ABSTRACT

OXIDATION OF DIMETHYL-ETHER AND ETHYLENE IN THE ATMOSPHERE AND COMBUSTION ENVIRONMENT AND THERMODYNAMIC STUDIES ON HYDROFLUOROCARBONS USING AB INITIO CALCULATION METHODS

by
Takahiro Yamada

Reaction pathways and kinetics are analyzed on $CH_3OC\bullet H_2$ unimolecular decay and on the complete $CH_3OC\bullet H_2 + O_2$ reaction system using thermodynamic properties ($\Delta H_f^{\circ}{}_{298}$, $S^{\circ}{}_{298}$, and $C_p(T)$ $300 \leq T/K \leq 1500$) derived by two *ab initio* calculation methods, CBS-q and G2. These are used to determine thermodynamic properties of reactants, intermediate radicals and transition state (TS) compounds. Quantum Rice-Ramsperger-Kassel (QRRK) analysis is used to calculate energy dependent rate constants, k(E), and master equation is used to account for collisional stabilization. Comparison of calculated fall-off with experiment indicates that the CBS-q and G2 calculated $E_{a,rxn}$ for the rate controlling transition state (β-scission reaction to $CH_2O + C\bullet H_2OOH$) needs to be lowered by factor of 3.3 kcal/mol and 4.0 kcal/mol respectively in order to match the data of Sehested et al. Experimental results on dimethyl-ether pyrolysis and oxidation reaction systems are compared with a detailed reaction mechanism model. The computer code CHEMKIN II is used for numerical integration. Overall agreement of the model data with experimental data is very good.

Reaction pathways are analyzed and kinetics are determined on formation and reactions of the adduct resulting from OH addition to ethylene using the above *ab initio* methods. Hydrogen atom tunneling is included by use of Eckart formalism. Rate constants are

compared with experimentally determined product branching ratios (C•H₂CH₂OH

stabilization : $CH_2O + CH_3$: $CH_3CHO + H$).

ab initio calculations are performed to estimate thermodynamic properties of nine

fluorinated ethane compounds (fluoroethane to hexafluoroethane), eight fluoropropane

(1-fluoropropane, 1,1- and 1,2-difluoropropane, 1,1,1- and 1,1,2-trifluoropropane,

1,1,1,2- and 1,1,2,2-tetrafluoropropane and 1,1,1,2,2-pentafluoropropane), and 2-

fluoro,2-methylpropane. Standard entropies and heat capacities are calculated using the

rigid-rotor-harmonic-oscillator approximation with direct integration over energy levels

of the intramolecular rotation potential energy curve. Enthalpies of formation are

estimated using G2MP2 total energies and isodesmic reactions. Thermodynamic

properties for fluorinated carbon groups C/C/F/H2, C/C/F2/H, C/C/F3, C/C2/F/H,

C/C2/F2 and C/C3/F for fluorinated alkane compounds, CD/F/H and CD/F2 for

fluorinated alkene compounds and CT/F for fluorinated alkyne compounds are estimated.

Fluorine-fluorine interaction terms F/F, 2F/F, 3F/F, 2F/2F, 3F/2F and 3F/3F for alkane

compounds, F//F, 2F//F and 2F/2F for alkene compounds, and F///F for alkyne compound

are also estimated.

OXIDATION OF DIMETHYL-ETHER AND ETHYLENE IN THE ATMOSPHERE AND COMBUSTION ENVIRONMENT AND THERMODYNAMIC STUDIES ON HYDROFLUOROCARBONS USING AB INITIO CALCULATION METHODS

by
Takahiro Yamada

A Dissertation
Submitted to the Faculty of
New Jersey Institute of Technology
in Partial Fulfillment of the Requirement for the Degree of
Doctor of Philosophy

Department of Chemical Engineering,
Chemistry and Environmental Science

January 1999

APPROVAL PAGE

OXIDATION OF DIMETHYL-ETHER AND ETHYLENE IN THE ATMOSPHERE AND COMBUSTION ENVIRONMENT AND THERMODYNAMIC STUDIES ON FLUOROHYDROCARBONS USING AB INITIO CALCULATION METHODS

Takahiro Yamada

Nov 5 1998

Dr. Joseph W. Bozzelli, Dissertation Adviser   Date
Distinguished Professor of Chemistry, NJIT

12-8-98

Dr. Richard B. Trattner, Committee Member   Date
Professor of Environmental Science, NJIT

12/8/98

Dr. Carol A. Venanzi, Committee Member   Date
Distinguished Professor of Chemistry, NJIT

12/08/98

Dr. Lev N. Krasnoperov, Committee Member   Date
Associate Professor of Chemistry, NJIT

11/5/98

Dr. Robert P. Hesketh, Committee Member   Date
Associate Professor of Chemical Engineering, Rowan University

BIOGRAPHYCAL SKETCH

Author: Takahiro Yamada

Degree: Doctor of Philosophy

Date: January 1999

Undergraduate and Graduate Education:

- Doctor of Philosophy in Environmental Science,
  New Jersey Institute of Technology, Newark, NJ, 1999

- Master of Science in Environmental Engineering,
  University of New Haven, West Haven, CT, 1994

- Master of Science in Marine Engineering
  State University of Osaka, Osaka, Japan 1987

- Bachelor of Science in Marine Engineering,
  State University of Osaka, Osaka, Japan 1985

Major: Environmental Science

Presentations:

Yamada, T.; Lay, T. H.; Bozzelli, J. W., "Ethylene + OH, Dimethyl-ether Radical + O_2, and the Respective Adduct Radical + O_2 Reactions", Chemical and Physical Processes in Combustion, 1996, p523, Proceedings, Combustion Institute, Pittsburgh, PA.

Lay, T. H.; Yamada, T.; Bozzelli, J. W., "Thermodynamic and Group Additivity Ring Correction for Three- to Six- Membered Oxygen Heterocyclic Hydrocarbons", J. Phys. Chem. A, 1997, v101, p2471

Yamada, T.; Bozzelli, J. W.; Lay, T. H., "Thermodynamic and Kinetic Analysis Using *ab initio* Calculations on Dimethyl-ether Radical + O2 Reaction System", 27th Int'l Symposium on Combustion, 1998, p31, Proceedings, Combustion Institute, Pittsburgh, PA.

Yamada, T.; Lay, T. H.; Bozzelli, J. W., "*ab initio* Calculations and Internal Rotor: Contributions for Thermodynamic Properties $S°_{298}$ and $C_p(T)$'s ($300 \leq T/K \leq 1500$): Group Additivity for Fluoroethanes, J. Phys. Chem. A, 1998, v102, p7286.

Publications in Process:

Thermodynamic Properties ($\Delta H_f^\circ{}_{298}$, $S^\circ{}_{298}$, $C_p(T)$'s $300 \leq T/K \leq 1500$) of Fluorinated Propanes. (Submitted)

Thermodynamic Properties of Groups and Interaction Terms for Fluorinated Alkanes, Alkenes, and Alkynes. (Submitted)

Kinetic and Thermodynamic Analysis on OH Addition to Ethylene: Adduct Stabilization, Isomerization, and Isomer Dissociations. (Submitted)

Kinetic and Thermodynamic Analysis on Dimethyl-ether Radical + O_2 Reaction (Application of *ab initio* Calculations, CBS-q and G2). (in process)

Presentations:

Yamada, T; Bozzelli, J. W.; Lay, T. H, "Ethylene + OH, Dimethyl-ether Radical + O_2, and the Respective Adduct Radical + O_2 Reactions", Eastern Section Combustion Institute Fall Technical Meeting, Hilton Head Island, South Carolina, December 9-11, 1996. Oral Presentation.

Yamada, T.; Bozzelli, J. W., Lay, T. H., "Dimethyl-ether Radical + O_2 and Respective Adduct Radical + O_2 Reactions", 4th International Conference on Chemical Kinetics, Gaithersburg, Maryland, July 14-18, 1997. Oral Presentation.

Yamada, T.; Bozzelli, J. W. ; Lay, T. H, "Ethylene + OH and the respective adduct Radical + O2 Reactions" 4th International Conference on Chemical Kinetics, Gaithersburg, Maryland, July 14-18, 1997. Poster.

Bozzelli, J. W.; Ing, W. C.; Yamada, T.; Sheng, C.; Dean, A. M., Pressure Dependent Reaction Mechanism for C1 and C2 Combustion System: 0.001 – 100 atm, 300 – 2500K" 4th International Conference on Chemical Kinetics, Gaithersburg, Maryland, July 14-18, 1997. Poster.

Yamada, T.; Bozzelli, J. W.; Lay, T. H, "Thermodynamic and Kinetic Analysis Using *ab initio* Calculations on Dimethyl-ether Radical + O2 Reaction System", 27th International Symposium on Combustion, Boulder Colorado, August 2 – 7. 1998. Oral Presentation.

Yamada, T.; Bozzelli, J. W.; Lay, T. H., "Kinetic and Thermodynamic Analysis on OH addition to Ethylene Using *ab initio* Calculation (G2 and CBS-q)", 27th International Symposium on Combustion, Boulder Colorado, August 2 – 7. 1998. Poster.

To my beloved family

ACKNOWLEDGEMENT

I wish to express my appreciation to Professor Joseph W. Bozzelli, my adviser, not only for his professional advice but also his encouragement, patience, and kindness. I am deeply indebted to him for the opportunities which he made available to me.

I would also like to thank to my dissertation committee members, Dr. Richard B. Trattner, Dr. Carol A. Venanzi, Dr. Lev N. Krasnoperov, and Dr. Howard Hesketh for their helpful corrections and productive comments.

It is my pleasure to thank Dr. Tsan H. Lay, who shared his knowledge with me and helped me with *ab initio* calculation analysis. In addition, I would like to thank my coworkers at NJIT, Samuel Chern, Chiung-Ju Chen, Chad Sheng, Byung Ik Park, Li Zhu , and Jongwoo Lee, for having dealt with me as a colleague, which has made my time at NJIT much more enjoyable and productive.

For love and inspiration I shall be eternally grateful to my parents, Seiryu and Chieko Yamada. Without their constant support and encouragement, I truly believe all of this would not have been possible.

TABLE OF CONTENTS
(Continued)

LIST OF TABLES

LIST OF TABLES
(Continued)

LIST OF FIGURES

Figure   **Page**

LIST OF FIGURES
(Continued)

LIST OF FIGURES
(Continued)

Figure   **Page**

PART I

OXIDATION OF DIMETHYL-ETHER AND ETHYLENE IN THE ATMOSPHERE AND COMBUSTION ENVIRONMENT

(THERMODYNAMIC AND KINETIC STUDY ON OXYGENATED HYDROCARBONS)

Overview

Thermodynamic and kinetic studies on oxidation of Dimethyl-ether and ethylene are discussed in Part I.

Dimethyl-ether radical + O_2 reaction, addition, isomerization, and dissociation, are described in Chapter 1. Dimethyl-ether is proposed as the alternative fuel for diesel engine by several petroleum companies and vehicle manufactures. Kinetic study based on *ab initio* determined thermodynamic properties is original work in this study. *ab initio* calculations are applied to calculate the thermodynamic properties ($\Delta H_f°_{298}$, $S°_{298}$, and $C_p(T)$'s, $300 \leq T/K \leq 1500$) of intermediate radicals and transition states (TS's). Quantum Rice-Rampsperger-Kassel (QRRK) analysis is performed based on these thermodynamic properties.

Further reaction of one important product from the reaction of dimethyl-ether radical with O_2, $C \bullet H_2OCH_2OOH$ with molecular oxygen is addressed in chapter 2. H atom abstraction reaction from dimethyl-ether by several major radicals, and dimethyl-ether and dimethyl-ether radical dissociation reactions are also analyzed in Chapter 2.

A detailed reaction mechanism is then constructed using results from analysis of the above reaction systems plus a previously constructed reaction mechanisms for methane, ethane, and methanol compounds. The product profiles (concentration vs. time) are

modeled and compared with experimental results. This mechanism and the results are described in Chapter 3.

ab initio calculations and kinetic analysis is also applied on ethylene + OH addition reaction in chapter 4. This reaction serves as a model reaction of OH addition to olefins in atmospheric photo chemistry as well as in low temperature combustion. Hydrogen tunneling effect is applied on this reaction system to match the experimentally determined product branching ratio. This addition reaction plays important role in low temperature combustion chemistry, but few detailed kinetic studies have been reported on it.

Thermodynamic properties ($\Delta H_f^\circ{}_{298}$, $S^\circ{}_{298}$, and $C_p(T)$'s. $300 \leq T/K \leq 1500$) of 34 oxygenated three- to six-membered cyclic oxy-hydrocarbons and group additivity ring corrections are calculated in chapter 5. Thermodynamic properties for 10 species are adopted from pervious study. Semiempirical molecular orbital (MO) method PM3 is performed to calculate thermodynamic properties for 34 cyclic oxy-hydrocarbons. Enthalpies of formation of above 10 species and PM3 calculation results are compared to derive the calibration. Thermodynamic properties on the remaining 24 species including 12 new species are evaluated in this study. The data presented in this chapter are of value because they allow the estimation of accurate thermodynamic properties ($\Delta H_f^\circ{}_{298}$, $S^\circ{}_{298}$, and $C_p(T)$'s. $300 \leq T/K \leq 1500$) of three- to six-membered cyclic oxy-hydrocarbons using group additivity and/or MOPAC-PM3, both of which are reasonable and straightforward calculations to perform.

CHAPTER 1

KINETIC AND THERMODYNAMIC ANALYSIS ON DIMETHYL-ETHER + O2 REACTION (APPLICATION OF *AB INITIO* CALCULATIONS, CBS-Q AND G2)

1.1 Introduction

Dimethyl-ether has a number of desirable properties that make it attractive for use as a diesel fuel. First, it has high cetane (i.e. low octane) number which is advantages for diesel use[1]. Second, when used in diesel engines, it significantly reduces combustion noise and emission of particles. Third, the trade-off between NOx emissions and soot using conventional diesel fuel is eliminated in dimethyl-ether-fueled engines because the combustion is soot free. A dimethyl-ether-fueled engine can, therefore, be tuned to give reduced NOx emissions. Engine tests have shown that dimethyl-ether-fueled diesel engines have emission levels that surpass those of the California ultra-low emission vehicle (ULEV) regulations for medium duty vehicles[1].

Although several experimental studies on the overall reaction have been reported for dimethyl-ether oxidation[1-4], theoretical analysis on the thermodynamic and kinetic reaction pathways has not been studied. Thermodynamic and kinetic studies are important to understand the impact of dimethyl-ether in both atmospheric and combustion environments. In this chapter, thermodynamic properties ($\Delta H_f^{\circ}_{298}$, S°_{298} and $C_p(T)$'s, $300 \leq T/K \leq 1500$) for stable molecules, radical intermediates and transition states are calculated using CBS-q//MP2(full)/6-31G(d,p) and G2. Isodesmic reactions are applied to estimate accurate $\Delta H_f^{\circ}_{298}$ (in kcal/mol) of reactant, $CH_3OC\bullet H_2$ and two intermediate radicals, $CH_3OCH_2OO\bullet$ and $C\bullet H_2OCH_2OOH$ and two species which are

3

necessary to estimate later two intermediate radicals, CH_3OCH_2OOH and $C\bullet H_2CH_2OOH$.

Quantum Rice-Ramsperger-Kassel (QRRK) analysis[5,6] is used to calculate energy

dependent rate constants, k(E) and master equation analysis is applied to account for

collisional stabilization in the reactions of $CH_3OC\bullet H_2 + O_2$.

1.2 Method

1.2.1 *ab initio* Calculations

Two established composite *ab initio* calculation methods, CBS-q[7] and G2[8], are used with

the Gaussian94 computer code[9]. These are one of the highest calculation methods which

are available at this moment. These *ab initio* methods are utilized to estimate $\Delta H_f^{\circ}{}_{298}$ for

reactant $CH_3OC\bullet H_2$, intermediate radicals $CH_3OCH_2OO\bullet$ and $C\bullet H_2OCH_2OOH$ and the

transition states:

(TS1) $CH_3O\overline{CH_2OO}\bullet$: Intra-molecular hydrogen shift to form a hydroperoxy alkyl

radical.

(TS2) $C\bullet H_2O$---CH_2OOH: β-scission reaction to form a formaldehyde plus a

hydroperoxy methyl radical. The hydroperoxy methyl radical rapidly dissociate to

a second $CH_2O + OH$ and

(TS3) $C\bullet H_2\overline{OCH_2O}$---OH : Dioxetane (CH_2OCH_2O)---OH.

The CBS-q calculation sequence is performed on the MP2(full)/6-31G(d,p)

geometry and followed by single point calculations at the theory level of QCISD(T)/6-

31G, MP4(SDQ)/6-31G(d'), MP2/6-31+D(d,p). MP2/6-31G(d,p) is used to obtain the

geometric structures and frequencies for $S^{\circ}{}_{298}$ (in cal/mol-K) and $C_p(T)$'s (in cal/mol-K),

while HF/3-21 G(d) is the suggested method for structure and frequencies with CBS-q.

G2 theory is based on MP2/6-31G(d) optimized structure and HF/6-31G(d)

determined vibrational frequencies. Treatment of electron correlation in G2 is by

MØller-Plesset (MP) perturbation theory and quadratic configuration interaction (QCI).

The final energies are effectively at the MP4/6-311+G(d,p) level, making certain

assumptions about additivity and appending a small higher-level empirical correlation to

accommodate remaining deficiencies. Transition state geometries are identified by the

existence of one imaginary frequency in the normal mode coordinate analysis.

1.2.2 Determination of Entropy (S°_{298}) and Heat Capacities ($C_p(T)$'s, $300 \leq T/K \leq 1500$)

S°_{298} and $C_p(T)$'s are calculated based on frequencies and moments of inertia of the

optimized MP2(full)/6-31G(d,p) structures for the CBS-q method; and frequencies of

optimized HF/6-31G(d) structures and moments of inertia of the optimized MP2(full)/6-

31G(d) structures for the G2 method. Contribution of rotational frequencies for S°_{298} and

$C_p(T)$'s are calculated separately based on rotational barrier height and moments of

inertia. Pitzer and Gwinn's [10] general treatment of internal rotation is used to calculate

hindered internal rotational contribution to S°_{298} and $C_p(T)$'s.

1.2.3 Determination of Enthalpies of Formation ($\Delta H_f^{\circ}_{298}$)

$\Delta H_f^{\circ}_{298}$ for the reactant, two intermediate radicals and two other species which are

necessary to calculate intermediate radicals are estimated using total energies obtained by

ab initio calculations and isodesmic reactions. Total energies are corrected by zero point

vibrational energies (ZPVE) which are scaled by 0.9608 as recommended by Scott et al.[11]. Thermal correction 0K to 298.15K is calculated to estimate $\Delta H_f°_{298}$ at 298.15K[12].

The vibrational frequencies are scaled by 1.0084 as recommended by Scott et al. for thermal correction[11].

$$\Delta H(T) = H_{trans}(T) + H_{rot}(T) + \Delta H_{vib}(T) + RT \qquad \text{---------- (1)}$$

$$H_{trans}(T) = 3/2RT$$

$$H_{rot}(T) = 3/2RT,$$

$$\Delta H_{vib}(T) = Nh\Sigma(v_i/(\exp(hv_i/kT)-1))$$

N: Avogadro constant, h: Plank constant, k: Boltzmann constant.

Five isodesmic reactions are used to determine the $\Delta H_f°_{298}$ of the three radicals.

For estimation of $CH_3OC\bullet H_2$

$$CH_3OC\bullet H_2 + CH_3OH \rightarrow CH_3OCH_3 + C\bullet H_2OH \qquad \text{---------- (2)}$$

For estimation of $CH_3OCH_2OO\bullet$

$$CH_3OCH_2OO\,\bullet\; + CH_3CH_2OOH \rightarrow CH_3OCH_2OOH + CH_3CH_2OO\bullet \qquad \text{---------- (3)}$$
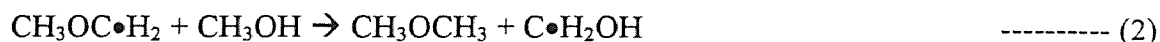
For estimation of $C\bullet H_2OCH_2OOH$
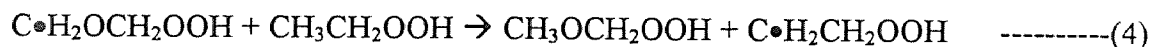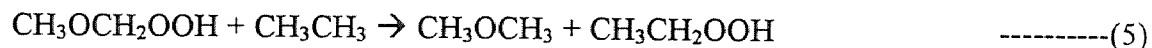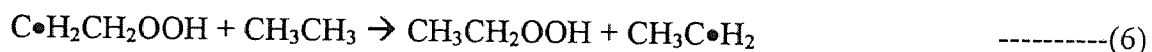
$$C\bullet H_2OCH_2OOH + CH_3CH_2OOH \rightarrow CH_3OCH_2OOH + C\bullet H_2CH_2OOH \qquad \text{----------(4)}$$

For estimation of CH_3OCH_2OOH

$$CH_3OCH_2OOH + CH_3CH_3 \rightarrow CH_3OCH_3 + CH_3CH_2OOH \qquad \text{----------(5)}$$

For estimation of $C\bullet H_2CH_2OOH$

$$C\bullet H_2CH_2OOH + CH_3CH_3 \rightarrow CH_3CH_2OOH + CH_3C\bullet H_2 \qquad \text{----------(6)}$$

The method of isodesmic reactions relies upon the similarity of bonding environment in the reactants and products that leads to cancellation of systematic errors in the *ab initio*

MO calculations [12]. The basic requirement of the isodesmic reaction is that the number of bonds of each formal chemical bond type is conserved in the reaction. In reaction (2), *ab initio* calculations with ZPVE and thermal correction are performed for all of four compounds. Since $\Delta H_f^\circ{}_{298}$ of three compounds (excepting) $CH_3OC\bullet H_2$ have been experimentally or theoretically calculated, the unknown $\Delta H_f^\circ{}_{298}$ of $CH_3OC\bullet H_2$ is obtained. The remaining four species are calculated in the same manner.

The $\Delta H_f^\circ{}_{298}$ of TS compounds are estimated by evaluation of $\Delta H_f^\circ{}_{298}$ of the stable radical adducts plus difference of total energies with ZPVE and thermal correction between these radical species and the transition state (TS).

1.2.4 High-pressure Limit A Factors (A_∞) and Rate Constants (k_∞) Determination with *ab initio* Calculations for Transition State Compounds

For the reactions where thermodynamic properties of transition states are calculated by *ab initio* methods, k_∞s are fit by three parameters A_∞, Δn and $E_{a,\infty}$ over a temperature range of 200 to 2,000K as expressed below.

$$k_\infty = A_\infty(T)^{\Delta n}\exp(-E_{a,\infty}/RT) \qquad \text{---------- (7)}$$

High-pressure limit A factors (A_∞) of unimolecular reactions are calculated using transition state theory (TST) along with *ab initio* data for the determination of the structure, and vibrational and rotational contributions to $S^\circ{}_{298}$ of transition states. Loss (or gain) of internal rotors and change of optical isomer and symmetry numbers are also incorporated into the calculation of $S^\circ{}_{298}$ for each TS. $S^\circ{}_{298}$ of reactants and TSs are then used to determine the pre-exponential factor, A, via classical TST[13] for a unimolecular

Reaction

$$A = (h_p T/K_b) \exp(\Delta S^{\neq}) \qquad \text{---------- (8)}$$

where h_p is Plank's constant, k_b is the Boltzmann constant and $\Delta S^{\neq}$ is equal to $S^{\circ}_{298,TS}$ -

$S^{\circ}_{298,reactant}$.

Activation energies of reactions are calculated as follows:

$$E_a = [\Delta H_f^{\circ}{}_{298,TS} - \Delta H_f^{\circ}{}_{298,reactant}]. \qquad \text{---------- (9)}$$

1.2.5 Quantum Rice-Ramsperger-Kassel (QRRK) Analysis with Master Equation

The $CH_3OC\bullet H_2 + O_2$ addition reactions along with subsequent chemically activated

reactions and unimolecular reactions are first analyzed by construction of potential

energy diagrams. Thermodynamic parameters, ($H_f^{\circ}{}_{298}$, S°_{298} and $C_p(T)$'s ($300 \leq T/K$

≤ 1500)), reduced vibration frequency sets and Lennard Jones parameters for species in

each reaction path are presented.

High pressure rate constants for each channel are obtained from literature or

referenced estimation techniques. The high-pressure limit rate constant (k_{∞}) for

$CH_3OC\bullet H_2 + O_2$ is taken from the generic reaction: $C_3H_7 + O_2$ and the reverse is

estimated from the principles of microscopic reversibility, MR. Kinetics parameters for

unimolecular and bimolecular (chemical activation) reactions are then calculated using

multi-frequency QRRK analysis for k(E)[14-16]. The master equation analysis[15] as

described by Gilbert and Smith[17] and their *UNIMOL* code[18] is used for fall-off (β

collision) with the steady state assumption on the energized adduct(s). Global rate

constants for loss of $CH_3OC\bullet H_2$ radical match the low pressure data of Masaki et al.[3] and Hoyermann et al.[4], when fall-off is accounted for.

Reactions which incur a change in number of moles, such as unimolecular dissociation, have energy of activation calculated as delta U_{rxn} plus an E_a for the reverse addition, where U is internal energy. (E_a reverse is usually 0.0 for simple association reactions). Recent modifications to the Quantum RRK calculation include;

1. use of a manifold of three frequencies plus incorporation of one external rotation for the density of states, $\rho(E)/Q$ and in calculation of $k(E)$ and of $F(E)$.

2. the collision efficiency βc is calculated with the calculated FE(T) factor instead of the previously assigned 1.15 value. βc is now calculated from Gilbert et al.[19], Eqn. 4.7.

3. the Leonard-Jones collision frequency Z_{LJ} is now calculated by $Z_{LJ} = Z \Omega (2,2)$ integral[20,21] obtained from fit of Reid et al.[21].

The QRRK analysis with the master equation and constant FE for fall-off has been used to analyze a variety of chemical activation reaction systems, Westmoreland et al.[14,22], Dean et al.[5] and Bozzelli et al.[23,24]. There are number of recent publications by other researchers, that utilize the QRRK formalism. Bauman notes its suitability for explanation of product ratios in ion molecule reaction systems. It is shown to yield reasonable results in these applications and provides a framework by which the effects of temperature and pressure can be evaluated.

1.3 Results and Discussion

1.3.1 Geometries of Two Intermediate Radicals and Transition States

Figure 1.1 to 1.4 show MP2(full)/6-31G(d) and MP2(full)/6-31G(d,p) determined

geometry of $CH_3OCH_2OO\bullet$, TS1, $C\bullet H_2OCH_2OOH$ and TS2 respectively and their

comparison between above two calculation methods. Since there is no significant

difference between two calculation methods, MP2(full)/6-31G(d,p) calculation result will

be discussed unless otherwise notice. Figure 1.2 shows TS1 structure. The H_5 atom is in

a bridge structure shifting from C_1 to radical site O_{10}. The bridging bond lengths H_5-C_1

and O_{10}-H_5 are calculated as 1.268Å and 1.257Å respectively with MP2(full)/6-31G(d,p)

determined geometry. Other bond lengths between carbon-oxygen and carbon-hydrogen

show near normal length with the O_{10}-O_9 bond at 1.401Å with MP2(full)/6-31G(d,p)

level of calculation, which is slightly shorter than normal bond length.

Figure 1.4 shows geometry of TS2. The bond lengths and angles of reactant

($C\bullet H_2OCH_2OOH$) are also shown in Figure 1.3 for comparison. The transition state

bond length of C_6-O_2 is calculated as 1.962Å with MP2(full)/6-31G(d,p) level of

calculation; the original length is 1.409Å. As O_2 and C_6 are being separated, the bond

length of C_1 and O_2 shortens to form a double bond. The transition state bond of C_1-O_2 is

calculated as 1.241Å; the original length is 1.374Å. It is interesting that that the same

level *ab initio* calculation, MP2/6-31G(d,p), for formaldehyde CH_2O shows C=O bond

length of C-O 1.265Å, which is longer than C=O bond length in this transition state. One

other significant difference in bond lengths between reactant and transition state is O_9-C_6,

which shows 0.052Å shorter bond length at the transition state, while bond length of
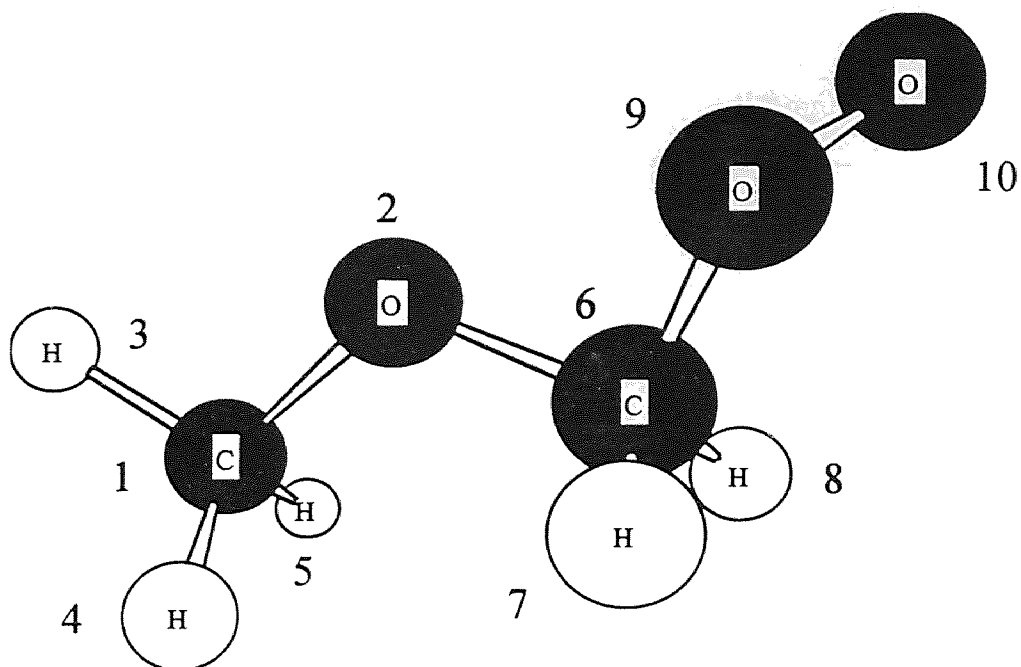
Bond Length (Å)	MP2(full)/6-31G(d)	MP2(full)/6-31G(d,p)
O2-C1	1.432	1.430
H3-C1	1.089	1.084
H4-C1	1.092	1.088
H5-C1	1.096	1.091
C6-O2	1.375	1.375
H7-C6	1.090	1.085
H8-C6	1.095	1.091
O9-C6	1.464	1.462
O10-O9	1.317	1.317

Bond Angle (Degree)	MP2(full)/6-31G(d)	MP2(full)/6-31G(d,p)
∠H3C1O2	105.8	106.0
∠H4C1O2	109.9	111.2
∠H5C1O2	110.7	110.7
∠C6O2C1	113.6	113.5
∠H7C6O2	113.7	113.6
∠H8C6O2	107.7	107.7
∠O9C6O2	111.8	111.8
∠O10O9C6	110.5	110.3

**Figure 1.1 MP2(full)/6-31G(d,p) Determined Geometry
CH3OCH2OO.**
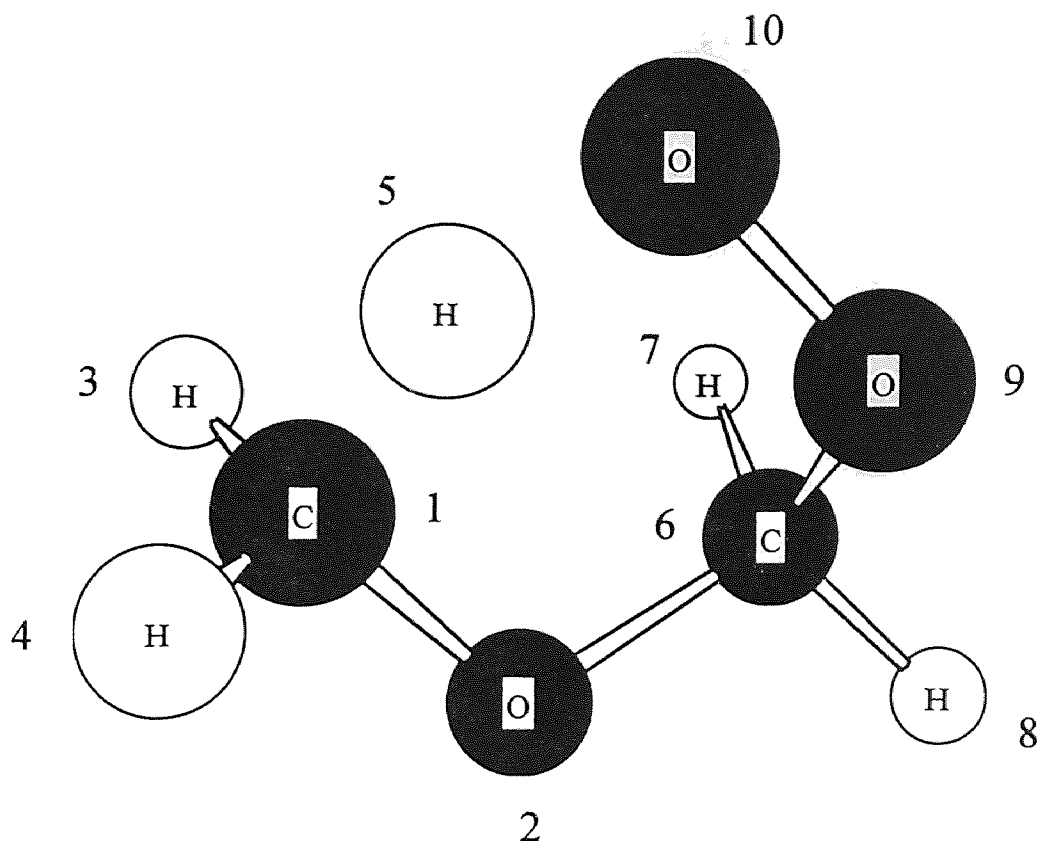
Bond Length (Å)	MP2(full)/6-31G(d)	MP2(full)/6-31G(d,p)
O2-C1	1.385	1.386
H3-C1	1.088	1.083
H4-C1	1.096	1.091
H5-C1	1.288	1.268
C6-O2	1.418	1.416
H7-C6	1.097	1.092
H8-C6	1.089	1.084
O9-C6	1.408	1.408
O10-O9	1.404	1.401
O10-H5	1.212	1.257

Bond Angle (Degree)	MP2(full)/6-31G(d)	MP2(full)/6-31G(d,p)
∠H3C1O2	110.1	110.2
∠ H4C1O2	114.3	114.2
∠C6O2C1	111.0	110.7
∠H7C6O2	111.1	111.1
∠H8C6O2	107.2	107.4
∠O9C6O2	107.9	107.9
∠ O10O9C6	106.0	105.9

Figure 1.2 MP2(full)/6-31G(d,p) Determined Geometry cyCH3OCH2OO. (TS1)
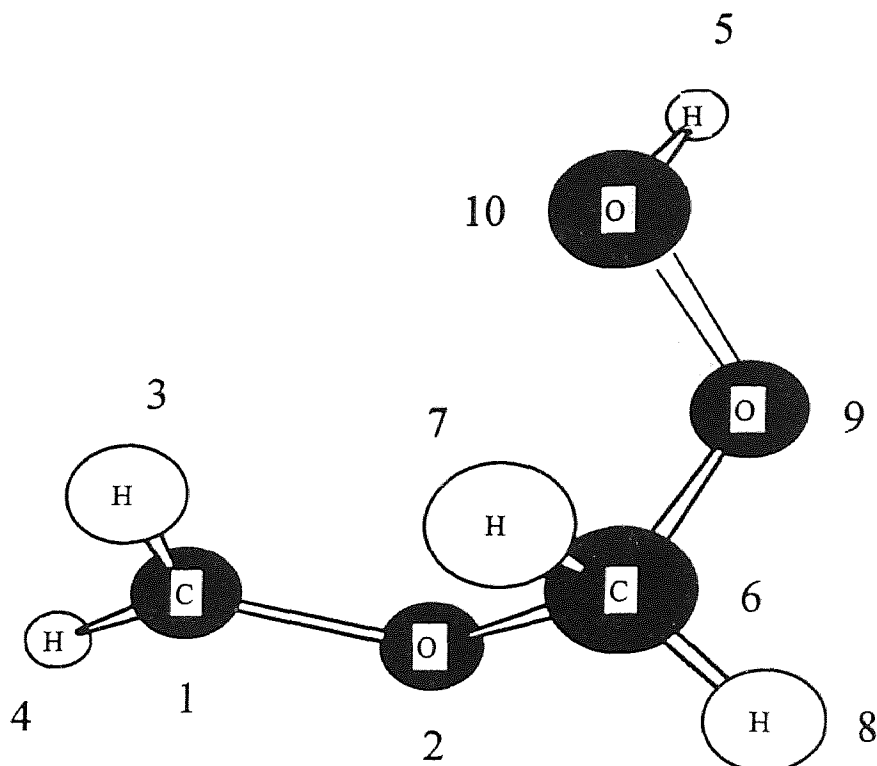
Bond Length (Å)	MP2(full)/6-31G(d)	MP2(full)/6-31G(d,p)
O2-C1	1.374	1.374
H3-C1	1.083	1.076
H4-C1	1.080	1.079
C6-O2	1.410	1.409
H7-C6	1.094	1.090
H8-C6	1.092	1.088
O9-C6	1.405	1.404
O10-O9	1.467	1.466
H5-O10	0.978	0.971

Bond Angle (Degree)	MP2(full)/6-31G(d)	MP2(full)/6-31G(d,p)
∠H3C1O2	117.8	117.6
∠ H4C1O2	112.2	112.3
∠C6O2C1	115.7	115.4
∠H7C6O9	110.5	110.5
∠H8C6O9	103.3	103.3
∠O9C6O2	112.5	112.7
∠ O10O9C6	105.8	105.8
∠ H5O10O9	98.9	98.8

Figure 1.3 MP2(full)/6-31G(d,p) Determined Geometry
C.H2OCH2OOH
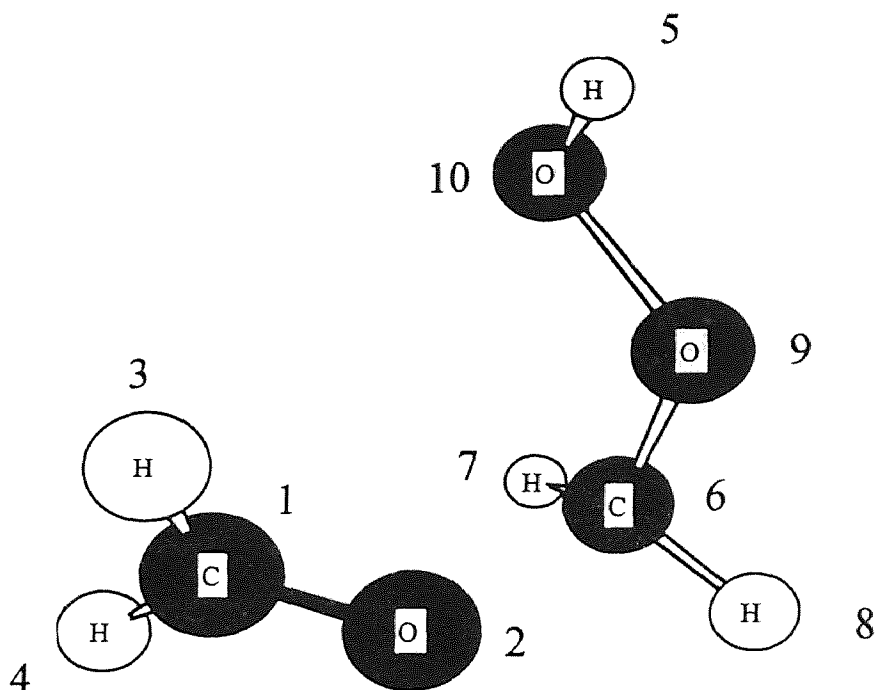
Bond Length (Å)	MP2(full)/6-31G(d)	MP2(full)/6-31G(d,p)
O2-C1	1.240	1.241
H3-C1	1.097	1.093
H4-C1	1.097	1.093
C6-O2	1.963	1.962
H7-C6	1.084	1.081
H8-C6	1.083	1.080
O9-C6	1.351	1.352
O10-O9	1.468	1.468
H5-O10	0.989	0.981

Bond Angle (Degree)	MP2(full)/6-31G(d)	MP2(full)/6-31G(d,p)
∠H3C1O2	121.2	121.2
∠H4C1O2	122.0	112.0
∠C6O2C1	116.0	116.0
∠H7C6O9	117.6	117.6
∠H8C6O9	111.0	111.0
∠O9C6O2	99.0	99.0
∠O10O9C6	105.9	105.9
∠H5O10O9	97.9	97.8

Figure 1.4 MP2(full)/6-31G(d,p) Determined Geometry C.H2O---CH2OOH (TS2)

O_{10}-O_9 stay in same bond length. This may indicate that the C•H$_2$OOH may be starting to dissociate to lower energy CH$_2$O + OH products in the transition state.

1.3.2   Entropy (S°$_{298}$) and Heat Capacity (C$_p$(T)'s (300≤T/K≤1500)) Estimation

S°$_{298}$ and C$_p$(T)'s are calculated by two methods, MP2(full)/6-31G(d,p) determined geometries and frequencies and MP2(full)/6-31G(d) determined geometries and HF/6-31G(d) determined frequencies. The calculation results using MP2(full)/6-31G(d,p) determined geometries and frequencies are summarized in Table 1.5. TVR, represents the sum of the contributions from translations, external rotations and vibrations for S°$_{298}$ and C$_p$(T)'s. Vibrational frequencies are scaled by 0.9608 as recommended by Scott et al[11]. Hindered internal rotational contribution for S°$_{298}$ and C$_p$(T)'s are estimated separately using the method of Pitzer and Gwinn[10]. Symmetry is incorporated in estimation of S°$_{298}$ as described in Table 1.5. There is no internal rotational contribution to S°$_{298}$ and C$_p$(T)'s for (TS1), hydrogen shift transition state since this is a cyclic structure. This results in smaller S°$_{298}$ and C$_p$(T) values than the reactant or product.

The calculation results using MP2(full)/6-31G(d,) determined geometries and HF/6-31G(d) determined frequencies are summarized in Table 1.6. Comparison of the stable radicals indicates that MP2/6-31G(d,p) and HF/6-31G(d) determined S°$_{298}$ and C$_p$(T)'s are in agreement. Differences are within 1 cal/mol-K for both S°$_{298}$ and C$_p$(T)'s except C$_p$(T)'s for C•H$_2$OCH$_2$OOH, where differences are 1 to 2 cal/mol-K. The differences of S°$_{298}$ of TS1 and TS3 are 2.01 and 1.90 cal/mol-K respectively, and that of TS2 is 5.42 cal/mol/K. The large difference of the low frequencies v6 to v9 in Table 1.1 and 1.2

Table 1.1 Vibrational Frequencies[a] (ν cm^{-1}) MP2(full)/6-31G(d,p) level of calculation

Species	v1	v2	v3	v4	v5	v6	v7	v8	v9	v10	v11	v12	v13	v14	v15	v16	v17	v18	v19	v20	v21	v22	v23	v24
$CH_3OC.H_2$	281	313	440	785	998	1171	1206	1289	1318	1512	1554	1558	1569	3109	3197	3205	3262	3369						
CH_3OCH_2OO	102	138	212	390	473	586	902	982	1151	1193	1213	1270	1283	1355	1446	1521	1551	1554	1572	3120	3137	3218	3257	3269
cyCH_3OCH_2OO (TS1)[b]	-2246[e]	257	412	489	495	614	742	957	1020	1148	1171	1218	1244	1262	1335	1407	1438	1528	1550	1742	3127	3138	3267	3283
$C.H_2OCH_2OOH$	104	163	247	299	379	466	601	719	868	1004	1078	1146	1253	1274	1352	1379	1452	1524	1555	3141	3235	3244	3397	3815
$C.H_2O\text{-}CH_2OOH$ (TS2)[c]	-1117[e]	103	192	225	359	432	535	621	735	943	999	1065	1167	1226	1289	1361	1474	1525	1652	3093	3195	3220	3372	3632
cy$CH_2OCH_2O\text{-}OH$ (TS3)[d]	-1637[e]	136	219	325	395	506	630	731	1010	1094	1108	1154	1183	1198	1204	1258	1428	1578	1619	3083	3160	3173	3293	3785

[a] non-scaled. [b,c,d] TS structure described in Method section. [e] Transition State compounds have one imaginary frequency.

Table 1.2 Vibrational Frequencies[a] (ν cm^{-1}) HF/6-31G(d) level of calculation

Species	v1	v2	v3	v4	v5	v6	v7	v8	v9	v10	v11	v12	v13	v14	v15	v16	v17	v18	v19	v20	v21	v22	v23	v24
$CH_3OC.H_2$	192	283	454	859	1066	1239	1295	1377	1400	1603	1646	1651	1656	3195	3255	3277	3319	3418						
CH_3OCH_2OO	100	135	213	407	503	646	1022	1078	1233	1254	1296	1355	1380	1474	1576	1630	1645	1659	1665	3208	3259	3279	3328	3358
cyCH_3OCH_2OO (TS1)[b]	-3094[e]	228	412	486	523	611	753	1044	1073	1197	1238	1264	1321	1327	1356	1444	1561	1624	1665	1730	3249	3257	3370	3382
$C.H_2OCH_2OOH$	99	163	229	314	409	483	658	812	1035	1096	1227	1254	1349	1373	1471	1569	1579	1616	1667	3265	3313	3339	3445	4081
$C.H_2O\text{-}CH_2OOH$ (TS2)[c]	-64[e]	19	59	89	96	135	262	341	534	885	1050	1299	1321	1337	1384	1580	1583	1680	2025	3156	3228	3319	3457	4080
cy$CH_2OCH_2O\text{-}OH$ (TS3)[d]	-211[e]	111	229	248	272	436	609	837	1075	1154	1242	1265	1314	1383	1419	1572	1590	1636	1713	3236	3298	3329	3456	4084

[a] non-scaled. [b,c,d] TS structure described in Method section. [e] Transition State compounds have one imaginary frequency.

which are derived by HF/6-31G(d) and MP2/6-31G(d,p) calculation methods result in large difference of $S°_{298}$. The negative frequency and first four frequencies, $v2$ to $v5$, which correspond to torsional frequencies are eliminated from the vibrational contribution for $S°_{298}$ and $C_p(T)$'s. The $C_p(T)$ determined by HF/6-31G(d) and MP2/6-31G(d,p) calculation methods for TS1 and TS3 are in good agreement. The $C_p(300K)$ for TS2 shows difference of 1.44 cal/mol-K.

1.3.3 Enthalpies of Formation ($\Delta H_f°_{298}$) Estimation using Total Energies and Isodesmic Reactions

CBS-q calculations are performed on the MP2(full)/6-31G(d,p) determined geometries and frequencies. G2 calculations are performed on the MP2(full)/6-31G(d) determined geometries and Hf/6-31G(d) determined frequencies.

Isodesmic reactions are applied to accurately estimate $H_f°_{298}$ of reactant, $CH_3OC•H_2$, intermediate radicals, $CH_3OCH_2OO•$ and $C•H_2OCH_2OOH$ and two other species, CH_3OCH_2OOH and $C•H_2CH_2OOH$. Zero point vibration energies (ZPVE's) and thermal corrections to 298.15K are taken into account. The total energies at 0 K including scaled ZPVE's, non-scaled ZPVE's, thermal corrections to 298.15 K and the total energies including scaled ZPVE's and thermal corrections are shown in Table 1.3 and 1.4 for CBS-q and G2 calculations respectively. Frequencies are scaled by 0.9608 for MP2/6-31G(d,p) determined frequencies as recommended by Scott et al.[11] and by 0.8929 as widely used for HF/6-31G(d) determined frequencies. The evaluated $\Delta H_f°_{298}$ for the molecules considered to have known $\Delta H_f°_{298}$ values, for use in the isodesmic reactions, are listed in Table 1.7. Both CBS-q and G2 calculation results are in good

Table 1.3   List of Total Energy, ZPVE, and Thermal Correction of CBS-q Calculation[a]

Compound	Total Energy at 0K[b]	ZPVE[c]	Thermal Correction[d]	Total Energy at 298 K
CH3OCH3	-154.8061777	0.082583	0.00519587	-154.8009819
CH3OC.H2[e]	-154.150071	0.068421	0.00522318	-154.1448478
CH3OH	-115.5767706	0.053035	0.00421923	-115.5725513
CH2OH	-114.9209789	0.038838	0.00415965	-114.9168193
CH3OCH2OOH	-305.0314795	0.090984	0.00720171	-305.0242778
C2H6	-79.6764427	0.077584	0.0043579	-79.672085
CH3C.H2	-79.01308383	0.061816	0.00477749	-79.00830634
CH3CH2OOH	-229.890461	0.085775	0.00625289	-229.8842081
C.H2CH2OOH	-229.2243005	0.070037	0.00677513	-229.2175254
CH3CH2OO.	-229.25602	0.074404	0.005704	-229.250316
CH3OCH2OO.	-304.3936408	0.079499	0.00662473	-304.3870161
C.H2OCH2OOH	-304.3748421	0.076763	0.00705772	-304.3677844
cyCH3OCH2OO. (TS1)[f]	-304.3604566	0.074824	0.00542956	-304.355027
C.H2O-CH2OOH (TS2)[g]	-304.3351877	0.073852	0.00683009	-304.3283576
cyCH2OCH2O-OH (TS3)[h]	-304.3244136	0.075796	0.00630109	-304.3181125

[a] Unit in Hartree 1 HF=627.51 kcal/mol. [b] Scaled ZPVE are included. Scaling factor is recommended as 0.96081 by Scott et al.[11] from Table 10 column of ZPVE for MP2(full)/6-31G(d). [c] Non-scaled. [d] Scaled by 1.0084 Scott et al.[11] [e] "." stands for radical site. [f,g,h] TS structure described in Method section.

agreement, where differences are within 1 kcal/mol. The values are listed in Table 1.8.

CBS-q determined enthalpy of reaction (2) ($\Delta H_{f298,rxn}$) is -0.25kcal/mol.

$\Delta H_f°_{298}(CH_3OC\bullet H_2)$ is evaluated from

$\Delta H_f°_{298,rxn} = H_f°_{298}(CH_3OCH_3) + H_f°_{298}(C\bullet H_2OH) - H_f°_{298}(CH_3OC\bullet H_2) - H_f°_{298}(CH_3OH)$

$-0.25 = -43.99 + (-4.2) - X - (-48.08)$ kcal/mol   ----- (10)

The $\Delta H_f°_{298}$ of $CH_3OC\bullet H_2$ obtained is 0.1 kcal/mol. G2 determined $\Delta H_f°_{298}$ is calculated in the same manner and determined as -0.1 kcal/mol.

The $\Delta H_f°_{298}$ for the two intermediate radicals (O_2 adducts) by CBS-q analysis are

obtained from use of isodesmic reactions (3) and (4); data result in $\Delta H_f°_{298}$ values of

Table 1.4   List of Total Energy, ZPVE, and Thermal Correction of G2 Calculation[a]

Compound	Total Energy at 0K[b]	ZPVE[c]	Thermal Correction[d]	Total Energy at 298K
CH3OCH3	-154.746681	0.086141	0.00534197	-154.741338
CH3OC.H2[e]	-154.093375	0.071040	0.0053997	-154.087975
CH3OH	-115.534891	0.055340	0.00429059	-115.530600
CH2OH	-114.881556	0.040226	0.00427716	-114.877279
CH3OCH2OOH	-304.938134	0.096682	0.00748454	-304.93065
C2H6	-79.630885	0.079757	0.004483	-79.626402
CH3C.H2	-78.970152	0.063364	0.004928	-78.965224
CH3CH2OOH	-229.812245	0.090392	0.006407	-229.805838
C.H2CH2OOH	-229.148794	0.074237	0.00696	-229.141834
CH3CH2OO.	-229.177477	0.077315	0.005861	-229.171616
CH3OCH2OO.	-304.301553	0.083616	0.006822	-304.294731
C.H2OCH2OOH	-304.284415	0.081664	0.00728465	-304.277131
cyCH3OCH2OO. (TS1)[f]	-304.266175	0.077717	0.00577018	-304.260405
C.H2O-CH2OOH (TS2)[g]	-304.245717	0.075	0.0091256	-304.236591
cyCH2OCH2O-OH (TS3)[h]	-304.240906	0.074023	0.00689177	-304.234015

[a] Unit in Hartree 1 HF=627.51 kcal/mol. [b] Scaled ZPVE, scaling factor=0.8929 [c] Non-scaled. [d] Scaled by 0.8929 [e] "." stands for radical site. [f,g,h] TS structure described in Method section.

-33.32 and -25.27 kcal/mol for $CH_3OCH_2OO\bullet$ and $C\bullet H_2OCH_2OOH$ respectively. G2 determined $\Delta H_f^\circ{}_{298}$ are calculated in the same manner and tabulated in Table 1.8. The values of other two species which are used to estimate the $\Delta H_f^\circ{}_{298}$ for two intermediate radicals are also shown in Table 1.8.

The activation energy of TS1 is estimated from the both reactant $CH_3OCH_2OO\bullet$ and product $C\bullet H_2OCH_2OOH$. The averaged result is 17.7 and 20.1 kcal/mol for the CBS-q and the G2 calculations respectively. The activation energy of TS2 is estimated by taking the difference of total energy between transition state and reactant, resulting in 24.7 and 25.4 kcal/mol for the CBS-q and the G2 calculations respectively. The activation energy of TS3 is also estimated by taking the difference of total energy between transition state

and reactant, resulting in 31.2 and 27.0 kcal/mol for the CBS-q and the G2 calculations

respectively. The overall energy diagram is illustrated in Figure 1.5.

Table 1.5   Ideal Gas Phase Thermodynamic Properties Using CBS-q//MP2/6-31G(d,p)[a]

Species and Symmetry #		Hf°$_{298}$	S°$_{298}$[b]	C$_{p300}$	C$_{p400}$	C$_{p500}$	C$_{p600}$	C$_{p800}$	C$_{p1000}$	C$_{p1500}$
CH3OC.H2	TVR[c]		57.00	11.73	14.68	17.57	20.13	24.30	27.47	32.51
(6)	Internal Rotor[d]		9.29	3.06	3.20	3.17	3.07	2.83	2.63	2.33
	Total[f]	0.1	67.67[e]	14.79	17.88	20.74	23.20	27.13	30.10	34.84
CH3OCH2OO.	TVR		65.11	14.70	18.99	23.04	26.53	31.94	35.85	41.73
(3)	Internal Rotor		16.61	6.64	6.60	6.26	5.82	5.06	4.51	3.78
	Total[f]	-33.9	83.10[e]	21.34	25.59	29.30	32.35	37.00	40.36	45.51
cyCH3OCH2OO.	TVR		69.54	18.41	23.48	27.96	31.68	37.22	41.03	46.54
(TS1)	Internal Rotor		0	0	0	0	0	0	0	0
(1)	Total[fg]	-16.2	72.30[e]	18.41	23.48	27.96	31.68	37.22	41.03	46.54
C.H2OCH2OOH	TVR		66.30	15.45	19.70	23.45	26.55	31.26	34.66	39.96
(2)	Internal Rotor		18.96	7.54	7.86	7.93	7.78	7.17	6.54	5.45
	Total[fg]	-26.5	88.02[e]	22.99	27.56	31.38	34.33	38.43	41.20	45.41
C.H2O-CH2OOH	TVR		65.97	14.86	18.91	22.44	25.37	29.84	33.11	38.26
(TS2)	Internal Rotor		19.00	7.54	7.86	7.93	7.78	7.17	6.54	5.45
(2)	Total[fg]	-1.8	87.73[e]	22.40	26.77	30.37	33.15	37.01	39.65	43.71
cyCH2OCH2O-OH	TVR		70.53	18.65	23.23	27.18	30.41	35.25	38.72	44.06
(TS3)	Internal Rotor		2.99	2.00	2.13	2.09	1.98	1.74	1.55	1.29
(1)	Total[fg]	4.7	74.90	20.65	25.36	29.27	32.39	36.99	40.27	45.35

[a] Thermodynamic properties are referred to a standard state of an ideal gas of pure enantiometer at 1 atm. [b] In cal mol^{-1}K^{-1}. [c] The sum of contributions from translations, external rotations, and vibrations. [d] Contribution from internal rotation. [e] Symmetry number is taken into account (-R x Ln (number of symmetry)) [f] Spin degeneracy contribution for entropy = 1.987 * Ln(2) (cal/mol-K) is taken into account. [g] Optical Isomer (OI) contribution for entropy = 1.987 * Ln(2) (cal/mol-K) is taken into account.

Table 1.6   Ideal Gas Phase Thermodynamic Properties Using G2[a]

Species and Symmetry #		Hf°$_{298}$	S°$_{298}$[b]	Cp$_{300}$	Cp$_{400}$	Cp$_{500}$	Cp$_{600}$	Cp$_{800}$	Cp$_{1000}$	Cp$_{1500}$
CH3OC.H2	TVR[c]		56.75	11.24	13.95	16.75	19.31	23.57	26.85	32.11
(6)	Internal Rotor[d]		9.29	3.06	3.20	3.17	3.07	2.83	2.63	2.33
	Total[f]	-0.1	67.42[e]	14.30	17.15	19.92	22.38	26.40	29.48	34.44
CH3OCH2OO.	TVR		64.63	13.80	17.75	21.69	25.20	30.79	34.89	41.13
(3)	Internal Rotor		16.61	6.64	6.60	6.26	5.82	5.06	4.51	3.78
	Total[f]	-34.1	82.62[e]	20.44	24.35	27.95	31.02	35.85	39.40	44.91
cyCH3OCH2OO.	TVR		70.29	19.02	24.12	28.61	32.31	37.79	41.55	46.91
(TS1)	Internal Rotor		0	0	0	0	0	0	0	0
(1)	Total[fg]	-14.0	70.29	19.02	24.12	28.61	32.31	37.79	41.55	46.91
C.H2OCH2OOH	TVR		65.64	14.26	18.18	21.86	25.03	29.98	33.60	39.27
(2)	Internal Rotor		18.96	7.54	7.86	7.93	7.78	7.17	6.54	5.45
	Total[fg]	-25.9	87.36[e]	21.80	26.04	29.79	32.81	37.15	40.14	44.72
C.H2O-CH2OOH	TVR		71.39	16.30	19.26	22.15	24.75	29.01	32.29	37.62
(TS2)	Internal Rotor		19.00	7.54	7.86	7.93	7.78	7.17	6.54	5.45
(2)	Total[fg]	-0.5	93.15[e]	23.84	27.12	30.08	32.53	36.18	38.83	43.07
cyCH2OCH2O-OH	TVR		72.43	19.06	23.23	27.90	30.20	36.18	38.83	43.07
(TS3)	Internal Rotor		2.99	2.00	2.13	2.09	1.98	1.74	1.55	1.29
(1)	Total[fg]	1.1	76.80	21.06	25.36	29.99	32.18	36.85	40.21	45.37

[a] Thermodynamic properties are referred to a standard state of an ideal gas of pure enantiometer at 1 atm. [b] In cal mol^{-1}K^{-1}. [c] The sum of contributions from translations, external rotations, and vibrations. [d] Contribution from internal rotation. [e] Symmetry number is taken into account (-R x Ln (number of symmetry)) [f] Spin degeneracy contribution for entropy = 1.987 * Ln(2) (cal/mol-K) is taken into account. [g] Optical Isomer (OI) contribution for entropy = 1.987 * Ln(2) (cal/mol-K) is taken into account.

Table 1.7 Molecular Considered to Have Known
ΔHf°$_{298}$ for Use in Isodesmic Reactions

Compounds	Hf°$_{298}$ (kcal/mol)
CH_3OCH_3	-43.99[a]
CH_3OH	-48.08[a]
$C.H_2OH$	-4.2[b]
CH_3CH_2OOH	-39.9[c]
$CH_3CH_2OO.$	-5.2[b]
CH_3CH_3	-20.24[a]
$CH_3C.H_2$	28.6[d]

[a] ref. 25. [b] ref. 26
[c] ref. 27 [d] ref. 28

Table 1.8 Comparison of CBS-q and G2 determined $H_f°_{298}$ Using Isodesmic Reactions (ZPVE's and Thermal Corrections are included)

Species	$H_f°_{298}$ (kcal/mol)		
	CBS-q	G2	Difference
CH_3OCH_2OOH	-70.7	-69.9	0.8
$C\bullet H_2CH_2OOH$	10.7	10.7	0.0
$C\bullet H_2OCH_3$	0.1	-0.1	0.2
CH_3OCH_2OO	-33.9	-34.1	0.2
$C\bullet H_2OCH_2OOH$	-26.5	-25.9	0.6

1.3.4 QRRK Calculation Results and CH_2O Yield

QRRK calculations for k(E) and master equation analysis for fall-off are performed and results are listed in Table 1.9 and 1.10 for CBS-q and G2 data respectively. ΔE down of 400 cal/mol is used. The ratio of rate constant for reaction (3) in QRRK result table against overall forward rate constant is used to estimate formaldehyde yield. The comparison of formaldehyde yields with CBS-q, G2 and experimental data are shown in Figure 1.6. The asterisk symbol represents experimental data of Sehested et al. at 296K and 0.38 to 940 Torr total pressure[1]. The dark thin line shows CH_2O yield based on CBS-q determined thermodynamic properties, the light thin line shows CH_2O yield based on G2 determined thermodynamic properties. Both calculation methods underestimates the rate constant compared to data of Sehested[1]. A QRRK fall-off plot matching the data of Sehested is obtained by lowering the E_a for TS2 by 3.3 kcal/mol, and use of other CBS-q determined thermodynamic properties, this data is illustrated via the bold dark line in Figure 1.6. Reduction of activation energy for TS2 by 4.0 kcal/mol is necessary for G2 determined thermodynamic properties to match the experimental data, this data is illustrated via bold light line and overlapped with CBS-q adjusted line in Figure 1.6.
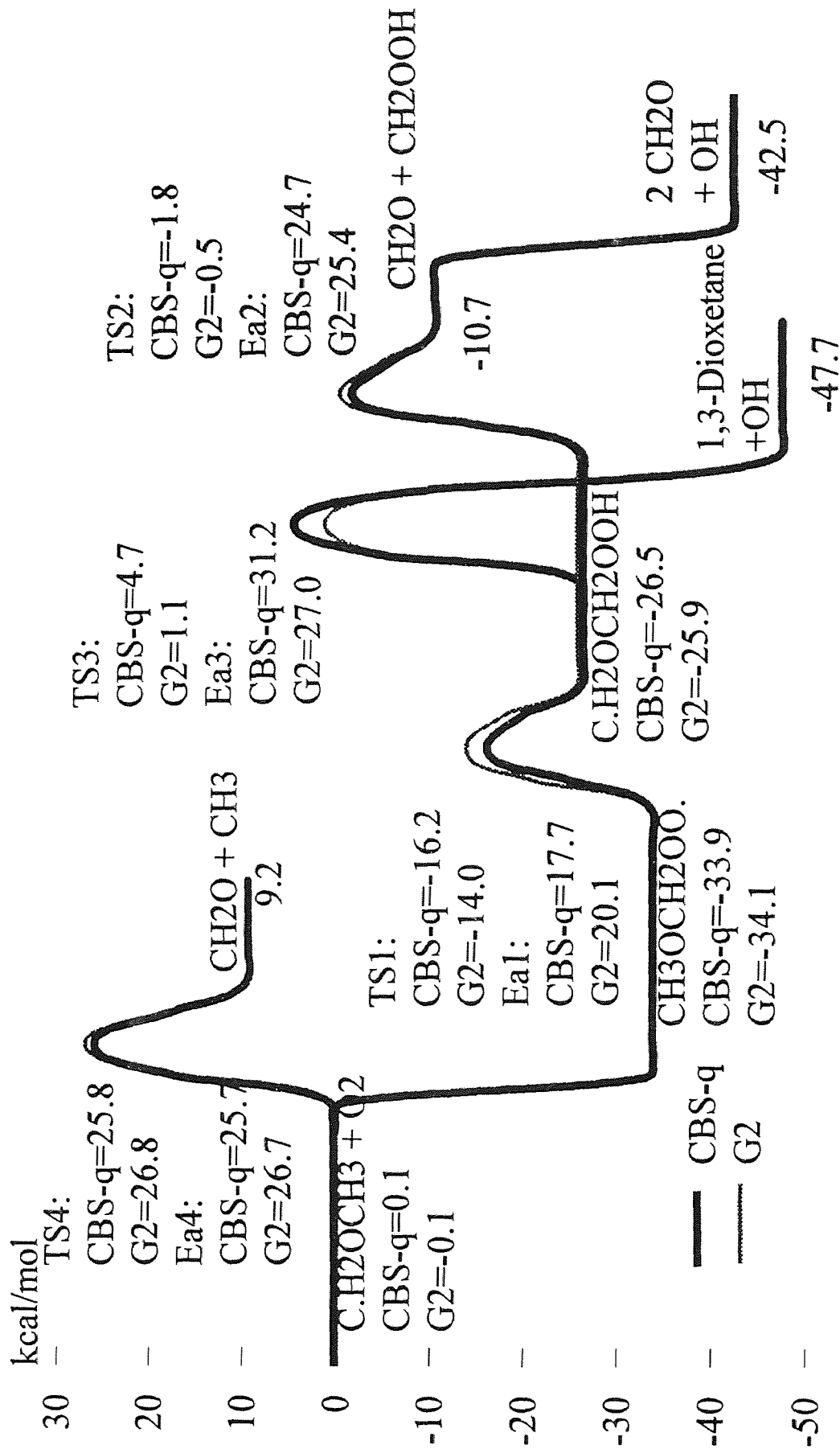
Figure 1.5 Potential Energy Diagram C.H2OCH3 + O2

kcal/mol

TS4:
CBS-q=25.8
G2=26.8
Ea4:
CBS-q=25.7
G2=26.7

CH2O + CH3
9.2

C.H2OCH3 + O2
CBS-q=0.1
G2=-0.1

TS3:
CBS-q=4.7
G2=1.1
Ea3:
CBS-q=31.2
G2=27.0

TS2:
CBS-q=-1.8
G2=-0.5
Ea2:
CBS-q=24.7
G2=25.4

CH2O + CH2OOH
-10.7

TS1:
CBS-q=-16.2
G2=-14.0
Ea1:
CBS-q=17.7
G2=20.1

CH3OCH2OO.
CBS-q=-33.9
G2=-34.1

C.H2OCH2OOH
CBS-q=-26.5
G2=-25.9

1,3-Dioxetane
+OH
-47.7

2 CH2O
+ OH
-42.5

CBS-q

G2

The reaction barriers of TS1 and TS2 are both lower in energy than the energy needed for reaction back to $CH_3OC \bullet H_2 + O_2$. These low barrier reactions provide a path for the exothermic, chain propagating combustion of dimethyl ether.

$$OH + CH_3OCH_3 \rightarrow CH_3OC \bullet H_2 + H_2O$$

$$\underline{CH_3OC \bullet H_2 + O_2 \rightarrow \quad 2\ CH_2O + OH}$$

$$CH_3OCH_3 + O2 \rightarrow 2\ CH_2O + H_2O$$
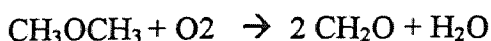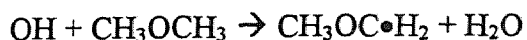
Figure 1.7 and 1.8 show rate constant k versus temperature (250 K to 2000 K) at 1 atm and 10 atm respectively. Results are based on MP2(full)/6-31G(d,p) determined geometry and frequencies and CBS-q calculation. The dissociation to 2 CH_2O + OH is major reaction over 700 K at 1 atm and the stabilization reaction to CH_3OCH_2OO. dominates below 700 K. That turning point is shifted to 1000 K at 10 atm. Figure 1.9 and 1.10 show rate constant versus pressure at 296 K and 1000 K. Results are based on same geometry, frequencies and calculation method as Figure 1.7 and 1.8. The dissociation to 2 CH_2O + OH is major reaction below 0.01 atm at 296 K and the stabilization reaction to CH_3OCH_2OO. dominates above 0.01 atm. That turning point is shifted to 10 atm at 1000 K. These results indicate that dimethyl-ether radical reacts with oxygen molecule to form energized adduct then it is stabilized as dimethyl-ether + O_2 adduct in the atmospheric environment, and the dimethyl-ether radical reacts with oxygen molecule to form energized adduct then it is decomposed to form two formaldehydes and hydroxy radical in the high temperature and pressure condition, such as internal combustion environment.
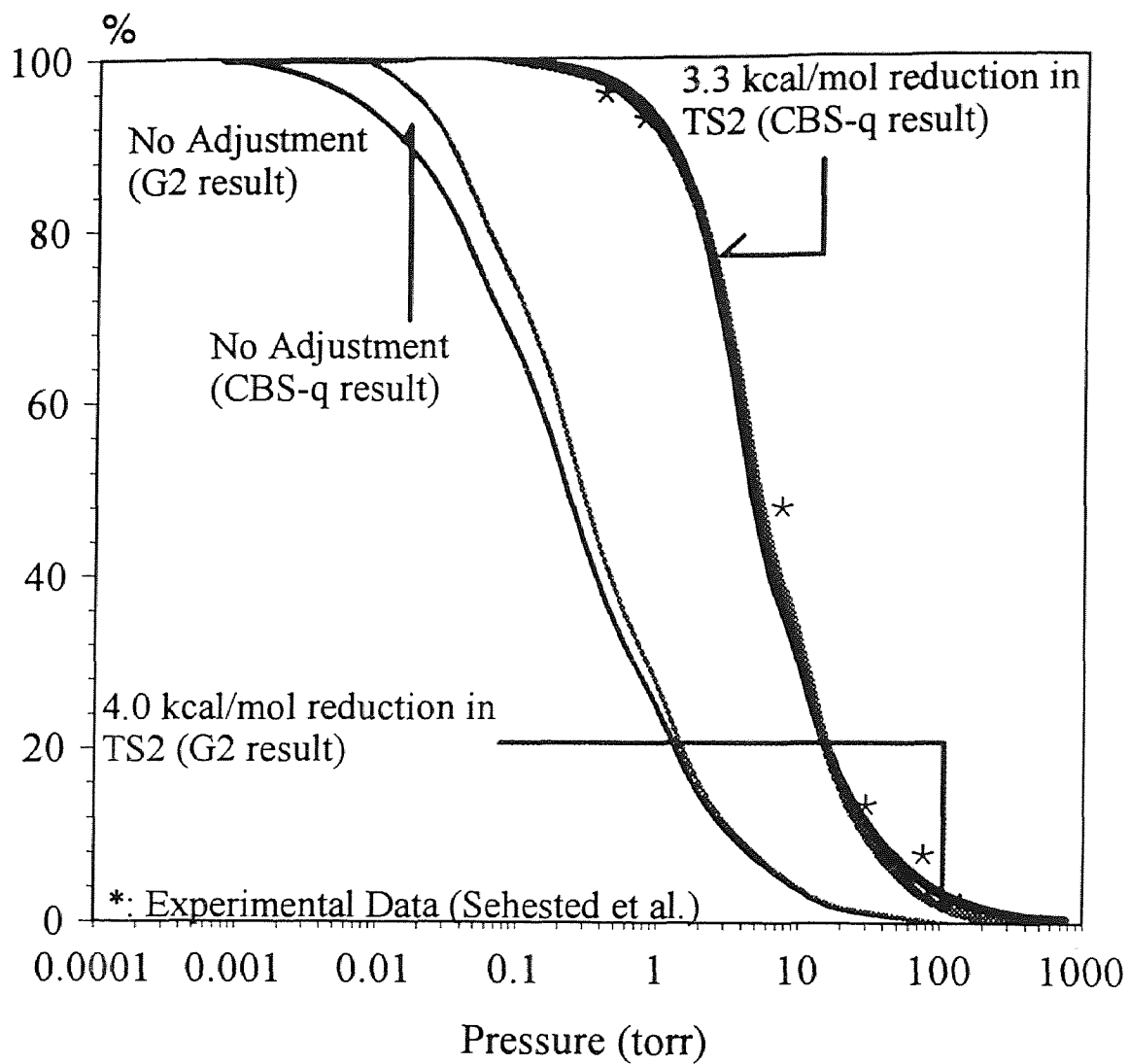
Figure 1.6 CH2O Yield Comparison
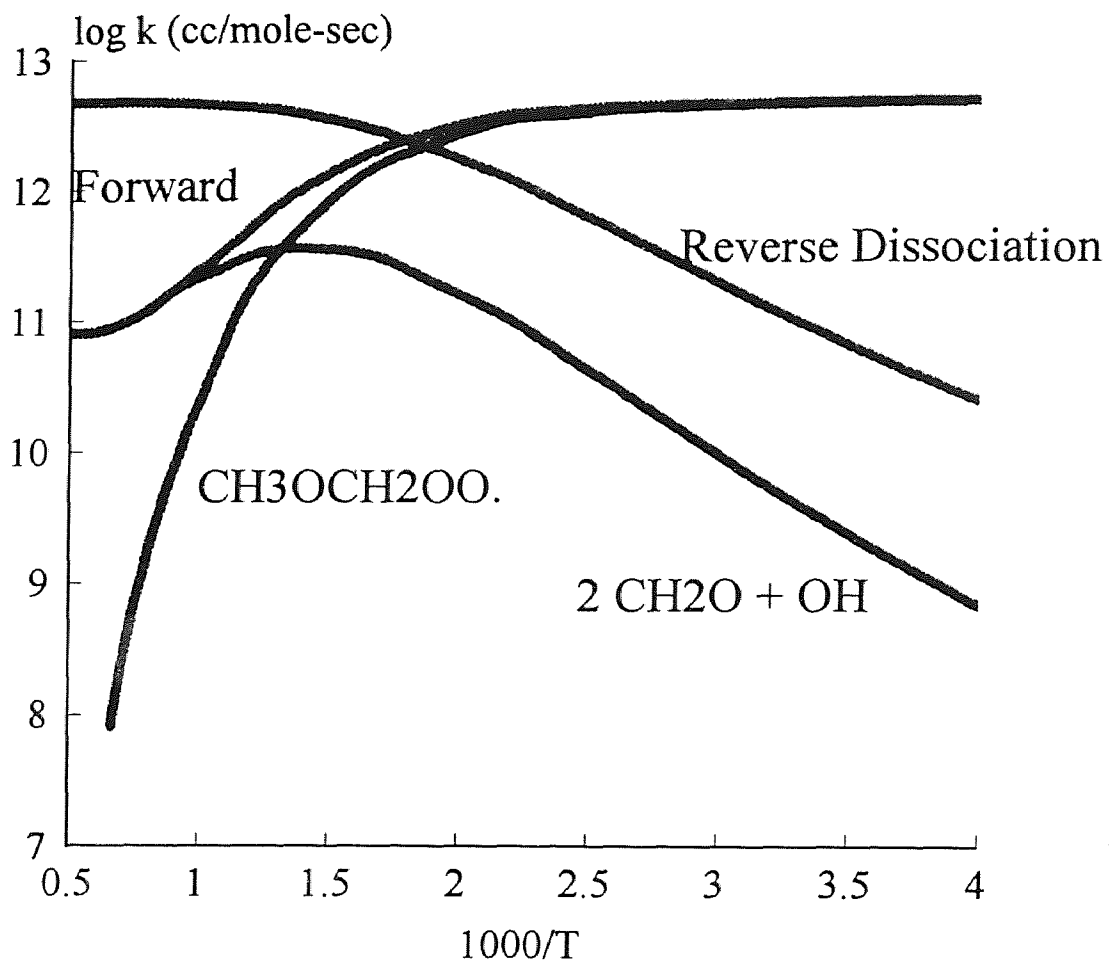
Figure 1.7 k vs. Temperature at 1 atm
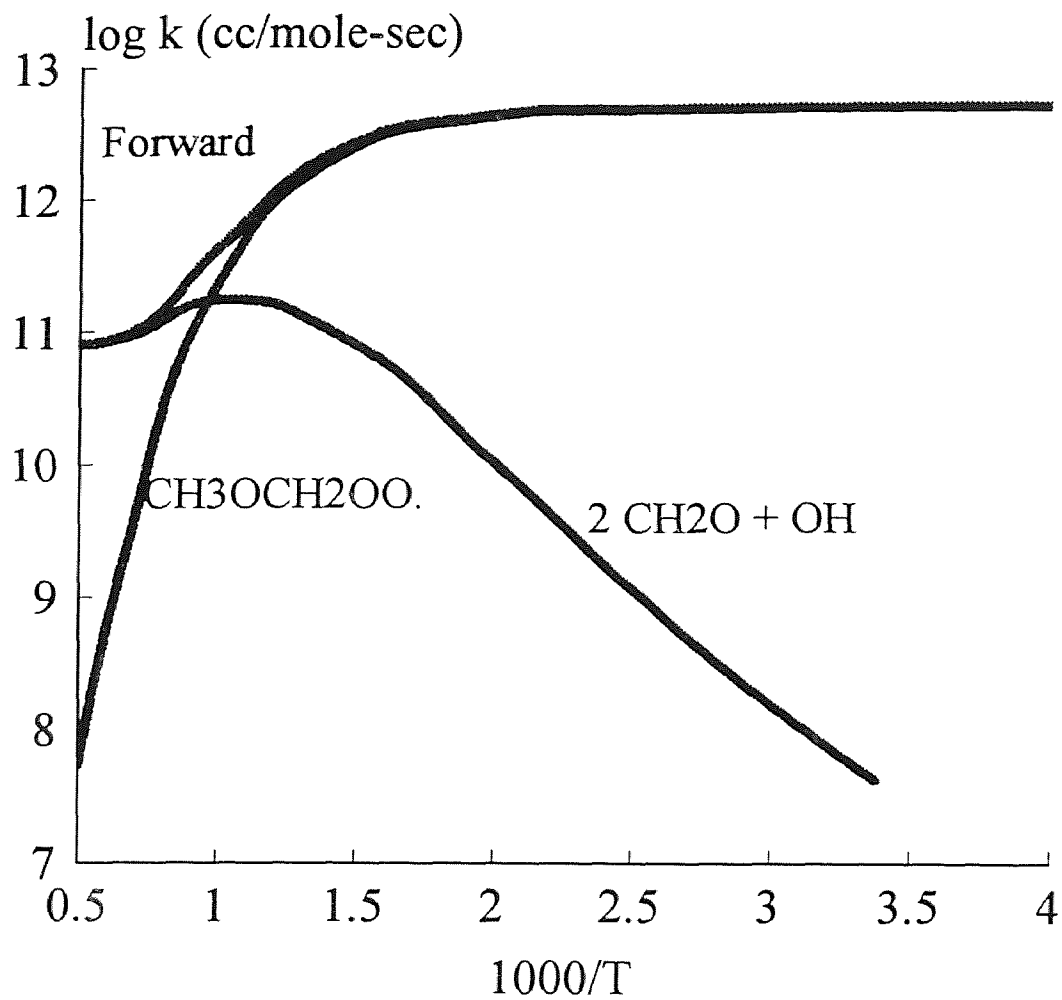
Figure 1.8 k vs. Temperature at 10 atm
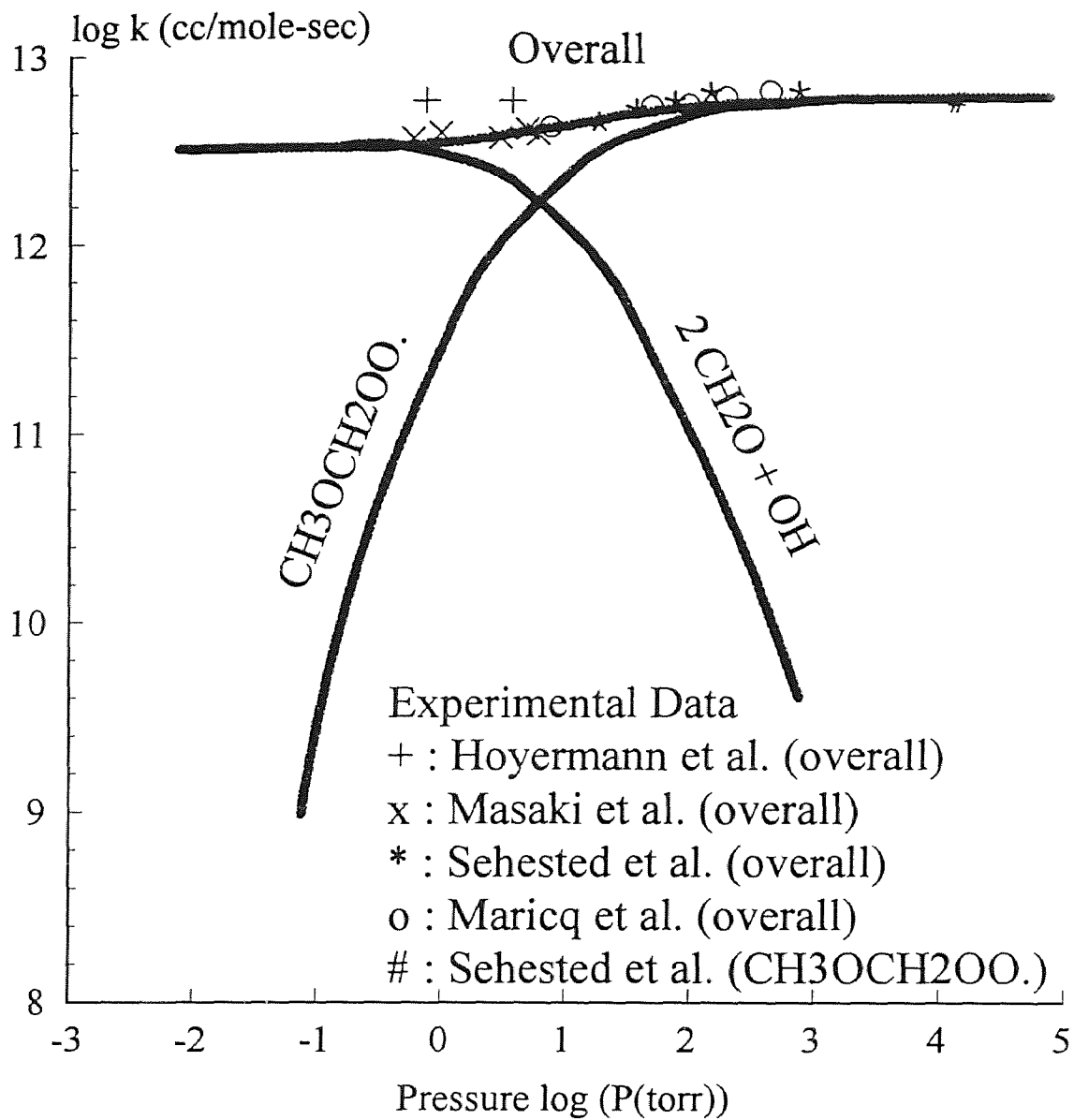
Figure 1.9 k vs. Pressure at 296 K
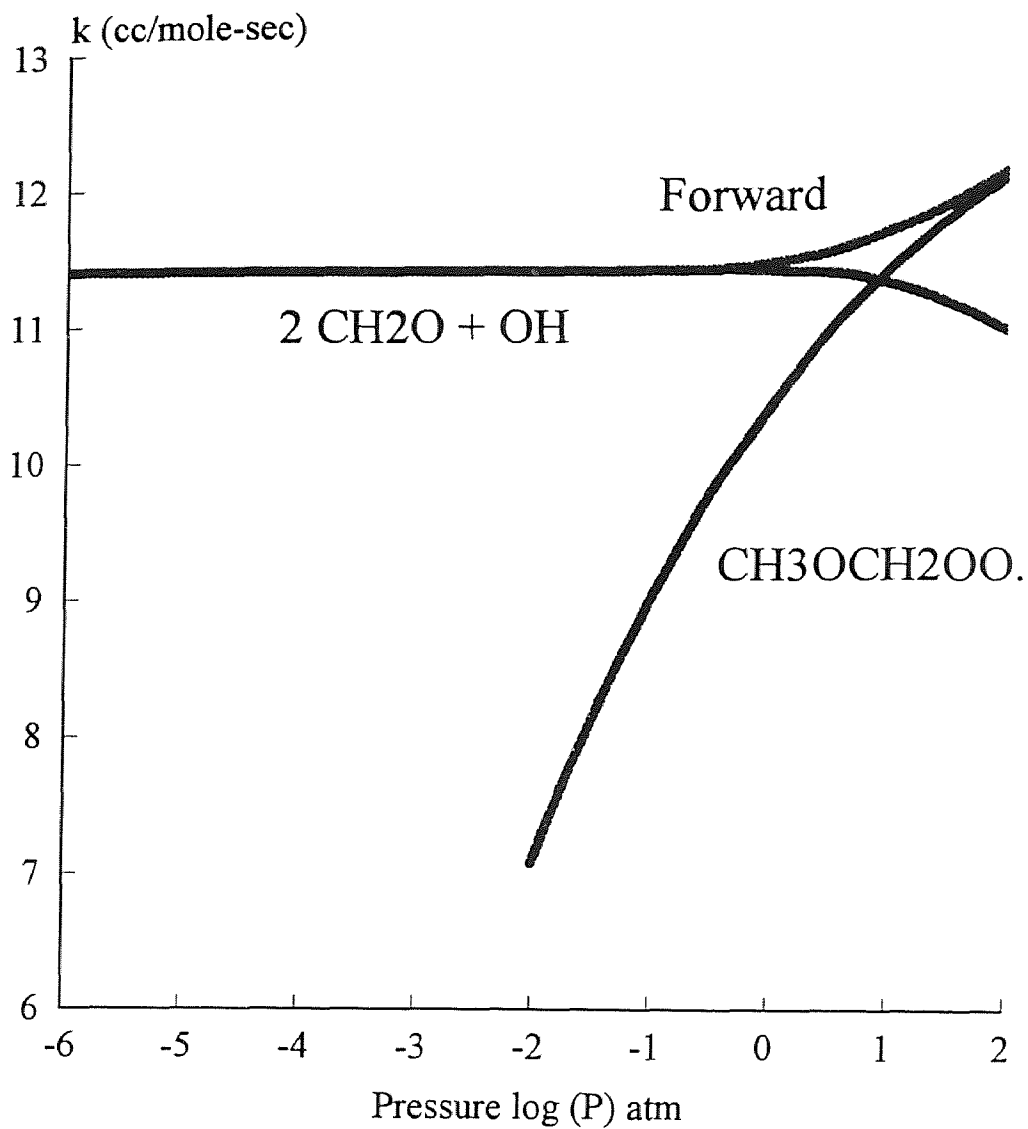
Figure 1.10 k vs. Pressure at 1000 K

1.3.5 Dioxetane (CH₂OCH₂O)+ OH Channel

The activation energies for (TS3) $CH_2OCH_2O\text{-}OH$ to dioxetane CH_2OCH_2O + OH are

31.2 and 27.0 kcal/mol for CBS-q and G2 calculation result. These are 4.6 and 1.2

kcal/mol above the reactants. QRRK analysis shows that this barrier makes this

cyclization reaction to form the cyclic diether not important in combustion of dimethyl-

ether.

Table 1.9 Input Parameters[a] and High - Pressure Limit Rate Constants $(K_\infty)^b$ for QRRK Calculations[c] and the Resulting Rate Constants (Temp=298 K) : CBS-q Result (Adjusted)

Input parameters for QRRK Calculations

High - Pressure Limit Rate Constants

k_∞

	Reaction	$A(S^{-1}$ or $cm^3/(mol\ s)$	n	E_a (kcal/mol)
1	$CH_3OC{\bullet}H_2 + O_2 \Rightarrow CH_3OCH_2OO{\bullet}^d$	4.82E+12	0.00	0.0
-1	$CH_3OCH_2OO{\bullet} \Rightarrow CH_3OC{\bullet}H_2 + O_2^e$	1.58+15	0.00	33.4
2	$CH_3OCH_2OO{\bullet} \Rightarrow C{\bullet}H_2OCH_2OOH^f$	1.10E+7	1.21	17.13
3	$C{\bullet}H_2OCH_2OOH \Rightarrow CH_2O + CH_2O + OH^g$	1.81E+12	0.38	22.19

Calculated Reaction Parameters at P=1atm, $k=A(T/K)^n(-E_a/RT)$ (Temp=200-2000K)

	Reaction	A	n	E_a (kcal/mol)	k_{298} (s^{-1} or $cm^3/(mol\ s)$
1	$CH_3OC{\bullet}H_2 + O_2 \Rightarrow CH_3OCH_2OO{\bullet}$	2.33E+63	-16.89	11.89	7.20E+12
3	$CH_3OC{\bullet}H_2 + O_2 \Rightarrow CH_2O + CH_2O + OH$	6.42E+29	-5.46	8.59	9.95E+09
4	$CH_3OCH_2OO{\bullet} \Rightarrow C{\bullet}H_2OCH_2OOH$	4.63E+21	-3.57	20.89	3.24E-03
5	$C{\bullet}H_2OCH_2OOH \Rightarrow CH_2O + CH_2O + OH$	1.34E+37	-8.09	26.20	7.84E-03

[a] Geometric mean frequency (from CPFIT, ref.[29] : 410.5cm⁻¹ (7.757); 1345.3cm⁻¹ (9.762); 3257.9cm⁻¹ (4.981). Lennard-Jones parameters: σ_{ij}=5.54Å, ϵ/k=460. [b] The units of A factors and rate constants k are s⁻¹ for unimolecular reactions and cm³/(mol s) for bimolecular reactions. [c] ΔE down of 400 cal/mol is used. [d] $k_{\infty,1}$: Atkinson et al.,[30]. [e] $k_{\infty,-1}$: MR. [f] A_2 is calculated using TST and entropy of transition state (TS1), $\Delta S^\ddagger_{298}$ from MP2(full)/6-31G(d,p) (see Table 1.), E_a from CBS-q calculation (see Table 3. and description for determination of E_a in Results section), All three parameters A, n, and E_a, are fit over the temperature range of 300 to2,000K. [g] A_3 is calculated using TST and entropy of transition state (TS1), $\Delta S^\ddagger_{298}$ from MP2(full)/6-31G(d,p) (see Table 1.), E_a from CBS-q calculation (see Table 3. and description for determination of E_a in Results section), All three parameters A, n, and E_a, are fit over the temperature range of 300 to2000K.

Table 1.10 Input Parameters[a] and High - Pressure Limit Rate Constants $(K_\infty)^b$ for QRRK Calculations[c] and the Resulting Rate Constants (Temp=298 K) : G2 Result (Adjusted)

Input parameters for QRRK Calculations

High - Pressure Limit Rate Constants

k_∞

	Reaction	$A(S^{-1}$ or $cm^3/(mol\ s)$	n	E_a (kcal/mol)
1	$CH_3OC\bullet H_2 + O_2 \Rightarrow CH_3OCH_2OO\bullet$ [d]	4.82E+12	0.00	0.0
-1	$CH_3OCH_2OO\bullet \Rightarrow CH_3OC\bullet H_2 + O_2$ [e]	1.78+15	0.00	34.0
2	$CH_3OCH_2OO\bullet \Rightarrow C\bullet H_2OCH_2OOH$ [f]	9.35E+4	2.03	19.1
3	$C\bullet H_2OCH_2OOH \Rightarrow CH_2O + CH_2O + OH$ [g]	5.98E+12	0.66	21.4

Calculated Reaction Parameters at P=1atm, $k=A(T/K)^n(-E_a/RT)$ (Temp=200-2000K)

	Reaction	A	n	E_a (kcal/mol)	k_{298} (s^{-1} or $cm^3/(mol\ s)$
1	$CH_3OC\bullet H_2 + O_2 \Rightarrow CH_3OCH_2OO\bullet$	3.10E+65	-17.59	12.53	6.03E+12
3	$CH_3OC\bullet H_2 + O_2 \Rightarrow CH_2O + CH_2O + OH$	5.51E+24	-3.89	6.80	1.35E+10
4	$CH_3OCH_2OO\bullet \Rightarrow C\bullet H_2OCH_2OOH$	1.97E+23	-3.96	23.85	1.03E-04
5	$C\bullet H_2OCH_2OOH \Rightarrow CH_2O + CH_2O + OH$	1.00E+10	0.64	17.54	5.28E-02

[a] Geometric mean frequency (from CPFIT, ref.[29] : 410.5cm^{-1} (7.757); 1345.3cm^{-1} (9.762); 3257.9cm^{-1} (4.981). Lennard-Jones parameters: σ_{ij}=5.54Å, ϵ/k=460. [b] The units of A factors and rate constants k are s^{-1} for unimolecular reactions and cm^3/(mol s) for bimolecular reactions. [c] ΔE down of 400 cal/mol is used. [d] $k_{\infty,1}$: Atkinson et al., [30]. [e] $k_{\infty,-1}$: MR. [f] A_2 is calculated using TST and entropy of transition state (TS1), $\Delta S^{\neq}_{298}$ from MP2(full)/6-31G(d,p) (see Table 1.), E_a from CBS-q calculation (see Table 3. and description for determination of E_a in Results section), All three parameters A, n, and E_a are fit over the temperature range of 300 to2,000K. [g] A_3 is calculated using TST and entropy of transition state (TS1), $\Delta S^{\neq}_{298}$ from MP2(full)/6-31G(d,p) (see Table 1.), E_a from CBS-q calculation (see Table 3. and description for determination of E_a in Results section), All three parameters A, n, and E_a are fit over the temperature range of 300 to2000K.

1.4 Summary

Thermodynamic properties of stable radicals and transition state are calculated using *ab initio* methods. $H_f°_{298}$'s are derived from 2 methods, CBS-q and G2 calculations. CBS-q calculations are performed based on MP2(full)/6-31G(d,p) optimized geometries and frequencies, and G2 calculations are performed based on MP2(full)/6-31G(d) optimized

geometries and HF/6-31G(d) optimized frequencies. ZPVE's and thermal corrections are taken into account with scaled frequencies. Isodesmic reactions are adopted to estimate the $\Delta H_f°_{298}$. $S°_{298}$ and $C_p(T)$'s are also determined by two methods. MP2(full)/6-31G(d,p) determined geometries and frequencies are used for $S°_{298}$ and $C_p(T)$ calculations and composed the thermodynamic properties with CBS-q determined $\Delta H_f°_{298}$. Hf/6-31G(d) determined frequencies and MP2(full)/6-31G(d) determined geometries are used for $S°_{298}$ and $C_p(T)$ calculations and composed the thermodynamic properties with G2 determined $\Delta H_f°_{298}$.

CH$_2$O formation based on both methods are compared with experimental data to evaluate thermodynamic properties derived from the calculation methods. Data from both levels of theory show good agreement. Activation energy for TS1 based on G2 calculation gives 4.2 kcal/mol lower energy than that of CBS-q calculations. Activation energy for TS2 based on both CBS-q and G2 calculations give similar activation energies. Reaction pathways and kinetics are analyzed on the CH$_3$OC•H$_2$ + O$_2$ reaction system using Quantum Rice-Ramsperger-Kassel (QRRK) for k(E) and master equation for fall off. CH$_2$O formation as a function of pressure at room temperature from data by the two calculation methods is compared with experiment, and a reduction of the E_a for TS2 by 3.3 and 4.0 kcal/mol is needed for CBS-q and G2 calculations respectively to match the experimental data. All steps in the chain propagation reaction CH$_3$OC•H$_2$ + O$_2$ → 2 CH$_2$O + OH have barriers below the $\Delta H_f°_{298}$ of the reactants.

CHAPTER 2

DIMETHYL-ETHER OXIDATION AND PYROLYSIS: OVERALL REACTION MECHANISM

2.1 Introduction

Reaction pathways and kinetics on $CH_3OC \bullet H_2 + O_2$ are analyzed in the previous chapter

using the thermodynamic properties derived by the composite *ab initio* calculation

methods, CBS-q and G2. To complete the reaction mechanism on dimethyl-ether

oxidation and pyrolysis, the following reactions are discussed in this chapter.

1. $C \bullet H_2OCH_2OOH + O_2$ and subsequent reactions.

2. Initiation reactions: H atom abstraction by the major radicals OH, HO_2, CH_3, $CH_3O \bullet$,

    O and H atom and O_2 from dimethyl-ether molecule.

3. Dimethyl-ether and dimethyl-ether radical dissociation reactions.

QRRK analysis is used to calculate energy dependent rate constants, k(E), as

expressed in Chapter 1. Modified strong collision approach of Gilbert et al.[19] for fall-off

is used to calculate rate constants over a range of temperature and pressure.

2.2 Method

2.2.1 Thermodynamic Properties ($\Delta H_{f\,298}^\circ$, S_{298}° and $C_p(T)$'s $300 \le T/K \le 1500$)

Thermodynamic properties for stable molecules are calculated using group additivity

$(GA)^{13,31}$ and THERM computer code[31]. The thermodynamic properties of free radical

species $(R \bullet)$ are determined using thermodynamic data of their corresponding parent

molecules (RH) and the hydrogen-atom-bond-increment (HBI) methods[28].

Enthalpies of formation ($\Delta H_f^\circ{}_{298}$ in kcal/mol) for TS's are estimated by $\Delta H_f^\circ{}_{298}$ of

reactant plus the difference of $\Delta H_f^\circ{}_{298}$ between TS and reactant derived by semiempirical

molecular orbital (MO) method PM3[32] in the MOPAC 6.0[33].

$\Delta H_f^\circ{}_{298,TS} = \Delta H_f^\circ{}_{298,reactant}$ (derived by THERM) + ($\Delta H_f^\circ{}_{298,TS}$ (derived by MOPAC) –

$\Delta H_f^\circ{}_{298,\,reactant}$ (derived by MOPAC)) $\times$ 0.8   --------- (1)

The activation energies estimated using MOPAC consistently overestimate the value.

The scaling factor of 0.8 gives a more accurate value. The correlation between PM3-

determined $\Delta H_f^\circ{}_{298}$ and experimentally determined $\Delta H_f^\circ{}_{298}$ on the series of monocyclic

and bicyclic hydrocarbons and oxyhydrocarbons is derived and explained in Chapter 5 as

expressed: $\Delta H_f^\circ{}_{298,expt} = -1.642 + 0.882 \times \Delta H_f^\circ{}_{298,\,PM3}$.

Entropy ($S^\circ{}_{298}$ in cal/mol-K) and heat capacities ($C_p(T)$'s in cal/mol-K) for TS's are

calculated using PM3[32]. Contribution of internal rotational to $S^\circ{}_{298}$ and $C_p(T)$'s are

calculated separately based on rotational barrier height and moments of inertia. Pitzer et

al.'s[10] general treatment of internal rotation is used to calculate the hindered internal

rotation contribution to $S^\circ{}_{298}$ and $C_p(T)$'s.

2.2.2 High-pressure Limit A Factors (A_∞) and Rate Constant (k_∞) Determination with Semi-empirical Calculations for Transition State Compounds

For the reactions where thermodynamic properties of transition states are calculated by

semi-empirical and *ab initio* methods , k_∞'s are expressed by

$$k_\infty = A_\infty(T)^n \exp(-E_{a,\infty}/RT). \qquad \text{---------- (2)}$$

High-pressure limit A factors (A_∞) of unimolecular reactions are calculated using

conventional transition state theory (TST)[13]. Semi-empirical and *ab initio* data for the

determination of the structure, vibrational and rotational contributions to $S°_{298}$ of

transition states, loss

(or gain) of internal rotors and change of optical isomer and symmetry numbers are

incorporated into the calculation of $S°_{298}$ for each TS. $S°_{298}$'s of reactants and TSs are

then used to determine the pre-exponential factor, A, via TST[13] for a unimolecular

reaction

$$A=(k_pT/h_b)exp(\Delta S^{\neq}) \qquad ---------(3)$$

where h_p is Plank's constant, k_b is the Boltzmann constant and $\Delta S^{\neq}$ is equal to $S°_{298,TS}$ -

$S°_{298,reactant}$.

Activation energies of reactions are calculated as follows:

$$E_a =\{\Delta H_f°_{298,TS} - \Delta H_f°_{298,reactant}\} \qquad ---------(4)$$

2.2.3 Kinetic Modeling

A kinetic modeling consisting of the $C\bullet H_2OCH_2OOH + O_2$ and subsequent reactions,

initiation reaction and unimolecular decomposition reactions are developed and explained

in this chapter. The $C\bullet H_2OCH_2OOH + O_2$ and subsequent reactions consist of:

i) $C\bullet H_2OCH_2OOH + O_2 \Rightarrow CH_2(OO\bullet)OCH_2OOH \Rightarrow$ Products

ii) $CH_2(OO\bullet)OCH_2(O\bullet) \Rightarrow$ Products

iii) $CH_2(OO\bullet)OCHO \Rightarrow CH2(OOH)C\bullet O \Rightarrow$ Products

iv) $CH_2O\bullet(OO\bullet) \Rightarrow CHO(OOH) \Rightarrow$ Products

v)   cy $\overline{CH_2OC\bullet HO} \Rightarrow C\bullet H2OCHO \Rightarrow$ Products

Initiation reactions consist of:

i) $CH_3OCH_3 + H \Rightarrow C\bullet H_2OCH_3 + H2$

ii) $CH_3OCH_3 + O \Rightarrow C\bullet H_2OCH_3 + OH$

iii) $CH_3OCH_3 + OH \Rightarrow C\bullet H_2OCH_3 + H_2O$

iv) $CH_3OCH_3 + HO_2 \Rightarrow C\bullet H_2OCH_3 + H_2O_2$

v) $CH_3OCH_3 + CH_3 \Rightarrow C\bullet H_2OCH_3 + CH_4$

vi) $CH_3OCH_3 + CH_3O\bullet \Rightarrow C\bullet H_2OCH_3 + CH_3OH$

vii) $CH_3OCH_3 + O_2 \Rightarrow C\bullet H_2OCH_3 + HO_2$

Dimethyl-ether parent and radical unimolecular dissociation reactions consist of:

i) $CH_3OCH_3 \Rightarrow CH_3O\bullet + CH_3$

ii) $CH_3OCH_3 \Rightarrow CH_2O + CH_4$

iii) $CH_3OCH_3 \Rightarrow C\bullet H_2OCH_3 + H$

iv) $C\bullet H_2OCH_3 \Rightarrow CH_2O + CH_3$

The overall dimethyl-ether kinetic modeling is constructed with above reaction mechanisms plus dimethyl-ether radical + O_2 reaction system, which is discussed in the previous chapter. CBS-q//MP2(full)/6-31G(d,p) results are chosen for the dimethyl-ether + O_2 reaction system. Elementary methane, ethane and methanol reaction mechanisms developed by Ing[34] comprise the remaining detailed mechanism. The detailed mechanism is presented in Table A.

2.2.4 Rate Constant Calculations for H atom Abstraction Reaction (Dimethyl-ether Radical Formation)

The hydrogen atom abstraction reaction scheme reported by Dean et al. is used to determine A, n and E_a[35] for H atom abstraction from dimethyl-ether by H, O, OH and CH_3.

$$k = n_H \, A \, T^n \exp(-\{E_0 - f(\Delta H_0 - \Delta H\}/RT) \, cm^3/(mole\text{-}sec)$$

where n_H : number of hydrogen atom, $R = 1.987$ cal/mol.

A, n, E_0, ΔH_0 and f depend on the radical species and are tabulated in Table 2.15.

2.2.5 Rate Constant Calculation for Dimethyl-ether Parent and Radical Unimolecular Dissociation

Arrhenius A factor for dimethyl-ether unimolecular dissociation reactions, $CH_3OCH_3 \Rightarrow CH_3 + CH_3O$ and $CH_3OCH_3 \Rightarrow C\bullet H_2OCH_3 + H$, are estimated from reverse reaction and microscopic reversibility (MR) along with QRRK analysis. Rate constant calculation for the disproportionation reaction $CH_3OCH_3 \Rightarrow CH_2O + CH_4$ through cyclic transition state formation where hydrogen atom moves from the carbon where the carbonyl bond is forming to the second carbon is estimated by thermodynamic properties of reactant, CH_3OCH_3 and the TS, which is estimated by Nash et al.[36].

Rate constant calculation for the important unimolecular dissociation reaction $C\bullet H_2OCH_3 \Rightarrow CH_2O + CH_3$ is estimated using thermodynamic properties determined by CBS-q//MP2(full)/6-31G(d,p) level of calculation.

2.3 Results and Discussion

2.3.1 Thermodynamic Properties ($\Delta H_f^\circ{}_{298}$, $S^\circ{}_{298}$ and ($C_p(T)$ (300 ≤ T/K ≤ 1500))

Thermodynamic properties ($\Delta H_f^\circ{}_{298}$, $S^\circ{}_{298}$ and ($C_p(T)$ (300 ≤ T/K ≤ 1500)) estimated by

use of THERM computer code[31], PM3[32] and *ab initio* methods are tabulated in Table

2.1, 2.2 (a) and 2.2 (b) respectively. TVR represents the sum of the contributions from

translations, external rotations and vibrations for entropy and heat capacities in Table 2.2

(a) and 2.2 (b).

2.3.2 C•H$_2$OCH$_2$OOH + O$_2$ Reaction System

High Pressure Limit Rate Constant as QRRK Input Parameters.

The potential energy diagram for the reaction C• H$_2$OCH$_2$OOH + O$_2$ ⇒

CH$_2$(OO•)OCH$_2$OOH adduct is illustrated in Figure 2.1.

$$k_5$$
i) C• H$_2$OCH$_2$OOH + O$_2$ ⇒ CH$_2$(OO•)OCH$_2$OOH
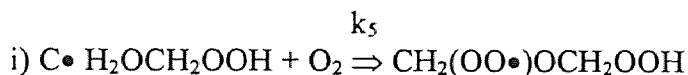
The well depth for O$_2$ addition to the radical is 35.7 kcal/mol. High pressure limit rate

constant has no barrier and A$_5$ is estimated as 4.82E+12 cm^3/(mol s), which is adopted

from Atkinson et al.'s study for n-C$_2$H$_7$ + O$_2$ ⇒ C$_3$H$_7$O$_2$•[30]. The reverse rate constant

k$_{-5}$ is calculated via the principle of MR, resulting in A$_{-5}$ = 1.78E+15 s^{-1} with E$_{a,-5}$ = 35.1

kcal/mol. This radical either isomerizes to form CH$_2$(OOH)OC•H(OOH) through a

hydrogen atom transfer or dissociates to form the diradical CH$_2$(OO•)OCH$_2$O• + OH.

$$k_6$$
ii) CH$_2$(OO•)OCH$_2$OOH ⇒ CH$_2$(OOH)OC.HOOH
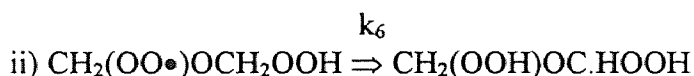
High pressure limit A$_{\infty,6}$ and E$_{a,6}$ activation energy along with those for reverse reaction

are estimated as 1.10+E7 s^{-1}, 17.1 kcal/mol, 4.88E+7 s^{-1} and 9.3 kcal/mol respectively.

Table 2.1 Thermodynamic Properties (ΔH°f 298, S°298, and Cp(T)'s (300 ≤ T/K ≤ 1500)) Used in Dimethyl-ether Oxidation Mechanism[a]

SPECIES	H°f 298	S°298	Cp 300	Cp 400	Cp 500	Cp 600	Cp 800	Cp 1000	Cp 1500	Reference	Elements	Phase
AA	0.00	66.85	15.29	17.95	20.30	22.33	25.55	28.07	30.59	THERM	C 1 H 4 N 2	G
BB	-9.50	35.30	10.49	12.34	14.22	16.02	19.05	21.38	25.01	THERM	C 1 H 3 N 1	G
*AR	0.00	36.98	4.97	4.97	4.97	4.97	4.97	4.97	4.97	L 5/66	AR 1	G
*N2	0.0	45.77	6.95	7.01	7.08	7.19	7.50	7.83	8.32	SAND	N 2	G
*O2	0.00	49.01	7.02	7.23	7.44	7.65	8.04	8.35	8.73	JANAF	O 2	G
*H	52.10	27.36	4.97	4.97	4.97	4.97	4.97	4.97	4.97	JANAF	H 1	G
*H2	0.00	31.21	6.90	6.95	6.99	7.02	7.10	7.21	7.72	JANAF	H 2	G
*O	59.55	38.47	5.23	5.14	5.08	5.04	5.01	5.01	4.98	JANAF	O 1	G
*OH	9.49	43.88	7.15	7.10	7.07	7.06	7.13	7.33	7.87	JANAF	H 1 O 1	G
H2O	-57.80	45.10	8.02	8.19	8.41	8.66	9.24	9.85	11.23	BSN	H 2 O 1	G
HO2	3.80	54.73	8.37	8.95	9.48	9.96	10.78	11.43	12.47	JANAF	H 1 O 2	G
H2O2	-32.53	55.66	10.41	11.48	12.37	13.11	14.26	15.14	16.84	JANAF	H 2 O 2	G
O3	34.10	57.09	9.42	10.44	11.27	11.91	12.74	13.15	13.67	SANDI	O 3	G
*NO	21.58	50.35	7.11	7.19	7.31	7.45	7.82	8.14	8.54	SANDI	O 1 N 1	G
NO2	7.91	57.34	8.83	9.64	10.33	10.93	11.89	12.49	13.17	SANDI	O 2 N 1	G
*CO	-26.42	47.21	6.96	7.02	7.13	7.27	7.61	7.94	8.41	JANAF	C 1 O 1	G
CO2	-94.05	51.07	8.90	9.85	10.65	11.31	12.30	12.97	13.93	JANAF	C 1 O 2	G
*C(S)	0.00	21.83	4.00	4.00	4.00	4.00	4.00	4.00	4.00	JANAF	C 1	S
*C	170.89	38.31	4.97	4.97	4.97	4.97	4.97	4.97	4.97	JANAF	C 1	G
*CH	142.00	43.72	6.97	6.97	7.03	7.12	7.41	7.77	8.74	JANAF	C 1 H 1	G
CH3	35.2	46.38	9.26	10.05	10.81	11.54	12.90	14.09	16.26	JANAF	C 1 H 3	G
CH2	92.35	46.32	8.28	8.62	8.99	9.37	10.15	10.88	12.22	JEFF	C 1 H 2	G
CH2S	101.45	44.15	8.33	8.77	9.21	9.64	10.45	11.16	12.47	JEFF	C 1 H 2	G
CH4	-17.90	44.48	8.51	9.77	11.10	12.44	15.00	17.20	20.61	JANAF	C 1 H 4	G
HC.O	10.40	53.60	8.20	8.70	9.20	9.70	10.70	11.50	12.50	EST	C 1 H 1 O 1	G
CH2O	-27.70	52.29	8.47	9.38	10.46	11.52	13.37	14.81	16.25	STULL	C 1 H 2 O 1	G
CH2O.O.	51.37	60.67	14.18	16.50	18.15	19.44	21.32	22.77	24.22	THERM	C 1 H 2 O 2	G
C.H2OH	-2.60	56.73	10.91	12.68	14.13	15.42	17.51	19.10	20.69	THERM	C 1 H 3 O 1	G
CH2OHO.	-39.07	66.10	13.12	14.65	16.28	17.92	20.73	22.76		10/25/96	C 1 H 3 O 2	G
C.H2Q	14.80	68.23	15.76	18.08	20.06	21.79	24.03	25.54	27.62	3/12/97 DBASE	C 1 H 3 O 2	G
CH2OHQ	-75.46	74.85	18.91	21.48	23.84	26.08	29.56	32.36	.00	11/25/96 THERM	C 1 H 4 O 3	G
CH2OHQ.	-40.36	76.80	16.86	18.64	20.29	21.99	24.84	27.39	.00	10/25/96	C 1 H 3 O 3	G
CH2O.Q	-23.50	73.39	17.93	20.18	22.23	24.19	27.18	29.56	.00	11/25/96 THERM	C 1 H 3 O 3	G
CH2O.Q.	12.60	73.61	15.88	17.34	18.68	20.10	22.46	24.59	.00	11/25/96	C 1 H 2 O 3	G
CH3O.	3.96	54.27	8.55	10.26	11.96	13.59	16.29	18.30	20.31	THERM	C 1 H 3 O 1	G
CH3OH	-48.00	57.30	10.49	12.34	14.22	16.02	19.05	21.38	25.01	THERM	C 1 H 4 O 1	G
CH3Q.	-4.97	62.08	13.70	16.12	18.22	20.03	22.86	25.04	27.22	THERM	C 1 H 3 O 2	G

[a] Thermodynamic properties are referred to a standard state of an ideal gas of pure enantiometer at 1 atm.
[b] In kcal/mol. [c] In cal/(mol K).

Table 2.1 Thermodynamic Properties ($\Delta H_{f,298}^{\circ}$, S_{298}°, and $C_p(T)$'s ($300 \leq T/K \leq 1500$)) Used in Dimethyl-ether Oxidation Mechanism (cont'd)

SPECIES	$H_{f,298}^{\circ}$	S_{298}°	C_p 300	C_p 400	C_p 500	C_p 600	C_p 800	C_p 1000	C_p 1500	Source	C	H	O	N	G
C.H2Q	15.27	65.44	15.77	18.33	20.23	21.74	24.01	25.80	27.59	THERM	1	3	2	0	2
CH3Q	-31.13	66.85	15.29	17.95	20.30	22.33	25.55	28.07	30.59	THERM	1	4	2	0	2
HOC.O	-46.29	60.12	10.78	12.19	13.34	14.29	15.67	16.57	17.70	SAND	1	1	2	0	1
O.CHO	-38.24	57.94	9.85	11.57	13.01	14.09	16.02	17.20	.00	9/ 9/96	1	1	2	0	0
HCOQ	-67.40	73.86	15.27	17.67	19.67	21.26	23.83	25.48	.00	12/23/96 THERM	1	2	3	0	2
HCOQ.	-31.30	74.08	13.22	14.83	16.12	17.17	19.11	20.51	.00	10/25/96	1	1	3	0	1
C.QOH	-32.56	80.40	19.05	20.64	22.18	23.78	26.38	28.57	.00	10/25/96	1	3	3	0	3
HOC.HOO.T	-13.00	77.58	17.19	18.34	19.27	20.32	22.17	24.00	.00	10/25/96	1	2	3	0	2
O.HC.OOHT	17.40	73.14	18.26	19.88	21.21	22.52	24.51	26.17	.00	10/25/96	1	2	3	0	2
HC*OOH	-90.20	59.40	10.83	12.87	14.62	15.98	18.40	20.00	.00	10/25/96	1	2	2	0	1
HOCHO.O	-31.01	72.22	15.48	16.90	18.41	19.96	22.61	24.28	.00	10/25/96	1	2	3	0	1
CH2O.Q	-23.50	73.39	17.93	20.18	22.23	24.19	27.18	29.56	.00	2/ 6/97	1	3	3	0	2
HC.QOH	-32.56	80.40	19.05	20.64	22.18	23.78	26.38	28.57	.00	10/25/96	1	2	3	0	3
HCOH	22.56	58.19	10.79	11.97	12.81	13.58	14.84	15.81	17.26	10/25/96	1	2	2	0	1
CH3NO	18.95	63.48	12.05	14.19	16.11	17.84	20.73	22.98	36.33	SAND	1	3	1	1	1
CH3NO2	-16.84	72.04	13.45	16.60	19.28	21.58	25.21	27.88	31.75	SAND	1	3	2	1	1
CH3ONO	-15.60	66.88	15.43	18.38	20.86	22.96	26.25	28.66	32.29	SAND	1	3	2	1	2
CH3ONO2	-28.60	71.64	17.72	21.48	24.62	27.24	31.23	34.02	37.81	SAND	1	3	3	1	2
COCQ	-70.86	84.07	24.20	28.52	32.12	35.44	40.97	45.12	.00	5/ 5/96 THERM	2	6	3	0	4
COCQ.	-33.9	83.10	21.34	25.59	29.30	32.35	37.00	40.36	45.51	3/11/98 CBS-q	2	5	3	0	3
C.OCQ	-26.5	88.02	22.99	27.56	31.38	34.33	38.43	41.20	45.41	3/11/98 CBS-q	2	5	3	0	4
COCHO	-84.39	71.53	17.13	20.02	22.82	25.31	29.55	32.77	.00	9/ 9/96 THERM	2	4	2	0	2
C.OCHO	-39.99	73.67	17.65	19.94	22.02	23.86	27.05	29.50	.00	9/ 9/96 THERM	2	3	2	0	3
COHOCHO	-127.42	81.79	20.74	23.63	26.49	29.10	33.61	36.95	.00	9/ 9/96 THERM	2	4	3	0	3
CO.OCHO	-75.46	80.33	19.76	22.33	24.88	27.21	31.23	34.15	.00	9/ 9/96 THERM	2	3	3	0	3
COC	-43.99	63.83	15.79	19.02	22.23	25.16	30.04	33.79	.00	7/23/98 Stull	2	6	1	0	2
CQOCQ	-98.32	101.62	32.62	37.66	41.74	45.50	51.48	56.10	.00	9/12/96 THERM	2	6	5	0	6
CQ.OCQ	-62.22	103.22	30.57	34.82	38.19	41.41	46.76	51.13	.00	9/12/96 THERM	2	5	5	0	5
CQOCHO	-111.85	90.46	25.55	29.16	32.44	35.37	40.06	43.75	.00	9/12/96 THERM	2	4	4	0	4
CQOCOH	-113.89	94.33	27.81	32.13	35.79	39.23	45.03	49.30	.00	9/12/96 THERM	2	6	4	0	5
CQOCO.	-61.93	92.87	26.83	30.83	34.18	37.34	42.65	46.50	.00	9/12/96 THERM	2	5	4	0	4
CQ.OCO.	-25.83	93.09	24.78	27.99	30.63	33.25	37.93	41.53	.00	9/12/96	2	4	4	0	4
CQOC.Q	-53.92	104.34	33.14	37.58	40.94	44.05	48.98	52.83	.00	9/12/96	2	5	5	0	5
COC.	0.1	67.67	14.79	17.88	20.74	23.20	27.13	30.10	34.84	7/23/98 Stull	2	5	1	0	2
COCOH	-86.43	75.40	19.39	22.99	26.17	29.17	34.52	38.32	.00	3/11/98 CBS-q	2	6	2	0	3
C.OCOH	-42.03	77.54	19.91	22.91	25.37	27.72	32.02	35.05	.00	9/19/96 THERM	2	5	2	0	3
C.OCO.	9.93	76.08	18.93	21.61	23.76	25.83	29.64	32.25	.00	9/19/96	2	4	2	0	2

Table 2.1 Thermodynamic Properties (ΔHf°298, S°298, and Cp(T)'s (300 ≤ T/K ≤ 1500)) Used in Dimethyl-ether Oxidation Mechanism (cont'd)

SPECIES	$H_f°_{298}$	$S°_{298}$	$C_{p}300$	$C_{p}400$	$C_{p}500$	$C_{p}600$	$C_{p}800$	$C_{p}1000$	$C_{p}1500$	Reference	C	H	O	N	G
CYCOCO	-57.24	64.10	14.00	18.30	22.20	25.30	29.90	33.10	37.70	12/02/96 Lay	2	4	2	0	G
COCH	-86.43	75.40	19.39	22.99	26.17	29.17	34.52	38.32	.00	12/16/96 THERM	2	6	2	0	G
COCO.	-34.47	73.94	18.41	21.69	24.56	27.28	32.14	35.52	.00	12/16/96 THERM	2	5	2	0	G
CQ.OCHO	-75.75	90.68	23.50	26.32	28.89	31.28	35.34	38.78	.00	2/ 4/97	2	3	4	0	G
CQOC.*O	-74.95	91.58	24.72	27.73	30.48	32.95	36.90	40.02	.00	2/ 6/97	2	3	4	0	G
COCC.	-2.60	78.35	20.00	24.87	28.89	32.41	38.40	42.73	.00	3/ 8/97 DBASE	2	7	1	0	G
HCOOCHO	-95.92	78.68	17.26	19.57	21.73	23.61	26.58	28.72	31.85	3/14/97 MOP+VIB	2	2	3	0	G
CQOC.Q.	-13.22	105.83	29.80	33.46	36.28	39.01	43.60	47.39	.00	3/16/97	2	4	5	0	G
COCOONO	-42.66	98.14	28.09	33.10	37.15	40.78	47.12	51.21	.00	5/ 8/96 THERM	2	5	4	1	G
CC	-20.40	55.00	12.38	15.68	18.80	21.58	26.04	29.54	35.16	3/ 7/97 THERM	2	6	0	0	G
HOC*C*O	-53.87	66.89	16.65	19.25	21.68	22.88	24.55	25.88	27.74	3/11/97 THERM	2	1	2	0	G
O.C*C*O	-1.91	65.43	15.67	17.95	20.07	20.99	22.17	23.08	24.15	3/11/97 THERM	2	2	2	0	G
CQ*C*O	-30.63	77.11	21.06	24.34	26.98	28.46	30.41	31.77	.00	3/11/97 THERM	2	2	3	0	G
CQ.*C*O	5.47	77.33	19.01	21.50	23.43	24.37	25.69	26.80	.00	3/11/97 THERM	2	1	3	0	G
CCOQ	-67.51	76.01	21.40	24.57	27.57	30.31	34.36	37.54	.00	3/12/97 THERM	2	4	3	0	G
C.COQ	-18.51	79.42	20.63	23.21	25.66	27.91	31.20	33.80	.00	3/12/97 THERM	2	3	3	0	G
COOQ.	-44.38	77.45	18.48	21.50	24.10	26.30	29.80	32.44	.00	3/12/97 DBASE	2	3	3	0	G
C*C	12.52	52.47	10.20	12.72	15.02	17.00	20.14	22.54	.00	3/ 8/97 TAK	2	4	0	0	G
C*C.	71.62	56.61	10.01	11.97	13.66	15.08	17.32	19.05	21.85	3/ 6/97 Jeff	2	3	0	0	G
CDCOH	-29.46	59.86	13.68	16.84	19.56	21.81	25.27	27.81	31.84	3/**/98 CBS-q	2	4	1	0	G
CCOH	-56.20	67.10	15.48	19.19	22.52	25.45	30.15	33.71	.00	3/ 6/97 BOZ	2	6	1	0	G
CC.	28.60	59.78	11.61	14.32	16.86	19.18	22.88	25.80	30.50	3/ 6/97 BOZ	2	5	0	0	G
C*C*O	-11.74	57.82	12.70	14.65	16.73	17.80	19.50	20.98	23.03	3/ 8/97 DBASE	2	2	1	0	G
C.*C*O	41.36	60.49	12.25	13.60	15.09	15.65	16.52	17.38	18.45	3/ 8/97 DBASE	2	1	1	0	G
CO.CO.	11.92	74.81	16.62	20.10	23.02	25.54	29.50	32.28	.00	6/ 8/96	2	4	2	0	G
CHOCHO	-21.54	73.48	16.55	18.77	20.73	22.52	25.94	28.21	.00	6/ 8/96	2	3	2	0	G
CQ.CHO	-50.60	66.79	14.90	17.54	19.64	21.40	24.28	25.80	.00	6/ 8/96 THERM	2	2	3	0	G
COHCOONO	-23.43	82.66	19.08	21.91	24.34	26.52	30.06	32.97	.00	6/ 8/96	2	5	4	1	G
CO.COONO	-48.23	100.48	27.28	32.81	37.22	40.93	46.86	50.77	.00	6/ 8/96 THERM	2	4	4	1	G
CHOCOONO	3.73	99.02	26.30	31.51	35.61	39.04	44.48	47.97	.00	6/ 8/96 THERM	2	3	4	1	G
C2H	-31.33	96.51	25.02	29.33	32.92	35.95	40.93	44.03	.00	6/ 8/96 THERM	2	1	0	0	G
C2H2	134.46	51.51	10.05	10.42	10.71	10.96	11.47	11.95	12.92	10/25/96	2	2	0	0	G
COHCQ.	53.86	48.02	10.56	11.98	12.98	13.74	14.94	15.92	17.70	10/25/96	2	5	3	0	G
C.*C*O	-41.33	86.98	21.34	25.39	28.64	31.50	35.99	39.71	.00	10/25/96	2	1	1	0	G
C.COH	41.36	60.49	12.25	13.60	15.09	15.65	16.52	17.38	18.45	10/25/96	2	5	1	0	G
CCO.	-7.20	70.51	14.71	17.83	20.61	23.05	26.99	29.97	.00	10/25/96	2	5	1	0	G
CC.OH	-4.24	65.64	14.50	17.89	20.91	23.56	27.77	30.91	.00	10/25/96	2	5	1	0	G
CC.OH	-14.30	67.88	15.81	18.89	21.50	23.78	27.48	30.32	.00	10/25/96	2	5	1	0	G

Table 2.1 Thermodynamic Properties ($\Delta H_{f\ 298}^{\circ}$, $S^{\circ}_{\ 298}$, and $C_p(T)$'s ($300 \le T/K \le 1500$)) Used in Dimethyl-ether Oxidation Mechanism (cont'd)

SPECIES	$H_{f\ 298}^{\circ}$	$S^{\circ}_{\ 298}$	$C_{p\ 300}$	$C_{p\ 400}$	$C_{p\ 500}$	$C_{p\ 600}$	$C_{p\ 800}$	$C_{p\ 1000}$	$C_{p\ 1500}$	Ref / Date	ELEMENTS (C H O N G)
CCQ.	-5.53	76.34	18.24	21.88	24.92	27.63	31.88	35.54	.00	10/25/96	C 2 H 5 O 2 N 0 G 2
CC.Q	2.27	79.94	20.43	23.88	26.81	29.42	33.42	36.72	.00	10/25/96	C 2 H 5 O 2 N 0 G 3
CCQ	-41.63	76.12	20.29	24.72	28.47	31.72	36.60	40.51	.00	10/25/96	C 2 H 6 O 2 N 0 G 3
C.CQ	6.87	79.53	19.52	23.36	26.56	29.32	33.44	36.77	.00	10/25/96	C 2 H 5 O 2 N 0 G 3
CCHO	-39.18	63.13	13.22	15.71	18.22	20.47	24.22	26.97	.00	10/25/96	C 2 H 4 O 1 N 0 G 1
CC.*O	-2.28	64.25	12.39	14.28	16.26	18.05	21.06	23.24	.00	10/25/96	C 2 H 3 O 1 N 0 G 1
CCO.Q	-35.47	81.86	23.87	28.17	32.19	35.18	39.44	43.04	.00	10/25/96	C 2 H 5 O 3 N 0 G 3
C.OHCQ	-35.53	87.54	23.72	27.93	31.17	33.92	38.04	41.29	.00	10/25/96	C 2 H 5 O 3 N 0 G 3
CO.CQ	-25.47	85.30	22.41	26.93	30.58	33.70	38.33	41.88	.00	10/25/96	C 2 H 5 O 2 N 0 G 2
CCQ.OH	-51.38	83.54	22.80	26.63	30.25	32.98	37.10	40.87	.00	10/25/96	C 2 H 5 O 3 N 0 G 3
C*COH	-29.61	62.91	14.15	17.32	19.97	22.08	25.19	27.44	31.09	10/25/96	C 2 H 4 O 1 N 0 G 1
C.CHO	3.12	60.40	12.92	15.31	17.44	19.24	22.10	24.12	.00	10/25/96	C 2 H 3 O 1 N 0 G 1
CYCCO	-8.81	58.14	11.58	15.09	18.25	20.85	24.78	27.60	31.88	3/16/97 LAY	C 2 H 4 O 1 N 0 G 0
CYC.CO	30.32	57.87	10.70	13.75	16.02	17.94	21.48	24.06	.00	7/21/93	C 2 H 3 O 1 N 0 G 0
CYC.OCO	30.32	57.87	10.70	13.75	16.02	17.94	21.48	24.06	.00	7/21/93	C 2 H 3 O 2 N 0 G 0
C*C.Q	50.53	74.94	18.22	21.20	23.33	25.14	27.71	29.42	.00	10/25/96	C 2 H 3 O 2 N 0 G 2
CC*OO.	-51.38	63.56	14.78	17.67	20.28	22.42	25.81	28.19	.00	10/25/96	C 2 H 3 O 2 N 0 G 1
COHCHO	-73.50	73.57	17.53	20.07	22.34	24.41	28.32	31.01	.00	9/19/96 THERM	C 2 H 4 O 2 N 0 G 2
CCC.	23.67	69.29	17.11	21.27	25.14	28.53	33.95	38.14	44.70	3/15/96	C 3 H 7 O 0 N 0 G 2
CCC	-25.33	64.50	17.88	22.63	27.05	30.93	37.11	41.88	49.36	3/15/96	C 3 H 8 O 0 N 0 G 2
COCOC	-81.83	81.86	24.68	30.03	34.45	38.53	45.93	51.08	.00	3/16/97 THERM	C 3 H 8 O 2 N 0 G 4
COCOC.	-32.83	85.27	23.91	28.67	32.54	36.13	42.77	47.34	.00	3/16/97 THERM	C 3 H 7 O 2 N 0 G 4
COC.Q	-26.46	85.41	24.72	28.44	31.32	33.99	38.47	41.85	.00	3/23/97	C 3 H 7 O 3 N 0 G 4
COC.OH	-42.03	76.33	20.67	23.92	26.37	28.62	32.69	35.55	.00	3/23/97	C 3 H 7 O 2 N 0 G 3
HCOOCHO	-87.40	77.10	17.46	19.44	21.34	23.16	26.80	29.00	.00	5/ 3/97 THERM	C 2 H 2 O 3 N 0 G 2
CHOOC.O	-43.00	79.82	17.98	19.36	20.54	21.71	24.30	25.73	.00	5/ 3/97 THERM	C 2 H 3 O 2 N 0 G 2
C.CHO	9.70	66.54	12.45	14.35	16.31	18.07	21.06	23.23	.00	5/ 3/97 THERM	C 2 H 3 O 1 N 0 G 1
CQCHO	-59.53	81.07	21.13	24.75	27.89	30.61	34.08	37.94	.00	5/ 3/97 THERM	C 2 H 4 O 3 N 0 G 3
CQ.CHO	-23.43	81.29	19.08	21.91	24.34	26.52	30.06	32.97	.00	5/ 3/97 THERM	C 2 H 3 O 3 N 0 G 3
CQC.O	-15.13	82.41	21.65	24.67	27.09	29.16	32.28	34.67	.00	5/ 3/97 THERM	C 3 H 5 O 2 N 0 G 2
C*C*O	-11.74	57.82	12.70	14.79	16.46	17.78	19.68	20.96	22.96	9/14/95 BOZDB	C 2 H 2 O 1 N 0 G 0
CCOCHO	-92.59	81.33	22.12	26.87	31.12	34.74	40.65	45.10	.00	5/14/97 THERM	C 3 H 6 O 2 N 0 G 3
C.QOCHO	-43.59	86.12	21.35	25.51	29.21	32.34	37.49	41.36	.00	4/20/98	C 2 H 3 O 4 N 0 G 4
COCC	-51.60	74.93	20.77	26.23	30.80	34.81	41.56	46.47	.00	7/23/98 THERM	C 3 H 8 O 1 N 0 G 3
COCQ	-70.86	84.07	24.20	28.52	32.12	35.44	40.97	45.12	.00	9/ 2/98 THERM	C 3 H 8 O 3 N 0 G 4
CYCOCOJ	-24.51	86.55	23.85	27.92	31.10	33.93	38.52	41.92	.00	9/15/98	C 2 H 3 O 2 N 0 G 0
COCHO	-84.39	71.53	17.13	20.02	22.82	25.31	29.55	32.77	.00	9/15/98 THERM	C 2 H 4 O 2 N 0 G 2
CJOCHO	-35.39	74.94	16.36	18.66	20.91	22.91	26.39	29.03	.00	9/15/98 THERM	C 2 H 3 O 2 N 0 G 2

Table 2.2 (a) Ideal Gas Phase Thermodynamic Properties Using PM3[a]

Species and Symmetry		$H_f°_{298}$	$S°_{298}$[b]	C_{p300}[b]	C_{p400}	C_{p500}	C_{p600}	C_{p800}	C_{p1000}	C_{p1500}
CH₃OC•HOOH	TVR[c]	-47.23	65.03	14.03	17.77	21.43	24.67	29.81	33.59	39.44
(3)	Internal Rotor[d]		22.76	7.65	7.08	6.49	5.99	5.31	4.90	4.43
	Total[f,g]	-47.23	90.55[e]	21.68	24.85	27.92	30.66	35.12	38.49	43.87
tCH3OCHO-OH[h]	TVR	-41.50	65.18	13.95	17.47	20.88	23.87	28.63	32.16	37.70
(3)	Internal Rotor		22.76	7.65	7.08	6.49	5.99	5.31	4.90	4.43
	Total	-41.50	90.70	21.60	24.55	27.37	29.86	33.94	37.06	42.13
CH₂(OO•)OCHO	TVR	-74.13	70.03	16.10	20.27	23.88	26.84	31.20	34.18	38.42
(2)	Internal Rotor		19.02	6.75	6.36	5.85	5.37	4.63	4.16	3.58
	Total	-74.13	89.05	24.23	26.63	29.73	32.21	35.83	38.34	42.00
tyOOCH₂OCHO[i]	TVR	-45.62	75.70	22.19	26.73	30.37	33.21	37.22	39.85	43.43
(2)	Total	-45.62	77.08	22.19	26.73	30.37	33.21	37.22	39.85	43.43
CH₂(OOH)OC•O	TVR	-86.73	70.73	16.24	19.88	23.02	25.60	29.44	32.13	36.13
(2)	Internal Rotor		14.24	6.10	6.46	6.58	6.55	6.21	5.73	4.71
	Total	-86.73	87.73	22.34	26.34	29.60	32.15	35.65	37.86	40.84
tCH₂(OOH)O-CO	TVR	-56.81	73.32	17.06	20.16	22.81	24.99	28.31	30.71	34.39
(2)	Internal Rotor		14.24	6.10	6.46	6.58	6.55	6.21	5.73	4.71
	Total	-56.81	90.32	23.16	26.62	29.39	31.54	34.52	36.44	39.10
tCH₂(OOH)—CO₂	TVR	-57.20	71.85	16.87	20.11	22.83	25.04	28.37	30.74	34.40
(2)	Internal Rotor		14.24	6.10	6.46	6.58	6.55	6.21	5.73	4.71
	Total	-57.20	88.85	22.97	26.57	29.41	31.59	34.58	36.47	39.11
CH2O•(OO•)	TVR	3.56	62.48	12.96	15.59	17.82	19.62	22.24	24.03	26.58
(2)	Internal Rotor		5.86	2.27	2.11	1.91	1.73	1.48	1.34	1.16
	Total	3.56	69.72	15.23	17.70	19.73	21.35	23.72	25.37	27.74
tCH2O—OO	TVR	21.79	62.14	11.90	14.02	15.93	17.55	20.06	21.84	24.45
(TS)	Internal Rotor		5.86	2.27	2.11	1.91	1.73	1.48	1.34	1.16
	Total	21.79	69.38	14.17	16.13	17.84	19.28	21.54	23.18	25.61
tyCH₂O(OO•)	TVR	19.36	67.65	15.46	17.61	19.48	21.10	23.58	25.26	27.46
	Total	19.36	70.41	15.46	17.61	19.48	21.10	23.58	25.26	27.46
yCH₂OC•HO[j]	TVR	-24.50	62.19	13.60	17.30	20.50	23.07	26.79	29.33	33.00
	Total	-24.50	63.57	13.60	17.30	20.50	23.07	26.79	29.33	33.00
tyCH2OC•.HO	TVR	-13.90	78.12	17.99	20.56	22.68	24.38	26.96	28.83	31.47
	Total	-13.90	79.50	17.99	20.56	22.68	24.38	26.96	28.83	31.47
CH₂OCHO	TVR	-35.40	61.71	12.15	14.62	16.82	18.69	21.63	23.80	27.16
	Internal Rotor		10.40	3.21	3.31	3.33	3.27	3.06	2.83	2.47
	Total	-35.40	73.49	15.36	17.93	20.15	21.96	24.69	26.63	29.63
tCH₂O--CHO	TVR	-13.90	62.95	13.01	15.40	17.45	19.18	21.95	24.03	27.30
	Internal Rotor		10.40	3.21	3.31	3.33	3.27	3.06	2.83	2.47
	Total	-13.90	74.73	16.22	18.71	20.78	22.45	25.01	26.86	29.77

[a] Thermodynamic properties are referred to a standard state of an ideal gas of pure enantiometer at 1 atm. [b] In cal mol⁻¹K⁻¹. [c] The sum of contributions from translations, external rotations, and vibrations.

[d] Contribution from internal rotation. [e] Symmetry number is taken into account (-R x Ln (number of symmetry)) [f] Spin degeneracy contribution for entropy = 1.987 * Ln(2) (cal/mol-K) is taken into account.

[g] Optical Isomer (OI) contribution for entropy = 1.987 x Ln(2) (cal/mol-K) is taken into account. [h] t stands for TS. [i] ty stands for Transition Cyclic conformation. [j] y stands for cyclic conformation.

Table 2.2 (b) Ideal Gas Phase Thermodynamic Properties Using *ab initio* Calculation[a]

Species and Symmetry		$H_f^\circ{}_{298}$	$S^\circ{}_{298}$[b]	C_{p300} [b]	C_{p400}	C_{p500}	C_{p600}	C_{p800}	C_{p1000}	C_{p1500}
tC•H₂O—CH₃[g]	TVR[c]	25.8	58.58	12.76	15.44	17.91	20.07	23.60	26.37	30.93
	(6) Internal Rotor		9.29	3.06	3.20	3.17	3.07	2.83	2.63	2.33
	Total[f]	25.8	69.25[e]	15.82	18.64	21.08	23.14	26.43	29.00	33.26
tyCH₂OCH₄[h]	TVR			15.16	19.46	22.90	25.59	30.68	34.24	39.86
	Total	45.5	65.62	15.16	19.46	22.90	25.59	30.68	34.24	39.86

[a] Thermodynamic properties are referred to a standard state of an ideal gas of pure enantiometer at 1 atm. [b] In cal $mol^{-1}K^{-1}$. [c] The sum of contributions from translations, external rotations, and vibrations. [d] Contribution from internal rotation. [e] Symmetry number is taken into account (-R x Ln (number of symmetry)) [f] Spin degeneracy contribution for entropy = 1.987 × Ln(2) (cal/mol-K) is taken into account. [g] t stands for TS. [h] ty stands for Transition Cyclic conformation.

These values are adopted from A_2, $E_{a,2}$, A_{-2} and $E_{a,-2}$ respectively since the two H shift reaction mechanisms are similar.

$$CH_3OCH_2OO\bullet \overset{k_{-2,2}}{\Longleftarrow\Longrightarrow} C\bullet H_2OCH_2OOH$$

iii) $CH_2(OOH)OC\bullet HOOH \overset{k_7}{\Longrightarrow} CH_2(OOH)OCHO + OH$
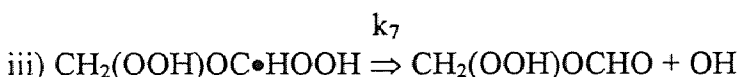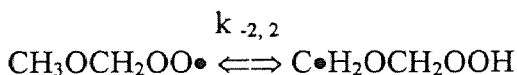
The high pressure limit A_7 is estimated based on TST of $CH_3OC\bullet HOOH \Rightarrow CH_3OCHO + OH$. $\Delta S^{\neq}{}_{298}$ is calculated based on molecular orbital (MO) method PM3[32] calculation and Pitzer et al.'s general treatment of hindered internal rotation contribution for entropy[10]. $E_{a,7}$ is estimated based on PM3 enthalpy $\Delta H_f^\circ{}_{298}$ calculation described in Table 2.3.
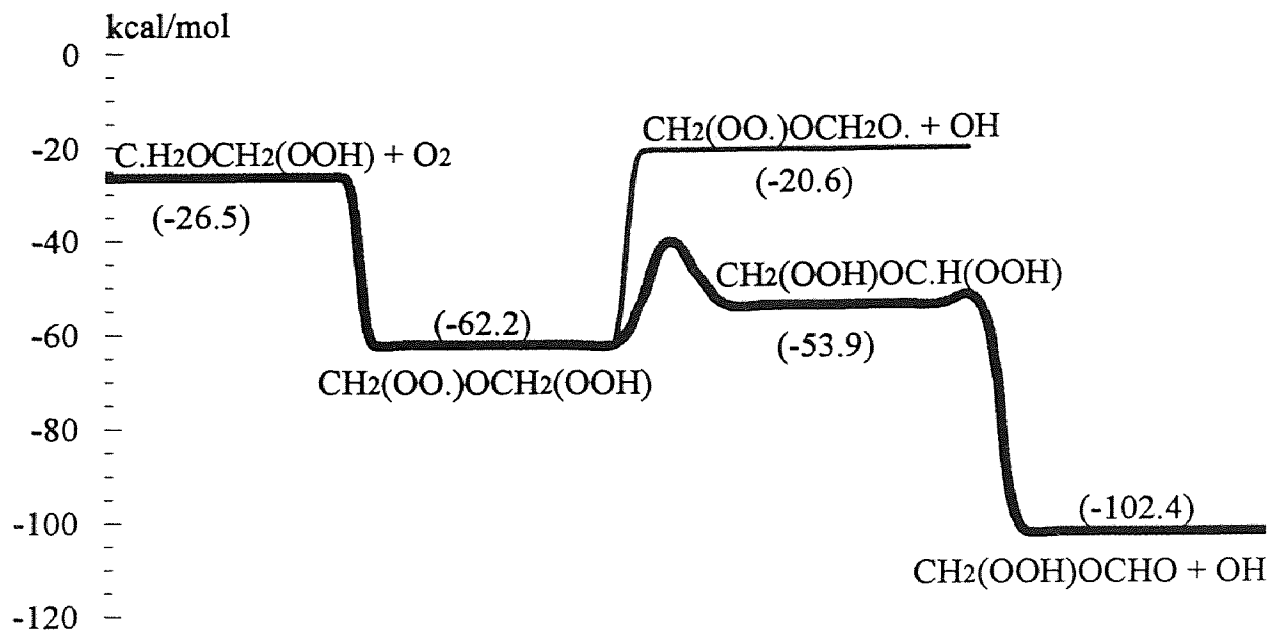
Figure 2.1 Potential Energy Diagram
C.H2OCH2OOH + O2 --> Products
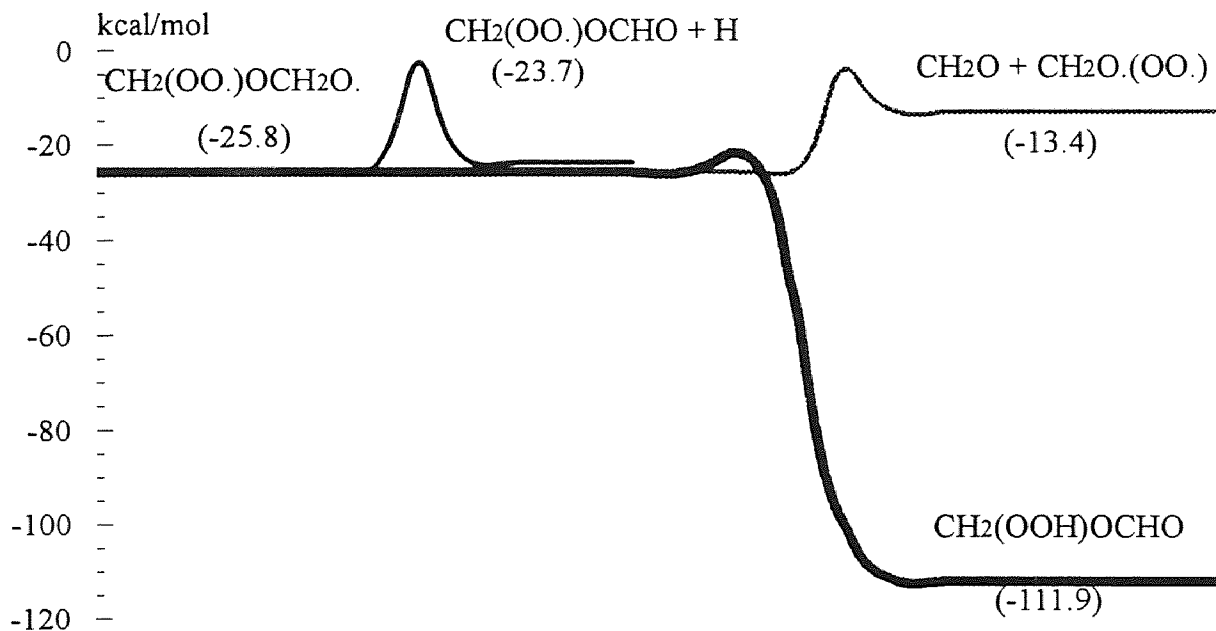
Figure 2.2 Potential Energy Diagram
CH2(OO.)OCH2O. --> Products
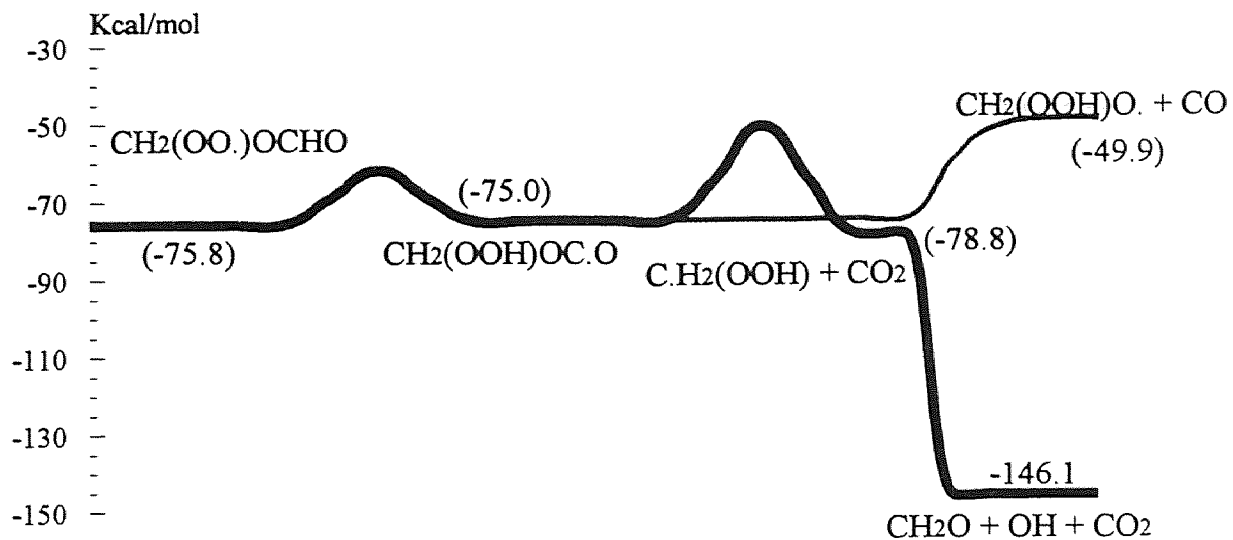
Figure 2.3 Potential Energy Diagram
CH2(OO.)CHO --> Products
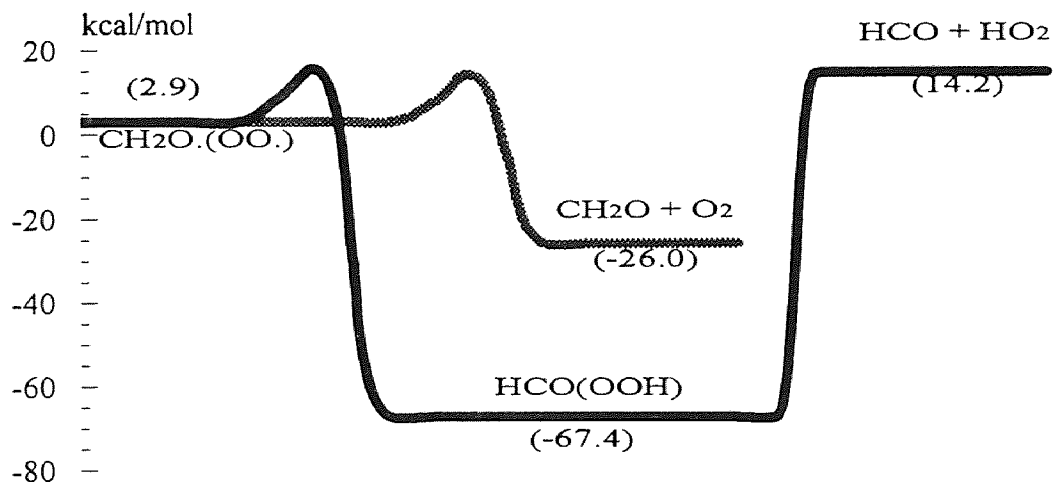
Figure 2.4 Potential Energy Diagram
CH2O.(OO.) --> Products
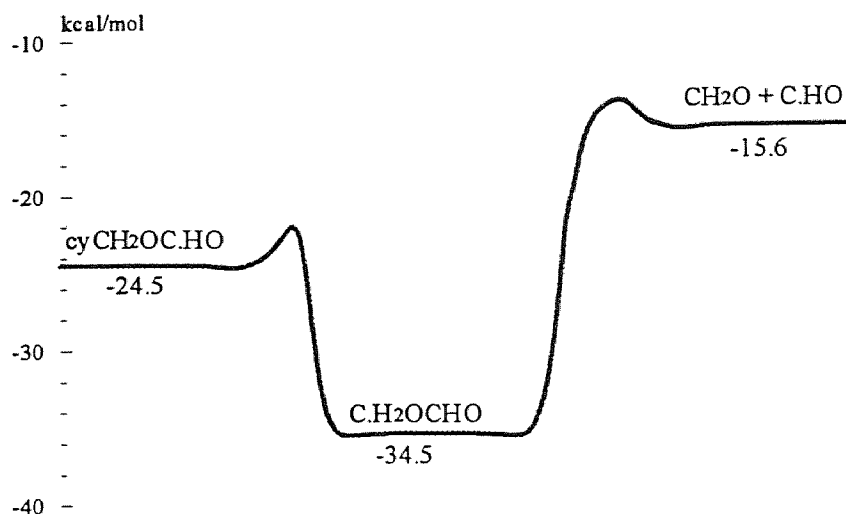
Figure 2.5 Potential Energy Diagram
cyCH2OC.HO —> Products

$$k_8$$
iv) $CH_2(OO\bullet)OCH_2OOH \Rightarrow CH_2(OO\bullet)OCH_2O\bullet + OH$
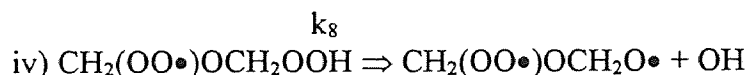
High pressure limit A_8 is estimated as $4.00E+15$ s^{-1} with barrier of 41 kcal/mol, which is adopted from Baulch et al.'s study for $C_2H_5OOH \Rightarrow C_2H_5O\bullet + OH$[37].

QRRK Analysis Results

The apparent rate constants at different temperatures ($298 \leq T/K \leq 2000$), 1 atm and 10 atm for each reaction channel are illustrated in Figure 2.6 and 2.7 respectively. Rate constants in the form $k = A(T/K)^n\exp(-E_a/RT)$ are obtained by least squares fitting the QRRK calculated rate constants in the temperature range 298 to 2000 K. There is no significant difference between two pressures. The stabilization reaction to form $CH_2(OO\bullet)OCH_2OOH$ dominates at low temperature and the reverse reaction dissociation back to reactants dominates at high temperature. The turning point where the reverse

reaction surpasses the stabilization reaction shifts from 670 K to 830 K as pressure increases from 1 atm to 10 atm. The apparent rate constants at different pressure, 1E-4 to 1E+2 atm and 298 and 1000 K for each reaction channel are illustrated in Figure 2.8 and 2.9 respectively. The stabilization reaction dominates at the pressure above 1E-3 atm at low temperature and reverse reaction dominates over the entire temperature range up to 100 atm at high temperature.

Table 2.3 Input Parameter for QRRK Calculations and the Results of Apparent Rate Constants : C•H$_2$OCH$_2$OOH + O$_2$ → CH$_2$(OO•)OCH$_2$OOH → Products

Input parameters for QRRK Calculations (T = 298 K)			
Reaction	High Pressure Limit Rate Constants		
	A(s-1 or cm3/(mol s)	n	Ea(kcal/mol)
5 C•H$_2$OCH$_2$OOH + O$_2$ ⇒ CH$_2$(OO•)OCH$_2$OOH	4.82E+12	0.00	0.0
-5 CH$_2$(OO•)OCH$_2$OOH ⇒ C.H$_2$OCH$_2$OOH + O$_2$	1.78E+15	0.00	35.1
6 CH$_2$(OO•)OCH$_2$OOH ⇒ CH$_2$(OOH)OC.HOOH	1.10E+07	1.21	17.1
-6 CH$_2$(OOH)OC•HOOH ⇒ CH$_2$(OO•)OCH$_2$OOH	4.88E+7	0.59	9.3
7 CH$_2$(OOH)OC•HOOH ⇒ CH$_2$(OOH)OCHO + OH	3.16E+11	0.60	4.8
8 CH$_2$(OO•)OCH$_2$OOH ⇒ CH$_2$(OO•)OCH$_2$O. + OH	4.00E+15	0.00	41.0

Frequencies/Degeneracies: 406.6 cm^{-1}/10.406, 401.0 cm^{-1}/4.909, 1906.2cm^{-1}/12.185
Lennard-Jones Parameters: σ=5.86Å, ∈/k=632.06 K. The Units of A factors and rate constasnts k are s^{-1} for unimolecular reactions and cm^3/(mol s) for bimolecular reactions. Bath Gas = Ar

K$_5$ A$_5$ and E$_{a,5}$ based on n-C$_3$H$_7$ + O$_2$ → n-C$_3$H$_7$O$_2$ from Atkinson et al.[30]
k$_{-5}$ Microscopic Reversibility (MR) Af/Ar=2.58E-2 E$_{a,-5}$=ΔH-RT
k$_6$ A$_6$ and E$_{a,6}$ are from A$_2$ and E$_{a,2}$ respectively
k$_{-6}$ A$_{-6}$ and E$_{a,-6}$ are from A$_2$ and E$_{a,-2}$ respectively
k$_7$ A$_7$ based on TST of CH$_3$OC•HOOH → CH$_3$OCHO + OH, ΔS$^{\neq}_{298}$ from MOPAC PM3 calculation (ΔS$_{298}$ of Transition State - ΔS°$_{298}$ of Reactant), E$_{a,7}$ from MOPAC PM3 calculation (ΔHf°$_{298}$ of Transition State - ΔHf°$_{298}$ of Reactant, scaled by ×0.8) All three parameters A, n, and E$_a$ are fit over the temperature range of 300 to2,000K.
k$_8$ A$_8$ and E$_{a,8}$ based on C$_2$H$_5$OOH → C$_2$H$_5$O• + OH from Baulch et al.[37]

**Table 2.4 QRRK Calculation Results: C•H$_2$OCH$_2$OOH + O$_2$ →
CH$_2$(OO•)OCH$_2$OOH → Products**

Calculated Apparent Reaction Parameters at P=1 atm, k=A(T/K)^n(-E$_a$/RT)(Temp=298–2000 K)

	Reaction	A	n	Ea	k$_{973}$ (s^{-1} or cm^3/(mol s))
5	C•H$_2$OCH$_2$OOH + O$_2$ ⇒ CH$_2$(OO•)OCH$_2$OOH	2.07E+37	-8.29	5.3	2.26E+11
-5	CH$_2$(OO•)OCH$_2$OOH ⇒ C•H$_2$OCH$_2$OOH + O$_2$	2.28E+39	-8.16	40.1	9.27E+05
6	C•H$_2$OCH$_2$OOH + O$_2$ ⇒ CH$_2$(OO•)OCH$_2$O. + OH	1.50E+21	-2.31	11.9	3.98E+11
7	C•H$_2$OCH$_2$OOH + O$_2$ ⇒ CH$_2$(OOH)OCHO + OH	8.90E+25	-4.45	6.4	1.64E+11
8	CH$_2$(OO•)OCH$_2$OOH ⇒ CH$_2$(OOH)OC.HOOH	3.42E+21	-4.91	18.4	5.36E+02
-8	CH$_2$(OOH)OC•HOOH ⇒ CH$_2$(OO•)OCH$_2$OOH	2.52E+13	-3.28	10.4	1.84E+01
9	CH$_2$(OOH)OC•HOOH ⇒ CH$_2$(OOH)OCHO + OH	2.38E+15	-1.99	2.9	6.01E+08

2.3.3 CH$_2$(OO•)OCH$_2$O• Reaction System

High Pressure Limit Rate Constant as QRRK Input Parameters.

The potential energy diagram for the reaction CH$_2$(OO•)OCH$_2$O• ⇒ Products is

illustrated in Figure 2.2.

$$k_9$$
i) CH$_2$(OO•)OCH$_2$O• ⇒ CH$_2$(OO•)OCHO + H
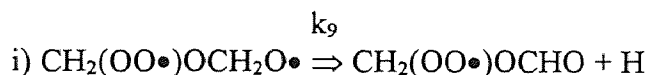
High pressure limit A$_9$ and activation energy E$_{a,9}$ are estimated as 3.64E+11 s^{-1}, 17.6

kcal/mol respectively. These values are adopted from the CH$_3$CH$_2$O• ⇒ CH$_3$CHO + H

reaction in C$_2$H$_4$ + OH addition reaction mechanism which is discussed in Chapter 4.

$$k_{10}$$
ii) CH$_2$(OO•)OCH$_2$O• ⇒ CH$_2$O + CH$_2$O•(OO•)
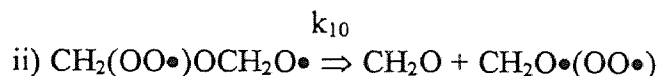
High pressure limit A$_{10}$ and activation energy E$_{a,10}$ are estimated as 5.90+E+11 s^{-1} and

13.6kcal/mol respectively. These values are adopted from CH$_3$CH$_2$O• ⇒ CH$_2$O + CH$_3$

reaction in the C$_2$H$_4$ + OH addition reaction mechanism.

$$k_{11}$$
iii) CH$_2$(OO•)OCH$_2$O• ⇒ CH$_2$OOHOCHO
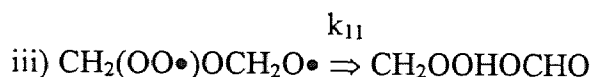
High pressure limit A_{11} and activation energy $E_{a,11}$ are estimated as 4.83E+10 s^{-1}, 4.0

kcal/mol respectively as described in Table 2.5.

Table 2.5 Input Parameter for QRRK Calculations and the Results of Apparent Rate Constants: $CH_2(OO\bullet)OCH_2O\bullet$ → Products

Input parameters for QRRK Calculations (T = 298 K)			
	High Pressure Limit Rate Constants		
Reaction	A(s-1 or cm3/(mol s)	n	Ea(kcal/mol)
9 $CH_2(OO\bullet)OCH_2O\bullet$ → $CH_2(OO\bullet)OCHO$ + H	3.64E+11	1.07	17.6
10 $CH_2(OO\bullet)OCH_2O\bullet$→ CH_2O + $CH_2O\bullet(OO\bullet)$	5.90E+11	0.67	13.6
11 $CH_2(OO\bullet)OCH_2O\bullet$ → $CH_2OOHOCHO$	4.83E+10	0.00	4.0

Frequencies/Degeneracies: 435.5 cm^{-1}/11.499, 2500.0 cm^{-1}/0.011, 2041.2cm^{-1}/10.99
Lennard-Jones Parameters: σ=5.55Å, ϵ/k=584.86 K. The Units of A factors and rate constasnts k are s^{-1} for unimolecular reactions and cm^3/(mol s) for bimolecular reactions. Bath Gas = Ar

K_9 A_9 and $E_{a,9}$ based on CH_3CH_2O. → CH_3CHO + H from C2H4 + OH mechanism (see Table 4.8)

k_{10} A_{10} and $E_{a,10}$ based on CH_3CH_2O → CH_2O + CH_3 from C2H4 + OH mechanism (see Table 4.8)

k_{11} A_{11} from TST, degeneracy = 2, $\Delta S^{\neq}$ (298)= -4.3 (cal/mol) × (number of rotor lost = 3) $E_{a,11}$ = ring strain (4.0 kcal/mol) + $E_{abstraction}$ (0.0 kcal/mol), $E_{abstraction}$ estimated from 12.5 kcal/mol - ΔH_{rxn} × 1/3 (Evans' Polanyi Plot)

QRRK Analysis Results

The apparent rate constants at different temperatures (298 ≤ T/K ≤ 2000) and 1 atm for

each reaction channel are illustrated in Figure 2.10. Isomerization reaction to form

$CH_2(OOH)OCHO$ dominates the reaction up to 1000 K. Dissociation reaction to form

$CH_2(OO\bullet)OCHO$ + H is important at higher temperature.

Table 2.6 QRRK Calculation Results: $CH_2(OO\bullet)OCH_2O\bullet \rightarrow$ Products

Calculated Apparent Reaction Parameters at P=1 atm, k=A(T/K)^n(-E$_a$/RT)(Temp=298 -2000K)

Reaction	A	n	Ea	k_{973} (s^{-1} or cm^3/(mol s))
10 $CH_2(OO\bullet)OCH_2O\bullet \rightarrow CH_2(OO\bullet)OCHO + H$	7.91E+31	-6.70	16.8	1.27E+08
11 $CH_2(OO\bullet)OCH_2O\bullet \rightarrow CH_2O + CH_2O\bullet(OO\bullet)$	6.68E+26	-4.93	19.0	6.69E+07
12 $CH_2(OO\bullet)OCH_2O\bullet \rightarrow CH_2OOHOCHO$	4.26E+36	-8.82	9.8	1.18E+08

2.3.4 $CH_2(OO\bullet)OCHO$ Reaction System

High Pressure Limit Rate Constant as QRRK Input Parameters.

The potential energy diagram for the reaction $CH_2(OO\bullet)OCH_2O\bullet \Rightarrow$ Products is

illustrated in Figure 2.3.

$$k_{12}$$
i) $CH_2(OO\bullet)OCHO \Rightarrow CH_2(OOH)OC\bullet O$
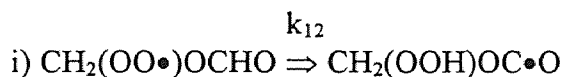
High pressure limit A_{12} and that for reverse direction A_{-12} are estimated as 2.89E+6 and

3.57E+6 s^{-1} respectively based on TST[13]. $\Delta S^{\neq}_{298}$ is calculated based on PM3[32]. There is

no rotor since the TS is cyclic formation. $E_{a,12}$ is estimated using ring strain and

$E_{a,abstraction}$ estimation as described in Table 2.7 since $E_{a,12}$ calculation based on PM3[32]

gives unreasonably high value (c.a. 22.4 kcal/mol).

$$k_{13}$$
ii) $CH_2(OOH)OC\bullet O \Rightarrow CH_2O\bullet(OOH) + CO$
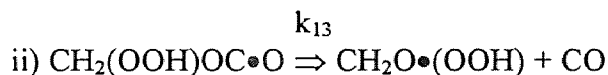
High pressure limit A_{13} is estimated as 2.53E+13 s^{-1} based on TST[13]. $\Delta S^{\neq}_{298}$ is

calculated based on PM3[32] and Pitzer et al.'s general treatment of hindered internal

rotation contribution for entropy[10]. $E_{a,13}$ is estimated as 24.6 kcal/mol based on PM3

calculation[32].

$$k_{14}$$
iii) $CH_2OOHOC\bullet O \Rightarrow CO_2 + CH_2O + OH$
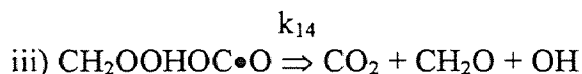
Table 2.7 Input Parameter for QRRK Calculations and the Results of Apparent Rate Constants: CH$_2$(OO•)OCHO → CH$_2$(OOH)OC•O → Products

Input parameters for QRRK Calculations (T = 298 K)

Reaction	High Pressure Limit Rate Constants		
	A(s-1 or cm3/(mol s)	n	Ea(kcal/mol)
12 CH$_2$(OO•)OCHO ⇒ CH$_2$(OOH)OC•O	2.89E+6	1.37	12.5
-12 CH$_2$(OOH)OC•O ⇒ CH$_2$(OO•)OCHO	3.57E+6	1.46	11.8
13 CH$_2$(OOH)OC•O ⇒ CH$_2$O•(OOH) + CO	2.35E+13	0.20	24.6
14 CH$_2$OOHOC•O ⇒ CO$_2$ + CH$_2$O + OH	9.19E+12	0.23	24.3

Frequencies/Degeneracies: 338.3 cm^{-1}/7.128, 401.1 cm^{-1}/2.593, 1760.5 cm^{-1}/9.779 Lennard-Jones Parameters: σ=5.83Å, ∈/k=492.5 K. The Units of A factors and rate constasnts k are s^{-1} for unimolecular reactions and cm^3/(mol s) for bimolecular reactions. Bath Gas = Ar

k$_{12}$	A$_{12}$ from Transition State Theory (TST), ΔS$^{≠}_{298}$ from MOPAC PM3 calculation (ΔS$_{298}$ of Transition State - ΔS$_{298}$ of Reactant), E$_{a,12}$ = ring strain (0.0 kcal/mol) + Eabstraction (12.2 kcal/mol) + ΔH (0.8kcal/mol), Eabstraction estimated from 12.5 kcal/mol - ΔHrxn × 1/3 (Evans' Polanyi Plot) All three parameters A, n, and E$_a$ are fit over the temperature range of 300 to2,000K.
k$_{-12}$	A$_{-12}$ from Transition State Theory (TST), ΔS$^{≠}_{298}$ from MOPAC PM3 calculation (ΔS$_{298}$ of Transition State - ΔS$_{298}$ of Product), E$_{a-12}$ from MR. All three parameters A, n, and E$_a$ are fit over the temperature range of 300 to2,000K.
k$_{13}$	A$_{13}$ from TST, ΔS$^{≠}_{298}$ from MOPAC PM3 calculation (ΔS$_{298}$ of Transition State - ΔS$_{298}$ of Reactant), E$_{a,13}$ from MOPAC PM3 calculation (ΔH$_{298}$ of Transition State - ΔH$_{298}$ of Reactant, scaled by ×0.8) All three parameters A, n, and E$_a$ are fit over the temperature range of 300 to2,000K.
k$_{14}$	A$_{15}$ from TST, ΔS$^{≠}_{298}$ from MOPAC PM3 calculation (ΔS$_{298}$ of Transition State - ΔS$_{298}$ of Reactant), E$_{a,14}$ from MOPAC PM3 calculation (ΔH$_{298}$ of Transition State - ΔH$_{298}$ of Reactant, scaled by ×0.8) All three parameters A, n, and E$_a$ are fit over the temperature range of 300 to2,000K. This reaction has two steps; First step; CH$_2$OOHOC.=O → C.H$_2$OOH + CO$_2$, Second step; C.H$_2$OOH → CH$_2$O + OH. The second reaction has very small barrier (c.a. 6 kcal/mol) and is fast under combustion environment.

Table 2.8 Input Parameter for QRRK Calculations and the Results of Apparent Rate Constants: CH$_2$(OO•)OCHO → CH$_2$(OOH)OC•O → Products

Calculated Apparent Reaction Parameters at P=1 atm, k=A(T/K)^n(-E$_a$/RT)(Temp=298 - 2000K)

Reaction	A	n	Ea	k$_{973}$ (s^{-1} or cm^3/(mol s))
13 CH$_2$(OO•)OCHO ⇒ CH$_2$(OOH)OC•O	2.42E+26	-4.59	24.2	1.71E+07
-13 CH$_2$(OOH)OC•O ⇒ CH$_2$(OO•)OCHO	7.52E+30	-6.48	18.2	2.66E+07
14 CH$_2$(OOH)OC•O ⇒ CH$_2$O•(OOH) + CO	3.85E+28	-4.77	31.9	1.47E+07
15 CH$_2$(OOH)OC•O ⇒ CO$_2$ + CH$_2$O + OH	1.81E+28	-4.76	31.7	8.19E+06

High pressure limit A_{14} is estimated as 9.19E+12 s^{-1} based on TST[13]. $\Delta S^{\neq}_{298}$ is

calculated based on PM3[32] and Pitzer et al.'s general treatment of hindered internal

rotation contribution for entropy[10]. $E_{a,14}$ is estimated as 24.3 kcal/mol based on PM3

calculation. After dissociation to $CH_2OOH + CO_2$, CH_2OOH rapidly decomposes to

$CH_2O + OH$ since activation energy is small (c.a. 6 kcal/mol); it is fast reaction under

combustion environment.

QRRK Analysis Results

The apparent rate constants at different temperatures ($298 \leq T/K \leq 2000$) and 1 atm for

each reaction channel are illustrated in Figure 2.11. Isomerization reaction to form

$CH_2(OOH)OC\bullet O$ dominates the reaction up to 1000 K. Dissociation reaction to form

$CH_2(OOH)O\bullet + CO$ is important at higher temperature. All reactions are slow and not

important in dimethyl-ether oxidation reaction.

2.3.5 CH2O•(OO•) Reaction System

High Pressure Limit Rate Constant as QRRK Input Parameters.

The potential energy diagram for the reaction $CH_2O\bullet(OO\bullet) \Rightarrow$ Products is illustrated in

Figure 2.4.

$$k_{15}$$
i) $CH_2O\bullet(OO\bullet) \Rightarrow HCO(OOH)$
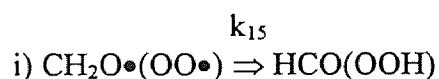
High pressure limit A_{15} and that for reverse direction A_{-15} are estimated as 1.30E+11 and

8.88E+9 s^{-1} respectively based on TST[13]. $\Delta S^{\neq}_{298}$ is calculated based on PM3[32] and

Pitzer et al.'s general treatment of hindered internal rotation contribution for entropy[10].

$E_{a,15}$ is estimated as 12.6 kcal/mol based on PM3 calculation[32].

$$k_{16}$$
ii) $HCO(OOH) \Rightarrow HCO + HO_2$
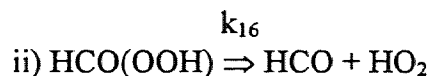
High pressure limit A_{16} is estimated as 1.55E+16 s^{-1} based on A_{-16} and MR. A_{-16} is

adopted from Tsang et al.'s study, $A = 3.01E+13$ cm^3/(mol s)[26].

$$k_{17}$$
iii) $CH_2O\bullet(OO\bullet) \Rightarrow CH_2O + O_2$
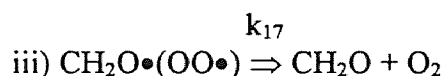
High pressure limit A_{17} is estimated as 1.66E+13 s^{-1} based on TST[13]. $\Delta S^{\neq}_{298}$ is

calculated based on PM3[32] and Pitzer et al.'s general treatment of hindered internal

rotation contribution for entropy[10]. $E_{a,17}$ is estimated as 11.1 kcal/mol based on PM3

calculation.

QRRK Analysis Results

The apparent rate constants at different temperatures (298 $\leq$ T/K $\leq$ 2000) and 1 atm for

each reaction channel are illustrated in Figure 2.12. Dissociation reaction to form CH_2O

+ O2 dominates $HCO + HO_2$ channel over the entire temperature range 298 to 2000 K at

1 atm.

2.3.6   cyCH2OC•HO (1,3-Dioxetane Radical) Reaction System

High Pressure Limit Rate Constant as QRRK Input Parameters.

The potential energy diagram for the reaction cyCH$_2$OC•HO $\Rightarrow$ C•H$_2$OCHO $\Rightarrow$ CH$_2$O +

HCO is illustrated in Figure 2.5.

Table 2.9 Input Parameter for QRRK Calculations and the Results of Apparent Rate Constants: $CH_2O\bullet(OO\bullet) \rightarrow$ Products

Input parameters for QRRK Calculations (T = 298 K)

Reaction	High Pressure Limit Rate Constants A(s-1 or cm3/(mol s)	n	Ea(kcal/mol)
15 $CH_2O\bullet(OO\bullet) \Rightarrow HCO(OOH)$	1.30E+11	0.92	12.6
-15 $HCO(OOH) \Rightarrow CH_2O\bullet(OO\bullet)$	8.88E+9	0.88	83.0
16 $HCO(OOH) \Rightarrow HCO + HO_2$	1.55E+16	0.00	81.6
17 $CH_2O\bullet(OO\bullet) \Rightarrow CH_2O + O_2$	1.66E+13	-0.01	11.1

Frequencies/Degeneracies: 338.3 cm^{-1}/7.128, 401.1 cm^{-1}/2.593, 1760.5 cm^{-1}/9.779
Lennard-Jones Parameters: σ=5.83Å, ϵ/k=492.5 K. The Units of A factors and rate constasnts k are s^{-1} for unimolecular reactions and cm^3/(mol s) for bimolecular reactions. Bath Gas = Ar

k_{15} A_{15} from Transition State Theory (TST), $\Delta S^{\neq}_{298}$ from MOPAC PM3 calculation (ΔS_{298} of Transition State - ΔS_{298} of Reactant), $E_{a,16}$ from MOPAC PM3 calculation (ΔH_{298} of Transition State - ΔH_{298} of Reactant, scaled by ×0.8) All three parameters A, n, and E_a are fit over the temperature range of 300 to2,000K.

k_{-15} A_{-15} from Transition State Theory (TST), $\Delta S^{\neq}_{298}$ from MOPAC PM3 calculation (ΔS_{298} of Transition State - ΔS_{298} of Product) All three parameters A, n, and E_a are fit over the temperature range of 300 to2,000K.

k_{16} MR (Af/Ar) = 5.14E+2 A_{-17} = 3.01E+13 from Tsang et al.

k_{17} A_{17} from TST, $\Delta S^{\neq}_{298}$ from MOPAC PM3 calculation (ΔS_{298} of Transition State - ΔS_{298} of Reactant), E_{a18} from MOPAC PM3 calculation (ΔH_{298} of Transition State - ΔH_{298} of Product, scaled by ×0.8) All three parameters A, n, and E_a are fit over the temperature range of 300 to2,000K.

Table 2.10 QRRK Calculation Results: $CH_2O\bullet(OO\bullet) \rightarrow$ Products

Calculated Apparent Reaction Parameters at P=1 atm, k=A(T/K)^n(-E$_a$/RT)(Temp=298 - 2000K)

Reaction	A	n	Ea	k_{973} (s^{-1} or cm^3/(mol s))
16 $CH_2O\bullet(OO\bullet) \Rightarrow HCO(OOH)$	6.03E+8	0.06	10.9	3.24E+06
-16 $HCO(OOH) \Rightarrow CH_2O\bullet(OO\bullet)$	4.73E+7	-0.01	81.5	2.17E-11
17 $CH_2O\bullet(OO\bullet) \Rightarrow HCO + HO_2$	1.39E-10	6.97	11.0	3.16E+08
18 $CH_2O\bullet(OO\bullet) \Rightarrow HCO + HO_2$	4.59E+11	0.75	12.8	1.07E+11

i) $cyCH_2OC\bullet HO \xrightarrow{k_{18}} C\bullet H_2OCHO$
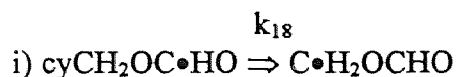
High pressure limit A_{18} and the reverse A_{-18} are estimated as 1.02E+11 and 3.20E+8 s^{-1}

respectively based on TST[13]. ΔS^*_{298} is calculated based on PM3[32]. There is no

rotational contribution for entropy. $E_{a,18}$ is estimated as 2.5 kcal/mol. PM3 calculation

result gives extremely high value (c.a. 20.8 kcal/mol).

ii) $C\bullet H_2OCHO \xrightarrow{k_{19}} CH_2O + HCO$
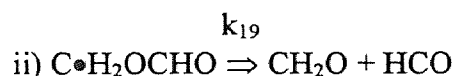
High pressure limit A_{19} is estimated as 2.55E+10 s^{-1} based on TST[13]. ΔS^*_{298} is

calculated based on PM3[32] and Pitzer et al.'s general treatment of hindered internal

rotation contribution for entropy[10]. $E_{a,19}$ is estimated as 21.3 kcal/mol based on PM3

calculation.

QRRK Analysis Results

The apparent rate constants at different temperatures ($298 \leq T/K \leq 2000$) and 1 atm for

each reaction channel are illustrated in Figure 2.13. The ring cleavage reaction to form

$C\bullet H_2OCHO$ dominates up to temperature of 800 K. The dissociation reaction to form

$CH_2O + HCO$ dominates at the higher temperature.

Table 2.11 Input Parameter for QRRK Calculations and the Results of Apparent Rate Constants: cyCH₂OC•HO → CH2OC•HO → CH2O + HCO

Input parameters for QRRK Calculations (T = 298 K)

Reaction	High Pressure Limit Rate Constants		
	A(s-1 or cm3/(mol s)	n	Ea(kcal/mol)
18 cyCH₂OC.HO ⟹ CH₂OCHO	1.02E+11	0.80	2.68
-18 CH₂OCHO ⟹ cyCH₂OC.HO	3.20E+8	0.75	13.2
19 CH₂OCHO⟹ CH₂O + HCO	2.55E+10	1.35	21.3

Frequencies/Degeneracies: 386.3 cm^{-1}/4.857, 800.3 cm^{-1}/1.368, 1793.6 cm^{-1}/7.776
Lennard-Jones Parameters: σ=5.18Å, ∈/k=357.0 K. The Units of A factors and rate constasnts k are s^{-1} for unimolecular reactions and cm^3/(mol s) for bimolecular reactions. Bath Gas = Ar

K_{18} A_{18} from Transition State Theory (TST), $\Delta S^{\neq}_{298}$ from MOPAC PM3 calculation (ΔS_{298} of Transition State - ΔS_{298} of Reactant), $E_{a,19}$ estimated by this study. All three parameters A, n, and E_a are fit over the temperature range of 300 to2,000K.

k_{-18} A_{-18} from Transition State Theory (TST), $\Delta S^{\neq}_{298}$ from MOPAC PM3 calculation (ΔS_{298} of Transition State - ΔS_{298} of Reactant) All three parameters A, n, and E_a are fit over the temperature range of 300 to2,000K.

k_{19} A_{19} from TST, $\Delta S^{\neq}_{298}$ from MOPAC PM3 calculation (ΔS_{298} of Transition State - ΔS_{298} of Reactant), $E_{a,20}$ from MOPAC PM3 calculation (ΔH_{298} of Transition State - ΔH_{298} of Product, scaled by ×0.8) All three parameters A, n, and E_a are fit over the temperature range of 300 to2,000K.

Table 2.12 QRRK Calculation Results: cyCH₂OC.HO → CH2OC.HO → CH2O + HCO

Calculated Apparent Reaction Parameters at P=1 atm, k=A(T/K)^n(-E$_a$/RT)(Temp=298 - 2000K)

Reaction	A	n	Ea	k_{973} (s^{-1} or cm^3/(mol s))
19 cyCH₂OC.HO ⟹ CH₂OCHO	1.68E+38	-8.06	10.1	7.45E+11
-19 CH₂OCHO ⟹ cyCH₂OC.HO	5.45E+35	-8.13	20.7	1.24E+07
20 cyCH₂OC.HO ⟹ CH₂O + HCO	4.05E+26	-3.54	13.8	8.50E+12
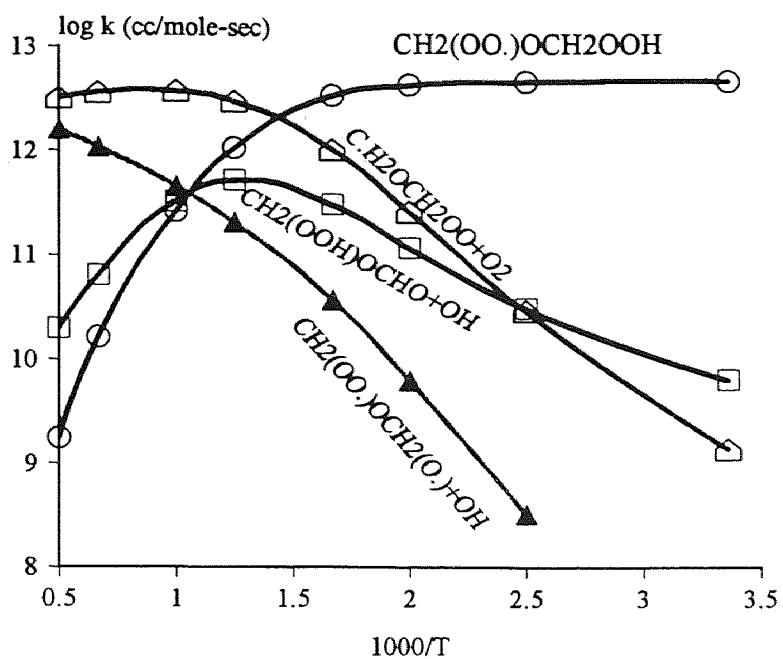
Figure 2.6 k vs. Temperature (1 atm)
C.H2OCH2OOH + O2
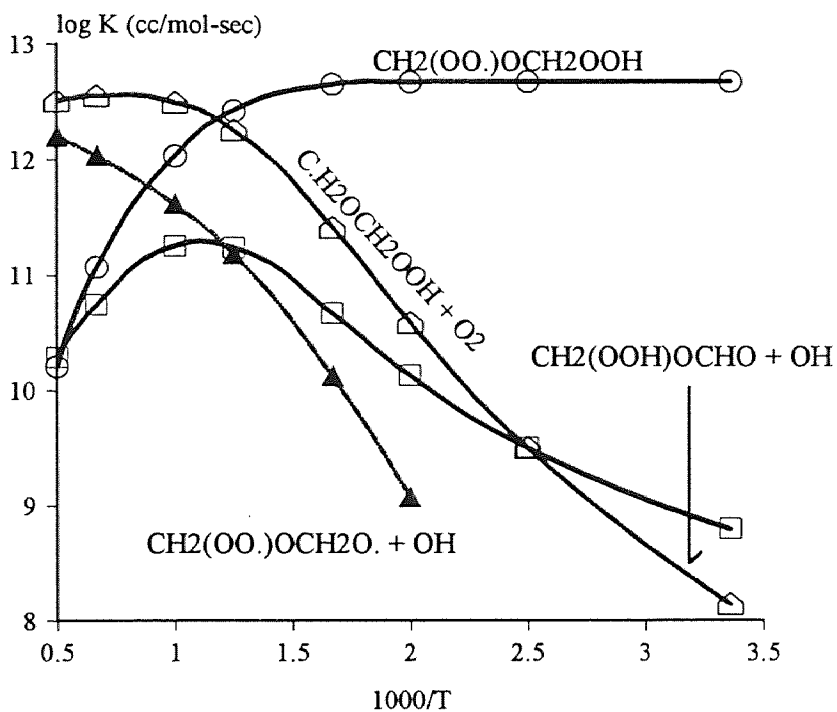
Figure 2.7 k vs. Temperature (10 atm)
C.H2OCH2OOH + O2
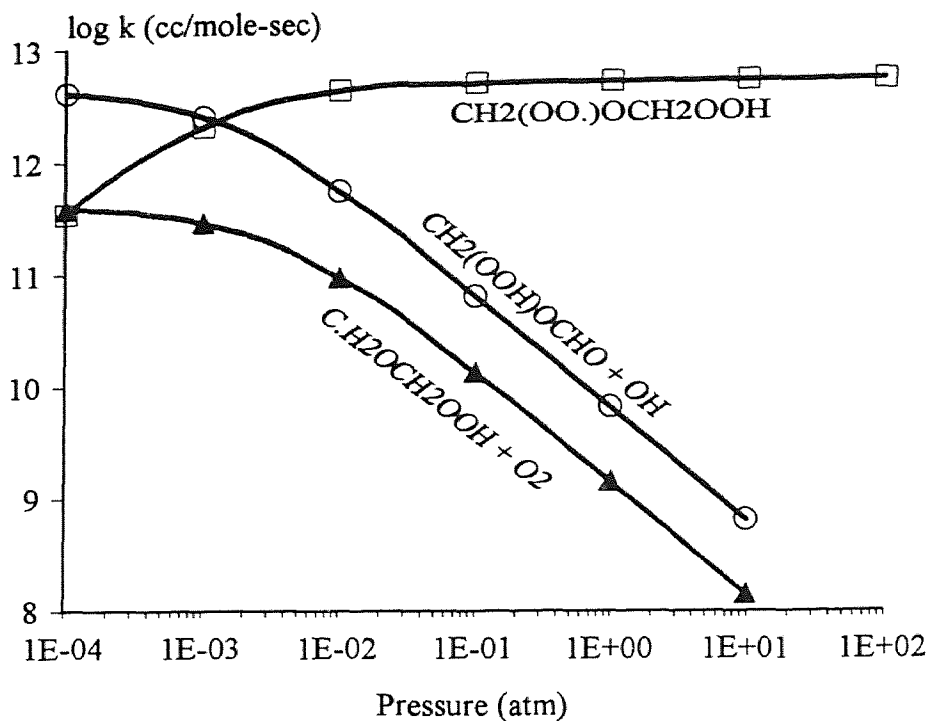
Figure 2.8 k vs. Pressure (298 K)
C.H2OCH2OOH + O2
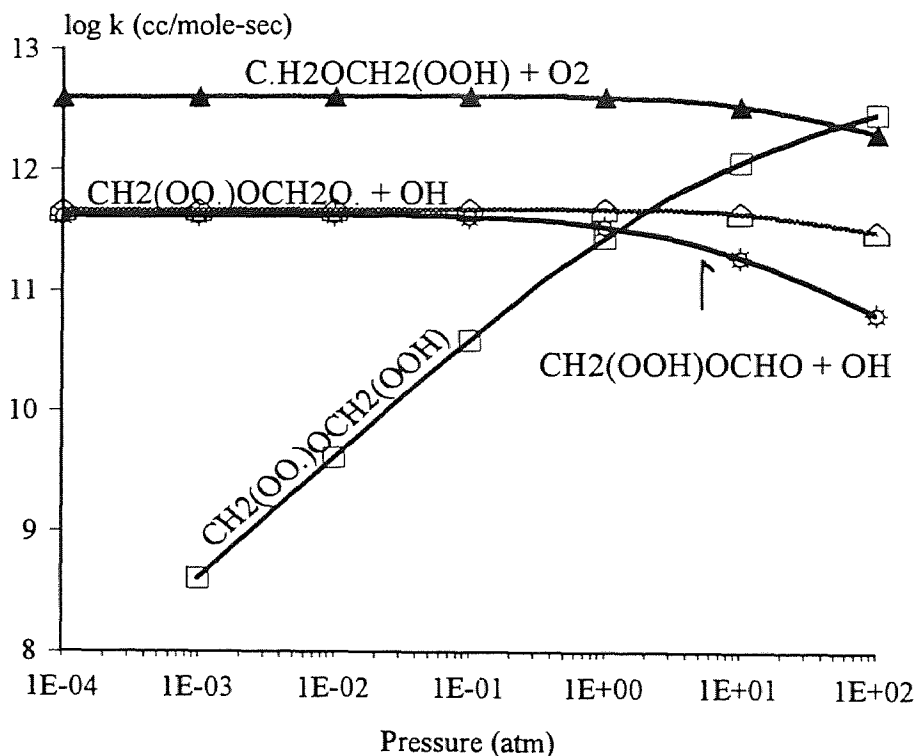
Figure 2.9 k vs. Pressure (1000 K)
C.H2OCH2OOH + O2
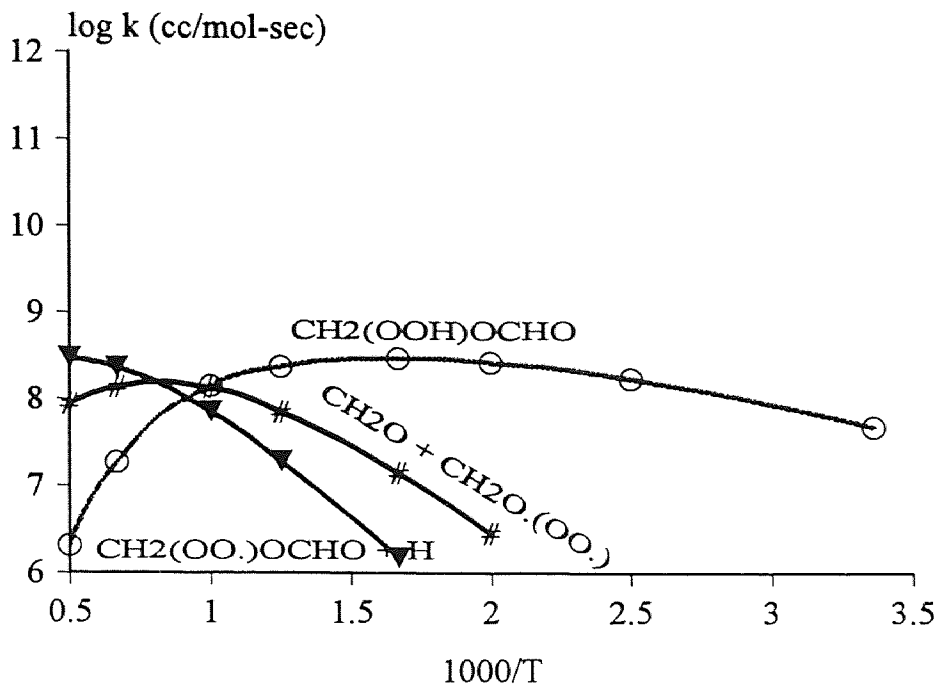
Figure 2.10 k vs. Temperature (1 atm)
CH2(OO.)OCH2O. --> Products
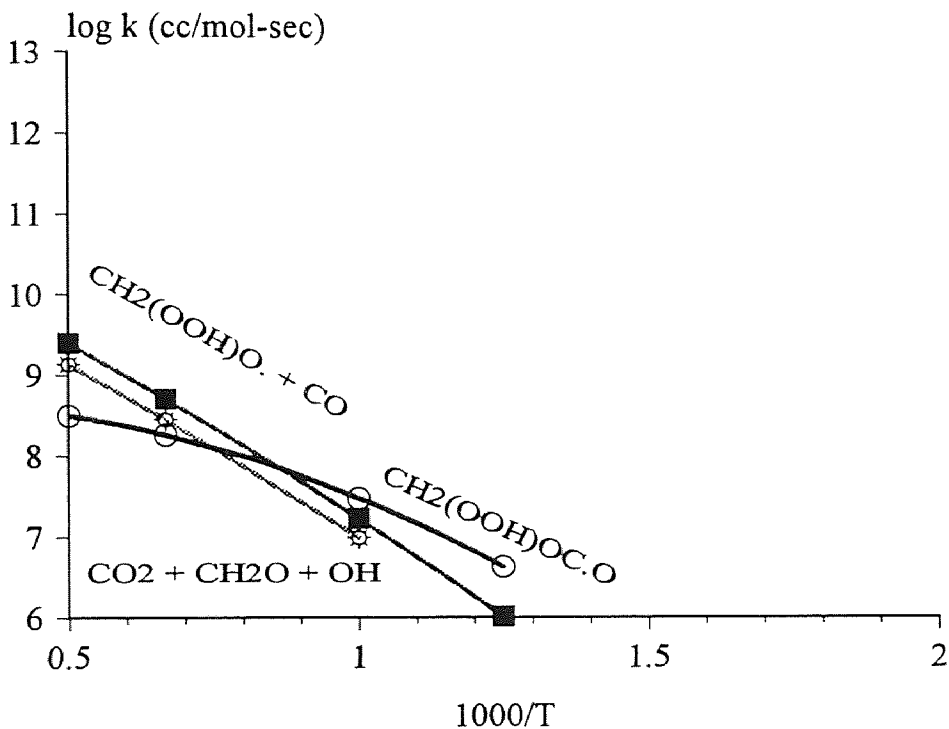
Figure 2.11 k vs. Temperature (1 atm)
CH2(OO.)OCHO --> products
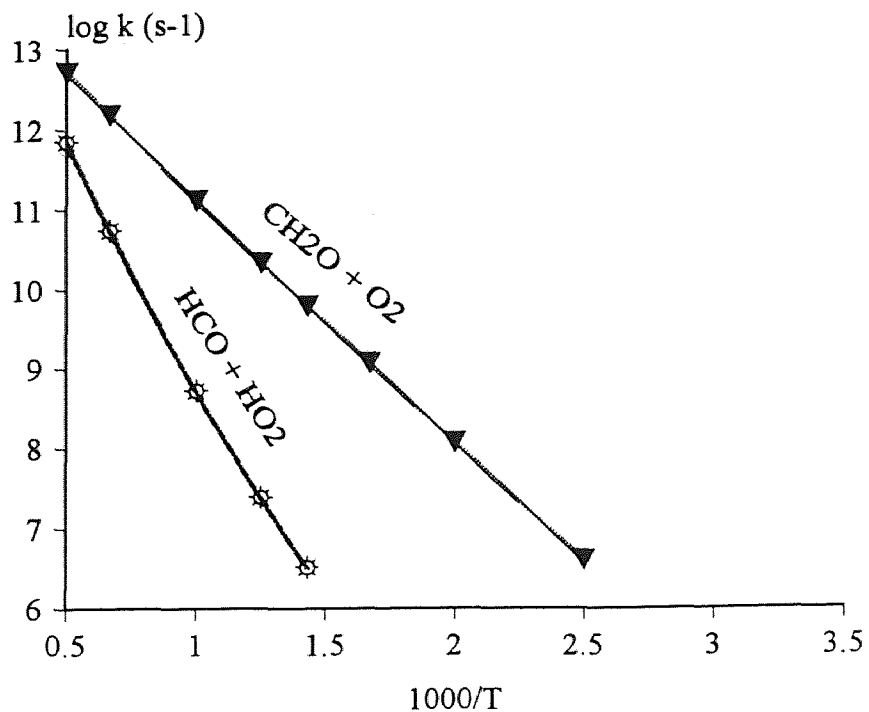
Figure 2.12 k vs. Temperature (1 atm)
CH2O.(OO.) --> Products
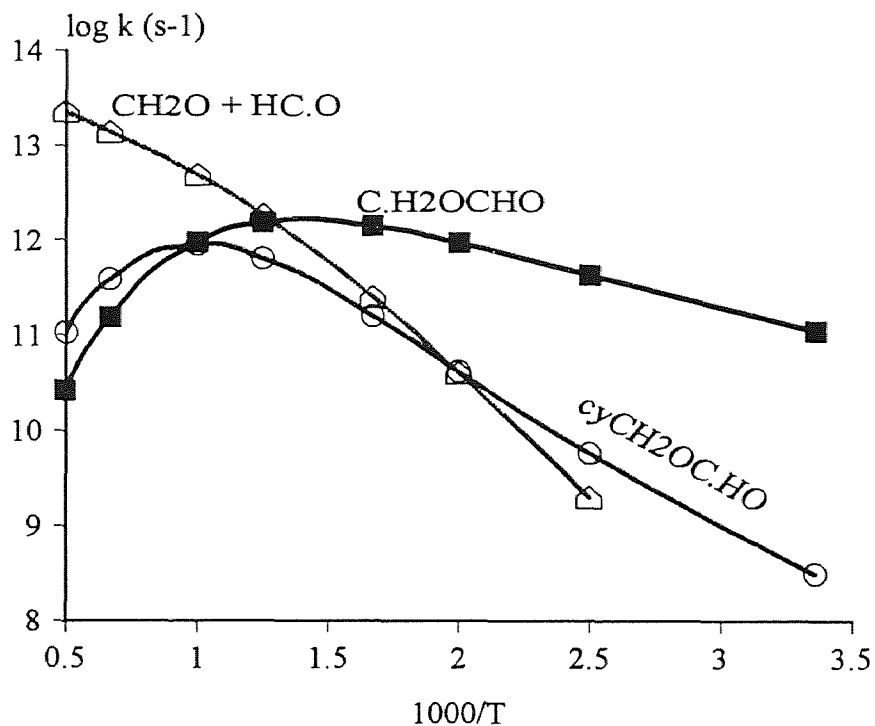
Figure 2.13 k vs. Temperature (1 atm)
cyCH2OC.HO --> C.H2OCHO --> CH2O + HC.O

2.3.7 Dimethyl-ether and Dimethyl-ether Radical Dissociation Reactions

High Pressure Limit Rate Constant as QRRK Input Parameters.

i) $CH_3OCH_3 \overset{k_{20}}{\Rightarrow} CH_3O\bullet + CH_3$
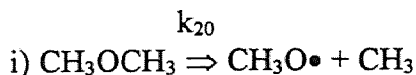
The high pressure limit A_{20} is estimated as 2.10E+16 s^{-1} from A_{-20} and MR. A_{-20} is

adopted from Tsan's study, A = 1.21E+13 $cm^3/(mol\ s)$[38].

ii) $CH_3OCH_3 \overset{k_{21}}{\Rightarrow} C\bullet H_2OCH_3 + H$
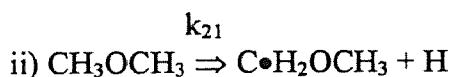
High pressure limit A_{21} is estimated as 1.03E+16 s^{-1} from A_{-21} and MR. A_{-21} is adopted

from Allara et al.'s study, A = 1.00E+14 $cm^3/(mol\ s)$[39].

iii) $CH_3OCH_3 \overset{k_{22}}{\Rightarrow} CH_2O + CH_4$
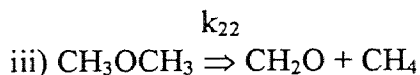
High pressure limit A_{22} is estimated as 1.10E+10 s^{-1} based on TST[13]. $\Delta S^{\neq}_{298}$ is

determined by S°_{298} of CH_3OCH_3 obtained from literature[25] and S°_{298} of TS obtained

from Nash et. al.'s TS geometry and frequencies determined by MP2/6-311G(2df,2p)

level of calculation[36]. There is no rotational contribution for entropy. $E_{a,22}$ is estimated

as 89.3 kcal/mol based on CCSD(T)/6-311++G(3df,3pd)//MP2/6-311G(2df,2p) level of

calculation by Nash et al.[36].

iv) $C\bullet H_2OCH_3 \overset{k_{23}}{\Rightarrow} CH_2O + CH_3$
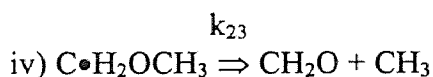
High pressure limit A_{23} is estimated as 3.94E+11 s^{-1} based on TST[13]. $\Delta S^{\neq}_{298}$ is

calculated based on CBS-q calculation and Pitzer et al.'s general treatment of hindered

internal rotation contribution for entropy[10]. The MP2(full)/6-31G(d,p) determined

geometry and frequencies which are scaled by 0.9608[11] are used to calculate S°_{298} of

reactant, $C \cdot H_2OCH_3$ and TS, CH_2O—CH_3. $E_{a,23}$ is estimated as 25.7 kcal/mol based on

CBS-q calculation. The MP2(full)/6-31G(d,p) determined geometries are used for the

CBS-q energy calculations. The Z.P.V.E.'s and thermal corrections to 298.15 K for

$\Delta H_f^{\circ}{}_{298}$ estimations are incorporated as described in Chapter 1. QRRK inputs and their

results for above four dissociation reactions are tabulated in Table 2.13and 2.14

respectively.

Table 2.13 Input Parameter for QRRK Calculations and the Results of Apparent Rate Constants: Dimethyl-ether and Radical Dissociation

Input parameters for QRRK Calculations (T = 298 K)			
	High Pressure Limit Rate Constants		
Reaction	A(s-1 or cm3/(mol s)	n	Ea(kcal/mol)
20 $CH_3OCH_3 \Rightarrow CH_3O\bullet + CH_3$	2.10E+16	0.00	82.0
21 $CH_3OCH_3 \Rightarrow C\bullet H_3OCH_3 + H$	1.03E+16	0.00	95.0
22 $CH_3OCH_3 \Rightarrow CH_2O + CH_4$	1.10E+10	1.22	89.3
23 $C\bullet H_2OCH_3 \Rightarrow CH_2O + CH_3$	3.94E+11	0.73	26.1

Frequencies/Degeneracies: 635.8 cm^{-1}/7.937, 1878.7 cm^{-1}/9.590, 3509.4 cm^{-1}/2.473
Lennard-Jones Parameters: σ=5.18Å, $\in$/k=357.0 K. The Units of A factors and rate
constasnts k are s^{-1} for unimolecular reactions and cm^3/(mol s) for bimolecular reactions.
Bath Gas = Ar

k_{20} Microscopic Reversibility (MR) Af/Ar=5.752E-4 $E_{a,20}=\Delta H-RT$. A_{-20} from Tsang
et al.[26]

k_{21} Microscopic Reversibility (MR) Af/Ar=9.372E-3 $E_{a,21}=\Delta H-RT$. A_{-21} from Allara
et al.[39]

k_{22} A_{22} from TST, $\Delta S^{\neq}{}_{298}$ from Nash et al.[36], calculated using their geometry and
frequencies determined by MP2/6-311G(2df,2p) level of calculation. $E_{a,22}$ from
Nash et al. based on CCSD(T)/6-311++G(3df,3pd)//MP2/6-311G(2df,2p) level of
calculation[36]. All three parameters A, n, and E_a are fit over the temperature range
of 300 to2,000K.

k_{23} A_{23} is calculated using TST and entropy of transition state (TS1), $\Delta S^{\neq}{}_{298}$ from
MP2(full)/6-31G(d,p) (see Table 2.2 (b)), $E_{a,23}$ from CBS-q calculation. All three
parameters A, n, and E_a are fit over the temperature range of 300 to2,000K.

Table 2.14 QRRK Calculation Results: Dimethyl-ether and Radical Dissociation

Calculated Apparent Reaction Parameters at P=1 atm, $k=A(T/K)^n(-E_a/RT)$(Temp=298 - 2000K)

Reaction	A	n	Ea	k_{973} (s^{-1} or cm^3/(mol s))
21 $CH_3OCH_3 \Rightarrow CH_3O + CH_3$	9.93E+30	-4.71	86.4	3.27E-03
21 $CH_3OCH_3 \Rightarrow C \bullet H_3OCH_3 + H$	8.03E+23	-2.52	97.4	3.13E-06
22 $CH_3OCH_3 \Rightarrow CH_2O + CH_4$	1.58E+12	0.53	90.0	3.68E-07
23 $C \bullet H_2OCH_3 \Rightarrow CH_2O + CH_3$	1.74E+47	-11.0	35.4	2.63E+06

2.3.8 H atom Abstraction Reactions (Dimethyl-ether Radical Formation)

$$k_{24}$$
i) $CH_3OCH_3 + H \Rightarrow C \bullet H_2OCH_3 + H_2$

$$k_{25}$$
ii) $CH_3OCH_3 + O \Rightarrow C \bullet H_2OCH_3 + OH$

$$k_{26}$$
iii) $CH_3OCH_3 + OH \Rightarrow C \bullet H_2OCH_3 + H_2O$

$$k_{27}$$
iv) $CH_3OCH_3 + CH_3 \Rightarrow C \bullet H_2OCH_3 + CH_4$
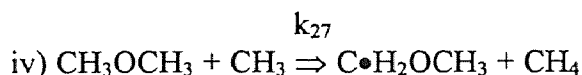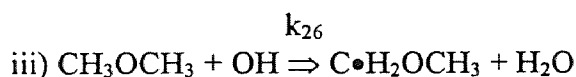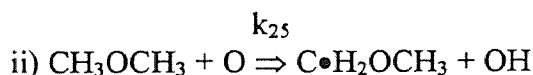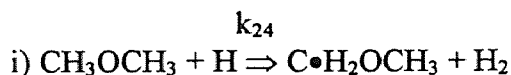
High pressure limit A, n and E_a values for H atom abstraction reactions (dimethyl-ether

radical formation) by H, O, OH and CH_3 are tabulated in Table 2.16.

$$k_{28}$$
v) $CH_3OCH_3 + CH_3O \bullet \Rightarrow C \bullet H_2OCH_3 + CH_3OH$
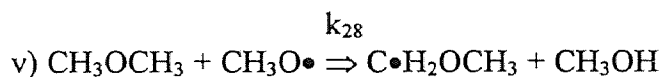
High pressure limit A_{28} and $E_{a,28}$ for H atom abstraction by methoxy radical are obtained

from those of $CH_3OH + CH_3O \bullet \Rightarrow C \bullet H_2OH + CH_3OH$ reported by Tsang, A=3.01E+11

and 4.07 kcal/mol[40]. The degeneracy factor, 2, is taken into account, since there are two

methyl group in dimethyl-ether.

$$k_{29}$$
vi) $CH_3OCH_3 + HO_2 \Rightarrow C\bullet H_2OCH_3 + H_2O_2$
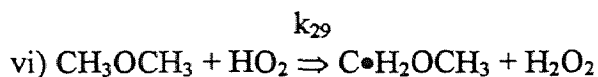
High pressure limit A_{29} and $E_{a,29}$ for H atom abstraction by hydroperoxy radical is

obtained from those of $CH_3OH + HO_2 \Rightarrow C\bullet H_2OH + H_2O_2$ reported by Tsang,

$A=9.64E+10$ $cm^3/(mol\ s)$ and $E_a=12.58$ kcal/mol[40]. The degeneracy factor, 2, is taken

into account.

$$k_{30}$$
vii) $CH_3OCH_3 + O_2 \Rightarrow C\bullet H_2OCH_3 + HO_2$
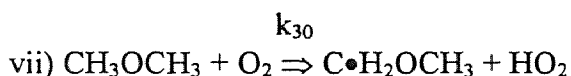
High pressure limit A_{30}, n and $E_{a,30}$ for H atom abstraction by oxygen molecule is

obtained from those of isobutane $+ O_2$ studied by Chen et al., $A=4.77E+5$ $cm^3/(mol\ s)$,

$n=2.69$ and $E_a=40.04$ kcal/mol[41]. Those numbers are tabulated in Table 2.16.

**Table 2.15 Parameters for Rate Constant Determination
of H Atom Abstractions**

R$\bullet$	A	n	E_0	ΔH_0	f
H	2.4E+8	1.5	7.4	-3.1	0.65
O	1.7E+8	1.5	5.8	-1.1	0.75
OH	1.2E+6	2.0	0.9	-18.3	0.50
CH3	8.1E+5	1.87	10.6	-3.7	0.65

Table 2.16 A, n, and E$_a$ for H atom abstraction Reactions

	Reaction	A (cm$_3$/(mol-sec))	n	E$_a$ (kcal/mol)	k$_{973}$ cm$_3$/(mol s)
24	CH$_3$OCH$_3$ + H $\Rightarrow$ C•H$_2$OCH$_3$ + H$_2$	1.44E+9	1.5	4.23	4.90E+12
25	CH$_3$OCH$_3$ + O $\Rightarrow$ C•H$_2$OCH$_3$ + OH	1.02E+9	1.5	2.18	1.00E+13
26	CH$_3$OCH$_3$ + OH $\Rightarrow$ C•H$_2$OCH$_3$ + H$_2$O	7.20E+6	2.0	0.00	6.82E+12
27	CH$_3$OCH$_3$ + CH$_3$ $\Rightarrow$ C•H$_2$OCH$_3$ + CH$_4$	2.43E+6	1.87	8.20	1.35E+10
28	CH$_3$OCH$_3$ + CH$_3$O• $\Rightarrow$ C•H$_2$OCH$_3$ + CH$_3$OH	6.02E+11	0.00	4.07	7.33E+10
29	CH$_3$OCH$_3$ + HO$_2$ $\Rightarrow$ C•H$_2$OCH$_3$ + H$_2$O$_2$	1.93E+11	0.00	12.58	2.88E-3
30	CH$_3$OCH$_3$ + O$_2$ $\Rightarrow$ C•H$_2$OCH$_3$ + HO$_2$	3.18E+5	2.69	40.04	3.52E+4

k$_{28}$ A$_{28}$ and E$_{a,28}$ is obtained from Tsang[38], CH$_3$OH + CH$_3$O• $\Rightarrow$ C•H$_2$OH + CH$_3$OH. The degeneracy factor 2 is taken into account.

k$_{29}$ A$_{29}$ and E$_{a,29}$ is obtained from Tsang[38], CH$_3$OH + HO2 $\Rightarrow$ C•H$_2$OH + H$_2$O$_2$. The degeneracy factor 2 is taken into account.

k$_{30}$ A$_{30}$ and E$_{a,30}$ is obtained from Chen et al.[41], isobutane + O$_2$ $\Rightarrow$ C•H$_2$C(CH$_3$)$_2$ + HO$_2$. The degeneracy factor 2/3 is taken into account.

2.4 Summary

H atom abstraction reaction from dimethyl-ether by several major radicals, and dimethyl-ether and dimethyl-ether radical dissociation reactions are studied. The further reaction of one important product (stabilized adduct) from the reaction of dimethyl-ether radical with O$_2$, C•H$_2$OCH$_2$OOH with molecular oxygen is also analyzed.

Group additivity[13,31], PM3[32] in MOPAC6[33] and *ab initio* calculations are used to estimate the thermodynamic properties of reactants, intermediate radicals, TS compounds and products. QRRK analysis is used to calculate energy dependent rate constants, k(E), with modified strong collision approach of Gilbert et al.[19] for fall-off.

In the reaction of C•H$_2$OCH$_2$OOH + O$_2$, the stabilization reaction to form CH$_2$(OO•)OCH$_2$OOH dominates at low temperature below 670 K and the reverse reaction dissociation back to reactants, C•H$_2$OCH$_2$OOH + O$_2$, dominates at high temperature at 1 atm.

CHAPTER 3

DIMETHYL-ETHER OXIDATION AND PYROLYSIS EXPERIMENT (773 K TO 1073 K): COMPARISON WITH MODEL

3.1 Experimental Method

3.1.1 Experimental Conditions

The oxidation and pyrolysis of dimethyl-ether is analyzed in a tubular flow reactor by varying temperature, residence time and fuel equivalence ratio. A temperature range from 773 to 1073 K is covered at points of 773, 823, 873, 923, 973, 1023 and 1073 K. Residence time ranges from 1.0 to 2.0 seconds with data points at 1.0, 1.25, 1.5, 1.75 and 2.0 sec. Four fuel to oxygen reaction ratios: pyrolysis, fuel rich (ϕ = 1.5), stoichiometry (ϕ = 1.0) and fuel lean (ϕ = 0.75) are studied using a uniform temperature tubular flow reactor. ϕ is fuel equivalence ratio; it is the ratio of fuel/O_2 for run conditions over the ratio fuel/O_2 stoichiometric.

3.1.2 Experimental Apparatus

A diagram of the experimental apparatus is shown in Figure 3.1.1. Dimethyl-ether is 99.5 % purity supplied by Liquid Carbonic Co. Argon and oxygen are reagent grade, 99.996 and 99.6 % purity respectively, supplied by PRAXAIR. Argon flow is used as make-up gas to achieve the 0.5 % dimethyl-ether concentration. Argon, Dimethyl-ether and oxygen flows are mixed in this respective order and controlled by a Hoke 3.2 mm needle valve, a Porter Instrument VCD-1000 controller and a Brooks Model 8744A flow control respectively. The mixed reactants are preheated to about 100 °C to prevent condensation and to improve reactor temperature control.

A 18.6 mm ID quartz tube by 100 cm long is employed as the reactor, which is housed within 63.5 cm length of a three-zone Clamshell 3.2 cm ID electric tube furnace equipped with three independent Omega Model CN-310 digital temperature controllers. A bypass line for reactant gas flow around the heated reactor is used to determine the initial concentration of reactants without going through the high temperature reactor.

Gas samples are drawn through the GC gas sampling port by means of a mechanical vacuum pump with a constant flow rate of 30 cm^3/min. The remaining 90-98 % of the total flow exits through a line to fume hood. A HP5890 Series II Gas Chromatography with two Flame Ionization Detectors is used on-line for analysis. Inlet to the GC is through gas sample valves with 1 ml heated sample loops. GC/MS (HP5890 Series II Gas Chromatography / HP5988A Mass Spectrometer (Quadrupole)) analysis is also performed on batch samples to identify and confirm gas species.

3.1.3   Temperature Control and Measurement

Temperature profile versus reactor length are obtained at each flow using a type K thermocouple probe moved axially within the 100 cm length reactor. Temperature control results in temperature profiles isothermal to within ± 5 °C over 60 % of the furnace length for each temperature.

3.1.4   Qualitative Analysis Using GC/MS

16.3 cm × 3.2 mm stainless steel tubing packed by Hayesep T (80/100 mesh) is used as a sampling tube. The gases after the combustion with fuel rich condition (ϕ=1.5) at 973 K and atmospheric pressure for 2 second is flowed into this sampling tube. The sampling

tube is cooled under -50 °C using cryogenic trap (Flexi-Cool FC-20-40-P3BF). The gas sample is trapped for 2 minutes at 50 cc/min flow rate. Two valves are mounted on the end of the 3.2 mm tube to isolate the sample.

The sampling tube is then connected directly to 6 port valve on the GC/MS to use as sampling loop as shown in Figure 3.1.2. The sampling tube is heated to 110 °C for 3 minutes before the valves on the both ends are opened. The sampling gas in the sampling loop is injected into GC column for two minutes. 10 cm × 1.6 mm steel tubing packed by HayeSep T (80/100) is used for separation with 1 ml/min N_2 carrier flow. Temperature program is used for the gas separation. Initial temperature is set as 35 °C for 5 min and temperature is increased by 8 °C/min up to 110 °C. The separated gases are then carried into quadrupole mass spectrometer and analyzed.

3.1.5   Qualitative and Quantitative Analysis Using GC

A HP-5890 Series II Gas Chromatograph with two parallel columns and Flame Ionization Detectors is used on-line to determine the concentration of reactants and products. Two six port VALCO gas sampling valves are employed to introduce the gas samples into the GC columns. Gas samples are passed through two sampling loops (1.0 cm^3 volume) in parallel at a constant flow rate of 30 cm^3/min, and then the valves are switched and the gases in the loop are injected into packed columns on the GC.

Two packed columns are used for separation. Two 180 cm × 3.2 mm stainless steel columns are packed with 80/100 HayeSep T and 80/100 Carbosphere for the separation of light hydrodcarbons, and CO, CO_2 and CH_2O respectively.

CH_2O is expected to be produced in dimethyl-ether pyrolysis and oxidation based on the model, and detailed chemical analysis of its reactions (see Chapter 1). Carbosphere is chosen as the stationary phase in qualitative and qualitative GC analysis of CH_2O because the retention time of the CH_2O is close but still fully separated from the un nown source gas contaminant. The CH_2O pea will overlap the pea of the un nown, if Hayesep T is used. Details and results on analysis of the contaminant in the source dimethyl-ether are discussed in this chapter.

In order to increase the accuracy of quantitative analysis for CO, CO_2 and CH_2O, a catalytic converter is connected in series after Carbosphere column with 5 % of 80/100 ruthenium on alumina catalyst. H_2 reactant is used to convert the CO, CO_2 and CH_2O to methane over the catalyst after separation in the converter. The temperature of catalyst is ept with 300 C to obtain the maximum conversion rate of CO, CO_2 and CH_2O to CH_4. A temperature program is used for this COx sample gas separation. The initial temperature is set as 50 C for 5 minutes and temperature is increased by 6 C/min up to 110 C.

Signal from the two FIDs, Hayesep T and Carbosphere, are integrated by Varian 2 0 and Spectra-Physics SP 2 0 integrators respectively.

Calibration for obtaining appropriate molar response factors and retention times of relevant compounds is performed by injecting nown concentrations of standard gases. The average retention times and relative response factors are shown in Table 3.1 and 3.2 for Hayesep T and Carbosphere respectively. Three point calibrations are used to identify dimethyl-ether concentration and expressed as follows:

$$X = 10^{\wedge}((\log(Y) - 8.2891)/0.9692) \qquad\text{---------}\qquad (1)$$

where X = concentration of dimethyl-ether, Y = Peak Area.

3.1.6   Qualitative and Quantitative Analysis on Dimethyl-ether Source Gas Contaminant Identified by GC/MS

The dimethyl-ether source gas is found to be contaminated via GC-FID analysis. It is critical to qualitate and quantitate this unknown to determine if it effects our experimental results. GC-FID analysis indicated the unknown is either formaldehyde, propane, or propene; retention times of these species are very close to the retention time of the unknown, if Hayesep T is used.

The source gas (Dimethyl-ether, 99.5% purity, Liquid Carbonic) is collected in the sampling bag (232-01 Sampling Bag, SKC Inc.) and injected into GC of the GC/MS. The sample gas is separated through a packed column (180 cm × 3.2 mm tubing packed by Hayesep T 80/100 Mesh) with 30 ml/min N_2 carrier flow. The flow is then split to 1 ml/sec using jet splitter before entering mass spectrometer source. A temperature program is used for the sample gas separation on the GC. Column initial temperature is set as 35 °C for 5 min and temperature is increased by 8 °C/min up to 110 °C.

3.2 Experimental Results

3.2.1 Temperature Control and Measurement

Temperature profiles, 773 to 1073 K (displayed as Celsius) are shown in Figures 3.1.3 to 3.1.7 for total gas flow corresponding to reaction times of 2.0 to 1.0 s respectively. There is small temperature decrease (c.a. 5 to 6 °C) due to slight separation in the electric tube furnace between central zone and end zones.

72
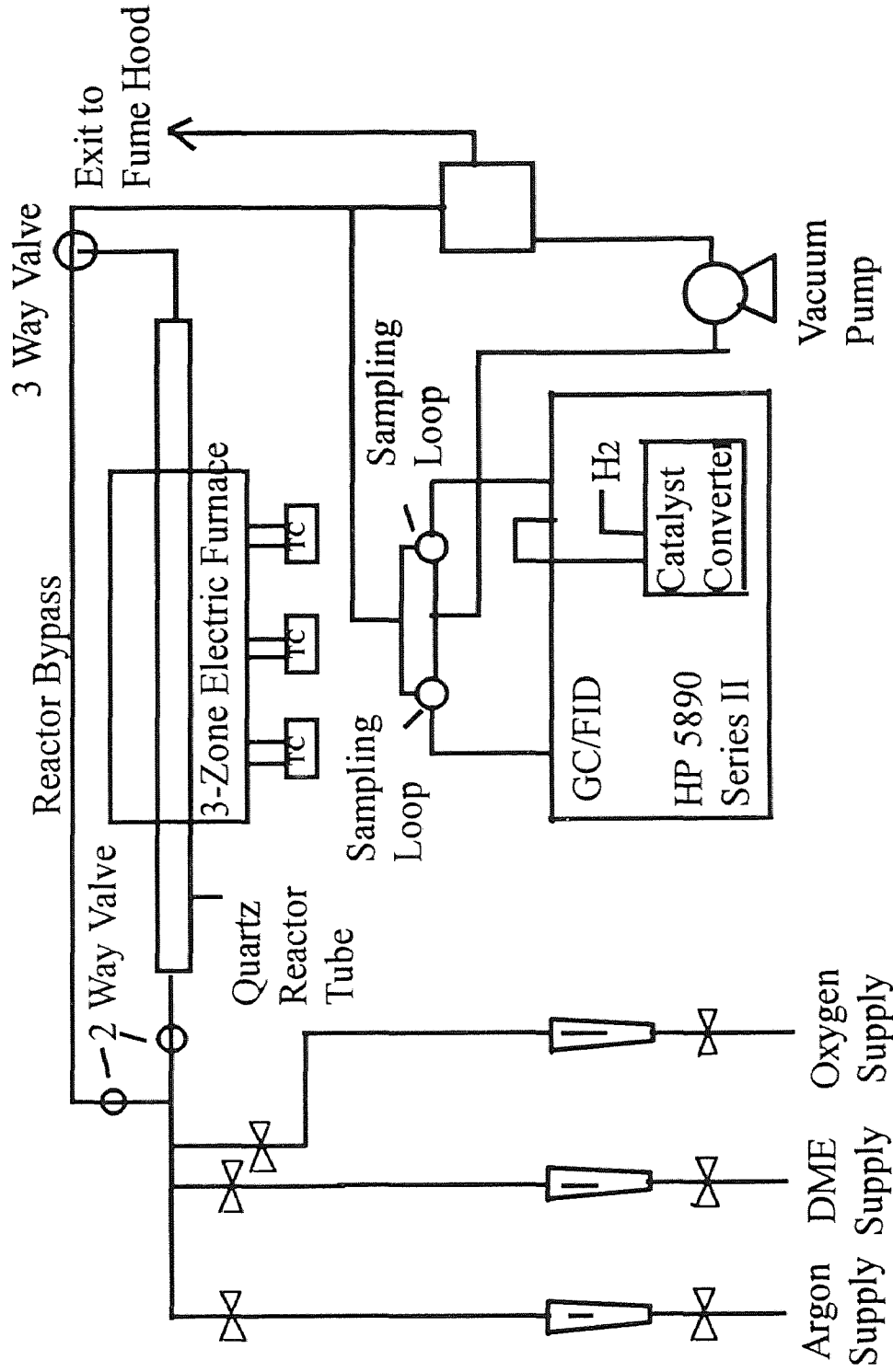
Figure 3.1.1 Experimental System

Sampling Tube

& Sample Loop
16.3 cm × 3.2 mm HayaSep T (80/100)
Packed Column

Column

Vacuum

N₂ (Carrier Gas)

Load
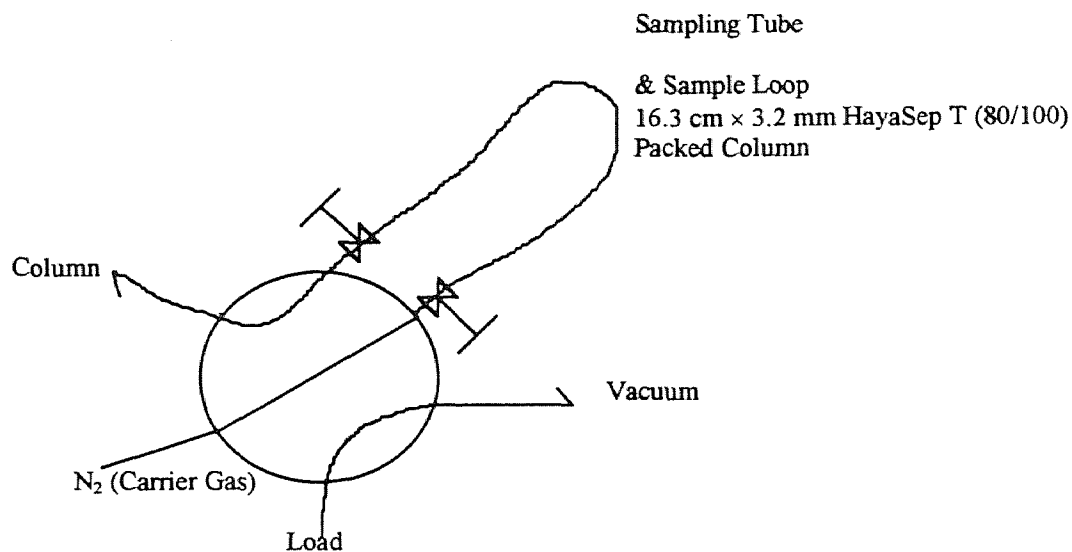
Figure 3.1.2 Sampling Tube Installation as Sample Loop (Inject Position) For GC/MS Analysis

Temperature (C)

Axial Distance (inches)

◾T=800 ✹T=750 �---T=700 ⬠T=650 ▲T=600 ◆T=550 ⟻T=500
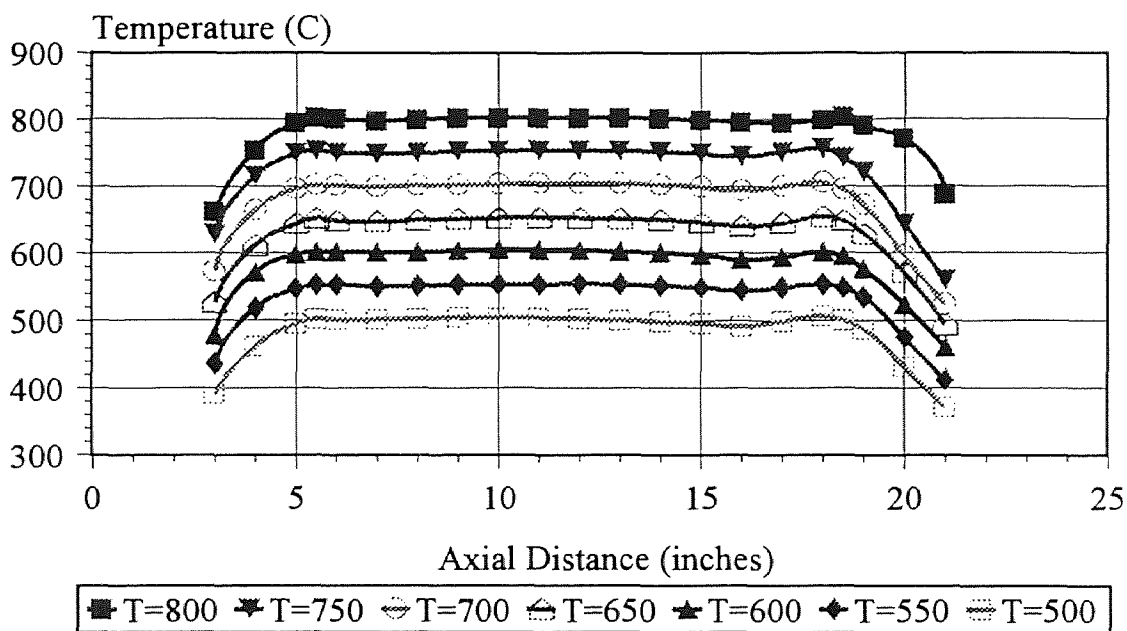
Figure 3.1.3 Temperature Profile (RT=2.0)
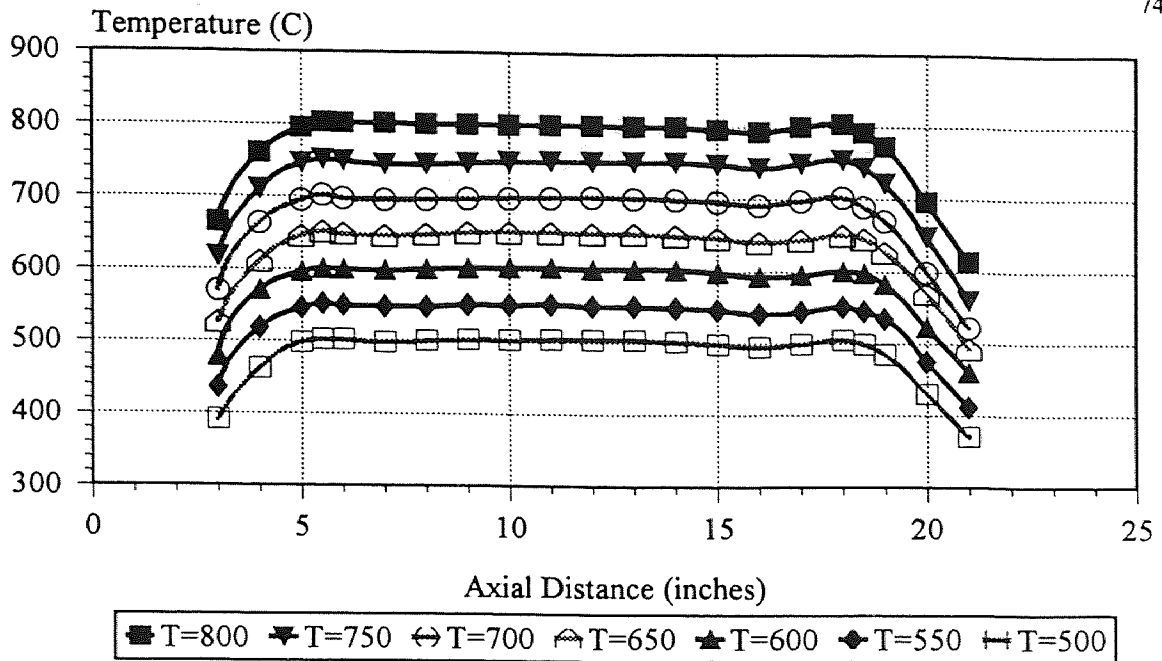
Figure 3.1.4 Temperature Profile (RT=1.75)
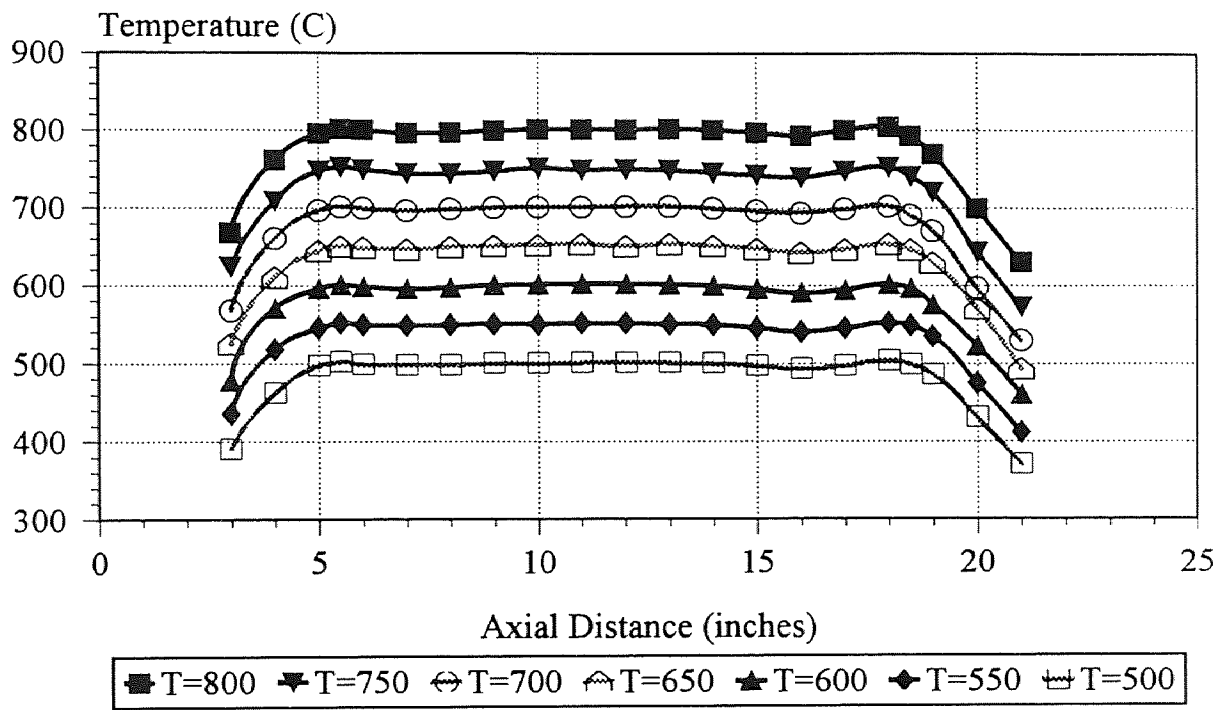
Figure 3.1.5 Temperature Profile (RT=1.5)
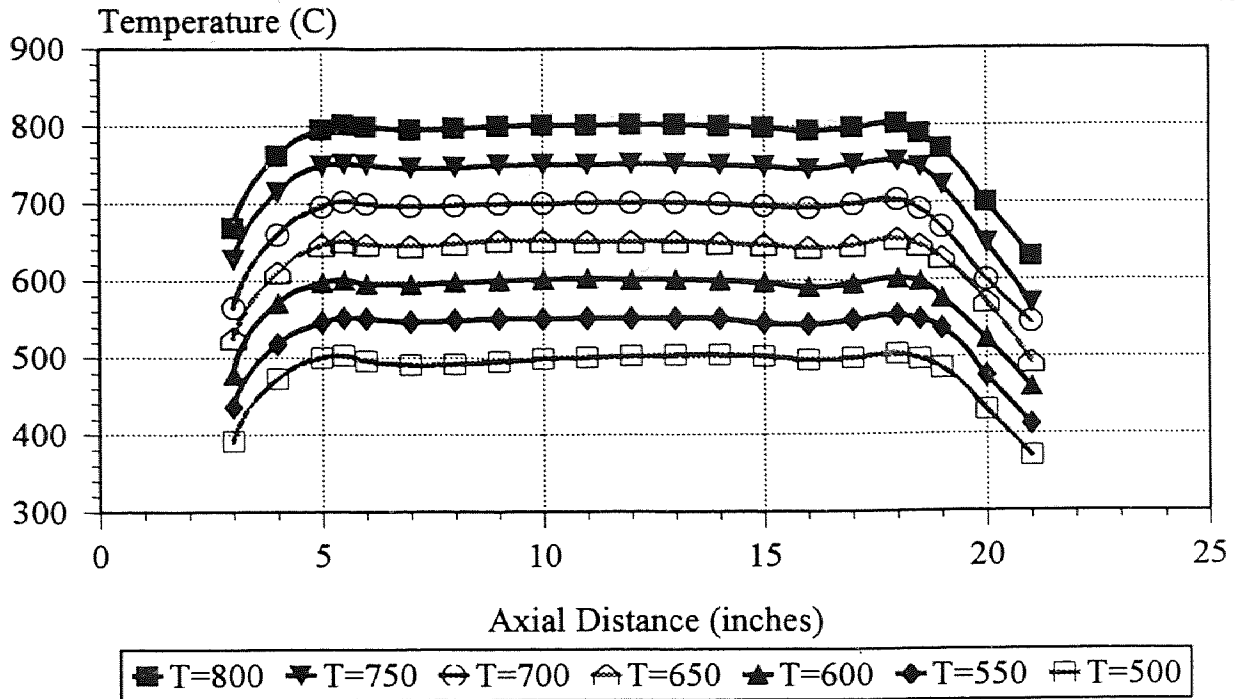
Figure 3.1.6 Temperature Profile (RT=1.25)
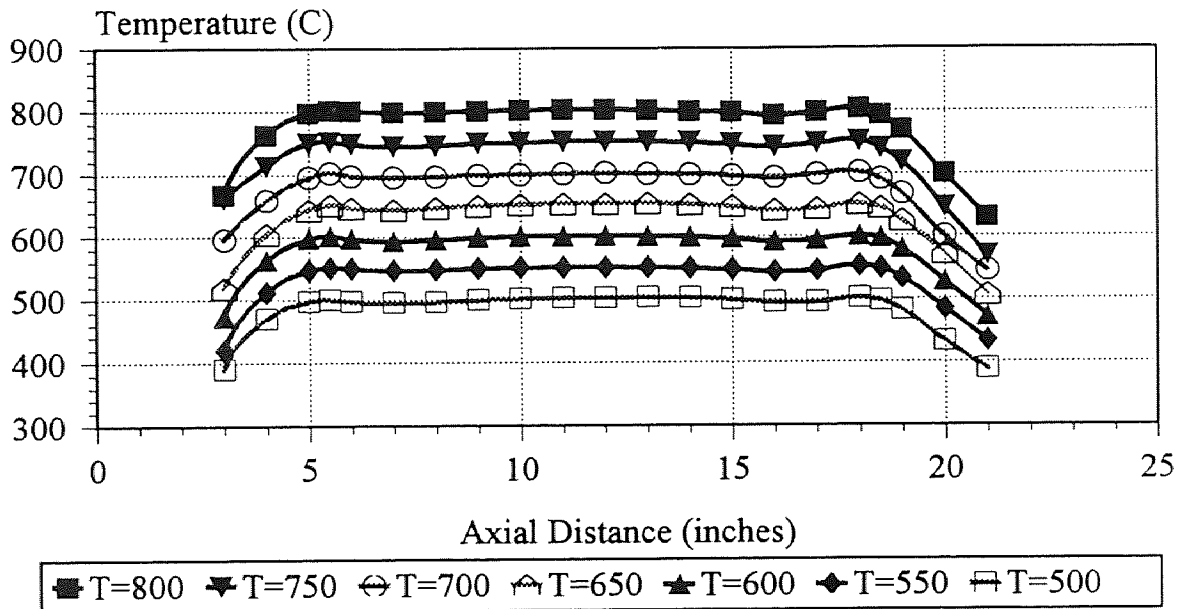
Figure 3.1.7 Temperature Profile (RT=1.0)

3.2.2 Qualitative and Quantitative Analysis on Dimethyl-ether Source Gas Contaminant Using GC/MS

Figure 3.2.1 shows GC chromatogram of dimethyl-ether from purchased compressed gas cylinder where signal between 11 to 15 minutes is magnified by the factor of 100. The small peak at 13.0 min, which is magnified by 100, is the unknown contaminant and second large peak at 15.7 min, which is no magnification, is dimethyl-ether. Figure 3.2.2 shows the spectra of magnified small peak with the background subtraction. The mass spectra result indicates that the unknown peak is propene. The mass 41 is propene radical and the mass 27 is vinyl radical (C_2H_3), which is one of the major fragments of propene. Since only mass over 20 are scanned, another major fragment, methyl radical $m/z=15$ is not shown. The GC-FID analysis on diluted dimethyl-ether (0.5 %) shows the concentration of propene is 2.59 ppm, which is close to detection limit of FID. The concentration of contaminant before dilution is estimated as 518 ppm. Since propene is not incorporated into the reaction mechanism, the modeling comparison with and without propene had not been performed. The model is exercised with ethane as surrogate for propene. Model results showed no effect from this concentration of ethane.

3.2.3   Qualitative Analysis Using GC/MS

Figure 3.2.3 shows the GC peaks on results of dimethyl-ether oxidation products (Reactor Temperature=973 K, Pressure=1 atm, fuel equivalence ratio=1.5 and reaction time=2 sec). The GC peaks at reaction times of 4 to 35 minutes are magnified by 50. Figures 3.2.4 and 3.2.5 show the time average mass spectra at 1.22 to 1.30 minutes and 2.12 to 2.43 minutes respectively. According to these spectra and their intensity, these are peaks of GC carrier gas nitrogen and the reactor carrier gas argon respectively.
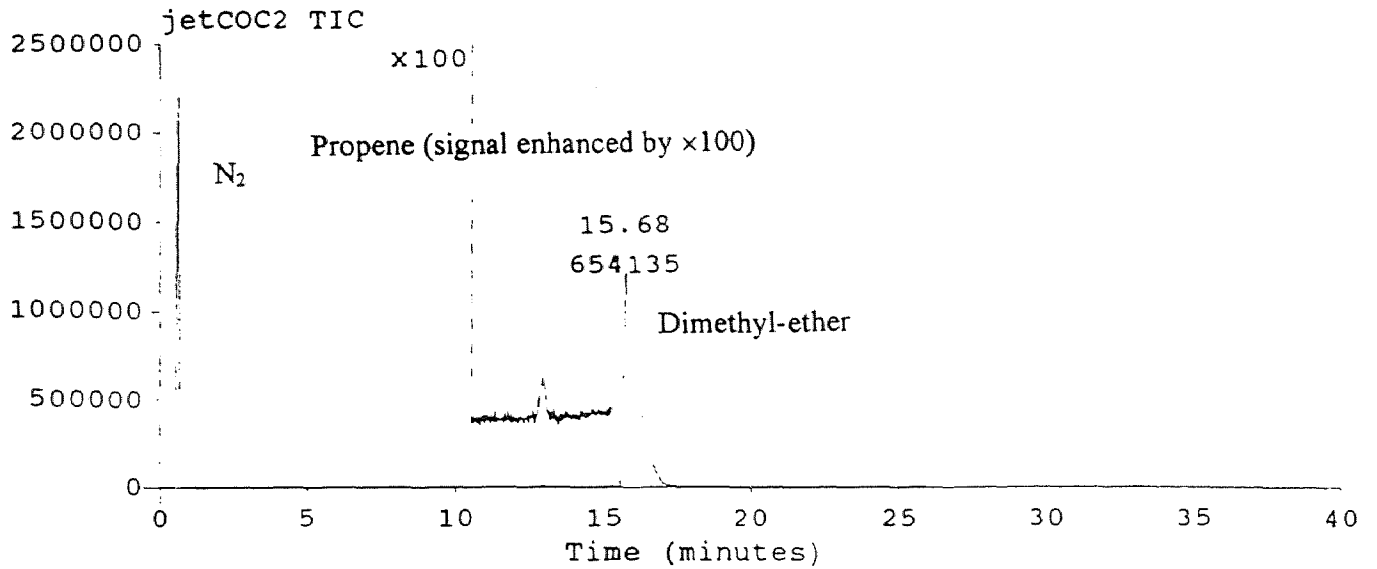
Figure 3.2.1 GC-FID Results on Dimethyl-ether Contaminant Analysis
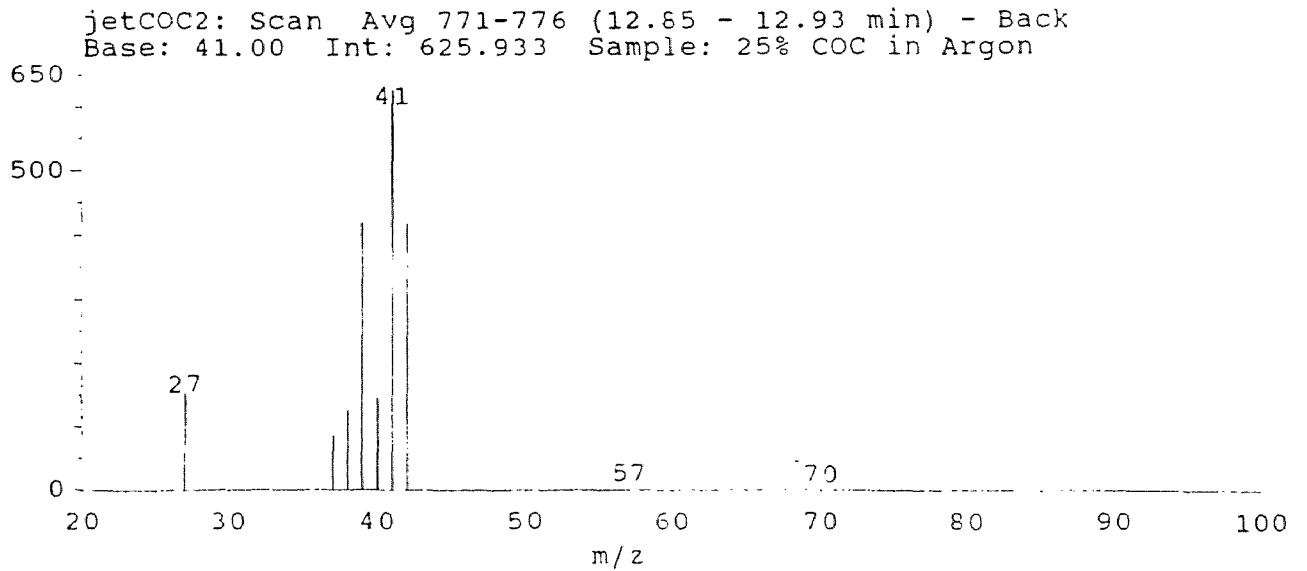
Figure 3.2.2 Dimethyl-ether Contaminant Mass Spectra

Signal enhanced by × 50
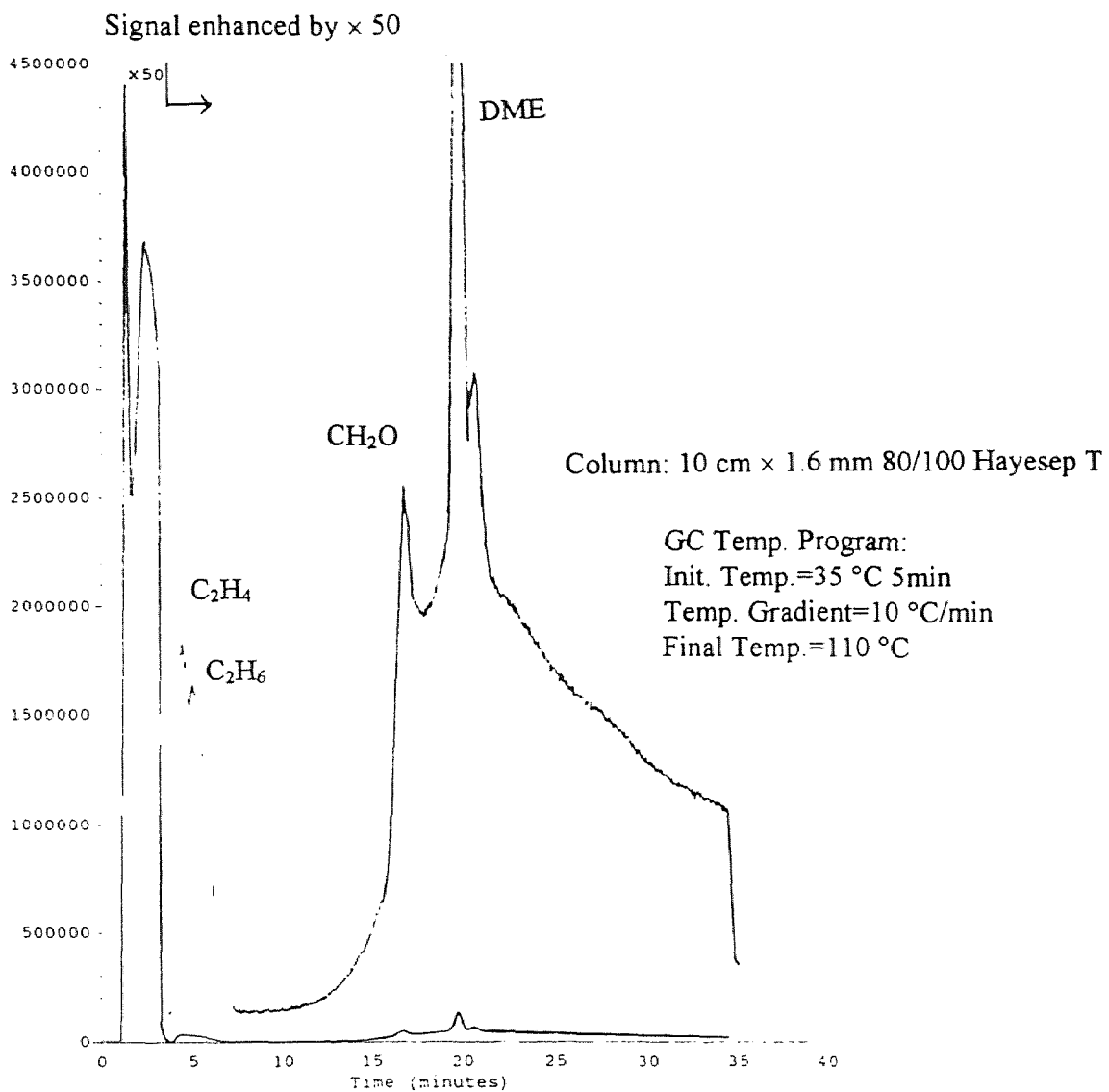
Figure 3.2.3 GC-FID Results on Dimethyl-ether Oxidation Products Analysis

0518dmel: Raw Bin Avg 127-146 (2.12 - 2.43 min)
Base: 40.00 Int: 1.46317e+006 Sample: coc 700

Figure 3.2.5 Mass Spectra (2.12-2.43 min without background subtraction)

0518dmel: Raw Bin Avg 73-78 (1.22 - 1.30 min)
Base: 28.00 Int: 2.14872e+006 Sample: coc 700

Figure 3.2.4 Mass Spectra (1.22-1.30 min without background subtraction)

Table 3.1 Average Retention Time and Relative Response Factors for Stainless Steel

Column (180 cm × 3.2 mm) Packed with 80/100 HayeSep T

Compound	Retention Time (min)	Relative Response Factor (RRF)
CH_4	0.70	1.00
C_2H_2	7.03	1.82
C_2H_4	2.95	1.97
C_2H_6	3.46	1.99
CH_3OCH_3	15.75	---

Table 3.2 Average Retention Time and Relative Response Factors for Stainless Steel Column (180 cm × 3.2 mm) Packed with 80/100 Carbosphere

Compound	Retention Time (min)	Relative Response Factor (RRF)
CO	1.25	0.944
CH_4	2.66	1.00
CO_2	7.29	0.883
CH_2O	17.86	0.944

Figure 3.2.6 shows the average spectra at 4.15 to 4.47 minutes without background spectra subtraction. These spectra indicate the combination of spectra from C_2H_4, CO_2, CO and CH_4. The intensity of mass 28 for C_2H_4 is supposed to be about twice as high as mass 27. The reason why the intensity of mass 28 is unusually large is because CO_2 fragment and CO spectra are present. Figure 3.2.7 shows the average spectra at 4.15 to 4.32 minutes with background spectra subtraction. The valley between two peaks in Figure 3.2.3 (around 5 minutes) is taken as a background. This spectra is combination of CO and CO_2, because CO_2 spectra does not have mass 12. Figure 3.2.8 shows the average spectra at 4.80 to 5.20 minutes without background subtraction. The spectra pattern around mass 28 and mass 14 indicate C_2H_4. Mass 44 is for CO_2. Figure 3.2.9

shows the average spectra at 4.97 to 5.17 minutes with background subtraction and the

pattern indicates the molecular is C_2H_6.

Figures 3.2.10 and 3.2.11 show average spectra around 16 minutes without and with

background subtraction respectively. These spectra indicate dimethyl-ether,

formaldehyde and H_2O. The mass spectra near $m/z = 18$ is for H_2O, $m/z = 29$ is for

formaldehyde and $m/z=45$ is for dimethyl-ether. The mass spectra in Figure 3.2.11,

where the background signal is subtracted, validates that this peak is formaldehyde.

Figures 3.2.12, 3.2.13 and 3.2.14, 3.2.15 show the average spectra around 19 minutes and

20 minutes without and with background subtraction respectively. These results indicate

the peak at 19 minutes is dimethyl-ether and that at 20 minutes is H_2O. The small peak

of mass 59 is shown in Figures, 3.2.12, 3.2.14 and 3.2.15. It might be ethyl, methyl-

ether, since it is possible to form this compound in dimethyl ether oxidation reaction:

$C \bullet H_2OCH_3 + CH_3 \Rightarrow CH_3OCH_2CH_3$.

3.2.4 Qualitative and Quantitative Analysis Using GC

Pyrolysis

Experimental results on dimethyl-ether pyrolysis are shown in Figures C.1 to C.6 for the

temperature of 823,873, 923, 973, 1023 and 1073 K respectively. No reaction is

observed at the temperature of 773 K. The data indicates that the important stable species

formed from dimethyl-ether decay are CH_4 and CO and initial reaction occurs on decay

of dimethyl-ether to produce CH_4 and CO and that these stable products decay slowly.

Only slight concentration change is observed versus reaction time for these compounds

through the temperature range of 823 to 1073 K. CO and CH_4 are observed throughout
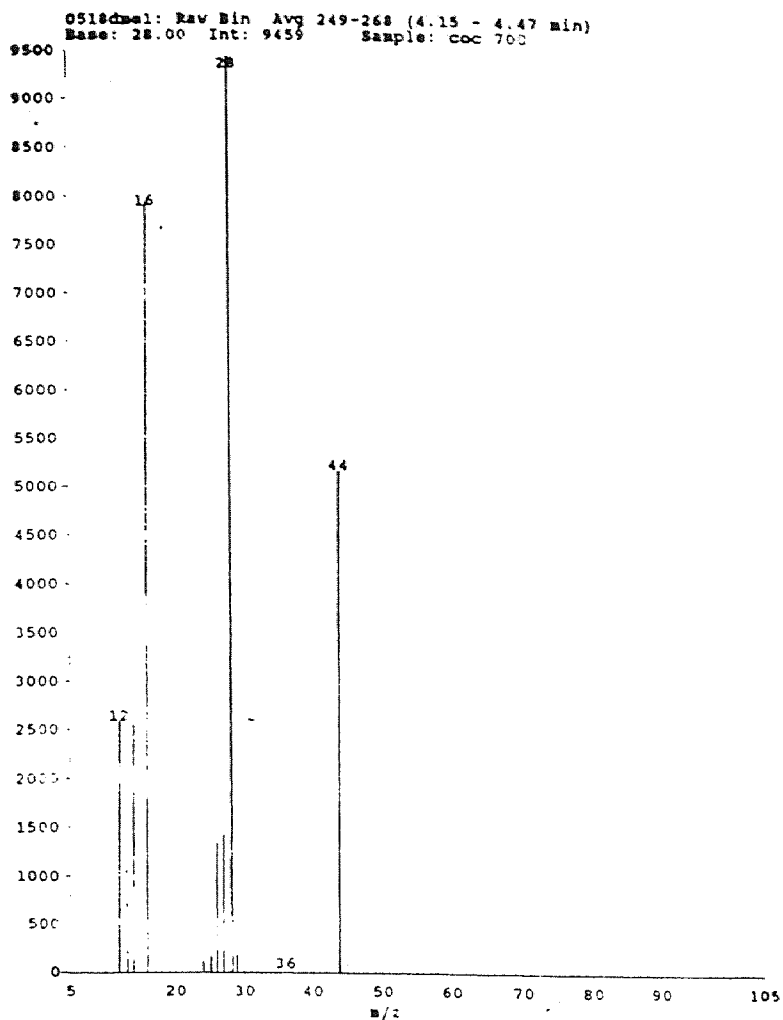
Figure 3.2.6 Mass Spectra (4.15–4.47 min without background subtraction)
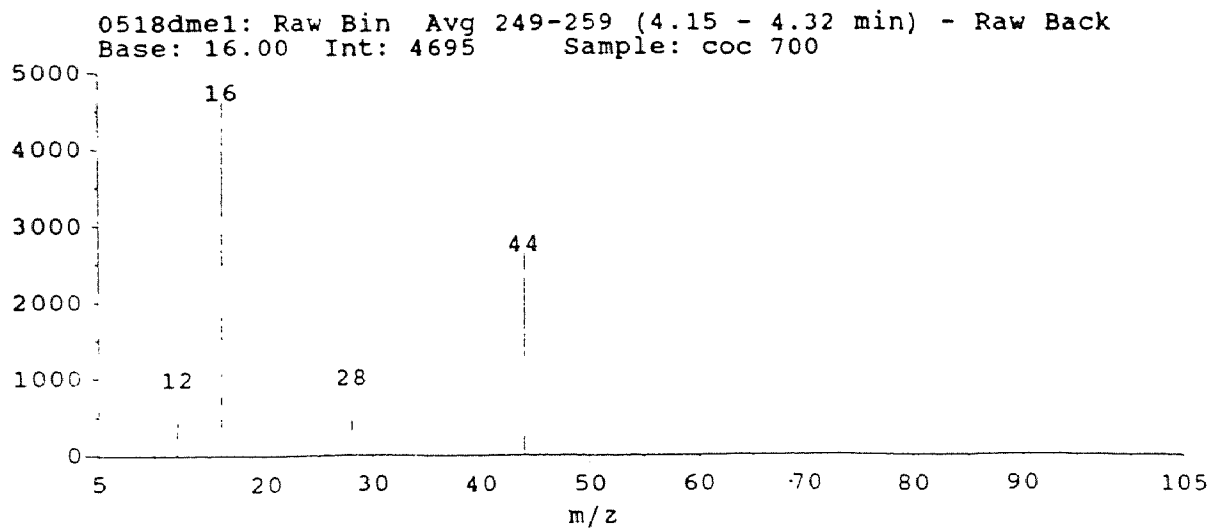
Figure 3.2.7 Mass Spectra (4.15–4.32 min with background subtraction)

0518dmel: Raw Bin Avg 288-312 (4.80 - 5.20 min)
Base: 28.00 Int: 8472 Sample: coc 700
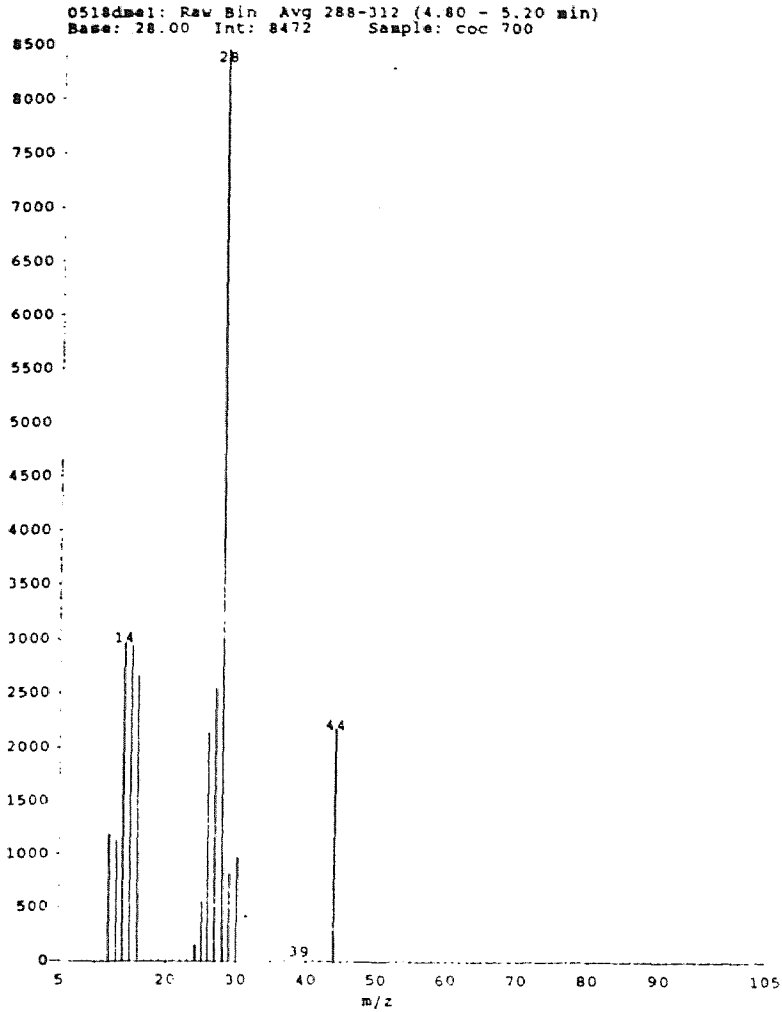
Figure 3.2.8 Mass Spectra (4.80-5.20 min without background subtraction)

0518dmel: Raw Bin Avg 298-310 (4.97 - 5.17 min) - Raw Back
Base: 15.00 Int: 2591 Sample: coc 700
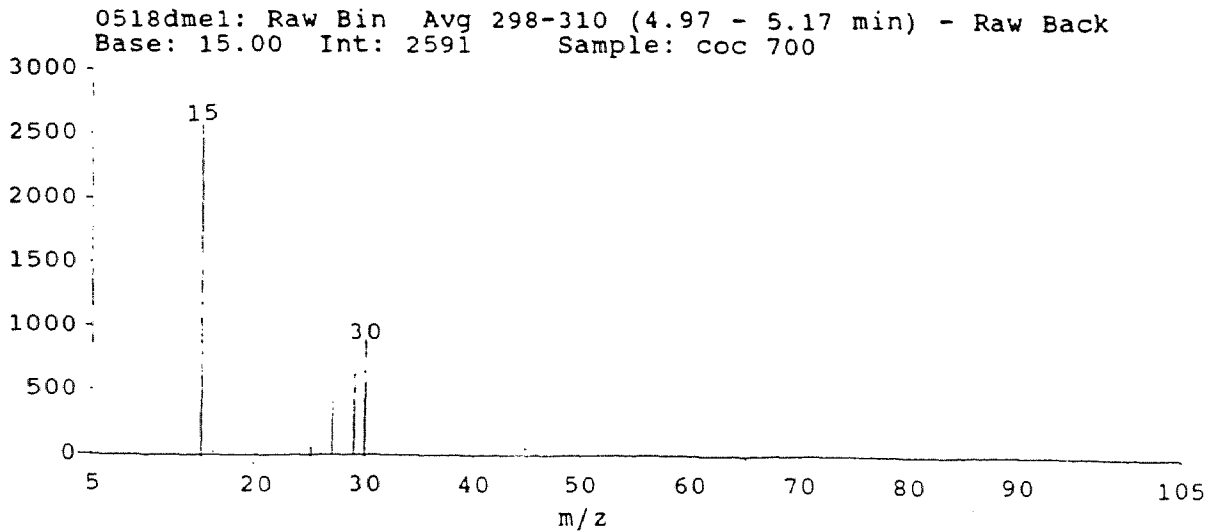
Figure 3.2.9 Mass Spectra (4.97-5.17 min with background subtraction)

0518dme1: Raw Bin Avg 990-1015 (16.50 - 16.92 min)
Base: 29.00 Int: 10662 Sample: coc 700
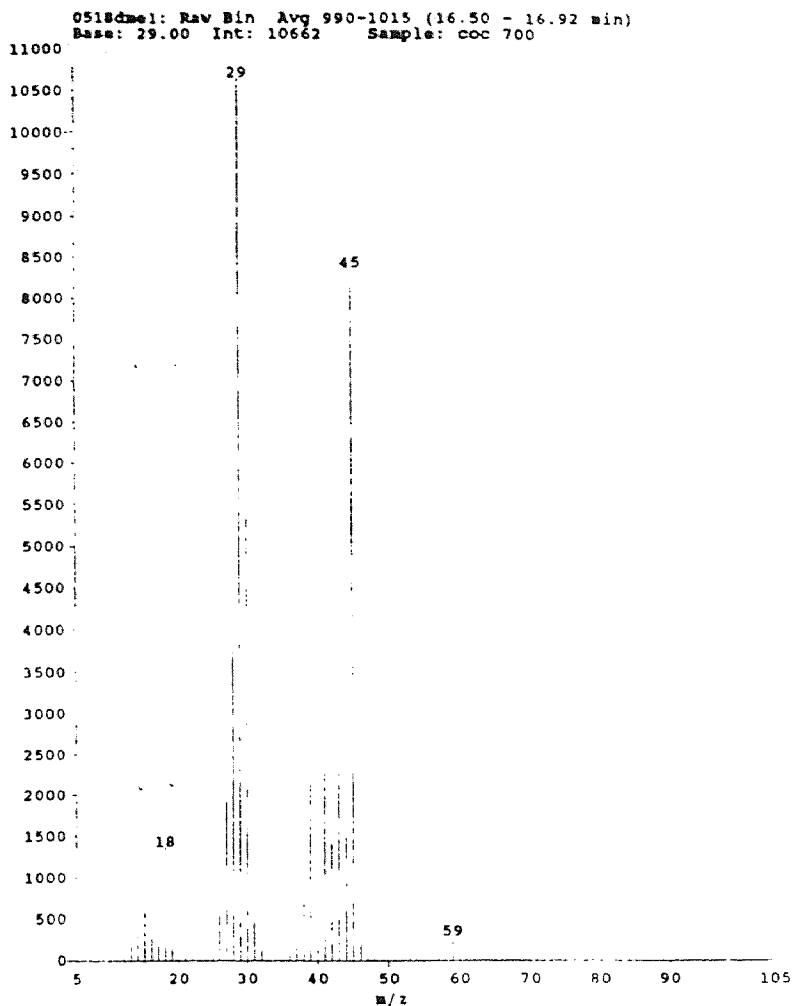
Figure 3.2.10 Mass Spectra (16.50-16.92 min without background subtraction)

0518dme1: Raw Bin Avg 995-1005 (16.58 - 16.75 min) - Raw Back
Base: 29.00 Int: 4834 Sample: coc 700
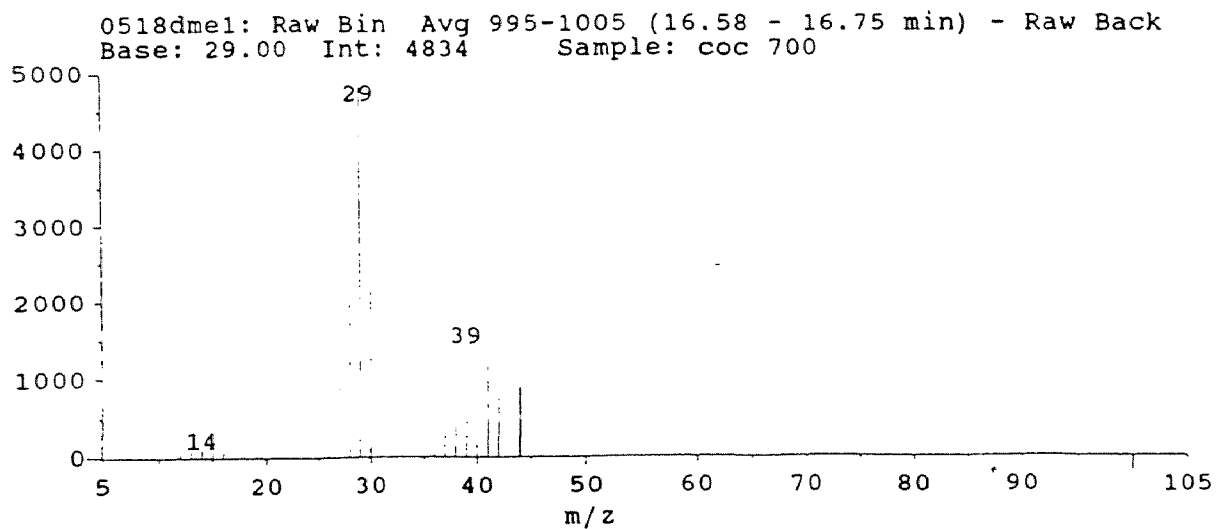
Figure 3.2.11 Mass Spectra (16.58-16.75 min with background subtraction)
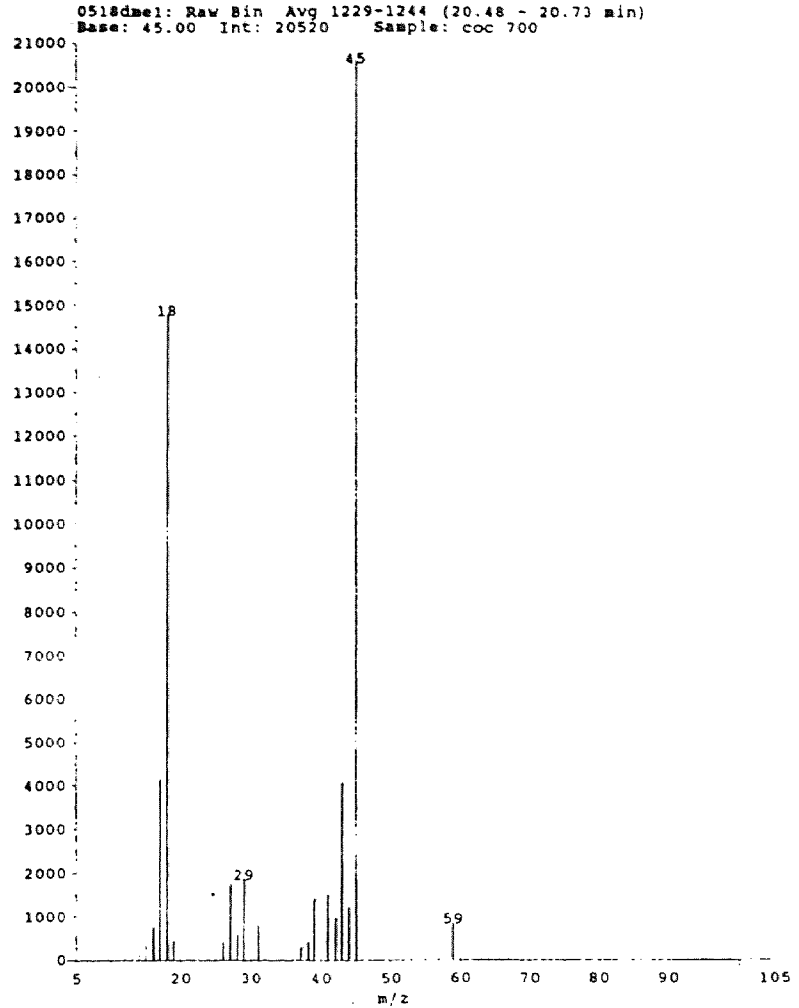
Figure 3.2.12 Mass Spectra (19.52-19.83 min without background subtraction)
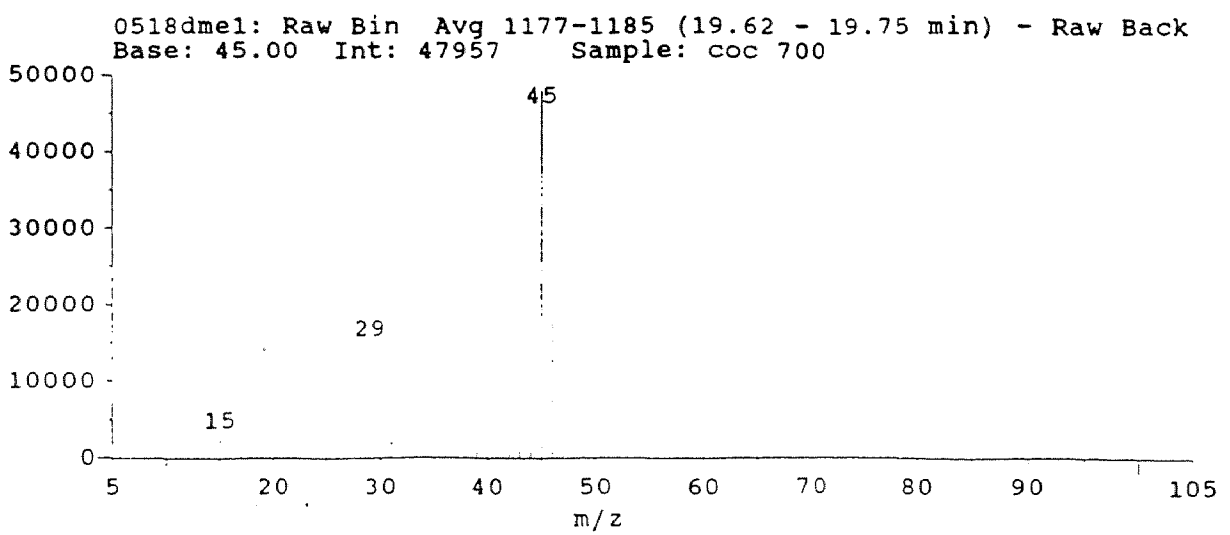
Figure 3.2.13 Mass Spectra (19.62-19.75 min with background subtraction)
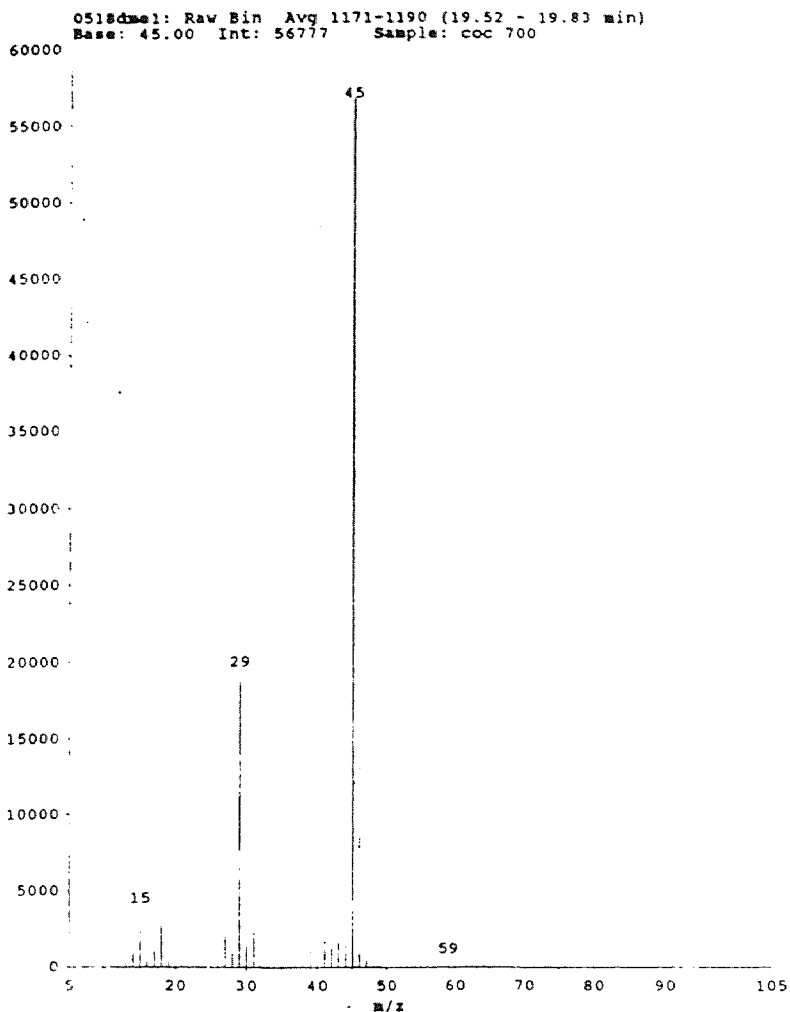
Figure 3.2.14 Mass Spectra (20.48-20.73 min without background subtraction)
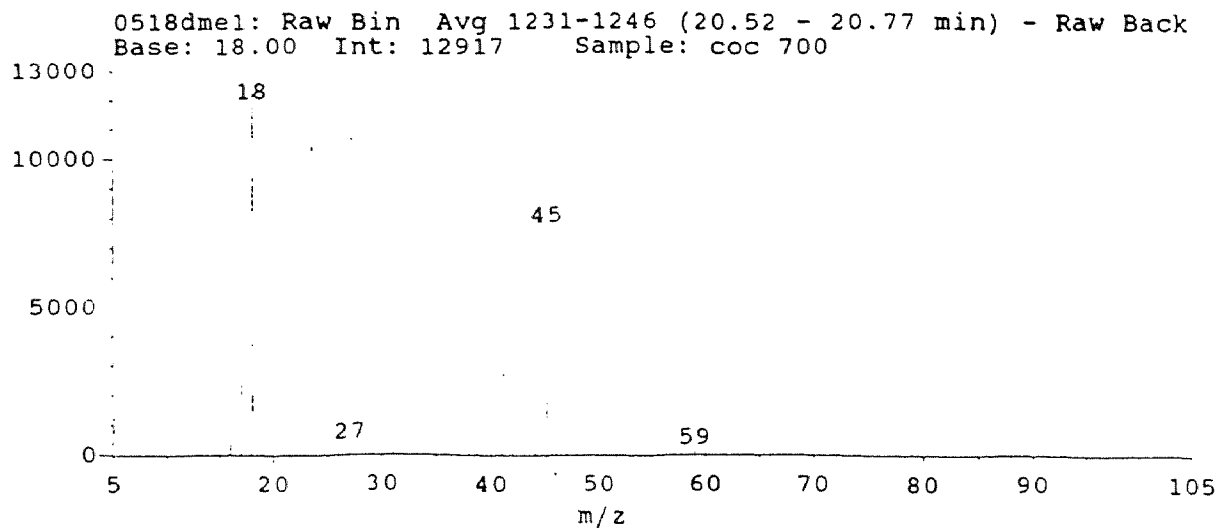
Figure 3.2.15 Mass Spectra (20.52-20.77 min with background subtraction)

the temperature range of 773 to 1073 K and their concentrations increases with temperature. C_2H_6 and CH_2O are observed at 823 K and above. Concentrations of C_2H_6 and CH_2O increase with temperature to 1023 K, then CH_2O decreases at 1073 K and above. C_2H_4 is observed at the temperature of 973 K or higher and its concentration increases with temperature; C_2H_4 is a product of C_2H_6 decay. C_2H_2 is observed only at the temperature of 1073 K, and is a product of C_2H_4 decay under pyrolysis conditions.

Fuel Rich Condition (ϕ = 1.5)

Experimental results on oxidation reaction under fuel rich condition are shown in Figures C.7 to C.13 for the temperatures of 773, 823, 873, 923, 973, 1023, and 1073 K respectively. Little or no dimethyl-ether decay is observed below 923 K. Dimethyl-ether concentration decreases from 3.5×10^{-3} to 8.8×10^{-5} (mole fraction) with reaction time (1 to 2 sec) at 973 K. The concentration of CH_4 increases with temperature and reaction time to 973 K, the maximum concentration of 2×10^{-3} (mole fraction) at T=973 K and 2 sec, then decreases with increased temperature and time. CO concentration increases with temperature. Its concentration dramatically increases with reaction time (1 to 2 sec), 6×10^{-4} to 6×10^{-3} (mole fraction) at 973 K. CO shows a maximum concentration (c.a. 8 $\times 10^{-3}$ mole fraction) at 1073 K. The concentration of CH_2O is about 1.0×10^{-4} (mole fraction) at temperatures to 923 K. The maximum concentration of CH_2O is 5.3×10^{-4} (mole fraction) at 973 K and reaction time of 1.25 sec. CH_2O concentration decreases with reaction time and no CH_2O is observed at the reaction time of 2 sec at 973 K. CH_2O is not observed at temperatures above 973 K. The concentration of C_2H_6 increases with temperature to 973 K. The maximum concentration is 2.1×10^{-4} (mole fraction) at 973 K

and reaction time of 1.25 sec. C_2H_6 decreases with temperature and reaction time above 973 K. The concentration of C_2H_4 increases with temperature to 1023 K. The maximum concentration is 2.8×10^{-4} (mole fraction) at 1023 K and reaction time of 1.0 sec.

Stoichiometric Condition ($\phi = 1.0$)

Experimental results on oxidation at stoichiometric reaction condition are shown in Figures C.14 to C.18 for temperatures of 773, 823, 873, 923 and 973 K respectively. Dimethyl-ether is completely destroyed to CO_2 at temperatures of 1023 and above. Mass balance at 1023 K and above shows 100 % of dimethyl-ether is converted to CO_2. Initial dimethyl-ether is 5.0×10^{-3} and CO_2 at 1023 K and above is 1.0×10^{-2} mole fraction. A very little dimethyl-ether decay is observed at the temperature below 823 K. Dimethyl-ether concentration decreases with temperature and reaction time at 923 and 973 K. The concentration of CH_4 increases to 1.8×10^{-3} (mole fraction) with increase of temperature and reaction time to 973 K and 1.25 sec, then CH_4 decreases with increase of reaction time. CH_4 is not observed at 973 K and 2 sec. The concentration of CO increases to 6.6 $\times 10^{-3}$ (mole fraction) with increase of temperature and reaction time to 973 K and 1.5 sec. CO decreases with increase of reaction time. CO_2 is initially observed at 823 K and all temperatures above. CO_2 concentration increases slowly with time at 973 K then rapidly increases between 1.75 to 2 sec. CH_2O concentration increases to 6.7×10^{-4} (mole fraction) with time at both 873 and 923 K. CH_2O decreases with time at 973 K with no CH_2O observed at 1.75 and 2.0 sec. at this temperature. C_2H_6 increases to 1.7×10^{-4} (mole fraction) with temperature and reaction time at 923 K. C_2H_6 decreases with reaction time with no C_2H_6 observed at 973 K and 2.0 sec. C_2H_4 is observed at both 923

K and 973 K. C_2H_4 increases to 2.1×10^{-4} (mole fraction) with temperature and reaction

time to 973 K and 1.5 sec. C_2H_4 decreases with reaction time. C_2H_4 is not observed at

973 K and 2 sec.

Fuel Lean Condition ($\phi = 0.75$)

Experimental results on oxidation reaction under fuel lean conditions are shown in

Figures C.19 to C.23 for the temperature of 773, 823, 873, 923 and 973 K respectively.

All of dimethyl-ether is destroyed to CO_2 at 1023 K. Only slight dimethyl-ether decay

(c.a. 20 %) is observed below 923 K. Dimethyl-ether concentration decreases with

temperature and reaction time at 923 and 973 K. Dimethyl-ether is all reacted at 973 K

and the reaction time of 2 sec. CH_4 concentration increases to $1.63 \times$

10^{-3} (mole fraction) with temperature and reaction time to 923 K. CH_4 then decreases

with time and no CH_4 is observed at 1.5 sec or longer at 973 K. CO concentration

increases to 7.3×10^{-3} (mole fraction) with temperature and time to 973 K and 1.25 sec.

CO then decreases and no CO is observed at 1.5 sec or longer at 973 K.

The CO_2 concentration increases dramatically between 1.25 and 1.5 sec. CH_2O is

observed in the mole fraction range of 1.0×10^{-4} to 10^{-3} below 973 K. CH_2O

concentration decreases with the time at 973 K and no CH_2O is observed at 1.5 sec or

longer at 973 K. The C_2H_6 concentration increases to mole fraction 1.7×10^{-4} with

temperature and time to 923 K. C_2H_6 concentration decreases with time and no C_2H_6 is

observed at 1.5 sec or longer at 973 K. C_2H_4 is observed at 923 and 973 K. C_2H_4

increases with time at 923 K and then decreases with time. C_2H_4 is not observed at 1.5

sec or longer at 973 K.

3.3 Model Comparison with Experiment

The experimental results are compared with a detailed reaction mechanism model, which

is assembled in this work and described in Table B.2. The computer code CHEMKIN II

[42] is used for numerical integration. Temperature of 873, 973 and 1073 K are selected

for the comparison with pyrolysis because no reaction occurs at 773 K. Temperature of

773, 873 and 973 K are selected for the comparison with oxidation reaction (ϕ = 1.5, 1.0

and 0.75) because only CO_2 is observed under oxidation condition at temperature above

973 K.

Pyrolysis

Figures C.24 to C.26 show the model comparison with experimental data under pyrolysis

at 873, 973 and 1073 K respectively. The model data on dimethyl-ether decay

underestimates by 50 % at 1073 K. The model data on CH_4 formation predicts the data

accurately. The model data on CO formation predicts correctly at 973 and 1073 K but

underestimates by the factor of ten at 873 K. The model data on CH_2O formation shows

the correct trends but overestimates the data by only 50 and 20 % at 973 and 1073 K

respectively. The model data on C_2H_4 formation underestimates the data by factors of

three and four at 973 and 1073 K respectively. The model data on C_2H_6 formation

underestimates by factor of two at 973 K but predicts correctly at 1073 K.

Fuel Rich Condition (ϕ = 1.5)

Figures C.27 to C.29 show the model comparison with experimental data under fuel rich

conditions (ϕ = 1.5) at 773, 873 and 973 K respectively. The model data on dimethyl-

ether decay and CH_4 formation data predict correctly at all temperatures. The model data on CO formation predicts well at 973 K, but does not fit at 773 K, factor of 100. The model data on CO_2 formation predicts correctly at 973 K, but does not fit at 873 K, factor of 100. The model data on CH_2O formation predicts correctly at 973 K, but underestimates by factor of 3 at 773 K and overestimates by factor of 2 at 873 K. The model data on C_2H_6 formation predicts well at 973 K, but underestimates by factor of 2 at 773 and overestimates by factor of 2 at 873 K. The model data on C_2H_4 formation underestimates by factor of 2 at 973 K.

Stoichiomerty Condition ($\phi = 1.0$)

Figures C.30 to C.32 show the model comparison with experimental data under stoichiometric condition ($\phi = 1.0$) at 773, 873, 973 K respectively. The model data on dimethyl-ether shows steep concentration drop at 1.5 sec and 973 K, while experimental results show slow decay. The model data on CH_4 formation predicts well, but decay is slightly earlier in the model than in the experiment at 973 K. The model data on CO formation predicts the experimental results well, where concentration increase with reaction time to 1.5 sec, then rapidly decrease at 973 K. The model data on CO formation underestimates by factor of ten and two at 773 and 873 K respectively. The model data on CO_2 formation shows rapid concentration increase at 1.7 sec and 973 K, while experimental results show rapid increase after 1.75 sec still the CO_2 formation profile is well predicted. The model data on CH_2O formation also predicts correctly at 873 and 973 K. The model data on CH_2O formation underestimates by factor of two at 773 K. The model data on C_2H_6 formation underestimates by factor of four to five at all

temperature between 773 to 973 K. The model data on C_2H_6 and C_2H_4 show rapid concentration decrease at 1.5 sec and 973 K, while experimental results show the corresponding decrease between 1.75 and 2.0 sec later in time than model.

Fuel Lean Condition ($\phi = 0.75$)

Figures C.33 to C.35 show the model comparisons with experimental data under fuel lean condition ($\phi = 0.75$) at 773, 873 and 973 K respectively. The model data on dimethyl-ether shows steep concentration decrease at 973 K between 1.25 and 1.5sec, while experimental results show slow decay. The model data on CH_4 formation accurately predicts. The model predicts CO formation accurately at 973 K, where the large concentration change occurs. The model data on CO formation underestimates by factor of ten and three at 773 and 873 K respectively. The model data on CO_2 predicts the rapid concentration increase at 1.5 sec at 973 K. The model data predicts CH_2O formation correctly at 773 and 873 K. The model data on C_2H_6 formation is good at 773 K, but underestimates by factor of four at 873 K. The model data on C_2H_6 and C_2H_4 show rapid concentration decrease at 1.5 sec at 973 K, while the experimental results show these decrease between 1.25 and 2.0 sec.

3.4 Summary

Experimental data are collected on dimethyl-ether reaction at temperatures of 773, 823, 873, 923, 973, 1023, 1073 K and reaction times of 1.0, 1.25, 1.5, 1.75 and 2.0 sec under pyrolysis and oxidation conditions of pyrolysis, fuel rich ($\phi=1.5$), stoichiometric ($\phi=1.0$) and fuel lean ($\phi=0.75$). The major stable products from both pyrolysis and initial

oxidation reaction are CH_4 and CH_2O, with C_2H_6 and C_2H_4, important minor products. Small amounts of acetylene are observed at high temperature pyrolysis. No reaction is observed at 773 K under pyrolysis condition. Only CO_2 is observed above 973 K under stoichiometric ($\phi=1.0$) and fuel lean ($\phi=0.75$) conditions. CO_2 is produced earlier when more O_2 is in the reactant fuel mixture. CO_2 is not observed in pyrolysis. Rapid concentration changes of CO CO_2 and CH_4 occur at 973 K with oxidation at the three fuel equivalence ratios ($\phi=1.5$, 1.0 and 0.75).

The model on dimethyl-ether decay and CH_4 formation predict reasonably accurately over all temperature ranges. The model data on CH_2O predicts correctly under stoichiometric ($\phi=1.0$) and fuel lean ($\phi=0.75$) conditions, but overestimates under pyrolysis. The model data on CO and CO_2 formation predict well at high temperature (T=973 K and above), but underestimate at low temperature, 773 and 873 K. The model data on C_2H_6 and C_2H_4 are consistently below the experimental results.

GC/MS analysis was performed to quantitatively identify and quantify the dimethyl-ether source gas contaminant. The results indicate that the contaminant is Propene and its concentration is estimated as 2.59 ppm under our reaction conditions, 0.5 % of dimethyl-ether gas. This amount does not cause adverse effects for the quantitative analysis on product.

GC/MS analysis is also performed on the dimethyl-ether oxidation products. The GC/MS analysis verified the product identification previously done by GC-FID analysis with standard gases.

CHAPTER 4

KINETIC AND THERMODYNAMIC ANALYSIS
ON OH ADDITION TO ETHYLENE:
ADDUCT STABILIZATION, ISOMERIZATION
AND ISOMER DISSOCIATION

4.1 Introduction

The OH plus ethylene addition reaction is important in low temperature (below 1200 K)

hydrocarbon combustion chemistry and in tropospheric photo-chemistry. The C - H bond

in ethylene is 111.6 kcal/mol and abstraction of this H by the OH radical has an

activation energy of c.a. 7 kcal/mol, while the addition of OH radical to the PI bond has

zero or negative activation energy and a similar pre-exponential factor[43-48]. At

atmospheric conditions, isomerization to CH_3CH_2O. or reaction to vinyl alcohol + H play

minor roles and stabilization and further reaction with O_2 is the important channel. This

peroxy radical can either react with NO or undergo H shift (Waddington mechanism) to

an alkoxy hydroperoxide, then dissociate to 2 CH_2O + OH. The addition reaction leads

to reverse dissociation plus formation of vinyl alcohol + H under higher temperature

combustion conditions. Vinyl alcohol has a very week O - H bond (ca. 85 kcal/mol); this

rapidly undergoes abstraction to form formyl methyl radical (loss of the O - H hydrogen

then electron rearrangement to $C\bullet H_2CHO$). Combustion models do not however always

include this pathway.

Several *ab initio* studies[47,49-51] have been performed on this reaction system and a

number of experimental studies[43-46,48,52-64] are available for data comparison. Sosa et

al. calculated barrier heights for C_2H_4 + OH using Unrestricted MØller-Presset

Perturbation Theory with spin annihilation[47]. They also studied reaction pathways for

adduct ($C\bullet H_2CH_2OH$) reaction to products using geometries optimized at HF/6-31G* and energy of up to MP4SDQ/6-31G** levels of calculations.

Villa et al. studied the activation energy and rate constant trends for C_2H_4 + OH addition to form $C\bullet H_2CH_2OH$ using canonical variational transition state theory and reaction potential-energy hypersurface using several *ab initio* methods[49]. Their calculations demonstrate a strong inverse dependence of the rate constant with temperature at T < 565 K, in agreement with the experimental evidence that this reaction has a negative activation energy at atmospheric temperatures.

Liu et al. studied the reaction using high temperature gas phase pulse radiolysis to determine the rate of the reaction and report a weak negative activation energy (-0.951 kcal/mol) below 560 K[55]. Atkinson et al. report absolute rate constants for the reaction of OH radical with ethylene using flash photolysis-resonance fluorescence technique and indicate that rate constants are independent of total pressure over the range 255 - 663 torr[44]. Bartels et al. studied the OH plus ethylene reaction at temperature of 295 K and low pressure (0.1 to 2 torr) using discharge flow and laval nozzle reactors with molecular beam mass spectrometric detection. They reported branching ratios at 295 K and 2 torr for $C\bullet H_2CH_2OH$ stabilization, CH_2O + CH_3, and CH_3CHO + H determined by direct calibration procedures. They also describe the reaction pathways of this chemical activation addition reaction system[54].

In this paper, thermodynamic properties ($\Delta H_f^\circ{}_{298}$, $S^\circ{}_{298}$, and $C_p(T)$'s, $300 \leq T/K \leq 1500$) of intermediate radicals, $C\bullet H_2CH_2OH$ and $CH_3CH_2O\bullet$, transition states, $\overline{C\bullet H_2CH_2OH}$, CH_3--CH_2O, CH_3CHO--H, and $C\bullet H_2CHOH$--H, and product, CH_2CHOH, are calculated using CBS-q//MP2(full)/6-31G(d,p) and G2 composite methods and

compared to literature data where available. Isodesmic reactions are applied to accurately estimate enthalpies of formation ($\Delta H_f^o{}_{298}$ in kcal/mol) of two intermediate radicals, $C\bullet H_2CH_2OH$ and $CH_3CH_2O\bullet$ and one product CH_2CHOH. The calculated activation energies of four TS's are compared with estimated values of Bartels et al.[54], previous *ab initio* determined reaction pathway analysis[50], and with group additivity using hydrogen bond increments. CBS-q//MP2(full)/6-31G(d,p) determined thermodynamic properties are chosen for the detailed kinetic analysis.

High-pressure limit A factors (A_∞) and rate constants (k_∞) determination with *ab initio* calculations for TS compounds are explained in Chapter 1. Quantum Rice-Ramsperger-Kassel (QRRK) analysis[5,6] is used to calculate energy dependent rate constants, k(E), and master equation analysis is applied to account for collisional stabilization in the OH + C_2H_4 adduct and isomers as expressed in Chapter 1.

Comparisons of the calculated branching ratio ($C\bullet H_2CH_2OH$ stabilization : CH_2O+CH_3 : CH_3CHO+H) at 2 torr and 295 K with the experimentally determined ratio suggests the need to invoke tunneling for the hydrogen shift transition state (TS1) $C\bullet H_2CH_2OH \rightarrow CH_3CH_2O\bullet$ and for the β-scission transition state (TS3) $CH_3CH_2O\bullet \rightarrow CH_3CHO + H$. Imaginary frequencies obtained at MP2(full)/6-31G(d,p) level of theory need to be adjusted downward to match the experimentally determined branching ratio with a chemical activation reaction analysis on the $(C\bullet H_2CH_2OH)^*$ adduct when tunneling is included.

4.2 Method

4.2.1 *ab initio* Calculations

Two established composite *ab initio* calculation methods, CBS-q [7] and G2[8], are used

with the Gaussian94 computer code[9]. These *ab initio* methods are utilized to estimate

thermodynamic properties ($\Delta H_f^\circ{}_{298}$, $S^\circ{}_{298}$, and $C_p(T)$'s($300 \leq T/K \leq 1500$) for two

intermediate radicals, $C\bullet H_2CH_2OH$ and $CH_3CH_2O\bullet$, one product C_2H_3OH, and four

transition states.

(TS1) $C\bullet H_2CH_2OH$: Intra-molecular hydrogen shift to form $CH_3CH_2O\bullet$.

(TS2) $CH_3\text{--}CH_2O$: β-scission reaction to form methyl radical plus formaldehyde.

(TS3) $CH_3CHO\text{--}H$: β-scission reaction to form acetaldehyde plus atomic hydrogen.

(TS4) $C\bullet H2CHOH\text{--}H$: β-scission reaction to form vinyl alcohol plus atomic hydrogen.

The CBS-q calculation sequence is performed on the MP2(full)/6-31G(d,p)

geometry and followed by single point calculations at the theory level of QCISD(T)/6-

31G, MP4(SDQ)/6-31G(d'), and MP2/6-31+D(d,p). MP2(full)/6-31G(d,p) is used to

obtain the geometric structures and frequencies for entropies ($S^\circ{}_{298}$ in cal/mol-K) and

heat capacities ($C_p(T)$'s in cal/mol-K), while HF/3-21 G(d) is the suggested method for

structure and frequencies with CBS-q.

G2 theory is based on MP2(full)/6-31G(d) optimized structure and HF/6-31G(d)

determined vibrational frequencies. Treatment of electron correlation in G2 is by

MØller-Plesset (MP) perturbation theory and quadratic configuration interaction (QCI).

The final energies are effectively at the MP4/6-311+G(d,p) level, making certain

assumptions about additivity and appending a small higher-level empirical correction[8].

Transition state geometries are identified by the existence of one imaginary frequency in

the normal mode coordinate analysis, analysis of structure, and atomic contributions to

the vibrational motion.

4.2.2 Entropy ($S°_{298}$) and Heat Capacities ($C_p(T)$'s)

$S°_{298}$ and $C_p(T)$'s of two intermediate radicals, $C•H_2CH_2OH$ and $CH_3CH_2O•$, four TS's,

TS1, TS2, TS3, and TS4 and one product C_2H_3OH are calculated based on frequencies

and moments of inertia of the optimized MP2(full)/6-31G(d,p) geometry for CBS-q

method, and with scaled frequencies of optimized HF/6-31G(d) geometry and moments

of inertia of MP2(full)/6-31G(d) for G2 method. $S°_{298}$ and $C_p(T)$'s for reactants and other

products are obtained from literature[25,65]. Vibrational frequencies are scaled by 1.0084

for MP2(full)/6-31G(d,p)[11] and by 0.8929 for HF/6-31G(d) calculation[12]; *ab initio*

calculated torsional frequencies are not included for $S°298$ and $C_p(T)$ calculations.

Contribution of internal rotational to $S°_{298}$ and $C_p(T)$'s are calculated separately based on

rotational barrier height and moments of inertia. Pitzer et al.'s [10] general treatment of

internal rotation is used to calculate the hindered internal rotational contribution to $S°_{298}$

and $C_p(T)$'s.

4.2.3 Determination of Enthalpies of Formation ($\Delta H_f°_{298}$)

$H_f°_{298}$ for two intermediate radicals and one product are estimated using total energies

obtained by *ab initio* calculations and isodesmic reactions. $\Delta H_f°_{298}$ for reactants and

other products are obtained from literature[25,65]. Total energies are corrected by zero

point vibrational energies (ZPVE) which are scaled by 0.9608 as recommended by Scott

et al.[11] for MP2(full)/6-31G(d,p) and 0.8929 for HF/6-31G(d)[12]. Thermal correction 0K

to 298.15K is calculated to estimate enthalpies of formation at 298.15K[12] as explained in

Chapter 1.

Three isodesmic reactions are used to determine the $\Delta H_f°_{298}$ of the two intermediate

radicals and one stable product.

For estimation of $C\bullet H_2CH_2OH$

$$C\bullet H_2CH_2OH + C_2H_6 \Rightarrow CH_3CH_2OH + C_2H_5 \qquad \text{---------- (1)}$$

For estimation of $CH_3CH_2O\bullet$

$$CH_3CH_2O\bullet + CH_3OH \Rightarrow CH_3CH_2OH + CH_3O\bullet \qquad \text{---------- (2)}$$
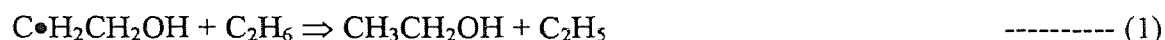
For estimation of vinyl alcohol

$$CH_2CHOH + CH_3CH_3 \Rightarrow CH_2CH_2 + CH_3CH_2OH \qquad \text{---------- (3)}$$

The method of isodesmic reactions relies upon the similarity of bonding environment in

the reactants and products that leads to cancellation of systematic errors in the *ab initio*

MO calculations[12]. A basic requirement of the isodesmic reaction analysis is the bond

type conservation, where the number of bonds of each formal chemical bond type is

conserved in the reactions. An isodesmic reaction will lead to more accurate $\Delta H_f°_{298}$

estimations if groups are conserved, where correlation of next-nearest-neighbor atoms in

reactants and products are conserved in addition to bond types[27]. Reaction (1) and (2)

conserve both bond and group types. *ab initio* calculations with ZPVE and thermal

correction are performed for all of four compounds in reaction (1). The unknown $\Delta H_f°_{298}$

of C•H$_2$CH$_2$OH is obtained from the calculated $\Delta H_f°_{298,rxn}$ and the experimental or theoretical calculated $\Delta H_f°_{298}$ of three other compounds in equation (1). The intermediate radical, CH$_3$CH$_2$O• and product C$_2$H$_3$OH are calculated in the same manner.

The $\Delta H_f°_{298}$ of TS compounds are estimated by evaluation of $\Delta H_f°_{298}$ of the stable intermediate radicals plus difference of total energies with ZPVE and thermal correction between these radical species and the TS.

4.2.4   Tunneling (Experimental Data Comparison)

Tunneling for the intramolecular hydrogen atom transfer reaction of TS1 and TS3, is applied, since the direct calculation results of branching ratios (C•H$_2$CH$_2$OH stabilization : CH$_2$O + CH$_3$: CH$_3$CHO + H) do not show good agreement with experimental values. We choose the CBS-q energies for use in the kinetic analysis because the G2 values for the reaction barriers are higher than the CBS-q , resulting in slower reactions and poorer agreement with experimental data.

Tunneling effects are taken into account using the Erwin-Henry computer code[66] to determine high-pressure limit rate constants (k_∞) of reactions 2 and 4. This program is based on Eckart's one-dimensional potential function. [67] Eckart evaluated in closed form, an expression for the probability, $\kappa(E)$, of crossing the barrier for a particle of energy E. The Erwin-Henry computer code requires input of vibrational frequencies, moments of inertia, and total energies at 0 K of reactants, transition states TS's, and products; imaginary frequencies are also required. Total energies are obtained from the CBS-q methods, vibrational frequencies and moments of inertia are obtained from MP2(full)/6-31G(d,p) level of calculation.

Imaginary frequencies are adjusted to fit the experimentally derived branching ratio, since the direct use of imaginary frequencies from MP2(full)/6-31G(d,p) gives unreasonably high correction factor Γ^* at low temperature. The Γ^* are calculated with the adjusted imaginary frequencies at temperatures, 290, 296, 325, 400, 524, 700, 900, and 1200 K. These numbers are convoluted into the A_∞ values determined from TST.

4.3 Results and Discussion

4.3.1   Geometries and Frequencies (*ab initio* Calculation Results)

Figure 4.1 to 4.6 show optimized geometries of two intermediate radicals and three TS compounds by MP2(full)/6-31G(d,p) and MP2(full)/6-31G(d) calculations. The two methods give similar results; geometric parameters from the higher theory are listed unless otherwise noted. Table 4.1 and 4.2 list the frequency calculation results of MP2(full)/6-31G(d,p) and HF/6-31G(d).

The C_2-C_1 bond length in TS1, H shift from the hydroxyl to the methyl, is 1.495 Å, which is slightly longer than C_2-C_1 bond length of reactant ($C\bullet H_2CH_2OH$), 1.482 Å, and shorter than C_2-C_1 bond length of product ($CH_3CH_2O\bullet$), 1.531 Å. The O_7-C_2 bond length is slightly stretched (1.446 Å) in TS1 (c.a. 0.02 Å) then shortened to 1.389 Å at product ($CH_3CH_2O\bullet$). The bond length of H_8-O_7 which is 0.963 Å in the reactant is stretched to 1.250 Å in TS1. The H_8-C_1 bond forming is 1.306 Å at TS1. The imaginary frequencies for TS1 show differences between MP2(full)/6-31G(d,p) and HF/6-31G(d) levels of theory, -2344 and -2909 cm^{-1} respectively.

Figure 4.4 shows the TS2 geometry, β-scission of $CH_3CH_2O\bullet \rightarrow CH_3 + CH_2O$. The bond length of C_2-C_1 in TS2 is 2.071 Å, which is 1.531 Å in $CH_3CH_2O\bullet$. The O_6-C_2
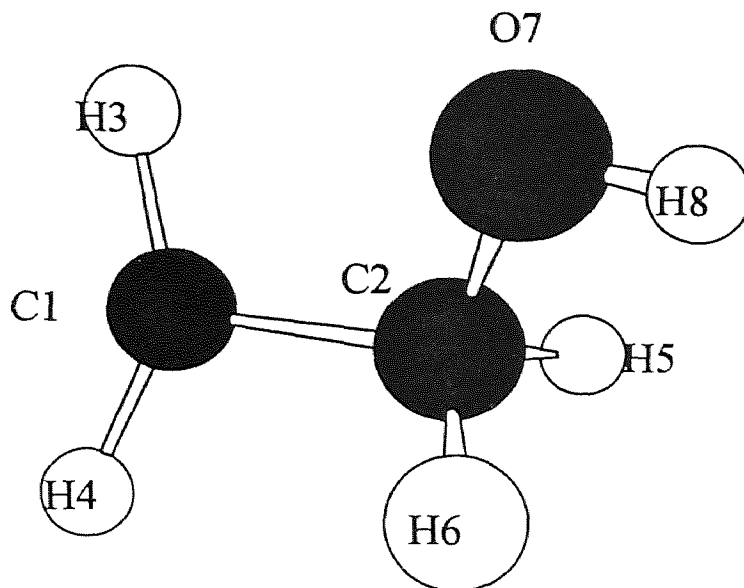
Description	MP2(full)/6-31G(d,p)	MP2(full)/6-31G(d)
C2-C1	1.482	1.483
H3-C1	1.077	1.082
H4-C1	1.076	1.081
H5-C2	1.100	1.105
H6-C2	1.096	1.101
O7-C2	1.425	1.427
H8-O7	0.963	0.971
∠3,1,2	120.1	120.3
∠4,1,2	118.9	119.0
∠5,2,1	110.4	110.5
∠6,2,1	110.0	110.1
∠7,2,1	108.1	107.9
∠8,7,2	107.4	107.5

**Figure 4.1 MP2(full)/6-31G(d,p) Determined Geometry
C.H2CH2OH**
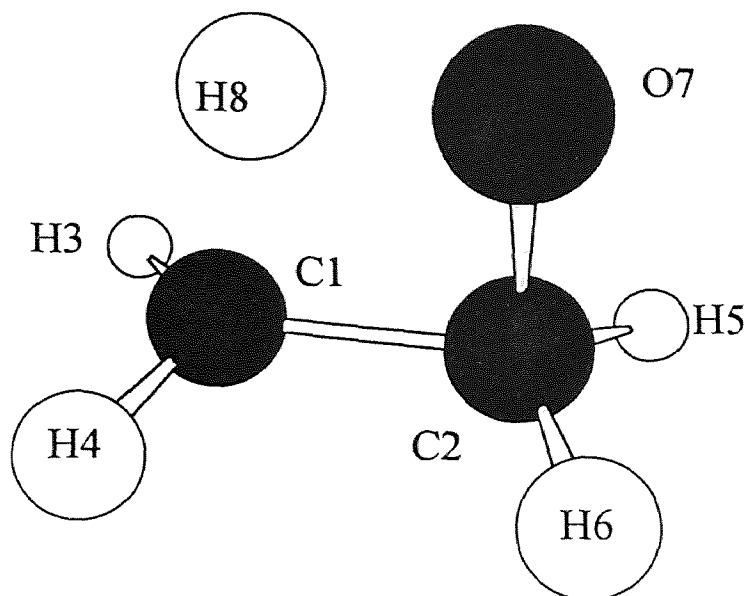
Description	MP2(full)/6-31G(d,p)	MP2(full)/6-31G(d)
C2-C1	1.495	1.495
H3-C1	1.081	1.086
H4-C1	1.081	1.086
H8-C1	1.306	1.332
H5-C2	1.088	1.093
H6-C2	1.088	1.093
O7-C2	1.446	1.449
H8-O7	1.250	1.249
∠3,1,2	117.8	118.0
∠4,1,2	117.8	118.0
∠5,2,1	115.9	115.9
∠6,2,1	115.9	116.0
∠8,1,2	81.0	81.1
∠7,2,1	88.0	88.2
∠7,8,1	104.3	105.0
∠8,7,2	84.9	85.7

**Figure 4.2 MP2(full)/6-31G(d,p) Determined Geometry
cyC.H2CH2OH (TS1)**
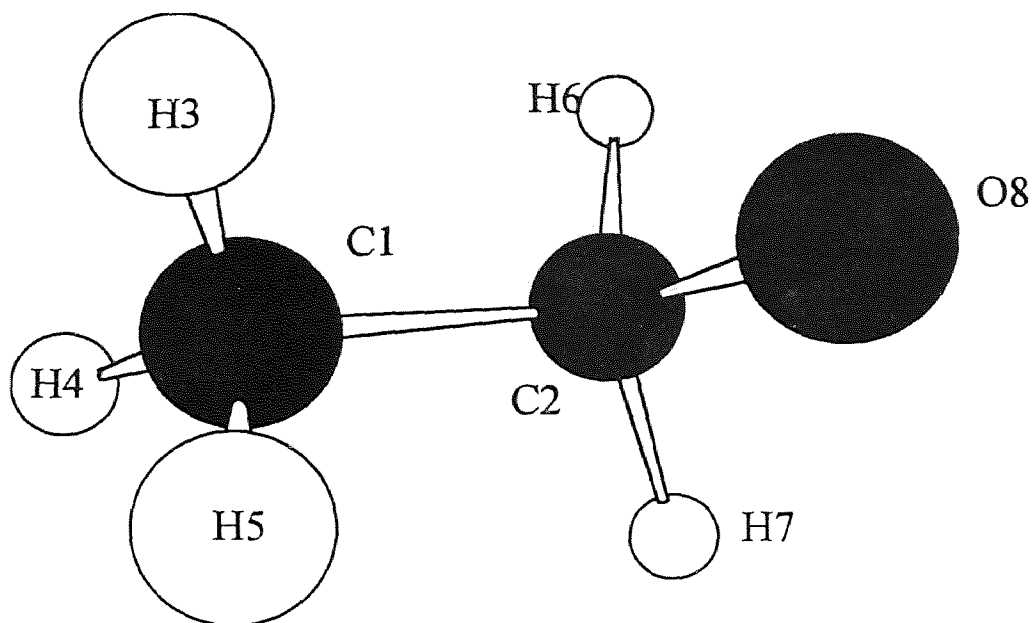
Description	MP2(full)/6-31G(d,p)	MP2(full)/6-31G(d)
C2-C1	1.531	1.533
H3-C1	1.086	1.091
H4-C1	1.087	1.093
H5-C1	1.086	1.091
O6-C2	1.389	1.390
H7-C2	1.093	1.098
H8-C2	1.093	1.098
∠3,1,2	110.3	110.3
∠4,1,2	109.2	109.3
∠5,1,2	110.3	110.3
∠6,2,1	106.1	106.0
∠7,2,1	109.5	109.6
∠8,2,1	109.5	109.6

Figure 4.3 MP2(full)/6-31G(d,p) Determined Geometry CH3CH2O.
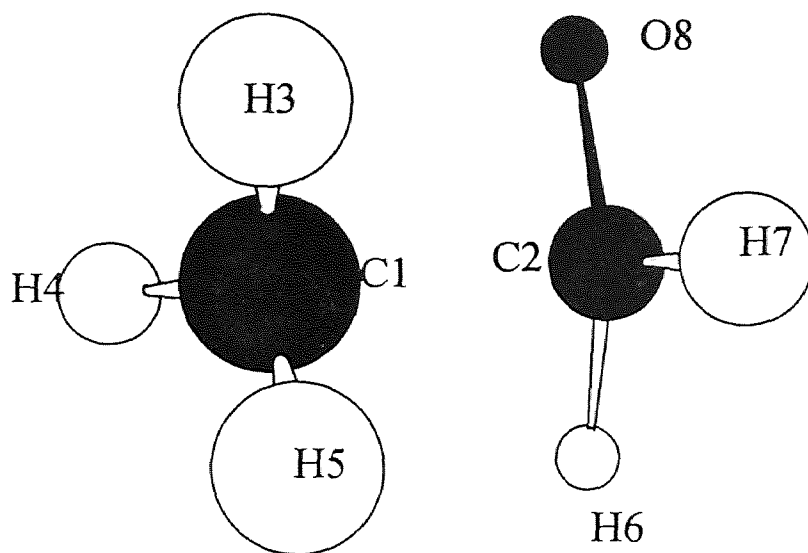
Description	MP2(full)/6-31G(d,p)	MP2(full)/6-31G(d)
C2-C1	2.071	2.071
H3-C1	1.080	1.080
H4-C1	1.077	1.077
H5-C1	1.077	1.077
O6-C2	1.220	1.220
H7-C2	1.102	1.102
H8-C2	1.102	1.102
∠3,1,2	100.9	100.2
∠4,1,2	100.2	100.1
∠5,1,2	100.2	100.1
∠6,2,1	102.9	102.8
∠7,2,1	91.1	91.3
∠8,2,1	91.0	91.3

Figure 4.4 MP2(full)/6-31G(d,p) Determined Geometry CH3---CH2O (TS2)
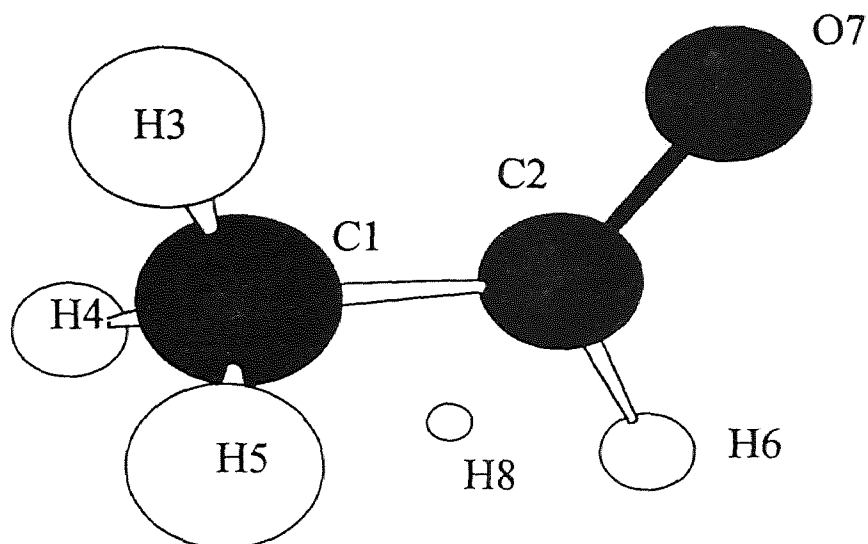
Description	MP2(full)/6-31G(d,p)	MP2(full)/6-31G(d)
C1-C2	1.512	1.514
H3-C1	1.090	1.095
H4-C1	1.085	1.090
H5-C1	1.087	1.092
O6-C2	1.220	1.225
H7-C2	1.107	1.111
H8-C2	1.622	1.600
∠3,1,2	107.1	107.3
∠4,1,2	109.9	109.8
∠5,1,2	112.0	112.1
∠6,2,1	123.0	122.7
∠7,2,1	114.6	114.8
∠8,2,1	98.3	98.7

Figure 4.5 MP2(full)/6-31G(d,p) Determined Geometry CH3CHO---H (TS3)
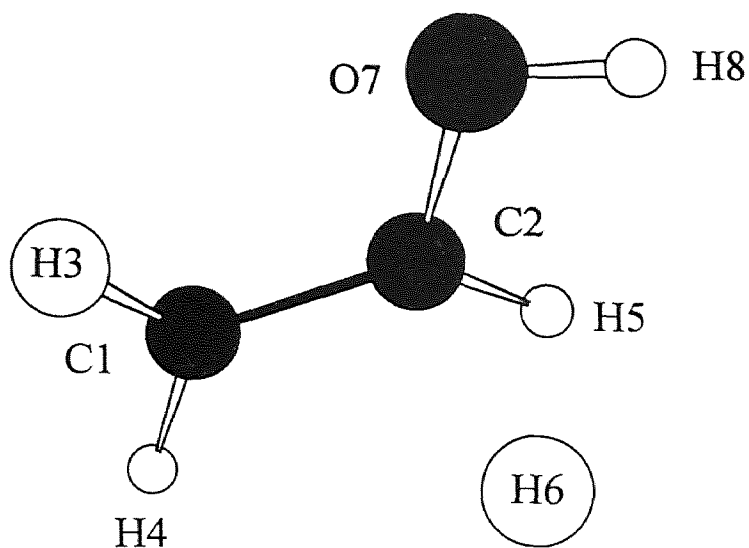
Bond Angle (degree)	MP2(full)/6-31G(d,p)	MP2(full)/6-31G(d)
C1-C2	1.340	1.345
H3-C1	1.076	1.081
H4-C1	1.077	1.082
H5-C2	1.083	1.088
H6-C2	1.795	1.772
O7-C2	1.371	1.376
H8-O7	0.963	0.971
∠3,1,2	119.9	120.1
∠4,1,2	120.6	12.07
∠5,2,1	120.9	120.8
∠6,2,1	99.4	100.5
∠7,2,1	120.1	119.5
∠8,2,1	108.6	108.6

Figure 4.6 MP2(full)/6-31G(d,p) Determined Geometry CH2CHOH--H (TS4)

bond length also changes from 1.389 Å to 1.220 Å, indicative of the CO double bond

formation in TS2 (bond length of the formaldehyde C=O double bond is1.219 Å at the

same level of theory). The imaginary frequencies at TS2 are -685 and -550 cm^{-1} for

MP2(full)/6-31G(d,p) and HF/6-31G(d) level of theory respectively.

The H_8-C_2 bond length is 1.622 Å, and O_6-C_2 is 1.220 Å at TS3 in Figure 4.5, which

is same as C-O bond length of TS2. The bond length of C_2-C_1 is slightly shorter (c.a.

0.02 Å) than that of reactant $CH_3CH_2O\bullet$. The imaginary frequencies are -1704 and -1118

cm^{-1} for MP2(full)/6-31G(d,p) and HF/6-31G(d) level of theory respectively.

Figure 4.6 shows the TS4 geometry, β-scission of $C\bullet H_2CH_2OH$ → CH_2CHOH + H.

The C_2-H_6 bond length is 1.795 and 1.772 Å with MP2(full)/6-31G(d,p) and MP2(full)/6-

31g(d) calculations respectively, slightly large difference between two calculations. The

C_1-C_2 bond length is 1.340 Å with MP2(full)/6-31G(d,p) calculation, almost forms C-C

double bond. The O_7-C_2 bond length, which is 1.371 Å, is slightly longer than normal O-

C bond length.

Table 4.1 Vibrational Frequencies^a (v cm^{-1}) MP2/6-31G(d,p) level of calculation

Species	v1[f]	v2	v3	v4	v5	v6	v7	v8	v9	v10	v11	v12	v13	v14	v15	v16	v17	v18
C•H₂CH₂OH	181	293	411	473	898	1011	1113	1154	1259	1301	1479	1532	1572	3025	3088	3277	3402	3902
C•H₂CH₂OH (TS1)[b]	-2344	383	767	854	968	1041	1136	1159	1180	1265	1332	1490	1595	2115	3152	3221	3227	3350
CH₃CH₂O•	266	396	673	932	988	1027	1172	1303	1376	1449	1545	1565	1608	3094	3152	3156	3257	3265
CH₃-CH₂O (TS2)[c]	-685	180	319	587	641	736	972	1207	1303	1489	1508	1572	1737	2990	3059	3207	3386	3406
CH₃CHO-H (TS3)[d]	-1704	222	488	563	622	883	958	1155	1227	1435	1460	1534	1541	1771	2979	3141	3238	3276
CH₂CH(OH) -H (TS4)[e]	-1318	297	472	546	555	730	887	984	1121	1186	1304	1362	1491	1694	3251	3288	3403	3913
CH₂CHOH	466	494	722	805	981	1012	1142	1355	1388	1496	1749	3258	3301	3373	3868			

^{a} non-scaled. ^{b,c,d,e} TS structure described in Method section. ^{f} Transition State
compounds have one imaginary frequency.

Table 4.2 Vibrational Frequencies[a] (v cm⁻¹) HF/6-31G(d) level of calculation

Species	v1	v2	v3	v4	v5	v6	v7	v8	v9	v10	v11	v12	v13	v14	v15	v16	v17	v18
C•H₂CH₂OH	172	301	418	481	948	1057	1158	1224	1359	1393	1565	1620	1668	3123	3174	3328	3437	4117
C•H₂CH₂OH (TS1)[b]	-2909	400	729	883	1038	1055	1162	1165	1272	1332	1452	1577	1683	1922	3249	3300	3313	3416
CH₃CH₂O•	261	425	452	973	974	1098	1239	1375	1497	1552	1627	1644	1692	3201	3221	3240	3293	3300
CH₃-CH₂O (TS2)[c]	-550	142	295	571	656	786	949	1157	1347	1486	1562	1574	1699	3204	3269	3291	3415	3433
CH₃CHO-H (TS3)[d]	-1118	201	493	552	600	938	1001	1192	1224	1490	1553	1608	1622	1655	3204	3218	3275	3315
CH₂CH(OH)-H (TS4)[e]	-843	290	463	494	530	674	829	1023	1035	1213	1361	1419	1567	1692	3349	3361	3450	4128
CH₂CHOH	459	533	785	965	1048	1129	1234	1447	1468	1595	1878	3333	3402	3433	4096			

[a] non-scaled. [b,c,d,e] TS structure described in Method section. [f] Transition State compounds have one imaginary frequenciy.

4.3.2 Entropy ($S°_{298}$) and Heat Capacities ($C_p(T)$'s ($300 \leq T/K \leq 1500$))

$S°_{298}$ and $C_p(T)$'s based on MP2(full)/6-31G(d,p) determined frequencies and geometry are summarized in Table 4.5. TVR, represents the sum of the contributions from translations, external rotations, and vibrations for $S°_{298}$ and $C_p(T)$'s. Symmetry is incorporated in estimation of $S°_{298}$ as described in Table 4.5. The internal rotational contribution to $S°_{298}$ and $C_p(T)$'s is lost in the cyclic structure of TS1. This results in a lower $S°_{298}$ (c.a. 9 cal/mol-K at 298 K) and $C_p(T)$ (c.a. 3.4 cal/mol-K at 300 K) than the reactant. $S°_{298}$ and $C_p(T)$'s increase in the TS2 by 1.5 cal/mol-K and 1.1 cal/mol-K respectively at 300 K relative to CH₃CH₂O•.

Table 4.6 lists $S°_{298}$ and $C_p(T)$'s used in G2 calculations estimated by the MP2(full)/6-31G(d) structure and HF/6-31G(d) frequencies. HF/6-31G(d) determined $S°_{298}$ and $C_p(T)$'s are consistently higher (c.a. 0.4 to 1.0 cal/mol-K) than MP2(full)/6-31G(d,p) determined values.

Table 4.3 List of Total Energy, ZPVE, and Thermal Correction of CBS-q Calculation[a]

	[b]Total energy at 0K	ZPVE[c]	Thermal Correction[d]	Total Energy at 298K
C•H₂CH₂OH	-154.1604228	0.066913	0.005493	-154.15493
C₂H₅OH	-154.8264197	0.08268	0.0051412	-154.82128
C₂H₆	-79.68450267	0.077584	0.0043579	-79.680145
C₂H₅	-79.01789109	0.06182	0.0047771	-79.013114
C.H₂CH₂OH (TS1)[e]	-154.1139293	0.064325	0.0044068	-154.10952
C₂H₅O•	-154.1537608	0.070772	0.0048373	-154.14892
CH₃OH	-115.5767701	0.053033	0.0042222	-115.57255
CH₃O•	-114.9078594	0.038596	0.0039123	-114.90395
CH₃-CH₂O (TS2)[f]	-154.1324838	0.064471	0.0052381	-154.12725
CH₃CHO-H (TS3)[g]	-154.1257077	0.060353	0.0050085	-154.1207
C₂H₃OH-H (TS4)[h]	-154.105946	0.060333	0.0050694	-154.10088
C₂H₃OH	-153.6154725	0.05789	0.0045408	-153.61093
C₂H₄	-78.45588667	0.052411	0.003971	-78.451916

[a] Unit in Hartree 1 HF=627.51 kcal/mol. [b] Scaled ZPVE are included. Scaling factor is recommended as 0.9608 by Scott et al.[11] [c] Non-scaled. [d] Scaled by 1.0084 Scott et al.[11] [e,f,g,h] TS structure described in Method section.

Table 4.4 List of Total Energy of G2 Calculation

Compound	Total Energy at 298K
C•H₂CH₂OH	-154.09549
C₂H₅OH	-154.759163
C₂H₆	-79.626402
C₂H₅	-78.965224
C•H₂CH₂OH (TS1)[b]	-154.0462645
C₂H₅O•	-154.09104
CH₃OH	-115.5306
CH₃O•	-114.863592
CH₃-CH₂O (TS2)[c]	-154.0654838
CH₃CHO-H (TS3)[d]	-154.0604102
C₂H₃OH-H (TS4)[e]	-154.0445236
C₂H₃OH	-153.554381
C₂H₄	-78.411923

[a] scaled ZPVE and Thermal correction 0K to 298.15K are taken into account. Unit in Hartree 1 Hartree=627.51 kcal/mol.
[b,c,d,e] TS structure described in Method section.

4.3.3 Enthalpies of Formation ($\Delta H_f^{\circ}{}_{298}$) Estimation using Total Energies and Isodesmic Reactions

Isodesmic reactions are applied to estimate $H_f^{\circ}{}_{298}$ of $C\bullet H_2CH_2OH$ and $CH_3CH_2O\bullet$, and

CH_2CHOH. The evaluated $\Delta H_f^{\circ}{}_{298}$ for the molecules considered to have known $\Delta H_f^{\circ}{}_{298}$

values, for use in the isodesmic reactions, are listed in Table 4.7. CBS-q determined

enthalpy of reaction (1) ($\Delta H_f^{\circ}{}_{298,rxn}$) is 0.43 kcal/mol. This near zero value of the

calculated $\Delta H_f^{\circ}{}_{298,rxn}$ supports our estimation of similar bonding environments for

reaction.

$\Delta H_f^{\circ}{}_{298}(C\bullet H_2CH_2OH)$ is evaluated from

$\Delta H_{f298,rxn} = \Delta H_f^{\circ}{}_{298}(C_2H_5OH) + \Delta H_f^{\circ}{}_{298}(C_2H_5) - \Delta H_f^{\circ}{}_{298}(C\bullet H_2CH_2OH) - \Delta H_f^{\circ}{}_{298}(C_2H_6)$

$$0.43 = -56.12 + 28.32 - X - (-20.24) \text{ kcal/mol} \qquad \text{----- (4)}$$

The $\Delta H_f^{\circ}{}_{298}n$ of $C\bullet H_2CH_2OH$ obtained is -7.99 kcal/mol. This $\Delta H_{f298,rxn}$ is also expressed

using the calculated reaction energy.

$\Delta H_{f298,rxn} = BDE(H-CH_2CH_3) - BDE(H-CH_2CH_2OH) = 0.43$ kcal/mol.

Since $BDE(H-CH_2CH_3)$ is known as 101.6 kcal/mol, one can estimate BDE(H-

CH_2CH_2OH) as 101.2 kcal/mol.

Sosa et al estimated $\Delta H_f^{\circ}{}_0$ for $C\bullet H_2CH_2OH$ as -5.1 kcal/mol. They used

frequencies and zero-point energies calculated by HF/3-21G* level of theory and

geometries optimized by HF/6-31G* level of theory[50]. Their total energies at the highest

level were estimated by adding the correction for spin contamination (PMP4/6-31G* -

MP4/6-31G*) and for zero-point energies to the MP4/6-31G** energies.

$\Delta H_f^{\circ}{}_{298}$ for the intermediate radical, $CH_3CH_2O\bullet$ is obtained from CBS-q analysis

with isodesmic reaction (2). Data result in the enthalpy values of -1.7 kcal/mol at 298 K.
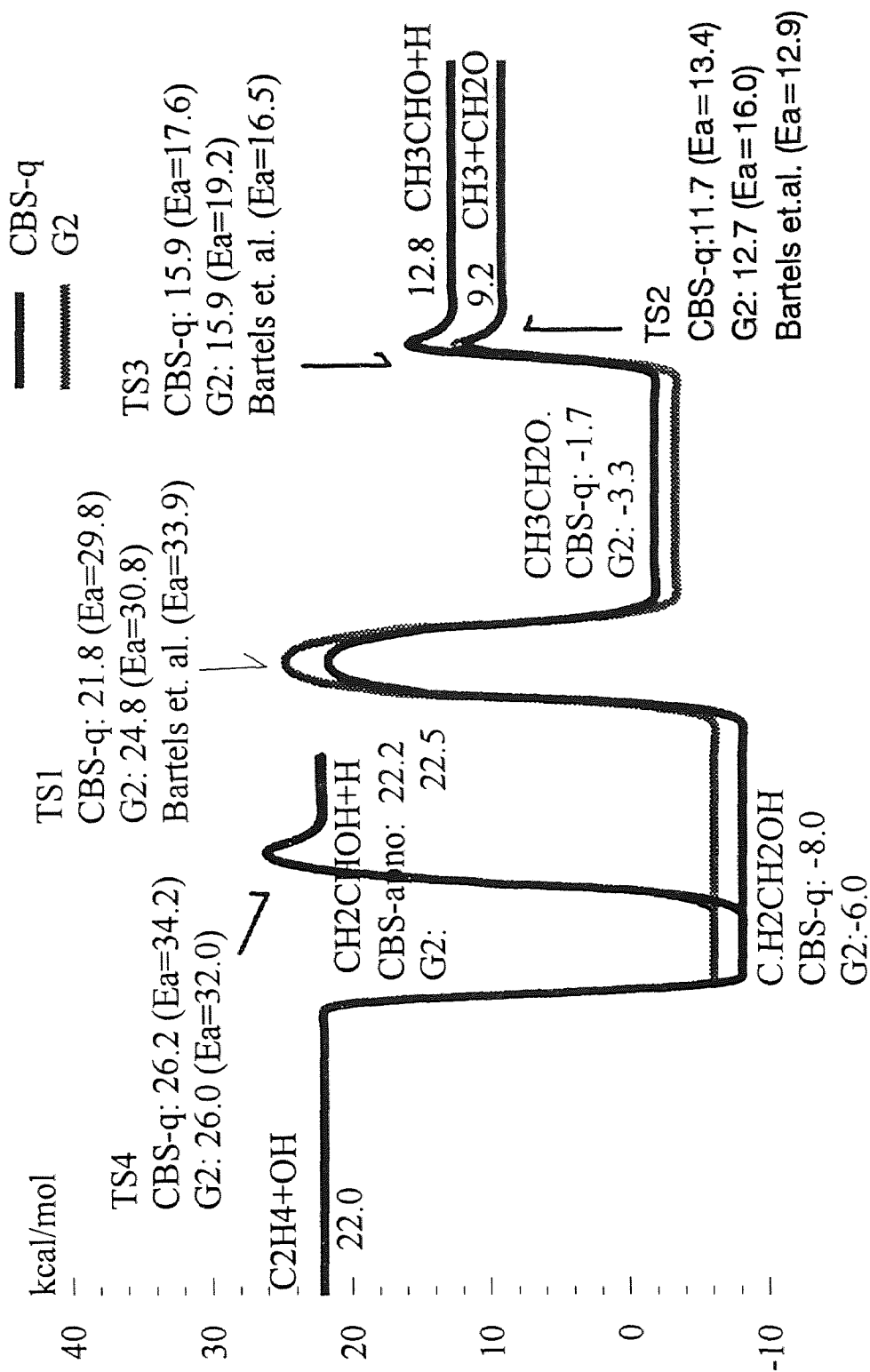
Figure 4.7 Potential Energy Diagram Determined by CBS-q//MP2(full)/6-31G(d,p) and G2

Table 4.5 Ideal Gas Phase Thermodynamic Properties Using CBS-q//MP2/6-31G(d,p)[a]

Species and Symmetry #		Hf°_{298}	S°_{298}[b]	Cp_{300}[b]	Cp_{400}	Cp_{500}	Cp_{600}	Cp_{800}	Cp_{1000}	Cp_{1500}
$C\bullet H_2CH_2OH$	TVR[c,d]		60.07	12.59	15.49	18.23	20.62	24.42	27.32	32.12
2	Internal Rotor[e]		7.94	3.07	3.04	2.96	2.86	2.65	2.49	2.26
	Total	-7.99	69.39[f]	15.66	18.53	21.19	23.48	27.07	29.81	34.38
$C\bullet H_2CH_2OH$	TVR		61.08	12.6	16.1	19.38	22.19	26.55	29.74	34.68
(TS1)[g]	Internal Rotor		0	0	0	0	0	0	0	0
2	Total	21.78	62.46[f]	12.6	16.1	19.38	22.19	26.55	29.74	34.68
$CH_3CH_2O\bullet$	TVR		58.99	12.24	15.36	18.4	21.09	25.43	28.73	33.99
3	Internal Rotor		3.99	2.04	2.19	2.17	2.07	1.82	1.62	1.34
	Total	-1.68	64.36[f]	14.28	17.55	20.57	23.16	27.25	30.35	35.33
CH_3-CH_2O	TVR		60.48	13.34	16.09	18.63	20.87	24.58	27.5	32.33
(TS2)[h]	Internal Rotor		3.99	2.04	2.19	2.17	2.07	1.82	1.62	1.34
3	Total	11.67	65.85[f]	15.38	18.28	20.8	22.94	26.4	29.12	33.67
CH_3CHO-H	TVR		59.17	13.02	16.14	19.03	21.54	25.55	28.53	33.17
(TS3)[i]	Internal Rotor		3.99	2.05	2.19	2.17	2.07	1.83	1.62	1.34
3	Total	15.92	64.54[f]	15.07	18.33	21.2	23.61	27.38	30.15	34.51
C_2H_3OH-H	TVR		62.22	16.29	19.91	22.89	25.28	28.84	31.42	35.51
(TS4)[j]	Internal Rotor		4.01	1.39	1.27	1.2	1.15	1.09	1.06	1.02
2	Total	26.19	67.61[f]	17.68	21.18	24.09	26.43	29.93	32.48	36.53
C_2H_3OH	TVR		59.88	13.77	16.93	19.62	21.82	25.17	27.64	31.64
	Internal Rotor		0	0	0	0	0	0	0	0
2	Total	-34.60	59.88	13.77	16.93	19.62	21.82	25.17	27.64	31.64

[a] Thermodynamic properties are referred to a standard state of an ideal gas of pure enantiometer at 1 atm. [b] In cal $mol^{-1}K^{-1}$. [c] The sum of contributions from translations, external rotations, and vibrations. [d] Symmetry number is taken into account (-1.987 x ln (number of symmetry)). [e] Contribution from internal rotation. [f] Spin degeneracy contribution for entropy = 1.987 * ln(2) (cal/mol-K) is taken into account. [g,h,i,j] TS structure described in Method section.

Sosa et al. estimated the energy of $CH_3CH_2O\bullet$ relative to $C_2H_4 + OH$ as -25.3 kcal/mol at 0 K[50]; our estimation is -23.7 kcal/mol at 298 K.

C_2H_3OH is calculated at CBS-APNO level of theory due to the surprisingly low $\Delta H_f^{\circ}_{298}$ obtained by CBS-q (-34.60 kcal/mol), where CBS-APNO value is -29.95 kcal/mol. Turecek et al. reported the $\Delta H_f^{\circ}_{298}$ of vinyl alcohol as -29.6 kcal/mol using G2MP2 determined total energy and same isodesmic reaction as our study[68]. Our G2 calculation results in -29.5 kcal/mol. Sosa et al. estimated relative energy of $C_2H_3OH +$

Table 4.6 Ideal Gas Phase Thermodynamic Properties Using G2^a

Species and Symmetry #		Hf°$_{298}$	S°$_{298}$^{b}	Cp$_{300}$^{b}	Cp$_{400}$	Cp$_{500}$	Cp$_{600}$	Cp$_{800}$	Cp$_{1000}$	Cp$_{1500}$
C•H$_2$CH$_2$OH	TVR^{c,d}		60.48	13.24	16.3	19.12	21.55	25.41	28.32	32.97
2	Internal Rotor^e		7.94	3.07	3.04	2.96	2.86	2.65	2.49	2.26
	Total	-5.99	69.80^f	16.31	19.34	22.08	24.41	28.06	30.81	35.23
C•H$_2$CH$_2$OH	TVR		61.57	13.59	17.37	20.76	23.6	27.64	31.04	35.65
(TS1)	Internal Rotor		0	0	0	0	0	0	0	0
2	Total	24.83	62.95^f	13.59	17.37	20.76	23.6	27.64	31.04	35.65
CH$_3$CH$_2$O•	TVR		59.87	13.46	16.69	19.75	22.43	26.77	30.02	35.01
3	Internal Rotor		3.99	2.04	2.19	2.17	2.07	1.82	1.62	1.34
	Total	-3.34	65.24^f	15.5	18.88	21.92	24.5	28.59	31.64	36.35
CH$_3$-CH$_2$O	TVR		61.32	14.44	17.44	20.08	22.35	26.02	28.85	33.35
(TS2)	Internal Rotor		3.99	2.04	2.19	2.17	2.07	1.82	1.62	1.34
3	Total	12.7	66.69^f	16.48	19.63	22.25	24.42	27.84	30.47	34.69
CH$_3$CHO-H	TVR		59.89	14.07	13.93	17.45	20.51	23.19	27.11	30.06
(TS3)	Internal Rotor		3.99	2.05	2.19	2.17	2.07	1.83	1.62	1.34
3	Total	15.88	65.26^f	16.12	19.62	22.58	25.02	28.73	31.4	35.42
C$_2$H$_3$OH-H	TVR		63.29	17.47	21.04	23.91	26.19	29.59	32.06	35.96
(TS4)	Internal Rotor		4.01	1.39	1.27	1.2	1.15	1.09	1.06	1.02
2	Total	25.99	68.68^f	18.86	22.31	25.11	27.34	30.68	33.12	36.98
C$_2$H$_3$OH	TVR		59.86	13.68	16.84	19.56	21.81	25.27	27.81	31.84
	Internal Rotor		0	0	0	0	0	0	0	0
2	Total	-29.46	59.86	13.68	16.84	19.56	21.81	25.27	27.81	31.84

^{a} Thermodynamic properties are referred to a standard state of an ideal gas of pure enantiometer at 1 atm. ^{b} In cal mol^{-1}K^{-1}. ^{c} The sum of contributions from translations, external rotations, and vibrations. ^{d} Symmetry number is taken into account (-1.987 x ln (number of symmetry)). ^{e} Contribution from internal rotation. ^{f} Spin degeneracy contribution for entropy = 1.987 * ln(2) (cal/mol-K) is taken into account. ^{g,h,i,j} TS structure described in Method section.

Table 4.7 Moleculs Considered to Have Known ΔHf°$_{298}$ for Use in Isodesmic Reactions

Compounds	ΔHf°298 (kcal/mol)
C2H6	-20.24[a]
C2H5OH	-56.12[a]
C2H5	28.32[b]
CH3OH	-48.08[a]
CH3O•	4.00[b]
C2H4	12.50[a]

^{a} reference[25] ^{b} reference[26]

H to C_2H_4 + OH as 5.5 kcal/mol[50], where our value is 0.15 kcal /mol using CBS-APNO

determined $\Delta H_f°_{298}$ of C_2H_3OH. Smith et al. calculated relative energy from

acetaldehyde using G1, results in 11.23 kcal/mol above acetaldehyde[51]. Estimated

$\Delta H_f°_{298}$ of vinyl alcohol is –28.53 kcal/mol. Espinosa has performed ab initio

calculations at several high levels of theory and used different isodesmic reaction to

evaluate $\Delta H_f°298$ of $C \bullet H2CH2OH$ radical. He reported a value of –4.0±1.0 Kcal/mol; 4

kcal/mol higher than the value used here and reported in the previous literature

The activation energy of TS1 is estimated from the both reactant $C \bullet H_2CH_2OH$, and

product $CH_3CH_2O \bullet$ direction. The averaged result is 29.77 kcal/mol for the CBS-q

calculation. Sosa et al. estimated Ea for TS1 as 31.9 kcal/mol using spin contamination

annihilation described above[50]. The activation energies of TS2, TS3, and TS4 are

estimated by taking the difference of total energy between transition state and reactant,

resulting in 13.35, 17.60, and 34.2 kcal/mol respectively with the CBS-q calculation.

Sosa et al. estimated these values as 18.2, 22.4, and 34.0 kcal/mol respectively, where

TS3 and TS4 were estimated from reverse directions (CH_3CHO + H $\rightarrow$ $CH_3CH_2O \bullet$ for

TS3 and C_2H_3OH + H $\rightarrow$ $C \bullet H_2CH_2OH$ for TS4)[50]. $\Delta H_f°_{298}$ using CBS-q composite

calculations are listed in Table 4.5: G2 values, which are determined in similar manner

are listed in Table 4.6.

The overall energy diagram for the reaction system is illustrated in Figure 4.7. The

calculated $\Delta H_f°_{298}$ of $C \bullet H_2CH_2OH$ using CBS-q and G2 are -7.99 and -5.99 kcal/mol

respectively. These values yield well depth for the C_2H_4 + OH $\rightarrow$ $C \bullet H_2CH_2OH$ addition

of –30.0 and –28.0 kcal/mol respectively. Sosa et al. estimated the well depth as 29.0

kcal/mol using G1. $\Delta H_f{}^o{}_{298}$ values of $CH_3CH_2O\bullet$ using CBS-q and G2 are -1.68 and -3.34 kcal/mol respectively. CBS-q and G2 enthalpies of formation of C_2H_3OH are -34.60 and -29.46 kcal/mol respectively. The activation energy of TS1 is 29.77 and 30.82 kcal/mol at CBS-q and G2 levels respectively. Both numbers for E_a are lower than the activation energy of Bartels et al. E_a=33.9 kcal/mol[54]. Sosa et al. estimated as 32.0 kcal/mol. The activation energy of TS2 is calculated as 13.35 and 16.04 kcal/mol with CBS-q and G2 calculation respectively and E_a of TS3 is calculated as 17.60 and 19.22 kcal/mol with CBS-q and G2 respectively. The calculation methods both show higher activation energies than the results of Bartels at. al. for both TS2 and TS3, who reports value of 12.9 and 16.5 kcal/mol respectively. Sosa et al. estimated as 18.2 and 22.4 kcal/mol respectively.

4.3.4 Tunneling Consideration and Imaginary Frequency Adjustment

The direct use of *ab initio* determined thermodynamic properties for QRRK analysis shows good agreement of overall forward rate constant $k_{\infty,f}$ with experimental data at temperature of 296 K and 524 K[46]. A large difference exists, however, in the branching ratio to products ($C\bullet H_2CH_2OH : CH_2O + CH_3 : CH_3CHO + H$) at 2 torr and 296K with the experimental data. The experimentally determined branching ratio is

($C\bullet H_2CH_2OH$ stabilization : $CH_2O + CH_3 : CH_3CHO + H$) = (21 : 44 : 35 = 1 : 2.1 : 1.7)

[54], where QRRK calculation with CBS-q and G2 result in

$(1 : 2.0 \times 10^{-2} : 8.2 \times 10^{-4})$ and $(1 : 1.9 \times 10^{-4} : 4.8 \times 10^{-6})$.

Our first attempt to match the experimental data involved lowering the activation energies for TS1 and TS3. A match of branching ratio with experimental data between

C•H$_2$CH$_2$OH and CH$_2$O + CH$_3$ can be obtained by reducing the activation energies of TS1 by 4.2 kcal/mol. The experimental branching ratio for CH$_3$CHO + H is not obtained even if the E$_a$ of TS3 is decreased to the energy of products (12.8 kcal/mol), which indicates zero activation energy for the reverse reaction (CH$_3$CHO + H → CH$_3$CH$_2$O•). The best fit of branching ratio underestimates the CH$_3$CHO + H channel by a factor of 4; is (1 : 2.1 : 0.4). We feel reducing the activation energy of TS1 by 4.2 kcal/mol is unrealistic, even though part of experimental data are matched. Tunneling is considered instead of decreasing activation energies. Sosa et. al also suggested that tunneling could be important[50].

The imaginary frequencies for TS1 and TS3 based on MP2(full)/6-31G(d,p) optimized structure are -2344 and -1704 cm^{-1} respectively, where HF/3-21G determined frequencies reported by Sosa et al. are -2599 and -805 cm^{-1} respectively[50]. Direct use of the MP2(full)/6-31G(d,p) values in the tunneling calculation give excessive correction of 7.84×10^6 and 5.25×10^3 for TS1 and TS3 respectively in the forward direction at 290K.

The imaginary (TST reaction coordinate) frequencies are adjusted as - 1580 and -550 cm^{-1} for TS1 and TS3 respectively. The calculated tunneling correction factors (Γ^*) correspond to these frequencies at 296 K are 824 for TS1 forward direction, 93 for TS1 reverse direction, and 21 for TS3 forward direction. These values are convoluted into the corresponding A$_\infty$ factors. The QRRK analysis performed at 296 K results in branching ratio obtained by Bartels et al.[54]; 1 : 2.1 : 1.7. William et al. applied tunneling effect into their *ab initio* study of transition state for C$_2$H$_5$ < -- > H + C$_2$H$_4$[69]. Their calculated activation energy and imaginary frequency were 3.5 kcal/mol and 860.0 cm^{-1} using QCISD/6-311+G(2df,p). The activation energy and imaginary frequency was adjusted

until the experimental rate constant was fit; their result is E_a of 2.00 kcal/mol and imaginary frequencies of 710 cm^{-1} [69].

4.3.5 QRRK Analysis

QRRK analysis are performed at each of the temperature points, 290, 296, 325, 400, 524, 700, 900, and 1200 K with the input A_∞ factor multiplied by the corresponding tunneling contribution. Results are shown in Figure 4.8 to 4.10. The high-pressure limit rate constant ($k_{\infty,1}$) for C_2H_4 + OH, reported by Villa et al., is adopted[49] and these Arrhenius A factors are multiplied by 2 to match the high pressure experimental data[44,53,59,70]. Villa et al.'s study indicates that A_∞ and $E_{a,\infty}$ both vary strongly with temperature. The rate constant expressions in Table 4.9 are adopted in order to use the calculated canonical vibrational transition state theory rate constants; A_∞ and $E_{a,\infty}$ are 1.44×10^{12} and -0.92kcal/mol respectively in the temperature range between 290 K to 450 K. A_∞ and $E_{a,\infty}$ are 5.56×10^{12} and 0 kcal/mol between 450 K and 700 K. A_∞ and $E_{a,\infty}$ are 8.84×10^{12} and 0.92kcal/mol at temperatures above 700 K. Small negative temperature activation energies are reported in other studies: -0.9 ± 0.2 kcal/mol is reported by Greiner and Tully, -0.7 ± 0.3 kcal/mol by Atkinson et al., and -0.6 ± 0.3 kcal/mol by Zellner et al. Table 4.8 lists the QRRK input parameters for this reaction system at temperature of 296 K. Table 4.9 summarizes A_∞, E_a, and Γ^* for TS1(forward), TS1(reverse), and TS3(forward) at each temperature used in QRRK analysis.

Figure 4.8 and 4.9 show QRRK analysis rate constant results vs. pressure 0.001 to 100 atm at 296K and 524K respectively. The calculation at 296 K for the overall forward rate constant shows higher values below 0.1 atm. than Zellner et al.'s experimental data

and does not show significant falloff, while the total forward rate constant without tunneling slightly underestimates the data of Zellner et al.[46].

The rate constants for $CH_2O + CH_3$, $CH_3CHO + H$, and reverse reaction back to reactants ($C_2H_4 + OH$) are very similar over the entire pressure range at 296 K. These reactions are important at pressure below 0.01 atm. The stabilization reaction to ethylene-OH adduct dominates the reaction at pressures above 0.01 atm.

The QRRK analysis at 524 K and of 0.001 to 100 atm. slightly underestimates the overall reaction rate compared with experimental data[46]. The dissociation reaction back to reactants dominates at pressure below 1 atm. and stabilization to ethylene-OH adduct dominates at high pressure.

Figure 4.10 shows k vs. temperature at 1 atm. Smooth curves are not obtained because tunneling is included and a different A_∞ and $E_{a,\infty}$ are used at each temperature for $C_2H_4 + OH \rightarrow C\bullet H_2CH_2OH$. Stabilization to form ethylene-OH adduct is major reaction at temperature up to 500 K. Energized adduct dissociation back to reactants is the major reaction at temperature above 500 K. The calculated and experimentally determined forward rate constants are also shown in Figure 4.10. The calculated forward rate constant shows falloff up to temperature of 700 K, then increases with increasing temperature due to increasing rate constant for $C_2H_4 + OH \rightarrow CH_2CHOH + H$ at high temperature. Our calculation underestimates the forward rate constant comparing with Liu et al.'s experimental result[48]. Their rate constant also increases over 700 K and show a large discrepancy, but their results includes the abstraction reaction channel $C_2H_4 + OH \rightarrow C_2H_3 + H_2O$, which is not included in our calculation.

Table 4.8 Input Parameters [a] and High - Pressure Limit Rate Constants (K_∞) [b] for QRRK Calculations [c] (Temp=296K) : CBS-q Result

Input parameters for QRRK Calculations

High - Pressure Limit Rate Constants

	Reaction	$A(S^{-1}$ or $cm^3/(mol\ s)$	n	E_a (kcal/mol)
1	$C_2H_4 + OH \Rightarrow C.H_2CH_2OH$ [d]	7.19E+11	0.00	-0.92
-1	$C.H_2CH_2OH \Rightarrow C_2H_4 + OH$ [e]	1.58E+13	0.00	29.41
2	$C.H_2CH_2OH \Rightarrow C_2H_3OH + H$ [f]	2.16E+5	2.84	32.82
3	$C.H_2CH_2OH \Rightarrow CH_3CH_2O$ [g]	9.63E+11	0.60	29.57
-3	$CH_3CH_2O \Rightarrow C.H_2CH_2OH$ [h]	4.29E+12	0.56	23.47
4	$CH_3CH_2O \Rightarrow CH_2O + CH_3$ [i]	5.90E+11	0.67	13.63
5	$CH_3CH_2O \Rightarrow CH_3CHO + H$ [j]	3.64E+11	1.07	17.58

[a] Geometric mean frequency (from CPFIT, ref.[29]: 401.1cm^{-1} (4.446); 1312.0cm^{-1} (7.795); 3415.6cm^{-1} (4.760). Lennard-Jones parameters: σ_{ij}=4.35Å, ϵ/k=423[b]. The units of A factors and rate constants k are s^{-1} for unimolecular reactions and cm^3/(mol s) for bimolecular reactions. [c] ΔE down of 400 cal/mol is used. [d] $k_{\infty,1}$: Villa et.al. [e] $k_{\infty,-1}$: MR. [f] A_2 is calculated using TST and entropy of transition state (TS1), $\Delta S^{\neq}_{298}$ from MP2(full)/6-31G(d,p) (see Table 4.5), E_a from CBS-q calculation (see Table 4.5 and description for determination of E_a in Results section). [g] A_3 is calculated using TST and entropy of transition state (TS1), tunneling correction=178.6 is taken into account, $\Delta S^{\neq}_{298}$ from MP2(full)/6-31G(d,p) (see Table 4.5), E_a from CBS-q calculation (see Table 4.5 and description for determination of E_a in Results section). [h] A_{-3} is calculated using TST and entropy of transition state (TS1), tunneling correction=32.5 is taken into account, $\Delta S^{\neq}_{298}$ from MP2(full)/6-31G(d,p) (see Table 4.5), E_a from CBS-q calculation (see Table 4.5 and description for determination of E_a in Results section). [i] A_4 is calculated using TST and entropy of transition state (TS2), tunneling correction=21.05 is taken into account, $\Delta S^{\neq}_{298}$ from MP2(full)/6-31G(d,p) (see Table 4.5), E_a from CBS-q calculation (see Table 4.5 and description for determination of E_a in Results section). [j] A_5 is calculated using TST and entropy of transition state (TS3), tunneling correction = 21.05, $\Delta S^{\neq}_{298}$ from MP2(full)/6-31G(d,p) (see Table 4.5), E_a from CBS-q calculation (see Table 4.5 and description for determination of E_a in Results section).
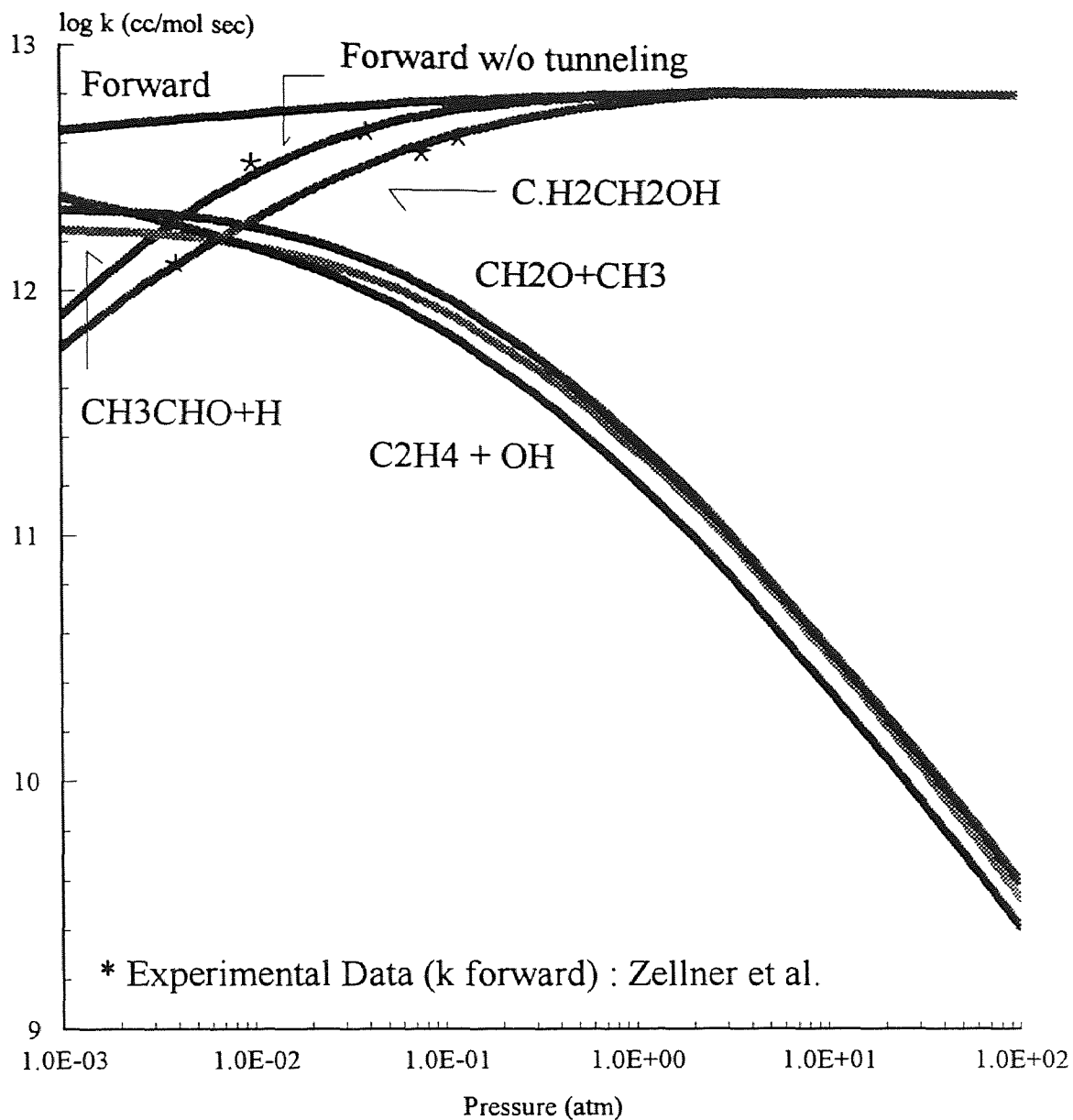
Figure 4.8 k vs Pressure at 296 K
C2H4 + OH --> Products
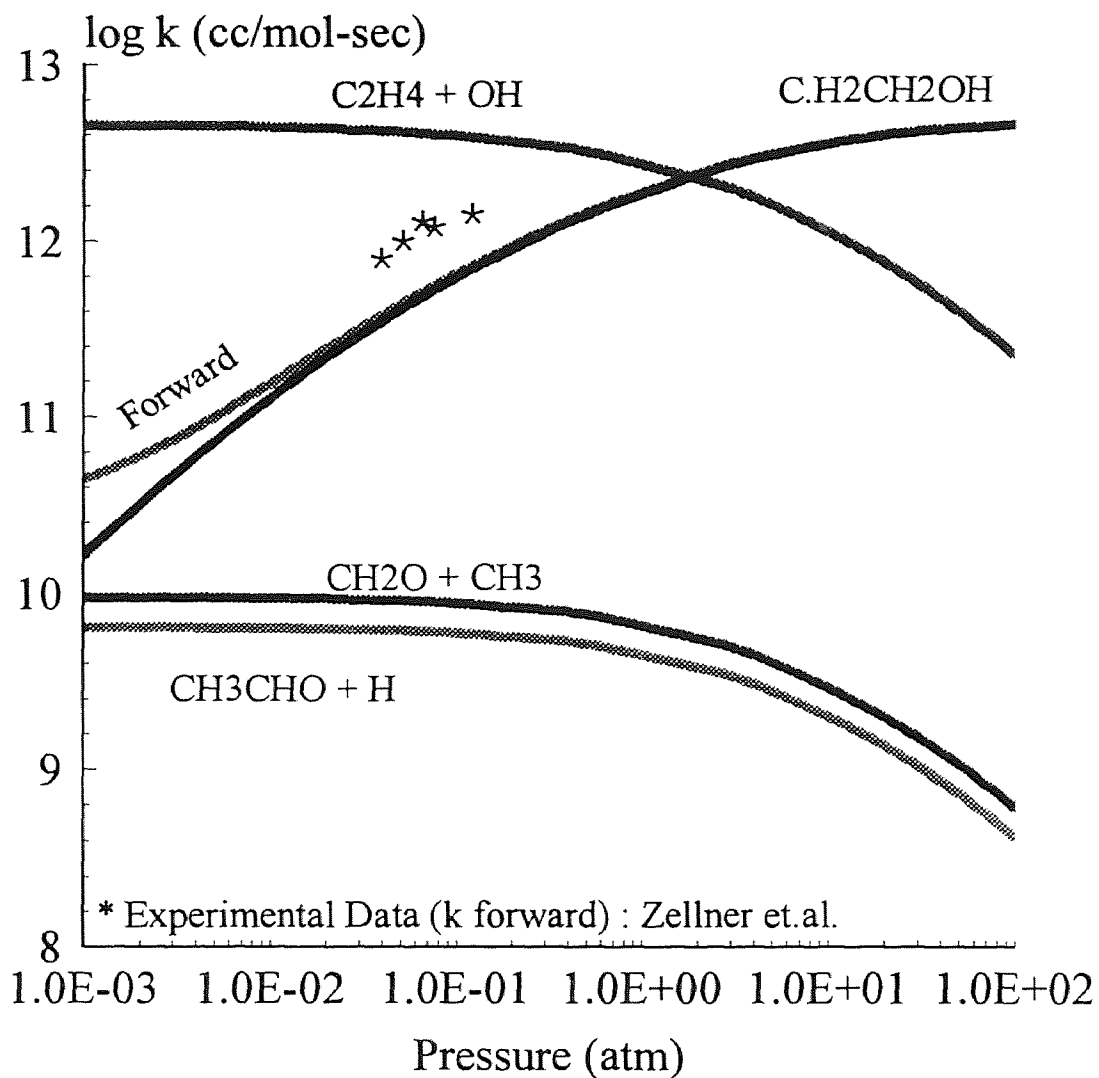
Figure 4.9 k vs. Pressure at 524 K
C2H4 + OH --> Products
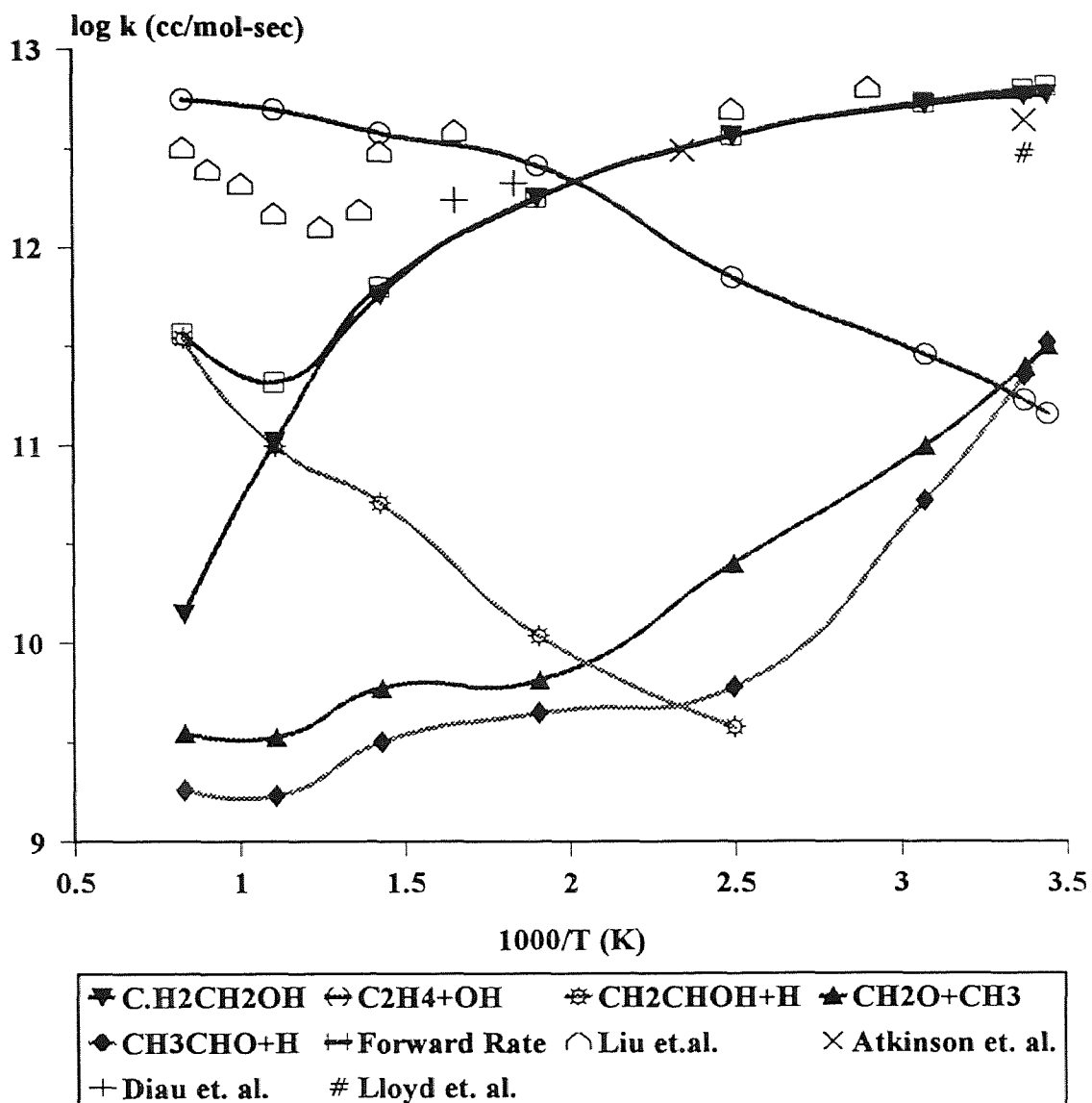
Figure 4.10 k vs. Temperature at 1 atm
C2H4 + OH --> Products

Table 4.9 Variables (A_1, $E_{a,1}$, and Γ^* for TS1(forward), TS1(reverse), and TS3(forward)

Temp (K)	A_1	$E_{a,1}$	Γ^* TS1(forward)	Γ^* TS1(reverse)	Γ^* TS3(forward)
290	1.44E+12	-0.92	1.39E+03	1.31E+02	2.46E+01
296	1.44E+12	-0.92	8.42E+02	9.31E+01	2.11E+01
325	1.44E+12	-0.92	1.26E+02	2.70E+01	1.13E+01
400	1.44E+12	-0.92	1.15E+01	5.90E+00	4.33E+00
524	5.56E+12	0.00	3.27E+00	2.49E+00	2.21E+00
700	5.56E+12	0.00	1.85E+00	1.62E+00	1.53E+00
900	8.84E+12	0.92	1.44E+00	1.34E+00	1.29E+00
1200	8.84E+12	0.92	1.23E+00	1.18E+00	1.16E+00

4.4 Summary

Thermodynamic properties of stable radicals and transition states are calculated using

composite *ab initio* methods, CBS-q//MP2(full)/6-31G(d,p) and G2 level of theory. A

potential energy diagram is developed and compared with previously reported *ab initio*

results and experimentally estimated values. Overall rate constants for OH addition to

ethylene and branching ratio (C•H_2CH_2OH stabilization : CH_2O+CH_3 : CH_3CHO+H) at 2

torr and 295K based on CBS-q//MP2(full)/6-31G(d,p) values and QRRK calculations are

compared with experimental result to evaluate thermodynamic properties derived from

the CBS-q calculation method and tunneling effects. S°_{298} and C_p(T)'s are calculated

based on MP2/6-31G(d,p) determined geometry and frequencies for CBS-q calculation

and MP2/6-31G(d) determined geometry and HF/6-31G(d) determined frequencies for

G2 calculation. Data from the CBS-q and G2 levels of theory show good agreement. $H_f°_{298}$ for the stable radicals $C\bullet H_2CH_2OH$ and $CH_3CH_2O\bullet$ are estimated using total energies derived from CBS-q and G2 calculations and isodesmic reactions, with ZPVE and thermal correction to 298.15K. $H_f°_{298}$ for CH_2CHOH are estimated using CBS-APNO and G2. QRRK analysis results with the composite *ab initio* determined thermodynamic properties show good agreement for overall rate constants with experimental data, but large differences exist for branching ratio. CBS-q determined thermodynamic properties are chosen for kinetic analysis and tunneling is considered in transition states TS1 and TS3, where H shift and H atom elimination reactions occur. The imaginary frequencies, which play a major role in the tunneling calculation, are adjusted to fit the experimental branching result; because unadjusted frequencies yield unrealistically high tunneling corrections. The tunneling correction in the rate constants at 296 K are 842, 93, and 21 for TS1 forward, TS1 reverse, and TS3 forward direction respectively. Three different A_∞'s and $E_{a,\infty}$'s are used for the reaction $C_2H_4 + OH \rightarrow C\bullet H_2CH_2OH$, which are derived using canonical variational TST.

CHAPTER 5

THERMODYNAMIC PARAMETERS AND GROUP ADDITIVITY RING CORRECTIONS FOR THREE- TO SIX-MEMBERED OXYGEN HETEROCYCLIC HYDROCARBONS

5.1 Introduction

Cyclic oxygenated hydrocarbons are important intermediates in chemical processes such as combustion, photochemical oxidation, and biological degradation of hydrocarbons. Many biological molecules including sugars, starches, nucleic acid segments etc, include cyclic ethers in addition to alcohol moieties. The initial breakdown products of cellulose and similar natural materials in pyrolysis and combustion are cyclic and bicyclic oxyhydrocarbons (often radicals). Reactions of alkyl radicals with molecular oxygen in combustion processes form peroxy species, which react to form cyclic ethers[71] and hydroperoxides. Thermodynamic properties of these radical intermediates are the controlling parameters for pseudo-equilibrium concentrations of these peroxy species, which in turn affect the overall rates of subsequent reactions leading to products in combustion process.[72] These reactions can strongly influence flame speeds and completeness of conversion or mineralization (formation of CO_2 and H_2O).

Cyclic peroxy intermediates are formed in reaction of allylic and propargyl radicals with O_2, which are important in biological,[73] combustion[24,71] and atmospheric photochemical oxidation systems.[74] For instance, the reaction of an allylic radical and O_2 initially forms allylic peroxy radical, $CH_2=CH-CH_2OO\bullet$, which may isomerize to form primary and secondary alkyl radicals of cyclic peroxides:
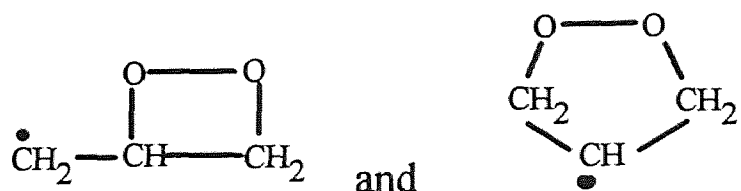
Cyclic peroxides are also formed in the reaction of vinyl, acetylenic, and phenyl radicals

with O_2. Here the reactions initially form a peroxy radical ($CH_2=CHOO\bullet$ or $CH\equiv COO\bullet$),

that reacts to form 3-membered ring, dioxirane alkyl radicals:
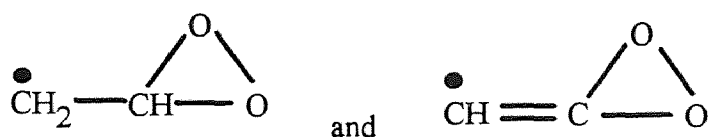
These radicals further react to carbonyl and alkoxy radicals, via cleavage of the weak O–

O bond.

Reactions of ozone with alkynes and alkenes in the atmosphere is another example,

where thermodynamic properties of cyclic oxygenated hydrocarbons are important. The

reactions of ozone with alkynes and alkenes are assumed to proceed by addition to form a

primary ozonide[75,76]:
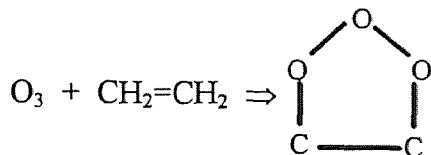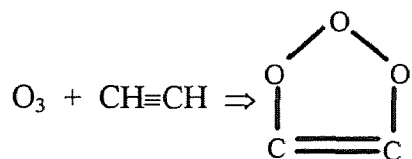
Ideal gas thermodynamic properties of twenty two oxygenated heterocyclic

compounds of three to six-membered rings were reported by Dorofeeva.[77,78] Enthalpies

of formation of 10 cyclic oxyhydrocarbons (furan, oxirane, oxetane, 3,4-dihydro-2H-

pyran, tetrahydrofuran, tetrahydro-2H-pyran, 1,3-dioxolane, 1,4-dioxane, 1,3-dioxane,

1,3,5-trioxane) in her paper were adopted from experimental values which were

originally quoted by Pedley et al.[79] Data on $\Delta H_f°_{298}$ for twelve other three to six-

membered ring species (oxirene, dioxirane, 1,2-dioxetane, 2,3-dihydrofuran, 2,5-

dihydrofuran, 1,2-dioxolane, 1,2,3-trioxolane, 1,2,4-trioxolane, 3,6-dihydro-2H-pyran ,

3,6-dihydro-1,2-dioxin, 2,3-dihydro-1,4-dioxin, 1,4-dioxin) in Dorofeeva's work were

estimated using a difference method, which is consistent with group additivity.[13] For

instance, the value of $\Delta H_f°_{298}$(3,6-dihydro-2H-pyran) was assumed to be the same as

$\Delta H_f°_{298}$(3,4-dihydro-2H-pyran). The enthalpy of formation of oxirene, as the second

example, was estimated based on the difference values between $-CH_2-$ and $-O-$ groups of

similar ring compounds:

$\Delta H_f°_{298}$(oxirene) $-\Delta H_f°_{298}$(cyclopropene) = $\Delta H_f°_{298}$(oxirane) - $\Delta H_f°_{298}$(cyclopropane).
(unknown)

The enthalpy of formation of dioxirane was also estimated by applying this enthalpy

difference method:

$\Delta H_f°_{298}$(dioxirane) - $\Delta H_f°_{298}$(oxirane) =
(unknown)
$\Delta H_f°_{298}$(dimethylperoxide) - $\Delta H_f°_{298}$(methoxyethane).

It is shown that the different method does not yield accurate results for small ring species,

i.e. 3 to 5 membered rings.

$\Delta H_f^\circ{}_{298}$ data obtained from semi-empirical molecular orbital method, PM3,[32] is compared with values previously reported. The experimentally determined enthalpies of formation of 10 cyclic oxyhydrocarbons listed above are used as reference data to calibrate PM3-determined enthalpies of formation. An empirical equation is then obtained and used to calculate enthalpies of formation for 12 new cyclic oxyhydrocarbons: dioxetane, dioxirene, 1,2-dioxolene, 1,3-dioxolene, 1,2,3-trioxolene, for 1,2-dioxane, 3,4-dihydro-1,2-dioxin, 2,4-dihydro-1,3-dioxin, 1,2,4-trioxane, 1,2,3-trioxane, 1,2,4-trioxene, 1,2,3-trioxane.

Structural parameters and fundamental frequencies resulting from either experiments or ab initio calculations have been adopted in Dorofeeva's work to calculate entropies and heat capacities for 13 oxygen heterocyclics.[77,78] Vibrational frequencies of remaining molecules in her work were estimated based on the force constants evaluated from related compounds. The frequencies of 1,2-dioxolane were calculated, for instance, using 20 force constants transferred from tetrahydrofuran and 1,2,4-trioxolane. It is known that the PM3 method provides an economical way to obtain molecular structural parameters, fundamental frequencies and subsequent thermodynamic properties.[80] Therefore, it is been interested in comparing PM3-determined values with the data reported by Dorofeeva. Uncertainties of entropies and heat capacities obtained using the PM3 method are evaluated and reported.

Benson's Group Additivity (GA) technique is commonly used for the estimation of ideal gas phase enthalpies of formation, heat capacities, and entropies.[13,21] The method assumes that the properties for a chemical substance are the sum of the contributions from each polyvalent atom (central atoms) in that molecule. In group additivity the "ring

groups" for cyclic compounds are needed to incorporate ring corrections as group values are derived from noncylic (chain) compounds. Groups for ring species considered in the present study are derived. The ring group corrections, once obtained, allow determination of the thermodynamic properties for cyclic compounds with alkyl substituents, which frequently appear in atmospheric oxidation systems. Examples are alkyl substituted ozonides:
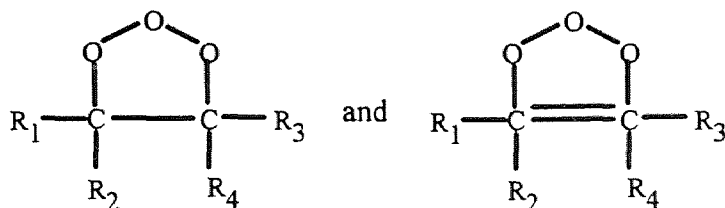
Thermodynamic properties ($\Delta H_f^{\circ}{}_{298}$, $S^{\circ}{}_{298}$ and $C_p(T)$, $300 \leq T/K \leq 1500$) on a total of 34 cyclic oxyhydrocarbons, which include 22 previously studied species and 12 new species listed above, are calculated in this study. The corresponding ring groups for use in group additivity are also derived.

5.2 Method

Thermodynamic properties are calculated for compounds in an ideal gas standard state at 1 atm. The standard state for molecules with optical isomers is defined as an equilibrium mixture of enantiomers at the total pressure 1 atm.

Optimized molecular geometry, moments of inertia for external rotation, and vibrational frequencies were obtained using the PM3 [32] method in the MOPAC 6.0 computer package. The restricted Hartree-Fock (RHF) method with the self-consistent-field (SCF) molecular orbital (MO) treatment using the PM3 parameter set is employed for the calculations of all molecules. It should be noted that PM3 parameters were

optimized to reproduce experimentally determined enthalpies of formation and molecular

geometries observed at 298 K; not the energies of molecules (E_{eq}) or equilibrium

geometry at 0 K.

Enthalpies of formation of 10 cyclic oxyhydrocarbons (furan, oxirane, oxetane, 3,4-

dihydro-2H-pyran, tetrahydrofuran, tetrahydro-2H-pyran, 1,3-dioxiolane, 1,4-dioxane,

1,3-dioxane, 1,3,5-trioxane) have been previously determined by experiments.[79] These

enthalpy values are used as reference data to calibrate PM3-determined enthalpies of

formation ($\Delta H_f^\circ{}_{298,PM3}$). Enthalpies of formation for species where no experimental data

exist are obtained using the PM3 method and corrected by this scaling equation.

Calculations of standard entropies and heat capacities are implemented by MOPAC 6.0

with its internal programs which are based on the statistical mechanics. The potentials of

ring inversion (ring puckering or pseudo-rotation) of oxetane, tetrahydrofuran, 2,3-

dihydrofuran, 2,5-dihydrofuran, 1,3-dioxolane, and 1,3,5-trioxane are included in the

determination of the thermodynamic properties in the literature.[77,78] For these five

molecules the inversion frequencies obtained using the PM3 method are excluded in

calculations of thermodynamic properties. They are replaced by the ring inversion or

pseudorotation contributions to entropies and heat capacities derived from the

lierature.[77,78]

The absolute standard deviation (s) of enthalpies of formation determined in this

work is calculated by root-mean-square: $s = [\ \Sigma\ \delta_i^2\ /\ (n-1)\ ]^{1/2}$. Experimentally determined

enthalpies of formation of the ten molecules listed above are used as reference data in the

calculation of the $s_{\Delta H_f^\circ 298}$ value of regressed, PM3-determined $\Delta H_f^\circ{}_{298}$ values. The

$\Delta H_f^\circ{}_{298}$ data estimated by Dorofeeva are neither used in the calibration of PM3-

determined $\Delta H_f^\circ{}_{298}$ nor in the calculation of absolute standard deviation (s).

Limited experimental data on entropies and heat capacities of these molecules are

available. The entropy and heat capacity data of 22 molecules reported by Dorofeeva are

therefore used as reference data to calculate the absolute standard deviations of entropies

at 298 K and heat capacities from 300 K to 1500 K resulting from the PM3 method. The

absolute standard deviations (s) for entropies and heat capacities determined in this work

are also calculated by root-mean-square.

Cyclic group parameters are derived using the thermodynamic properties from the

literature or those obtained in the present study as described later for each molecules.

Derivation of cyclic group values utilizes non-cyclic group values reported by Benson

and Cohen, [13,81] and authors' reassignments based on recent literature data[13,24,74,82-

84] on standard enthalpies of formation for certain compounds.

5.3 Results and Discussion

Vibrational frequencies and moments of inertia are listed in Table 5.1. Thermodynamic

properties, $\Delta H_f^\circ{}_{298}$, $S^\circ{}_{298}$ and $C_p(T)$ ($300 \leq T/K \leq 1500$), are listed in Table 5.2. Parameters

of ring groups are listed in Table 5.3.

The comparison of experimental versus PM3-determined enthalpies of formation is

illustrated in Figure 5.1. A regressed line with an R-squared value equal to 0.993 is

obtained:

$$\Delta H_f^\circ{}_{298,expt.} = -1.642 + 0.882 \times \Delta H_f^\circ{}_{298,PM3.} \qquad \text{---------- (1)}$$

Table 5.1 Vibrational Frequencies (v: cm^{-1}) and Moments of Inertia (I: 10^{-40} g-cm^2) Calculated Using the PM3 Method
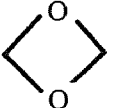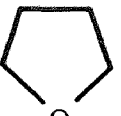
1	Oxirane	v: 793, 893, 916, 932, 1015, 1072, 1142, 1176, 1300, 1358, 1575, 3038, 3053, 3063, 3064. I: 32.50, 39.08, 60.57.
2	Oxirene	v: 669, 748, 844, 937, 1021, 1195, 1948, 3245, 3295. I: 26.16, 29.34, 55.50.
3	Dioxirane	v: 750, 923, 924, 1006, 1193, 1265, 1552, 2938, 2949. I: 27.97, 37.38, 59.78.
4	Oxetane	v: 263, 825, 840, 873, 949, 957, 976, 999, 1012, 1064, 1116, 1190, 1207, 1262, 1314, 1374, 1397, 1440, 3001, 3007, 3045, 3049, 3057, 3122. I: 70.87, 71.10, 125.96.
5	1,2-Dioxetane	v: 250, 800, 830, 840, 948, 977, 980, 1012, 1085, 1207, 1288, 1290, 1373, 1420, 2982, 2997, 3038, 3038. I: 61.87, 72.24, 123.38.
6	1,3-Dioxetane	v: 234, 906, 914, 922, 923, 947, 988, 1005, 1059, 1213, 1229, 1334, 1360, 1427, 2956, 2960, 2970, 2974, I: 59.91, 66.05, 114.9.
7	Dioxirene	v: 441, 775, 842, 863, 927, 980, 1011, 1276, 1339, 1756, 3154, 3180. I: 51.38, 60.52, 111.90.
8	Tetrahydro-furan	v: 75, 116, 679, 716, 780, 828, 932, 975, 1001, 1022, 1026, 1066, 1075, 1108, 1117, 1127, 1132, 1282, 1290, 1303, 1359, 1377, 1392, 1413, 1433, 2964, 2968, 2984, 2998, 3033, 3036, 3070, 3075. I: 117.68, 122.22, 217.55.

Table 5.1 Vibrational Frequencies (v: cm^{-1}) and Moments of Inertia (I: 10^{-40} g-cm^2) Calculated Using the PM3 Method (cont'd)
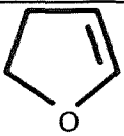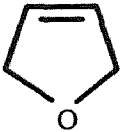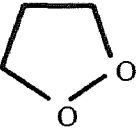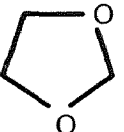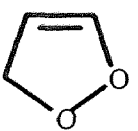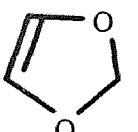
9	2,3-Dihydro-furan	v: 220, 442, 732, 766, 826, 840, 924, 951, 981, 1034, 1037, 1057, 1079, 1089, 1173, 1258, 1312, 1369, 1393, 1417, 1789, 2980. 2996, 3038, 3066, 3111, 3163. I: 103.96, 107.84, 201.22.
10	2,5-Dihydro-furan	v: 209, 395, 756, 760, 796, 889, 939, 954, 977, 982, 1003, 1046, 1074, 1080, 1152, 1242, 1322, 1348, 1377, 1390, 1816, 2960, 2964, 3011, 3013, 3137, 3155. I: 103.99, 107.98, 201.22.
11	Furan	v: 502, 516, 764, 774, 872, 877, 883, 944, 979, 1026, 1069, 1102, 1290, 1313, 1486, 1611, 1697, 3128, 3134, 3166, 3178. I: 89.96, 92.47, 182.43.
12[a]	1,2-Dioxolane	v: 85, 165, 649, 666, 784, 794, 905, 999, 1000, 1042, 1058, 1084, 1092. 1119, 1123, 1291, 1334, 1343, 1383, 1387, 1421, 2961, 2962, 2996, 3029. 3030, 3076. I: 110.65, 121.72, 213.21.
13	1,3-Dioxolane	v: 143, 172, 683, 738, 831, 908, 995, 956, 986, 998, 1038, 1073, 1085. 1100, 1142, 1275, 1288, 1350, 1365, 1380, 1403, 2917, 2972, 2983. 2987. 3037, 3040. I: 109.5, 110.95, 201.57.
14	1,2-Dioxolene	v: 183, 416, 686, 747, 759, 880, 886, 952, 981, 998, 1048, 1052, 1191. 1348, 1366, 1393, 1789, 2956, 2999, 3098, 3165. I: 95.70, 109.32, 199.61.
15	1,3-Dioxolene	v: 216, 436, 712, 776, 864, 865, 917, 919, 941, 999, 1036, 1098, 1248. 1252, 1349, 1386, 1780, 2939, 2955, 3127, 3148. I: 96.12, 97.41, 188.01.

Table 5.1 Vibrational Frequencies (ν: cm^{-1}) and Moments of Inertia (I: 10^{-40} g-cm^2) Calculated Using the PM3 Method (cont'd)
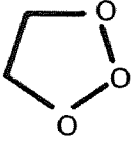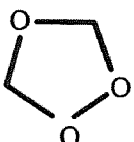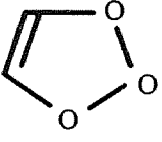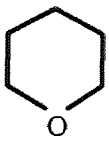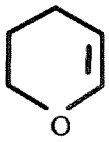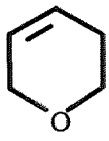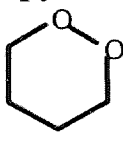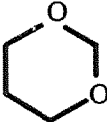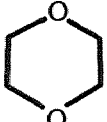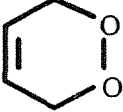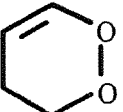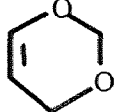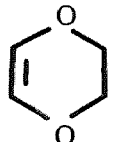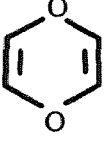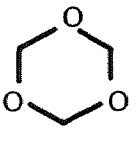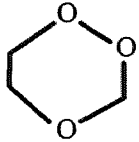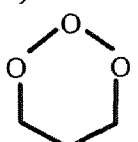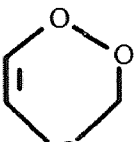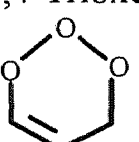
16	1,2,3-Trioxolane	ν: 113, 239, 450, 578, 718, 750, 832, 976, 1003, 1044, 1064, 1069, 1111, 1301, 1330, 1374, 1384, 2965, 2978, 3041, 3045. I: 105.80, 112.96, 200.04.
17	1,2,4-Trioxolane	ν: 147, 248, 619, 666, 785, 895, 904, 942, 980, 1034, 1058, 1140, 1150, 1324, 1355, 1360, 1375, 2905, 2909, 2981, 2989. I: 96.09, 113.82, 192.88.
18	1,2,3-Trioxolene	ν: 203, 393, 609, 619, 749, 777, 861, 904, 962, 991, 1280, 1381, 1806, 3103, 3123. I: 92.73, 102.87, 195.60.
19	Tetrahydro-2H-pyran	ν: 182, 225, 356, 479, 482, 620, 823, 871, 936, 948, 958, 970, 1002. 1038, 1076, 1080, 1112, 1133, 1137, 1141, 1150, 1157, 1278, 1319, 1321. 1346, 1365, 1373, 1380, 1404, 1411, 1414, 2941, 2944, 2959, 2971, 2978. 3039, 3041, 3042, 3050, 3055. I: 179.03, 187.20, 323.64.
20	3,4-Dihydro-2H-pyran	ν: 153, 238, 406, 519, 534, 735, 775, 872, 932, 941, 967, 993, 1025, 1051. 1052, 1089, 1108, 1130, 1148, 1150, 1293, 1330, 1341, 1370, 1390, 1412. 1434, 1855, 2951, 2958, 2978, 3033, 3035, 3054, 3070, 3092. I: 162.17, 176.05, 312.14.
21	3,6-Dihydro-2H-pyran	ν: 127, 277, 366, 532, 539, 704, 789, 864, 952, 968 983, 995, 1026, 1040, 1053, 1088, 1099, 1110, 1138, 1164 1262, 1379, 1346, 1353, 1383, 1392, 1428, 1873, 2924, 2943 2959, 3025, 3034, 3041, 3060, 3081. I: 165.55, 172.94, 313.30.
22	1,2-Dioxane	ν: 226, 228, 372, 462, 498, 630, 693, 870, 907, 948, 979, 982, 1043, 1081, 1089, 1117, 1127, 1133, 1142, 1149, 1289, 1327, 1347, 1352, 1370, 1375, 1400, 1411, 2944, 2953, 2972, 2981, 3034, 3042, 3044, 3050. I: 177.58, 181.37, 319.11.

Table 5.1 Vibrational Frequencies (v: cm⁻¹) and Moments of Inertia (I: 10⁻⁴⁰ g-cm²) Calculated Using the PM3 Method (cont'd)

23	1,3-Dioxane	v: 170, 250, 362, 484, 516, 644, 862, 897, 938, 974, 985, 1009, 1032, 1047, 1107, 1110, 1120, 1125, 1128, 1158, 1279, 1307, 1330, 1343, 1365, 1369, 1378, 1406, 2890, 2943, 2945, 2987, 3022, 3042, 3043, 3063. I: 171.50, 172.33, 307.14.
24	1,4-Dioxane	v: 168, 278, 349, 510, 512, 672, 833, 929, 963, 977, 986, 1021, 1036, 1041, 1076, 1091, 1117, 1124, 1129, 1150, 1302, 1306, 1334, 1359, 1366, 1371, 1378, 1379, 2953, 2955, 2965, 2967, 3041, 3044, 3048, 3051. I: 165.84, 182.59, 312.98.
25	3,6-Dihydro-1,2-dioxin	v: 196, 300, 394, 501, 541, 718, 741, 855, 902, 975, 1021, 1022, 1038, 1064, 1067, 1097, 1114, 1153, 1275, 1330, 1351, 1376, 1418, 1868, 2936, 2936, 3024, 3024, 3070, 3089. I: 159.50, 171.20, 305.83.
26	3,4-Dihydro-1,2-dioxin	v: 120, 278, 405, 503, 535, 695, 741, 825, 899, 952 979, 1021, 1046, 1082, 1095, 1114, 1129, 1146, 1316, 1347 1376, 1389, 1445, 1857, 2949, 2964, 3036, 3041, 3063, 3089. I: 161.82, 169.81, 310.45.
27	2,4-Dihydro-1,3-dioxin	v: 165, 278, 408, 520, 568, 758, 827, 897, 937, 965 993, 1015, 1031, 1054, 1078, 1099, 1111, 1159, 1274, 1322 1340, 1366, 1418, 1838, 2908, 2943, 3016, 3025, 3076, 3107. I: 154, 161, 294.
28	2,3-Dihydro-1,4-dioxin	v: 174, 228, 434, 556, 557, 769, 793, 872, 933, 974 998, 1012, 1043, 1056, 1081, 1102, 1110, 1200, 1316, 1330 1359, 1375, 1405, 1840, 2958, 2971, 3038, 3042, 3081, 3099. I: 150, 170, 301.

Table 5.1 Vibrational Frequencies (ν: cm^{-1}) and Moments of Inertia (I: 10^{-40} g-cm^2) Calculated Using the PM3 Method (cont,d)

29	1,4-Dioxin	ν: 142, 386, 475, 597, 654, 774, 779, 876, 898, 921 1026, 1036, 1044, 1047, 1137, 1182, 1316, 1383, 1814, 1880 3078, 3082, 3096, 3101. I: 135.11, 155.73, 290.84.
30	1,3,5-Trioxane	ν: 223, 232, 369, 499, 501, 656, 927, 930, 934, 938, 957, 1054, 1071, 1076, 1079, 1105, 1141, 1146, 1236, 1325, 1328, 1337, 1360, 1361, 2887, 2889, 2891, 3018, 3018, 3023. I: 159.06, 159.80, 286.41.
31	1,2,4-Trioxane	ν: 213, 245, 369, 475, 491, 660, 705, 884, 960, 988, 998, 1025, 1034, 1085, 1099, 1110, 1121, 1160, 1299, 1323, 1337, 1367, 1371, 1379, 2901. 2952, 2965, 3017, 3040, 3048, I: 162.30, 174.04, 301.83.
32	1,2,3-Trioxane	ν: 213, 244, 369, 475, 491, 660, 705, 884, 960, 988, 998, 1025, 1034, 1085, 1099, 1110, 1121, 1160, 1299, 1323, 1337, 1367, 1371, 1379, 2901. 2952, 2965, 3017, 3040, 3048 I: 162.30, 174.04, 301.83.
33	1,2,4-Trioxene	ν: 109, 296, 433, 514, 528, 678, 773, 865, 874, 951, 984, 1009, 1042. 1072, 1130, 1203, 1282, 1367, 1423, 1804, 2913, 3004, 3071, 3095. I: 147.41, 161.58, 289.06.
34	1,2,3-Trioxene	ν: 161, 303, 366, 409, 483, 576, 680, 753, 865, 907, 991, 1022, 1041. 1069, 1095, 1123, 1319, 1344, 1423, 1845, 2947, 3030, 3067, 3107. I: 151.24, 164.60, 294.66.

[a] Frequencies calculated at the RHF/6-31G* level of theory for 1,2-dioxolane (scaled by 0.9): 114, 326, 657, 685, 800, 901, 912, 930, 959, 1010, 1112, 1155, 1224, 1243, 1245, 1306, 1333, 1387, 1478, 1493, 1508, 2915, 2917, 2930, 2956, 2981, 2986

The standard deviation of the scaled PM3 enthalpies of formation using equation 1 versus experimental values is 3.16 kcal/mol. Enthalpies of formation of this work listed in Table 5.2 are calculated using equation 1. Absolute differences between enthalpies of formation obtained using equation 1 versus those reported by Dorofeeva range from 0.5 (1,4-dioxane) to 16.8 kcal/mol (1,2,3-trioxolane).

There is no experimental data on $\Delta H_f^{\circ}{}_{298}$(1,2,3-trioxolane). It was estimated by Dorofeeva to be -23.90 kcal/mol[77] using the difference method described above. The value determined using equation 1 is, however, -7.09 kcal/mol. Jungkamp and Seinfeld[85] recently report enthalpies of formation for three trioxy compounds: HOOOH, CH_3OOOH, and C_2H_5OOOH to be: -21.82, -21.34, and -28.52 kcal mol^{-1}, respectively. These values are determined using ab initio calculations at the G2, G2M, and G2M/MP2 levels of theory. The $\Delta H_f^{\circ}{}_{298}$ data calculated by PM3 for these three species are: -27.39, -22.86, and -25.92 kcal mol^{-1}, and after scaling by equation 1, they are: -25.80, -21.80, and -24.50 kcal mol^{-1}, respectively, as shown in Table 5.4. The maximum deviation of scaled PM3-calculated $\Delta H_f^{\circ}{}_{298}$ data from the values reported by Jungkamp et al. is 4.02 kcal mol^{-1}. The PM3-determined $\Delta H_f^{\circ}{}_{298}$(1,2,3-trioxolane) value with 4.02 kcal/mol uncertainty, -7.09±4.02 kcal mol^{-1}, indicates that Dorofeeva's data: -23.90 kcal mol^{-1} could be ca. 12.8 kcal mol^{-1} too low.

The enthalpies of formation of two other molecules: dioxirane, and 1,2-dioxolane determined using equation 1 are also significantly lower than Dorofeeva's values by 10.83 and 6.97 kcal/mol, respectively. The experimental data on $\Delta H_f^{\circ}{}_{298}$ of these two molecules are again not available. A study[74] of enthalpies of formation of cyclic alkyl peroxides using ab initio calculations at the MP4SDTQ/6-31G*//MP2/6-31G* level of

theory combined with the isodesmic reactions results in $\Delta H_f^\circ{}_{298}$(dioxirane) = -2.91±1.34

kcal/mol and $\Delta H_f^\circ{}_{298}$(1,2-dioxolane) = -27.43±0.91 kcal/mol. These values are more

consistent with the values determined using equation 1: $\Delta H_f^\circ{}_{298}$(dioxirane) = -2.47

kcal/mol and $\Delta H_f^\circ{}_{298}$(1,2-dioxolane) = -27.42 kcal/mol, and ≥7 kcal/mol different from

the Dorofeeva's $\Delta H_f^\circ{}_{298}$ data. These two $\Delta H_f^\circ{}_{298}$ values determined at the MP4SDTQ/6-

31G* level of theory are included in the data of Figure 5.1 and recalculate the standard

deviation (s) of regressed PM3-determined $\Delta H_f^\circ{}_{298}$ to be 2.89 kcal/mol.

The standard deviation of the PM3-determined entropy versus Dorofeeva's data is

1.15 cal mol^{-1} K^{-1} (e.u.). The PM3-determined entropies of six species (oxirene,

tetrahydrofuran, 1,2,4-trioxolane, 1,3-dioxane, 3,6-dihydro-1,2-dioxin, 1,3,5-trioxane)

differ from those in Dorofeeva's work by more than 1.0 but less than 2.0 e.u. For the

remaining fifteen molecules, the entropy differences are smaller than 1 e.u. The largest

difference in the entropies is 3.26 e.u as for 1,2-dioxolane, which mainly results from

difference in vibrational frequencies. The frequencies of 1,2-dioxolane were

calculated[77,78] using 20 force constants transferred from tetrahydrofuran and 1,2,4-

trioxolane. The vibrational contribution to entropy ($S^\circ{}_{298,vib}$) of 1,2-dioxolane is 8.27 e.u.

from the PM3-calculated vibrational frequencies, while it is 5.07 e.u. from Dorofeeva's

frequencies.

Vibrational frequencies of 1,2-dioxolane are further calculated at the RHF/6-31G*

level of theory using the Gaussian 94[9] system of programs. The default optimization

criteria and the analytical method for vibrational frequency calculation are employed.

The value of $S^\circ{}_{298,vib}$ is 6.29 e.u. from the frequencies obtained at the RHF/6-31G*

(scaled by 0.9),[12] which is 1.98 e.u. lower than the PM3 $S^\circ{}_{298,vib}$, and 1.22 e.u. higher

than Dorofeeva's value. At this step, Dorofeeva's data on entropies and heat capacities for 1,2-dioxolane in the derivation of the ring group values is adopted.

The standard deviations of PM3-determined heat capacities from Dorofeeva's data for temperatures of 300 K through 1500 K are all smaller than 1.0 cal mol^{-1} K^{-1}: 0.79, 0.91, 0.92, 0.83, 0.82, 0.62, 0.45, 0.29 cal mol^{-1} K^{-1} for $C_{p,300}$, $C_{p,400}$, $C_{p,500}$, $C_{p,600}$, $C_{p,800}$, $C_{p,1000}$, and $C_{p,1500}$, respectively. The deviation is more than 1 cal mol^{-1} K^{-1} for four molecules: oxirene, 1,2,4-trioxolane, 1,3-dioxane, and 1,3,5-trioxane. The largest difference observed is that for $C_{p,500}$ of 1,3,5-trioxolane as 2.45 cal mol^{-1} K^{-1}, which results from the differences in vibrational frequencies. Vibrational frequencies of 1,3,5-trioxane adopted by Dorofeeva are experimentally determined.[86]

A recent ab initio study[87] by Vacek et al. indicates that the C_{2v} structure of oxirene is a transition state, with an imaginary frequency corresponding to a ring-opening normal coordinate, according to DFT (BLYP, B3LYP) calculations, and the MP4 and CCSD(T) methods with large *spd* basis sets. Other methods (RHF, MP2, CISD, and CCSD(T)) indicate it is a true minimum.[87] At the highest level of theory performed by Vacek et al., CCSD (T) with basis set of triple-ζ quality including multiple *pdf* shells, oxirene is a true minimum with the lowest harmonic vibrational frequency in the range of 139-163 cm^{-1}. The lowest vibrational frequency adopted by Dorofeeva is, however, 450 cm^{-1},[77] which is also supported by the calculations at the RHF/QZ3P(f,d) level of theory.[87] The vibrational frequencies of oxirene are still not well characterized since significant controversy exists between different levels of theory. At this step, the entropy and heat capacity data of oxirene reported by Dorofeeva are adopted in the derivation of ring groups.

Table 5.2 Thermodynamic Properties [a] of Cyclic Oxyhydrocarbons

	Compound	$\Delta H_f^{\circ}{}_{298}$	$S^{\circ}{}_{298}$	C_{p300}	C_{p400}	C_{p500}	C_{p600}	C_{p800}	C_{p1000}	C_{p1500}
1	Oxirane (σ=2 , OI=1)[b]									
	This work	-8.81	58.14	11.58	15.09	18.25	20.85	24.78	27.60	31.88
	Ref. 8	-12.57	57.98	11.30	14.74	17.90	20.55	24.57	27.46	31.28
2	Oxirene (σ=2, OI=1)									
	This work	44.63	57.50	11.22	13.44	15.22	16.62	18.69	20.18	22.49
	Ref. 8	40.63	58.70	13.00	15.12	16.68	17.86	19.62	20.89	22.91
3	Dioxirane (σ=2, OI=1)									
	This work	-2.47	57.81	10.47	12.71	14.69	16.30	18.69	20.34	22.75
	Ref. 8	8.36	57.69	10.53	12.80	14.78	16.38	18.73	20.35	22.72
4	Oxetane (σ=2, OI=1)									
	This work	-25.20	64.78	14.82	20.27	25.20	29.27	35.38	39.71	46.24
	Ref. 8	-19.24	64.87	14.80	20.07	24.91	28.99	35.24	39.70	46.35
5	1,2-Dioxetane (σ=2, OI=1)									
	This work	-6.38	62.90	14.25	18.58	22.36	25.42	29.98	33.05	37.64
	Ref. 8	2.39	62.23	13.62	17.80	21.57	24.71	29.49	32.73	37.53
6	1,3-Dioxetane (σ=2, OI=1)									
		-57.24	64.10	14.00	18.30	22.20	25.30	29.90	33.10	37.70
7	Dioxirene (σ=2, OI=1)									
		25.08	61.36	12.81	15.91	18.47	20.49	23.38	25.33	28.12
8	Tetrahydrofuran (σ=2, OI=1)									
	This work	-46.87	71.53	19.54	26.81	33.39	38.85	47.09	52.94	61.72
	Ref. 8	-44.02	72.26	18.45	25.59	32.13	37.64	46.07	52.08	60.97
9	2,3-Dihydro-furan (σ=1, OI=1)									
	This work	-23.52	69.40	17.19	23.44	28.91	33.37	40.02	44.70	51.67
	Ref. 8	-17.92	69.92	17.86	24.01	29.40	33.82	40.46	45.14	52.03
10	2,5-Dihydro-furan (σ=2, OI=1)									
	This work	-20.90	67.69	17.69	23.93	29.38	33.81	40.40	45.03	51.93
	Ref. 8	-16.73	67.95	18.20	24.41	29.80	34.20	40.79	45.42	52.24
11	Furan (σ=2, OI=1)									
	This work	-5.19	64.21	15.75	20.97	25.38	28.91	34.05	37.58	42.76
	Ref. 8	-8.34	63.87	15.74	21.22	25.77	29.34	34.45	37.91	42.95

Table 5.2 Thermodynamic Properties [a] of Cyclic Oxyhydrocarbons (cont'd)

12	1,2-Dioxolane (σ=2, OI=2)									
	This work	-27.42	71.93	18.81	24.91	30.28	34.68	41.22	45.80	52.89
	Ref. 8	-21.51	68.67	18.51	24.78	30.26	34.73	41.37	46.01	52.79
13	1,3-Dioxolane (σ=2, OI=1)									
	This work	-74.38	72.37	17.48	23.64	29.11	33.58	40.20	44.82	51.63
	Ref. 8	-71.22	71.66	17.08	22.89	28.22	32.72	39.56	44.39	51.47
14	1,2-Dioxolene (σ=1, OI=1)									
		-4.62	68.16	17.18	22.24	26.48	29.87	34.80	38.20	43.15
15	1,3-Dioxolene (σ=2, OI=1)									
		-49.03	66.11	16.87	22.00	26.32	29.76	34.75	38.18	43.16
16	1,2,3-Trioxolane (σ=1, OI=1)									
	This work	-7.09	71.28	18.84	23.71	27.78	31.00	35.68	38.88	43.56
	Ref. 8	-23.90	71.87	18.72	23.54	27.62	30.89	35.65	38.92	43.64
17	1,2,4-Trioxolane (σ=2, OI=2)									
	This work	-59.12	69.85	17.77	22.78	27.03	30.43	35.35	38.71	43.53
	Ref. 8	-50.19	68.17	16.55	21.44	25.77	29.32	34.54	38.12	43.24
18	1,2,3-Trioxolene (σ=1, OI=1)									
		16.72	68.21	16.94	20.72	23.65	25.89	29.02	31.10	34.02
19	Tetrahydro-2H-pyran (σ=1, OI=1)									
	This work	-52.28	74.43	23.83	32.96	41.17	48.00	58.32	65.67	76.67
	Ref. 9	-53.39	73.72	23.86	32.77	40.87	47.73	58.27	65.80	76.94
20	3,4-Dihydro-2H-pyran (σ=1, OI=2)									
	This work	-31.00	74.89	22.48	30.44	37.45	43.22	51.90	58.06	67.23
	Ref. 9	-29.90	74.36	22.17	29.96	36.96	42.82	51.73	58.04	67.35
21	3,6-Dihydro-2H-pyran (σ=1, OI=2)									
	This work	-29.24	75.12	22.52	30.49	37.51	43.29	51.98	58.13	67.29
	Ref. 9	-29.90	74.54	22.75	30.69	37.69	43.49	52.26	58.46	67.58
22	1,2-Dioxane (σ=2, OI=2)									
		-32.96	73.79	23.12	31.11	38.13	43.88	52.48	58.54	67.52
23	1,3-Dioxane (σ=1, OI=1)									
	This work	-79.06	73.84	22.66	30.71	37.84	43.68	52.39	58.50	67.54
	Ref. 9	-81.81	72.44	21.50	29.05	36.04	42.01	51.19	57.71	67.25

Table 5.2 Thermodynamic Properties [a] of Cyclic Oxyhydrocarbons (cont'd)

24	1,4-Dioxane (σ=2, OI=1)									
	This work	-74.95	72.31	22.53	30.62	37.76	43.61	52.33	58.44	67.49
	Ref. 9	**-75.48**	**71.53**	**22.16**	**29.82**	**36.80**	**42.70**	**51.70**	**58.08**	67.43
25	3,6-Dihydro-1,2-dioxin (σ=2, OI=2)									
	This work	**-9.80**	72.73	21.62	28.49	34.35	39.09	46.09	50.96	58.13
	Ref. 9	**-4.78**	**71.34**	**20.91**	**27.74**	**33.65**	**38.50**	**45.73**	**50.78**	**58.11**
26	3,4-Dihydro-1,2-dioxin (σ=1, OI=2)									
		-11.45	75.07	21.78	28.54	34.34	39.04	46.02	50.89	58.08
27	2,4-Dihydro-1,3-dioxin (σ=1, OI=1)									
		-57.44	72.62	21.31	28.22	34.15	38.94	46.01	50.92	58.12
28	2,3-Dihydro-1,4-dioxin (σ=2, OI=2)									
	This work	**-53.62**	72.78	21.25	28.13	34.04	38.82	45.89	50.81	58.03
	Ref. 9	-57.36	**72.07**	**20.46**	**27.39**	**33.30**	**38.19**	**45.49**	**50.58**	**57.99**
29	1,4-Dioxin (σ=4, OI=1)									
	This work	**-30.87**	68.72	19.74	25.50	30.23	34.00	39.43	43.16	48.57
	Ref. 9	-33.46	**69.42**	**19.54**	**25.37**	**30.14**	**33.89**	**39.28**	**42.95**	**48.23**
30	1,3,5-Trioxane (σ=3, OI=1)									
	This work	-109.62	70.89	21.71	28.68	34.68	39.51	46.58	51.45	58.48
	Ref. 9	**-111.35**	**68.95**	**19.69**	**26.23**	**32.22**	**37.26**	**44.88**	**50.20**	**57.85**
31	1,2,4-Trioxane (σ=1, OI=2)									
		-59.82	74.68	22.00	28.90	34.80	39.60	46.60	51.40	58.40
32	1,2,3-Trioxane (σ=1, OI=1)									
		-13.05	74.80	23.40	30.10	35.70	40.30	47.00	51.60	58.50
33	1,2,4-Trioxene (σ=1, OI=2)									
		-38.08	74.68	20.80	26.50	31.20	34.90	40.20	43.80	49.00
34	1,2,3-Trioxane (σ=1, OI=1)									
		9.14	73.60	21.90	27.50	31.90	35.40	40.50	44.00	49.10

$\Delta H_f^{\circ}{}_{298}$(dimethylperoxide) - $\Delta H_f^{\circ}{}_{298}$(methoxyethane). [a] The numbers in bold are selected in the derivation of ring group values in Table 5.3.

[b] σ: symmetry number, OI: number of optical isomers. Assignments of σ and OI are consistent with those of Dorofeeva in ref. 8 and 9.

Ring Correction Groups of Group Additivity Method

The selection of thermodynamic properties to derive values for ring group corrections is

described as follows. The experimental data for enthalpies of formation of ten molecules

Table 5.3 Ring Group Values of Cyclic Oxyhydrocarbons

Molecule	$\Delta H_f^\circ{}_{298}$	$S^\circ{}_{298}$	C_{p300}	C_{p400}	C_{p500}	C_{p600}	C_{p800}	C_{p1000}
Oxirane	26.83	31.08	-2.08	-2.66	-2.40	-2.11	-2.05	-1.80
Oxirene	56.42	34.08	1.20	1.42	1.38	1.06	0.02	-0.51
Dioxirane	41.96	32.57	-2.77	-2.77	-2.67	-2.65	-2.98	-3.59
Oxetane	25.16	28.55	-4.08	-4.28	-3.64	-3.02	-2.45	-1.90
1,2-Dioxetane	31.39	26.93	-4.16	-4.52	-4.23	-3.83	-3.37	-3.53
1,3-Dioxetane	24.96	27.90	-3.82	-2.99	-1.75	-1.03	-1.07	-0.83
Dioxirene	19.97	26.50	-2.59	-1.83	-1.03	-0.81	-1.28	-1.25
Tetrahydro-furan	5.20	26.52	-5.93	-5.71	-4.67	-3.72	-2.69	-1.86
2,3-Dihydro-furan	8.02	24.65	-4.52	-4.04	-3.43	-2.94	-2.44	-2.32
2,5-Dihydro-furan	2.89	25.11	-3.76	-3.07	-2.16	-1.58	-1.35	-1.04
Furan	-6.11	26.49	-4.98	-4.06	-3.03	-2.30	-1.85	-1.71
1,2-Dioxolane	12.49	22.57	-4.77	-4.49	-3.79	-3.16	-2.56	-2.59
1,3-Dioxolane	12.18	26.66	-5.20	-5.16	-4.03	-3.09	-2.53	-1.81
1,2-Dioxolene	-2.05	23.73	-3.70	-2.83	-2.00	-1.61	-1.72	-1.82
1,3-Dioxolene	15.69	22.67	-4.85	-3.57	-2.73	-2.27	-2.16	-2.56
1,2,3-Trioxolane	15.74	25.79	-1.26	-2.42	-2.38	-1.99	-1.83	-2.24
1,2,4-Trioxolane	27.41	23.57	-5.65	-4.78	-3.63	-2.86	-2.64	-2.76
1,2,3-Trioxolene	2.14	22.57	-0.66	-0.66	-0.05	0.25	-0.26	-0.38
Tetrahydro-2H-pyran	1.01	17.18	-6.02	-5.48	-4.18	-2.98	-1.56	-0.48
3,4-Dihydro-2H-pyran	1.04	18.29	-5.71	-5.04	-4.12	-3.29	-2.24	-1.76
3,6-Dihydro-2H-pyran	-4.12	19.14	-4.20	-3.64	-2.57	-1.72	-0.99	-0.33
1,2-Dioxane	7.10	18.27	-5.66	-5.11	-4.17	-3.36	-2.52	-2.40
1,3-Dioxane	6.59	16.64	-6.28	-5.95	-4.46	-3.15	-1.97	-0.83
1,4-Dioxane	3.32	16.35	-4.60	-4.98	-3.80	-2.62	-1.54	-0.44
3,6-Dihydro-1,2-dioxin	4.44	18.72	-5.45	-4.66	-3.81	-3.16	-2.65	-2.68
3,4-Dihydro-1,2-dioxin	-2.87	19.46	-4.09	-3.38	-2.44	-1.87	-1.61	-1.46
2,4-Dihydro-1,3-dioxin	7.12	19.05	-4.98	-3.63	-2.33	-1.54	-1.25	-1.15
2,3-Dihydro-1,4-dioxin	2.02	17.07	-5.74	-4.93	-4.10	-3.35	-2.57	-2.48
1,4-Dioxin	-1.88	20.17	-4.06	-2.03	-0.46	0.29	0.08	0.15
1,3,5-Trioxane	20.65	16.83	-7.01	-5.72	-3.63	-2.19	-1.53	-0.62
1,2,4-Trioxane	7.04	18.53	-4.65	-4.05	-2.93	-2.11	-1.77	-1.82
1,2,3-Trioxane	11.77	19.26	-2.05	-2.83	-2.53	-1.96	-1.58	-1.87
1,2,4-Trioxene	3.81	23.14	-5.47	5.84	-5.50	-5.01	-4.46	-4.16
1,2,3-Trioxene	3.87	21.54	-1.69	-2.71	-2.59	-2.23	-2.11	-2.07

described above are selected. The values of $\Delta H_f^\circ{}_{298}$(dioxirane), $\Delta H_f^\circ{}_{298}$(1,2-dioxetane)

and $\Delta H_f^\circ{}_{298}$(1,2-dioxolane) determined by ab initio study and isodesmic reactions are

used. Enthalpies of formation determined using equation 1 are used for the remaining

molecules. Values of entropies and heat capacities reported by Dorofeeva are adopted to

derive the $S°_{298}$ and $C_p(T)$ group contributions wherever available, otherwise, the values

obtained using PM3 method are used. The diffrences between PM3-determined and

literature $S°_{298}$ and $C_p°$ values are, however, insignificant except for those of 1,2-

dioxolane ($S°_{298}$) and 1,3,5-trioxolane ($C_p°_{500}$).

Some enthalpy corrections for ring groups in Table 5.3 have negative values,

resulting from the use of group values listed in Table 5.5. Benson states the ring

correction derived from group additivity reflects the strain energy of the corresponding

cyclic compound since group values are derived from open-chain, "unstrained"

compounds. However, he also recognizes the difficulty to separate strain energy from

resonance energy using group additivity for some ring compounds. The ring strain of

benzene, if calculated with a Benson type analysis, is -33.0 kcal mol^{-1}.[13] The negative

enthalpy corrections for several ring groups in Table 5.3 may result from the combination

of resonance and ring strain, such as occurs in furan, phenol and other vinyl or

unsaturated ether compounds.[13] Resonance through chemical bonds on unsaturated

carbon and adjacent oxygen atoms is evidenced by the weaker O–H bonds (ca. 85 kcal

mol^{-1})[88] in $CH_2=CHOH$, $CH\equiv COH$, and phenol, compared to CH_3O–H and CH_3CH_2–

OH (bond energy 104 kcal mol^{-1}).[89]

The ring correction values for use in group additivity, based on the group values

listed in Table 5.5 are reported. Additional study is needed to separate and identify ring

strain and resonance effects in oxyhydrocarbon species, and this may lead to redefinition

of several oxygen-carbon-hydrogen groups, and subsequent revision of ring groups for

some cyclic oxyhydrocarbons.

Table 5.4 Comparison of Enthalpies of Formation (kcal/mol) for HOOOH, CH₃OOOH, and C₂H₅OOOH

	Data in ref. 24 (Calculation method)	PM3, unscaled (diff.)	PM3, scaled [a] (diff.)
HOOH	-21.82 (G2)	-27.39 (-5.57)	-25.80 (-3.98)
CH₃OOOH	-21.34 (G2M)	-22.86 (-1.52)	-21.80 (-0.46)
C₂H₅OOOH	-28.52 (G2M/MP2)	-25.92 (+2.6)	-24.50 (+4.02)

[a] Scaled using equation 1, see text.

Table 5.5 Group Values Used to Derive the Ring Corrections in Table 5.3

Group	$\Delta H_f^\circ{}_{298}$	$S^\circ{}_{298}$	C_{p300}	C_{p400}	C_{p500}	C_{p600}	C_{p800}	C_{p1000}	Note
C/H2/O2	-20.80	9.42	5.50	6.95	8.25	9.35	11.07	12.34	a
C/C/CD/H2	-4.80	9.80	5.12	6.86	8.32	9.49	11.22	12.48	ref. 18
C/C/H2/O	-8.10	9.80	4.99	6.85	8.30	9.43	11.11	12.33	ref. 11
C/C2/H2	-5.00	9.42	5.50	6.95	8.25	9.35	11.07	12.34	ref. 18
C/CD/H2/O	-6.76	9.80	5.12	6.86	8.32	9.49	11.22	12.48	ref. 18
C/CD2/H2	-4.30	10.20	4.70	6.80	8.40	9.60	11.30	12.60	ref. 18
CD/H/O	2.03	6.20	4.75	6.46	7.64	8.35	9.10	9.56	b
CD/C/H	8.55	7.97	4.16	5.03	5.81	6.50	7.65	8.45	ref. 18
CD/CD/H	6.78	6.38	4.46	5.79	6.75	7.42	8.35	9.11	ref. 18
O/C/CD	-23.62	9.70	3.91	4.31	4.60	4.84	5.32	5.80	c
O/C2,	-23.20	8.68	3.40	3.70	3.70	3.80	4.40	4.60	ref. 18
O/CD2	-19.85	10.00	3.40	3.70	3.70	3.80	4.40	4.60	d
O/CD/O	1.64	10.12	3.50	3.87	3.95	4.15	4.73	4.89	e
O/C/O	-6.40	8.54	3.90	4.31	4.60	4.84	5.32	5.80	f
O/O2	9.30	9.40	2.20	3.64	4.20	4.34	4.62	4.90	g

The groups derived by authors, based on:

a. $CH_2(OH)_2$, $\Delta H_f^\circ{}_{298}$ = -96.6 kcal mol⁻¹ (Melius, C. F., *BAC-MP4 Heats of Formation and Free Energies* **1993**, Sandia National Laboratories, Livermore, California.)

b. O/CD/H = -37.9 and $\Delta H_f^\circ{}_{298}$(vinyl alcohol)[83,90] = -29.8 kcal mol⁻¹.

c. $\Delta H_f^\circ{}_{298}$($CH_3CH_2OCHCH_2$)[84] = -33.63 kcal mol⁻¹

d. $\Delta H_f^\circ{}_{298}$($CH_2CHOCHCH_2$)[84] = -3.27 kcal mol⁻¹.

e. O/H/O = -16.3, and, $\Delta H_f^\circ{}_{298}$(CH_2CHOOH)[24] = -6.37 kcal mol⁻¹.

f. $\Delta H_f^\circ{}_{298}$(CH_3OOH)[27] = -32.2 kcal mol⁻¹.

g. $\Delta H_f^\circ{}_{298}$(HOOOH) = -22.94 kcal mol⁻¹, and CH₃OOOH, $\Delta H_f^\circ{}_{298}$ = -23.8 kcal mol⁻¹, authors' unpublished results.
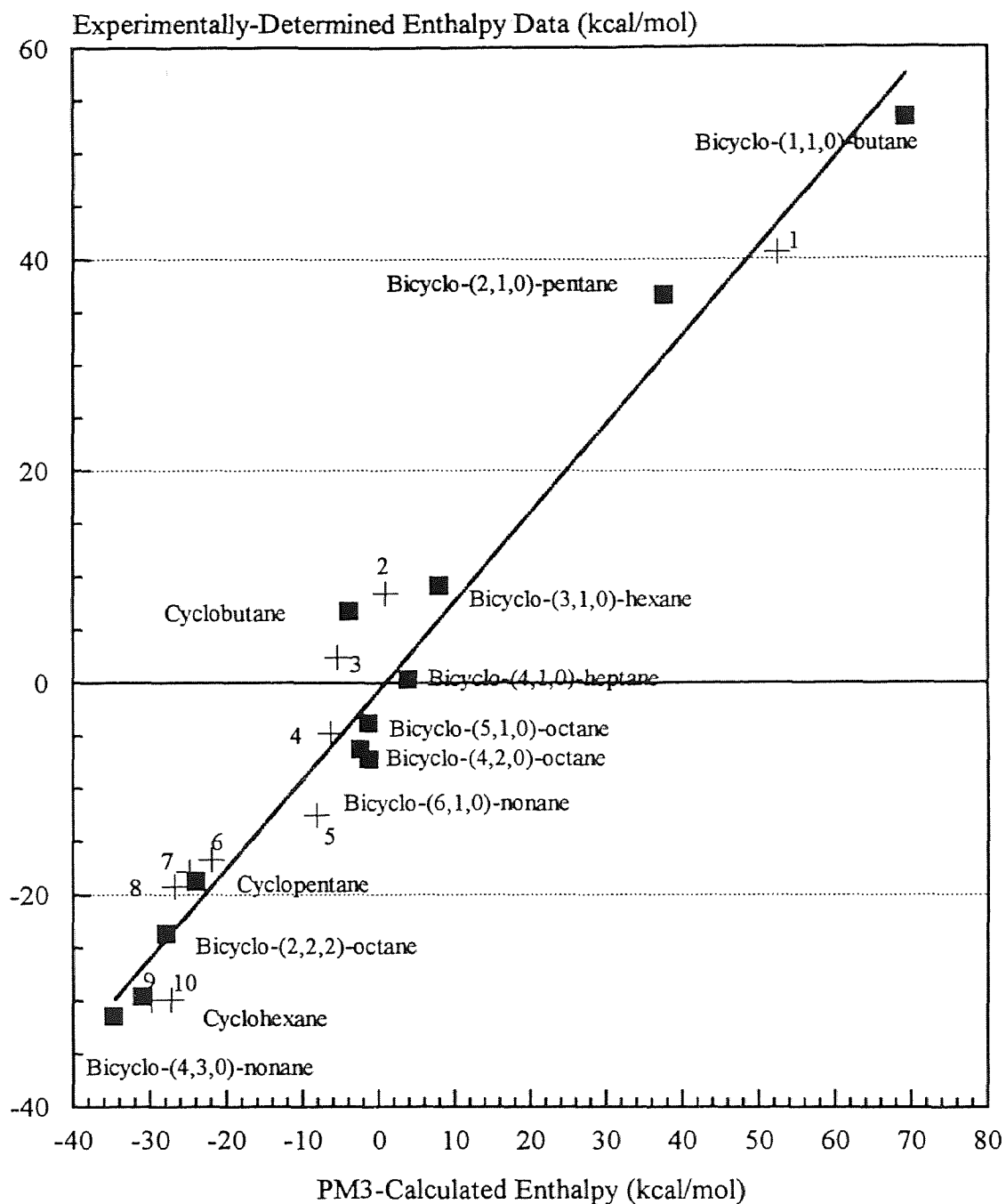
Figure 5.1 Analysis of Correlation Factor for PM3 Determined Enthalpies to Experimentally Determined Enthalpies

5.4 Summary

Thermodynamic properties ($\Delta H_f^\circ{}_{298}$, $S^\circ{}_{298}$ and $C_p(T)$, $300 \leq T/K \leq 1500$) of 34 cyclic oxyhydrocarbons are calculated using the PM3 method and scaled using equation 1, including 12 species which were not previously studied. The standard deviations of PM3-determined $\Delta H_f^\circ{}_{298}$ and $S^\circ{}_{298}$ are evaluated as 2.89 kcal/mol and 1.15 cal mol^{-1} K^{-1}. The standard deviations of PM3-determined heat capacities are determined less than 0.92 cal mol^{-1} K^{-1}. Ring groups corresponding to the 34 compounds are derived using thermodynamic properties selected from literature or this work. The PM3 method is a convenient and economic approach compared to ab initio methods. It is, therefore, valuable to determine the deviations of ideal-gas thermodynamic properties for cyclic oxyhydrocarbons using the PM3 method. Enthalpies of formation obtained using PM3 method after calibration are particularly valuable when no other data are available.

APPENDIX A

TABLE A DETAILED MECHANISM FOR DIMETHYL-ETHER OXIDATION

ELEMENTS
C H O N AR
END

SPECIES

AR	N2	O2	H2	O
H	H2O	OH	HO2	
H2O2				

CH4	CH3OH	CO	CO2
CH2O			
C.H2OH	CH3O.	CH3	CH2
CH2S			
CH	HC.O	CH2OHO.	CH2OHQ.
HC*OOH			
HCOQ	CH2O.Q	HC.QOH	HCOQ.
HCOH			
HOC.HOO.T	O.HC.OOHT	HOCHO.O.	CH3Q.
O.CHO			
CH3Q	CH2O.Q.	HOC.O	

C*C	CC	C2H2	C2H
COHCQ.			
C*C.	CC.	C.*C*O	C.COH
CCO.			
CCQ.	CCOQ.	CC.OH	CQC.O
CC*OO.			
CCOH	CCQ	C.CQ	CCHO
C*C*O			
CC.*O	CCO.Q	C.OHCQ	CO.CQ
CCQ.OH			
C*COH	CCOQ	CYC.CO	C.CHO
CYCCO			
C.COQ	CQ.*C*O	CQ.CHO	CQCHO
COHCHO			
CDCOH			
COC.	COCQ.	C.OCQ	C.OCO.
CYCOCO			
COCO.	C.OCOH	CQ.OCQ	CQ.OCO.
CQOCHO			
CQOC.Q	CQ.OCHO	CQOC.*O	CO.OCHO
HCOOCHO			
COC	COCOH	C.OCHO	COCQ
CYCOCJO			
CJOCHO			

COCOC	COCOC.	CCC.	CCC
COCC			

END

REACTIONS	A	n	E$_a$ (kcal/mol)
O + O + M = O2 + M	1.88E+13	0.0	-1788. !86TSANG
AR/1.0/			
H + O + M = OH + M	4.71E+18	-1.0	0. !86TSANG
H + O2 = O + OH	2.50E+14	0.0	16802. !92BAULCH
Org 1.99e14			
H + O2 + M = HO2 + M	8.75E+16	-0.41	1116. !98 Dryer
Yetter Org 8.75e16			
AR/1.0/ H2/3.41/ N2/2.29/ H2O/2.53/			
H + H + M = H2 + M	6.52E+17	-1.0	0. !92BAULCH
AR/1.0/			
H2 + O = H + OH	5.12E+04	2.67	6285. !92BAULCH
Org 5.12e4			
OH + H + M = H2O + M	8.34E+21	-2.0	0. !92BAULCH
AR/1.0/ N2/2.65/ H2O/16.96/			
OH + H2 = H + H2O	2.04E+08	1.60	3298. !92BAULCH
Org 1.02e8			
OH + OH = H2O + O	1.51E+09	1.14	99. !92BAULCH
HO2 + O = OH + O2	1.75E+13	0.0	-397.
!89ATK/BAU,86TSA			
HO2 + H = OH + OH	1.69E+14	0.0	874. !86 TSANG
Org 1.69e14			
HO2 + H = H2 + O2	6.62E+13	0.0	2126. !86 TSANG
HO2 + H = H2O + O	3.01E+13	0.0	1721. !92BAULCH
HO2 + OH = H2O + O2	2.89E+13	0.0	0.
!92BAU/COB			
HO2 + HO2 = OH + OH + O2	1.00E+13	0.0	11980.
!BOZZELLI(MODEL OF TROE)Org=4.20e14 7/23/98			
HO2 + HO2 = H2O2 + O2	1.87E+12	0.0	1540.
!92BAULCH/500-1250K			
H2O2 + M = OH + OH + M	1.29E+33	-4.86	53247. !86 TSANG
AR/0.7/ N2/1.0/ O2/0.7/ H2O/6.0/			
H2O2 + H = H2O + OH	2.41E+13	0.0	3974. !86 TSANG
H2O2 + H = H2 + HO2	4.82E+13	0.0	7949. !86 TSANG
H2O2 + O = OH + HO2	9.63E+06	2.0	3974. !86 TSANG
H2O2 + OH = H2O + HO2	1.75E+12	0.0	318. !89
ATK/BAU, 86TSA			
CO + O + M = CO2 + M	1.80E+10	0.0	10200. !72
BALDWIN,86TSANG			
AR/1.0/ N2/2.0/ CO/3.0/ CO2/7.0/ O2/12.0/			
CO + OH = CO2 + H	3.16E+06	1.50	-497. !92
BAULCH Org. A=6.32E6			
CO + O2 = CO2 + O	2.53E+12	0.00	47693. !86 TSANG
CO + HO2 = CO2 + OH	1.51E+14	0.00	23648. !86 TSANG
Org. A=1.51e14			
CH + O2 = CO + OH	3.31E+13	0.0	0. !92
BAULCH			
CH + O2 = HC.O + O	3.31E+13	0.0	0. !92
BAULCH			
CH + H2 = CH2 + H	1.45E+14	0.00	3497. !92
BAULCH			
CH + H2 = CH3	1.45E+14	0.00	3497. !92
BAULCH			
HC.O + M = CO + H + M	1.87E+17	-1.00	17000.
!87TIMONEN Org. A=1.87e17			

```
HC.O + O = CO + OH                         3.01E+13    0.00      0.
!92BAULCH/86TSANG
HC.O + H = CO + H2                         9.04E+13    0.00      0. !92
BAULCH Org. A=9.04e13
HC.O + OH = CO + H2O                       1.02E+14    0.00      0. !92
BAULCH Org. A=1.02e14
HC.O + O2 = CO2 + OH                       5.45E+14   -1.15   2018. !93JWB/AD
Org. A=5.45E14
HC.O + O2 = CO + HO2                        6.25E+15   -1.15   2018. !93JWB/AD
Org. A=6.25e15
HC.O + O2 = HCOQ.                          2.12E+24   -3.89   2633. !93JWB/AD
HC.O + CH3 = CH4 + CO                      1.21E+14    0.00      0. !86 TSANG
Org. A=1.21e14
CH2 + O2 = HC.O + OH                       1.00E+14    0.00   3700. !JWB
CH2O+O
CH2 + O = CO + H2                          1.20E+13    0.00      0. !NIST+BOZ
.3*1.2E14
CH2 + O = HC.O + H                         1.20E+13    0.00      0. !NIST+BOZ
.3*1.2E14
CH2 + O = H + H + CO                       1.20E+13    0.00      0. !NIST+BOZ
.3*1.2E14
CH2 + OH = CH + H2O                        2.70E+11    0.67   2570. !JWB
CH+H2O??
CH2S + M = CH2 + M                         1.00E+13    0.0       0. !MILLER
       AR/1.0/ N2/1.67/
CH2S + CH4 = 2CH3                          4.00E+13    0.0       0. !MILLER
CH2S + CCC = CH3 + CCC.                    0.60E+14    0.0       0. !JWB***
CH2S + CCC = 2CC.                          0.60E+14    0.0       0. !JWB***
CH2S + CC = CH3 + CC.                      1.20E+14    0.0       0. !MILLER
CH2S + O2 = CO + OH + H                    3.00E+13    0.0       0. !MILLER
CH2S + H2 = CH3 + H                        7.00E+13    0.0       0. !MILLER
CH2S + H = CH2 + H                         2.00E+14    0.0       0. !MILLER
HCOH = CH2O                                2.11E+19   -3.07   9541. !CHEM251
HCOH + O2 = HC*OOH + O                     2.66E+16   -1.21    944. !CHEM262
HCOH + O2 = HC.O + HO2                     6.08E+07    0.64   1860. !CHEM262
HCOH + O2 = O.CHO + OH                     4.32E+15   -0.98    870. !CHEM262
HCOH + O2 = CO2 + H2O                      4.40E+13   -0.82    764. !CHEM262
HC*OOH + H = HOC.O + H2                    2.40E+08    1.50  12000. !An FROM
DEANEST Ea FROM BOZ MAY97
HC*OOH + H = O.CHO + H2                    2.40E+08    1.50  10500. !An FROM
DEANEST Ea FROM BOZ MAY97
HC*OOH + O = HOC.O + OH                    2.40E+08    1.50  12000. !An FROM
DEANEST Ea FROM BOZ MAY97
HC*OOH + O = O.CHO + OH                    2.40E+08    1.50  10500. !An FROM
DEANEST Ea FROM BOZ MAY97
HC*OOH + OH = HOC.O + H2O                  3.00E+12    0.00   4000. !BOZEST
MAY97
HC*OOH + OH = O.CHO + H2O                  3.00E+12    0.00   5000. !BOZEST
MAY97
HOC.O = CO2 + H                            1.21E+12    0.00   2000. !TAKEST
FROM C=C=C + H & MR 72WAG/ZEL
HOC.O = CO + OH                            2.50E+13    0.00  33000. !TAKEST
FROM C2H4 + OH & MR A=2.28E12 MR=1/21.97 Org 5.01e13, 30000.
CH2O = HC.O+H                              2.54E+25   -5.16  71501. !CHEM211
Org 2.54e25
CH2O = H2+CO                               2.26E+25   -4.65  81990. !CHEM211
```

```
CH2O + OH = HC.O + H2O                  3.44E+09    1.18    -447. !92
BAULCH/86 TSANG Org. a=3.44e9
CH2O + H = HC.O + H2                     4.58E+10    1.05    3279. !92
BAULCH Org=2.29e10 7/23/98
CH2O + O = HC.O + OH                     4.16E+11    0.57    2762. !92
BAULCH
CH2O + O2 = HC.O + HO2                   2.05E+13    0.0    38949. !86 TSANG
CH2O + CH3 = HC.O + CH4                  1.11E+04    2.81    5862. !86 TSANG
Org=5.54e3 7/23/98
CH2O + HO2 = HC.O + H2O2                 1.99E+12    0.0    11665. !86 TSANG
CH2O + HO2 = CH2OHQ.                     8.01E+20   -4.00    1487. !CHEMDIS
ING93
CH2O + HO2 = CH2OHO. + O                 6.91E+17   -1.97   43664. !CHEMDIS
ING93
CH2O + HO2 = HC*OOH + OH                 1.19E+22   -3.81   25799. !CHEMDIS
ING93
CH2O + HO2 = HCOQ + H                    3.45E+10   -0.94   24320. !CHEMDIS
ING93
CH3 + O = CH2O + H                       1.34E+14   -0.08      79. !CHEM221
CH3 + O = C.H2OH                         6.57E+12    0.04     -24. !CHEM221
CH3 + HO2 = CH3O. + OH                   1.85E+13    0.0       0. !MV TO
TROE=1/2=1.35e13 Org. 2.70e13
CH3 + HO2 = CH4 + O2                     1.20E+12    0.00      0. !86
TSANG Org A=3.61e12
CH3 + CH2 = C*C + H                      3.00E+13    0.00      0. !N
CHEMACT
CH3 + O2 = CH3Q.                         3.36E+34   -7.43    5960. !CHEMACT
CH3 + O2 = O + CH3O.                     7.89E+14   -0.46   31150. !CHEMACT
CH3 + O2 = OH + CH2O                     4.50E+11    0.03   10420. !CHEMACT
Org A=1.58e11
CH3 + OH = CH2S + H2O                    9.08E+15   -0.99    2909. !CHEM241
CH3 + OH = HCOH + H2                     4.81E+18   -1.84    3304. !CHEM241
CH3 + OH = CH2O + H2                     4.04E+12   -0.51    2839. !CHEM241
CH3 + OH = C.H2OH + H                    6.55E+13   -0.31    4619. !CHEM241
CH3 + OH = CH3O. + H                     5.61E+12   -0.23   12444. !CHEM241
CH3 + CH3 = CC                          0.085E+54  -12.0   19400. !ADM87
Org A=0.17E+54
CH3 + CH3 = CC. + H                      0.80E+15    0.0    26500. !ADM87
CH3 + C*C. = CH4 + C2H2                  7.84E+11    0.0       0. !86 TSANG
Org A=3.92E11
CH3 + CC. = CH4 + C*C                    2.30E+12    0.0       0. !92
BAULCH Org. A=1.15E12
CH3O. = CH2O + H                         6.13E+28   -5.65   31351. !CHEM221
CH3O. + CH3O. = CH3OH + CH2O             8.50E+7     1.5       0. !ABST
TAK97
CH3O. + CH2O = CH3OH + HC.O              1.02E+11    0.00    2981. !86 TSANG
Org. A=1.02e11
CH3O. + CC = CC. + CH3OH                 2.41E+11    0.00    7094. !86 TSANG
CH3O. + CH3 = COC. + H                   1.94E+10    0.83   15975. !CHEMDIS
ING93
CH3O. + CH2O = COCO.                     7.67E+26   -5.56   10713. !CHEMDIS
ING93
CH3O. + CH2O = C.OCOH                    2.99E+38   -8.85   15925. !CHEMDIS
ING93
CH3O. + CH2O = COC. + O                  7.60E+13    0.04   83562. !CHEMDIS
ING93
C.H2OH = CH2O + H                        8.15E+34   -7.27   40135. !CHEM231
```

C.H2OH = CH3O.	3.16E+30	-6.25	42714. !CHEM231
C.H2OH + H = CH2O + H2	6.03E+12	0.0	0. !87 TSANG
C.H2OH + O = CH2O + OH	4.22E+13	0.0	0. !87 TSANG
C.H2OH + OH = CH2O + H2O	2.41E+13	0.0	0. !87 TSANG
C.H2OH + CH3OH = CH3OH + CH3O.	7.83E+09	0.0	12062. !87 TSANG
C.H2OH + CH3 = CCOH	1.67E+21	-2.59	2416. !CHEMDIS
TAK97			
C.H2OH+O2 = CH2OHQ.	2.65E+21	-3.65	888. !CHEMDIS
ING93			
C.H2OH+O2 = CH2OHO. + O	6.95E+12	-0.03	23578. !CHEMDIS
ING93			
C.H2OH+O2 = CH2O + HO2	1.37E+23	-3.32	3207. !CHEMDIS
ING93			
C.H2OH+O2 = HC*OOH+OH	5.81E+09	0.14	4703. !CHEMDIS
ING93			
C.H2OH+O2 = HCOQ+H	4.86E-01	2.69	3850. !CHEMDIS
ING93			
C.H2OH + CH3O. = COCOH	5.65E+32	-6.10	6407. !CHEMDIS
ING93			
C.H2OH + CH3O. = COC. + OH	3.90E+09	1.27	15238. !CHEMDIS
ING93			
C.H2OH + CH3O. = COCO. + H	5.05E+10	0.48	20718. !CHEMDIS
ING93			
C.H2OH + CH2O = C.OCOH	3.76E+35	-7.94	18195. !CHEMDIS
ING93			
C.H2OH + CH2O = COCO.	1.55E+35	-8.26	20621. !CHEMDIS
ING93			
C.H2OH + CH2O = CH3O. + CH2O	4.31E+19	-2.62	20606. !CHEMDIS
ING93			
C.H2OH + CH2O = COC.+O	3.79E+15	-0.86	91157. !CHEMDIS
ING93			
CH3Q. = CH2O + OH	5.61E+28	-4.94	49601. !CHEMDIS
TAK97			
CH3Q. + CH4 = CH3 + CH3Q	1.12E+13	0.00	24640.
CH3Q. + CH2O = CH3Q + HC.O	5.60E+12	0.00	13600.
CH3Q. + CC = CC. + CH3Q	1.70E+13	0.00	20460.
CH3Q. + CH3OH = C.H2OH + CH3Q	6.30E+12	0.00	21360.
CH3Q. + CH3 = CH3O. + CH3O.	3.80E+12	0.00	-1200.
CH3Q. + CC. = CH3O. + CCO.	3.80E+12	0.00	-1200.
CH3Q. + CH3Q. = CH2O + CH3OH + O2	3.00E+10	0.00	-830
CH3Q. + CH3Q. = CH3O. + CH3O. + O2	3.00E+10	0.00	-830
CH3Q. + C*C = CYCCO + CH3O.	2.82E+11	0.00	17110.
CH3Q. + H = CH3O. + OH	9.64E+13	0.00	0.
!83TSA/HAM			
CH4 + H = CH3 + H2	1.33E+04	3.00	8038. !92
BAULCH			
CH4 + OH = CH3 + H2O	1.57E+07	1.83	2782. !92
BAULCH			
CH4 + O = CH3 + OH	2.13E+06	2.21	6480. !83
MICHAEL			
CH4 + HO2 = CH3 + H2O2	9.04E+12	0.00	24641. !92
BAULCH			
CH3OH = CH3 + OH	1.24E+41	-8.16	99516. !CHEM241
CH3OH = CH2S + H2O	1.79E+39	-7.85	97607. !CHEM241
CH3OH = HCOH + H2	7.26E+33	-6.23	91610. !CHEM241
CH3OH = CH2O + H2	2.10E+38	-8.14	99501. !CHEM241
CH3OH = C.H2OH + H	1.64E+39	-7.95	101760. !CHEM241

```
CH3OH = CH3O. + H                            1.88E+34    -6.96    108119. !CHEM241
CH3OH + OH = C.H2OH + H2O                     9.96E+04     2.5       -960. !86TSANG
CH3OH + OH = CH3O. + H2O                      1.32E+05     2.5       -960. !86TSANG
CH3OH + H = C.H2OH + H2                        1.70E+07     2.10      4869. !86 TSANG
CH3OH + H = CH3O. + H2                         4.24E+06     2.10      4869. !86 TSANG
CH3OH + CH3 = C.H2OH + CH4                     2.43E+06     1.87      8050. !97
BOZ/DEN
CH3OH + CH3 = CH3O. + CH4                      8.10E+05     1.87     28306. !97
BOZ/DEN
CH3OH + O = C.H2OH + OH                        2.91E+05     2.50      3080. !86 TSANG
CH3OH + O = CH3O. + OH                         9.70E+04     2.50      3080. !86 TSANG
CH3OH + HO2 = C.H2OH + H2O2                    9.64E+10     0.0      12579. !86 TSANG
CH3OH + HO2 = CH3O. + H2O2                     6.75E+8      3.1      22400. !97
TAKEST An FROM CH3OH + CH3 Ea FROM C2H6 + HO2 +3 (104 - 101)
CH3Q = CH3O. + OH                             3.13E+15     0.00     44600. !97
BOZEST
CH3Q + O2 = CH3Q. + HO2                        3.00E+12     0.00     39000.
CH2OHQ. = CH2O.Q                               1.60E+17    -4.12     21243. !CHEMDIS
ING93
CH2OHQ. = HC.QOH                               8.68E+19    -4.60     38602. !CHEMDIS
ING93
CH2OHQ. = HC*OOH + OH                          2.11E+21    -3.81     38357. !CHEMDIS
ING93
CH2OHQ. = HCOQ + H                             2.11E+10    -1.12     36834. !CHEMDIS
ING93
CH2O.Q = HC.QOH                                1.51E-18     4.80     -1850. !CHEMDIS
ING93
C2H + O2 = HC.O + CO                           9.00E+11     0.0          0. !JWB NCA
C2H + O2 = C.*C*O + O                          9.00E+11     0.0          0. !JWB NCA
C2H2 + O2 = C*C*O + O                          4.00E+12     0.0      28000. !JWB Org.
A=4.00E12 Ea=28000
C2H2 + H = C2H + H2                            4.80E+08     1.5      26378. !97
BOZ/DEN
C2H2 + OH = C2H + H2O                          0.73E+04     2.68     12042. !92 JPCRD
Org. A=1.45E4 Ea=12042
C2H2 + O = C.*C*O + H                          9.04E+12     0.0       4541. !86 TSANG
C2H2 + OH = C*C*O+H                            3.20E+11     0.0        201. !77
VANDOOREN
C2H2 + O = CH2+CO                              1.75E+13     0.00      3200. !TSANG86
C*C. = C2H2 + H                                9.36E+27    -4.89     43443. !CHEMDIS
TAK97 Org A=4.68E27
C*C. + H = C2H2 + H2                           2.42E+13     0.0          0. !92
BAULCH Org A=1.21E13
C*C. + O2 = C2H2 + HO2                         7.69E+11    -0.09      1765. !JWB/AD93
10ATM
C*C. + O2 = HC.O + CH2O                        2.05E+13    -0.26      1564. !JWB/AD93
10ATM
C*C. + O2 = C.CHO + O                          6.61E+06     1.90       977. !JWB/AD93
10ATM
C*C. + CH3Q = C*C + CH3Q.                      7.00E+11     0.0       1000. !CH3
C*C. + CCQ = C*C + CCQ.                        7.00E+11     0.0       1000. !CH3
C*C. + HO2 = C.CHO + OH                        1.00E+13     0.0          0. !JWB
C*C. + HO2 = C*C + O2                          1.00E+12     0.0          0. !JWB
C*C. + H2O2 = C*C + HO2                        1.00E+12     0.0          1. !JWB EST
C*C + CH3 = C*C. + CH4                         1.62E+06     1.87     18252. !97
BOZ/DEN Org 3.24E06 Ea=18252
```

```
C*C + H = C*C. + H2                        9.60E+08    1.50     13965. !97
BOZ/DEN
C*C + OH = C*C. + H2O                       2.40E+06    2.00      5955. !97
BOZ/DEN Org 4.80E6 Ea=5955
C*C + O = CH2O + CH2                        6.40E+10    0.63      1369.
!1/2(O+C2H4->PROD),84PERRY Org 6.40e10
CC.      = C*C + H                          4.89E+09    1.19     37204
!86TSA/HAM JPCRD 1986,15,1087 Org A=4.89E+9
CC. + HO2 = CCO. + OH                       3.00E+13    0.00        0. !90
BOZZELLI
CC. + CC. = CC + C*C                        1.45E+12    0.00        0. !92
BAULCH
CC. + H = CC                                1.59E+14   -1.68     1578. !97TAK
Org A=7.95E13
CC. + O =CCHO + H                           8.02E+13    0.0         0. !86 TSANG
CC. + O =CH2O + CH3                         1.61E+13    0.0         0. !86 TSANG
CC. + O2=C*C+ HO2                           1.00E+27   -4.826     9468. !BOZZELLI
CC. + O2=CCO.+ O                            1.10E+13   -0.21     27934. !BOZZELLI
CC. + O2=CCQ.                               4.85E+12    0.0         0. !BOZZELLI
CC. + C*C. = C*C + C*C                      3.00E+12    0.00        0.
CC. + OH = CCOH                             3.44E+23   -3.18      2939. !CHEMDIS
TAK97
CC.OH = C*COH + H                           5.00E+13    0.0      36490.
CC.OH = CCHO + H                            5.00E+13    0.0      26620.
CC.OH + O2 = CCQ.OH                         3.54E+49  -11.134    15638.
CC.OH + O2 = CCHO + HO2                     0.93E+39   -7.740    27178.
CC.OH + O2 = C*COH + HO2                    1.34E+39   -7.740    27178.
COC. + OH = COCOH                           1.01E+09   -0.59      -237. !CHEMDIS
ING93
COC. + OH = COCO. + H                       4.64E+11    0.08    103553. !CHEMDIS
ING93
COC. + CH3O. = COCOC                        9.22E+37   -7.73      8060. !CHEMDIS
ING93
COC. + CH3O. = COCOC. + H                   1.67E+06    2.25     16005. !CHEMDIS
ING93
COC. + CH3 = COCC                           1.00E+13    0.0         0.       !Boz
Est 7/23'98
COCO. = COC. +O                            6.75E+15   -1.44     95040.
!CHEMDIS ING93
COCO. + CH3 = COCOC                         1.61E+35   -6.86      7224. !CHEMDIS
ING93
COCO. + CH3 = COC. + CH3O.                  2.13E+05    2.56     12943. !CHEMDIS
ING93
COCO. + CH3 = COCOC. + H                    4.25E+09    1.38     21340. !CHEMDIS
ING93
C.OCOH = COC. + O                           3.37E+19   -2.88    102839. !CHEMDIS
ING93
CC + O2 = CC. + HO2                         6.03E+13    0.00     51866. !92
BAULCH
CC + HO2 = CC. + H2O2                       1.70E+13    0.00     20460. !86
BALDWIN
CC + CH3 = CC. + CH4                        0.75E-07    6.00      6047. !92
BAULCH Org 1.51E-07 Ea=6047
CC + H = CC. + H2                           1.44E+09    1.50      7412. !92
BAULCH
CC + OH = CC. + H2O                         3.61E+06    2.00       864. !92
BAULCH Org 7.22E6 Ea=864
```

```
CC + O = CC. + OH                        9.99E+08     1.50        5803. !92
BAULCH
CCOH + O2 = C.COH +HO2                    2.00E+13     0.0        53800.
CCOH + O2 = CC.OH+HO2                     1.33E+13     0.0        48400.
CCOH + OH = C.COH + H2O                   3.60E+06     2.00        1138. !97
BOZ/DEN
CCOH + OH = CC.OH + H2O                   2.40E+06     2.00        1138. !97
BOZ/DEN
CCOH + OH = CCO. + H2O                    1.20E+06     2.00        2385. !97
BOZ/DEN
CCOH + H = C.COH + H2                     7.20E+08     1.50        7400. !97
BOZ/DEN
CCOH + H = CC.OH + H2                     4.80E+08     1.50        3435. !97
BOZ/DEN
CCOH + H = CCO. + H2                      2.40E+08     1.50        9325. !97
BOZ/DEN
CCOH + O = C.COH + OH                     5.10E+08     1.50        5830. !97
BOZ/DEN
CCOH + O = CC.OH + OH                     3.40E+08     1.50        1255. !97
BOZ/DEN
CCOH + CH3 = C.COH + CH4                  2.43E+06     1.87       10392. !97
BOZ/DEN
CCOH + CH3 = CC.OH + CH4                  1.62E+06     1.87        6427. !97
BOZ/DEN
CCOH + CC. = C.COH + CC                   5.00E+10     0.0        13400.
CCOH + CC. = CC.OH + CC                   3.30E+10     0.0        10400.
CCOH + HO2 = C.COH + H2O2                 8.40E+12     0.0        20430.
CCOH + HO2 = CC.OH + H2O2                 5.60E+12     0.0        17700.
CCOH + C*C. = C.COH + C*C                 5.00E+11     0.0        10400.
CCOH + C*C. = CC.OH + C*C                 3.30E+11     0.0         5200.
COC        = CH3 + CH3O.                  9.93E+30    -4.71       86357.        !
1.00E+00 (1.00E+00) atm,    300-1500 K,   25% err, 1.00 x N2  Org=9.93E+30
COC        = COC. + H                     8.03E+23    -2.52       97417.        !
1.00E+00 (1.00E+00) atm,    300-1500 K,   13% err, 1.00 x N2
COC        = CH2O + CH4                   1.58E+12     .53       90038.        !
1.00E+00 (1.00E+00) atm,    300-1500 K,    1% err, 1.00 x N2
COC + O = COC. + OH                       1.02E+9      1.5        2180. !97BOZEST
COC + H = COC. + H2                       0.72E+9      1.5        4230. !97BOZEST
Org A=1.44e9
COC + OH = COC. + H2O                     7.20E+6      2.0        0000. !97BOZEST
COC + CH3 = COC. + CH4                    2.43E+6      1.87       8200. !97BOZEST
Org A=4.86E+6 Ea=7200
COC + CH3O. = COC. + CH3OH               6.02E+11     0.00        4070. !Tsang,
W. JPCRD 1987, 16, 471, k(CH3O. + CH3OH = CH3OH + C.H2OH)x2
COC + HO2 = COC. + H2O2                   1.93E+11     0.0       12580.
!CH3OH+HO2-->CH2OH+H2O2 87TSA JPCRD1987/16/471 A*2
COC + O2  = COC. + HO2                    3.18E+5      2.69      40036.
!98CHIUNG-JU Isobutene + O2
COCOH = COCO. + H                         4.15E+43    -9.18      113297. !CHEMDIS
ING93
COCOC. = COC. + CH2O                      1.37E+41    -9.06      30590. !CHEMDIS
ING93
COCOC = COCOC. + H                        4.52E+46    -9.45      107474. !CHEMDIS
ING93
C.*C*O + H = CH2S + CO                    2.37E+13     0.11      33459. !CHEMDIS
TAK97
C.*C*O + O2 = HC.O + CO2                  3.33E+11    -0.19         104.
```

```
C.*C*O + O2 = O.CHO + CO                 4.53E+10      0.13      -58.
C.*C*O + O = HC.O + CO                   1.10E+14     -0.01       13.
CCO.Q = CCHO + HO2                       5.00E+12      0.0     11000.
CCQ.OH = CCO.Q                           9.00E+11      0.0     27000.
CCQ = CCO. + OH                          6.46E+14      0.00    43000.
CCQ + O2 = CCQ. + HO2                     3.00E+12      0.00    39000.
C.CQ = CYCCO + OH                        4.70E+11      0.00    19000.
C.CQ = C*C + HO2                         5.00E+12      0.00    16000.
CCQ. = C.CQ                              2.80E+12      0.0     27000.
CCQ. + CH2O = CCQ + HC.O                 5.60E+12      0.00    13600.
CCQ. + CCQ. = CCO. + CCO. + O2           6.00E+10      0.00     -830.
CCQ. + CH3Q. = CCO. + CH3O. +O2          6.00E+10      0.00     -830.
CCQ. + CH4 = CH3 + CCQ                   1.12E+13      0.00    24640.
CCQ. + CH3OH = C.H2OH + CCQ              6.30E+12      0.00    21336.
CCQ. + CC  = CC. + CCQ                   1.70E+13      0.00    20460.
CCQ. + C*C = CYCCO + CCO.                2.82E+11      0.00    17110.
CCOQ. = CC.*O + O2                       5.00E+14      0.00    37300.
CCOQ. = C.COQ                            1.33E+27     -4.22     3596.         !
1.00E+00 (1.00E+00) atm,    300-1500 K,   12% err, 1.00 x N2
CCOQ. = C*C*O + HO2                      6.61E+33     -5.45    17272.         !
1.00E+00 (1.00E+00) atm,    300-1500 K,    3% err, 1.00 x N2
C.COQ = C*C*O + HO2                      2.30E+29     -5.52    22698.         !
1.00E+00 (1.00E+00) atm,    300-1500 K,    2% err, 1.00 x N2
CCOQ. + HO2 = CCOQ+ O2                   8.00E+11      0.00     1000.
CCHO + O2 = CC.*O + HO2                  2.00E+13      0.50    42200.
CCHO + OH = CC.*O + H2O                  1.20E+06      2.00     1192. !97
BOZ/DEN
CCHO + H = CC.*O + H2                    2.40E+08      1.50      894. !97
BOZ/DEN
CCHO + O = CC.*O + OH                    1.70E+08      1.50      894. !97
BOZ/DEN
CCHO + HO2 = CC.*O + H2O2                1.70E+12      0.00    10700.
CCHO + CH3 = CH4 + C.CHO                 5.00E+11      0.00     8000.
CCHO + CH3Q. = CH3Q + CC.*O             2.80E+12      0.00    13600.
CCHO + CCOQ. = CC.*O + CCOQ             2.80E+12      0.00    13600.
CYCCO + OH = CYC.CO + H2O                4.80E+06      2.00    25335. !97
BOZ/DEN
CYCCO + H = CYC.CO + H2                  9.60E+08      1.50     3435. !97
BOZ/DEN
CYCCO + CH3Q. =CYC.CO + CH3Q            2.83E+12      0.00    20000.
CYCCO + CCQ.= CYC.CO + CCQ              2.83E+12      0.00    20000.
CYCCO + CH3 = CYC.CO + CH4              1.07E+12      0.00    11830.
CYC.CO = C.CHO                          7.50E+13      0.00     7800.
C.CHO = C*C*O + H                        5.00E+13      0.0     39980.
C.CHO + O2 = C*C*O + HO2                 4.15E+39     -7.740   27178.
C*COH + OH = H2O + C.CHO                 1.00E+13      0.0       440.
C*COH + H = H2 + C.CHO                   4.00E+13      0.0      3200.
C*COH + O = C.CHO + OH                   1.50E+13      0.0      1790.
C*COH + CH3 = CH4 + C.CHO               5.00E+11      0.0      6600.
C*COH + HO2 = H2O2 + C.CHO               4.00E+11      0.0      9178.
C*C*O + H = CH3 + CO                     5.60E+12      0.00     3400. !JWB NCA
C*C*O + O = HC.O + HC.O                  7.80E+12      0.00     2400.
C*C*O + O =  C.*C*O + OH                 1.10E+12      0.0      8000. !MILLER
C*C*O + O = CH2 + CO2                    1.74E+12      0.0      1350. !MILLER
C*C*O + H = C.*C*O + H2                  4.80E+08      1.50    10065. !97
BOZ/DEN
```

```
C*C*O + OH = C.*C*O + H2O          2.40E+06    2.00     2960.  !97
BOZ/DEN
C*C*O + OH = CH2O + HC.O            5.70E+12    0.0       250.
CC.*O = CH3 + CO                   2.50E+13    0.0     16380.  !GUTMAN92
 C.*C*O + O2 <=> CQ.*C*O           1.53E+10   -1.15    -1164.     !
1.00E+00 (1.00E+00) atm,  250-1500 K,  11% err, 1.00 x N2
 CQ.*C*O   <=> CO + O.CHO          3.52E+21   -3.69    12887.     !
1.00E+00 (1.00E+00) atm,  250-1500 K,  14% err, 1.00 x N2
 CQ.*C*O   <=> CO2 + HC.O          1.08E+28   -5.71    11483.     !
1.00E+00 (1.00E+00) atm,  250-1500 K,  14% err, 1.00 x N2
 C.CHO + O <=> CQ.CHO              1.72E+40   -9.34     6251.     !
1.00E+00 (1.00E+00) atm,  250-2000 K,  21% err, 1.00 x N2
 C.CHO + O2 <=> CQC.O              2.52E+21   -4.12     3219.     !
1.00E+00 (1.00E+00) atm,  250-2000 K,  11% err, 1.00 x N2
 CQ.CHO    <=> CQC.O               1.30E+31   -7.12    28161.     !
1.00E+00 (1.00E+00) atm,  250-2000 K,  36% err, 1.00 x N2
 CQ.CHO    <=> C*C*O + HO2         2.04E+35   -7.76    30433.     !
1.00E+00 (1.00E+00) atm,  250-2000 K,  41% err, 1.00 x N2
 CQC.O     <=> C*C*O + HO2         3.29E+15   -1.86     4479.     !
1.00E+00 (1.00E+00) atm,  250-2000 K,  17% err, 1.00 x N2
 COC.      <=> CH2O + CH3          1.74E+47  -11.00    35354.     !
1.00E+00 (1.00E+00) atm,  298-1500 K,  22% err, 1.00 x AR
 COC. + O2 <=> COCQ.               3.16E+62  -16.60    11689.     !
1.00E+00 atm,  250-2000 K,  58% err  ::CM  :comments:
 COC. + O2 <=> C.OCQ               4.63E+66  -17.94    15204.     !
1.00E+00 atm,  250-2000 K,  74% err  ::CM  :comments:
 COC. + O2 <=> CH2O + CH2O + OH    1.17E+30   -5.52     9136.     !
1.00E+00 atm,  250-2000 K,  25% err  ::CM  :comments:
 COC. + O2 <=> CYCOCO + OH         1.83E+16   -2.72    10186.     !
1.00E+00 atm,  250-2000 K,  15% err  ::CM  :comments:

 CYCOCO + CH3 =  CYCOCJO + CH4     1.95E+11    0.0      8418.   !DUKE,
M.G. J.CHEM.SOC.F.T. 1980,76,1232
 CYCOCO + OH =  CYCOCJO + H2O      6.21E+12    0.0        0.
!DAGAUT,P J.PHYS.CHEM. 1990,94,1881

 CYCOCJO <=> CJOCHO                8.79E+27   -5.67     4600.     !
1.00E+00 (1.00E+00) atm,  298-2000 K,  14% err, 1.00 x AR
 CYCOCJO  <=> CH2O + HC.O          7.79E+13    .21     12335.     !
1.00E+00 (1.00E+00) atm,  298-2000 K,   8% err, 1.00 x AR
 CJOCHO   <=> CH2O + HC.O          6.47E+21   -3.63    22516.     !
1.00E+00 (1.00E+00) atm,  298-2000 K,  12% err, 1.00 x AR

 COCQ.       <=> C.OCQ             4.63E+21   -3.57    20889.     !
1.00E+00 atm,  250-2000 K,  27% err  ::CM  :comments:
 C.OCQ       <=> CH2O + CH2O + OH  8.78E+37   -8.32    27433.     !
1.00E+00 atm,  250-2000 K,  22% err  ::CM  :comments:
 C.OCQ       <=> CYCOCO + OH       2.55E+46  -12.81    37825.     !
1.00E+00 atm,  250-2000 K,  29% err  ::CM  :comments:
 COC. + CH3O. = COC + CH2O         2.41E+13    0.0        0.
!CURRAN
 COC. + CH2O = COC + HC.O          5.49E+03    2.80     5862.
!CURRAN Org. A=5.49e3
 COC. + HO2 = COCO. + OH           9.64E+12    0.00       0.
!CURRAN
 COCQ. + COC = COCQ +COC.          1.00E+13    0.00    17686.
!CURRAN
```

```
   COCQ. + CH2O = COCQ + HC.O            1.99E+12     0.00      11665
!CURRAN
   COCQ        = COCO. + OH              1.83E+20    -1.54      44150.
!CURRAN

   C.OCQ+O2    <=> CQ.OCQ                2.28E+43   -10.09       7890.    !
1.00E+00 (1.00E+00) atm,  298-2000 K,  13% err, 1.00 x AR
   C.OCQ+O2    <=> CQ.OCO.+OH            5.82E+25    -3.67      14515.    !
1.00E+00 (1.00E+00) atm,  298-2000 K,  13% err, 1.00 x AR
   C.OCQ+O2    <=> CQOC.Q                2.90E+32    -7.68       8868.    !
1.00E+00 (1.00E+00) atm,  298-2000 K,  45% err, 1.00 x AR
   C.OCQ+O2 <=> CQOCHO+OH                1.11E+36    -7.45      10951.    !
1.00E+00 (1.00E+00) atm,  298-2000 K,  35% err, 1.00 x AR
   CQ.OCQ      <=> CQ.OCO.+OH            1.09E+42    -9.04      46434.    !
1.00E+00 (1.00E+00) atm,  298-2000 K,  21% err, 1.00 x AR
   CQ.OCQ      <=> CQOC.Q                3.79E+25    -6.12      20225.    !
1.00E+00 (1.00E+00) atm,  298-2000 K,  54% err, 1.00 x AR
   CQ.OCQ      <=> CQOCHO+OH             3.88E+29    -6.05      23534.    !
1.00E+00 (1.00E+00) atm,  298-2000 K,  48% err, 1.00 x AR
   CQOC.Q      <=> CQ.OCO.+OH            1.12E+33    -7.61      39556.    !
1.00E+00 (1.00E+00) atm,  298-2000 K,  12% err, 1.00 x AR
   CQOC.Q      <=> CQOCHO+OH             2.62E+09     -.21        145.    !
1.00E+00 (1.00E+00) atm,  298-2000 K,  11% err, 1.00 x AR

   CQ.OCO.     <=> CH2O + CH2O.Q.        1.06E+37    -8.47      17138.    !
1.00E+00 (1.00E+00) atm,  298-2000 K,  41% err, 1.00 x AR
   CQ.OCO.     <=> CQ.OCHO + H           8.36E+26    -5.22      17634.     !
1.00E+00 (1.00E+00) atm,  298-2000 K,  36% err, 1.00 x AR
   CQ.OCO.     <=> CQOCHO                5.41E+32    -8.06      17224.     !
1.00E+00 (1.00E+00) atm,  298-2000 K,  39% err, 1.00 x AR

   CQOCHO      <=> CO.OCHO + OH          7.67E+50   -11.43      53817.     !
1.00E+00 (1.00E+00) atm,  298-2000 K,  45% err, 1.00 x N2
   CO.OCHO     <=> CH2O + O.CHO          5.90E+11     0.63      13630       !
FROM MY MECHANISM CH3CH2O. --> CH3 + CH2O  1ATM 298 1200K

   CH2O.Q.     <=> HCOQ                  2.36E+09     -.11      11259.     !
1.00E+00 (1.00E+00) atm,  250-2000 K,  16% err, 1.00 x AR
   CH2O.Q.     <=> HC.O + HO2            1.21E-10     6.99      10926.     !
1.00E+00 (1.00E+00) atm,  250-2000 K,  15% err, 1.00 x AR

   HCOQ        <=> HC.O + HO2            6.09E+39    -7.73      87830.     !
1.00E+00 (1.00E+00) atm,  250-2000 K,  37% err, 1.00 x N2
   CH2O.Q.     = CH2O + O2               2.01E+13    -0.03      14560.     !
MOP+AFACT2g2 04-21-98
   O.CHO       <=> OH + CO               1.21E+14     0.53      33980       !
NIST 88LAR/STE
   O.CHO       <=> H + CO2               1.0E+13     0.307      32930       !
NIST 88LAR/STE

   CQ.OCHO     <=> CQOC.*O               2.47E+26    -5.11      18771.     !
1.00E+00 (1.00E+00) atm,  298-2000 K,  16% err, 1.00 x AR
   CQ.OCHO     <=> CH2O + HO2 + CO       5.05E+27    -4.32      38127.     !
1.00E+00 (1.00E+00) atm,  298-2000 K,   9% err, 1.00 x AR
   CQ.OCHO     <=> CH2O + OH + CO2       7.59E+26    -4.20      40461.     !
1.00E+00 (1.00E+00) atm,  298-2000 K,   7% err, 1.00 x AR
```

```
   CQ.OCHO    <=> HCOOCHO + OH          3.57E+14   -1.20     62473.      !
1.00E+00 (1.00E+00) atm,  298-2000 K,    1% err, 1.00 x AR
   CQOC.*O    <=> CH2O + HO2 + CO        3.31E+32   -6.40     34342.      !
1.00E+00 (1.00E+00) atm,  298-2000 K,   16% err, 1.00 x AR
   CQOC.*O    <=> CH2O + OH + CO2        2.67E+31   -6.21     36728.      !
1.00E+00 (1.00E+00) atm,  298-2000 K,   21% err, 1.00 x AR
   CQOC.*O    <=> HCOOCHO + OH           2.22E+16   -2.48     58401.      !
1.00E+00 (1.00E+00) atm,  298-2000 K,   21% err, 1.00 x AR


   CQ.OCHO    <=> C.OCHO + O2            2.06E+35   -7.17     39528.      !
1.00E+00 (1.00E+00) atm,  298-2000 K,   26% err, 1.00 x N2
   CH2O.Q      = CH2O + HO2              8.47E+13    0.0       6300.      !
NIST 72KER/PAR C2H4+HO2 A=5.01E+11 Ea=5000. Af/Ar=1.69E+2
   CQOCHO + OH = CQOC.*O + H2O           1.20E+6     2.00        0.      !
BOZ97 NEW EST
   CQOCHO + CH3  CQOC.*O + CH4           8.10E+5     1.87      2480.      !
BOZ97 NEW EST
   CQOCHO + H  = CQOC.*O + H2            2.40E+8     1.50      6500.      !
BOZ97 NEW EST
   CQOCHO + HO2 = CQOC.*O + H2O2         3.01E+12    0.0      11923.      !
NIST 92BAU/COB CH3CHO + H2O                                   !  BOZ97
NEW EST
   CQOCHO + OH = CQ.OCHO + H2O           1.20E+6     2.00        0.      !
BOZ97 NEW EST
   CQOCHO + CH3 = CQ.OCHO + CH4          8.10E+5     1.87      2000.      !
BOZ97 NEW EST
   CQOCHO + H  = CQ.OCHO + H2            2.40E+8     1.50      6500.      !
BOZ97 NEW EST
   CO.OCHO + OH = HCOOCHO + H2O          2.40E+6     2.00        0.      !
BOZ97 NEW EST
   CO.OCHO + CH3 = HCOOCHO + CH4         1.62E+6     1.87        0.      !
BOZ97 NEW EST
   CO.OCHO + H = HCOOCHO + H2            4.80E+8     1.50        0.      !
BOZ97 NEW EST
   CO.OCHO + HO2 = HCOOCHO + H2O2        3.01E+11    0.0         0.      !
NIST 86TSA/HAM CH3O. + HO2
   C*C + OH   <=> C.COH                  3.63E+51  -12.70     12428.      !
1.00E+00 atm,  700-1200 K,    0% err ::CM  :comments: from my c2h4+oh
master with cbsq
   C*C + OH   <=> CDCOH + H              1.09E+13     .09      7878.      !
1.00E+00 atm,  700-1200 K,    0% err ::CM  :comments:
   C*C + OH   <=> CCO.                   1.04E+34  -11.78      7690.      !
1.00E+00 atm,  700-1200 K,    0% err ::CM  :comments:
   C*C + OH   <=> CH2O + CH3             3.16E+20   -3.00      6345.      !
1.00E+00 atm,  700-1200 K,    0% err ::CM  :comments:
   C*C + OH   <=> CCHO + H               3.80E+14   -1.39      6034.      !
1.00E+00 atm,  700-1200 K,    0% err ::CM  :comments:
   C.COH      <=> CDCOH + H              6.22E+42   -9.77     42513.      !
1.00E+00 atm,  700-1200 K,    0% err ::CM  :comments:
   C.COH      <=> CCO.                   7.43E+40   -9.46     37976.      !
1.00E+00 atm,  700-1200 K,    0% err ::CM  :comments:
   CCO.       <=> CH2O + CH3             1.78E+26   -5.22     16123.      !
1.00E+00 atm,  700-1200 K,    0% err ::CM  :comments:
   CCO.       <=> CCHO + H               1.73E+21   -3.98     16128.      !
1.00E+00 atm,  700-1200 K,    0% err ::CM  :comments:
   C.COH + O2  = COHCQ.                  1.23E+25   -4.61     -1269.      !
1.00E+00 (1.00E+00) atm,  700-2000 K,   12% err, 1.00 x N2
```

```
C.COH + O2   = COHCHO + OH        6.26E+13   -0.64     9472.      !
1.00E+00 (1.00E+00) atm,  700-2000 K,   2% err, 1.00 x N2
C.COH + O2   = CO.CQ              1.95E+57  -14.21    21140.      !
1.00E+00 (1.00E+00) atm,  700-2000 K,   6% err, 1.00 x N2
C.COH + O2   = CH2O + CH2O + OH   1.08E+35   -7.02    18211.      !
1.00E+00 (1.00E+00) atm,  700-2000 K,   1% err, 1.00 x N2
C.COH + O2   = CQCHO + H          1.73E+35   -6.72    18325.      !
1.00E+00 (1.00E+00) atm,  700-2000 K,   1% err, 1.00 x N2
C.COH + O2   = C.OHCQ            6.30E+29   -6.09     5408.      !
1.00E+00 (1.00E+00) atm,  700-2000 K,   1% err, 1.00 x N2
C.COH + O2   = C*COH + HO2        1.83E+27   -4.24     8969.      !
1.00E+00 (1.00E+00) atm,  700-2000 K,   1% err, 1.00 x N2
COHCQ.       = COHCHO + OH        9.86E+25   -4.90    40386.      !
1.00E+00 (1.00E+00) atm,  700-2000 K,  12% err, 1.00 x N2
COHCQ.       = CO.CQ              2.04E+61  -15.57    43135.      !
1.00E+00 (1.00E+00) atm,  700-2000 K,   2% err, 1.00 x N2
COHCQ.       = CH2O + CH2O + OH   1.48E+51  -12.09    55572.      !
1.00E+00 (1.00E+00) atm,  700-2000 K,   8% err, 1.00 x N2
COHCQ.       = CQCHO + H          1.66E+51  -11.76    55737.      !
1.00E+00 (1.00E+00) atm,  700-2000 K,   8% err, 1.00 x N2
COHCQ.       = C.OHCQ            4.52E+71  -18.38    46242.      !
1.00E+00 (1.00E+00) atm,  700-2000 K,   2% err, 1.00 x N2
COHCQ.       = C*COH + HO2        2.10E+52  -12.09    43381.      !
1.00E+00 (1.00E+00) atm,  700-2000 K,  13% err, 1.00 x N2
CO.CQ        = COHCHO + OH        2.20E+45  -10.87    40583.      !
1.00E+00 (1.00E+00) atm,  700-2000 K,   4% err, 1.00 x N2
CO.CQ        = CH2O + CH2O + OH   3.95E+36   -7.60    37226.      !
1.00E+00 (1.00E+00) atm,  700-2000 K,   4% err, 1.00 x N2
CO.CQ        = CQCHO + H          1.01E+37   -7.36    37642.      !
1.00E+00 (1.00E+00) atm,  700-2000 K,   4% err, 1.00 x N2
CO.CQ        = C.OHCQ            1.65E+59  -14.91    33488.      !
1.00E+00 (1.00E+00) atm,  700-2000 K,   9% err, 1.00 x N2
CO.CQ        = C*COH + HO2        2.36E+56  -13.40    37941.      !
1.00E+00 (1.00E+00) atm,  700-2000 K,   4% err, 1.00 x N2
C.OHCQ       = COHCHO + OH        4.36E+22   -4.54    30056.      !
1.00E+00 (1.00E+00) atm,  700-2000 K,   0% err, 1.00 x N2
C.OHCQ       = CH2O + CH2O + OH   2.38E+40   -9.51    42107.      !
1.00E+00 (1.00E+00) atm,  700-2000 K,   4% err, 1.00 x N2
C.OHCQ       = CQCHO + H          5.69E+40   -9.28    42465.      !
1.00E+00 (1.00E+00) atm,  700-2000 K,   4% err, 1.00 x N2
C.OHCQ       = C*COH + HO2        1.24E+24   -4.14    17343.      !
1.00E+00 (1.00E+00) atm,  700-2000 K,   1% err, 1.00 x N2
END
```

APPENDIX B

DIMETHYL-ETHER PYROLYSIS AND OXIDATION EXPERIMENTAL RESULTS AND MODEL COMPARISON
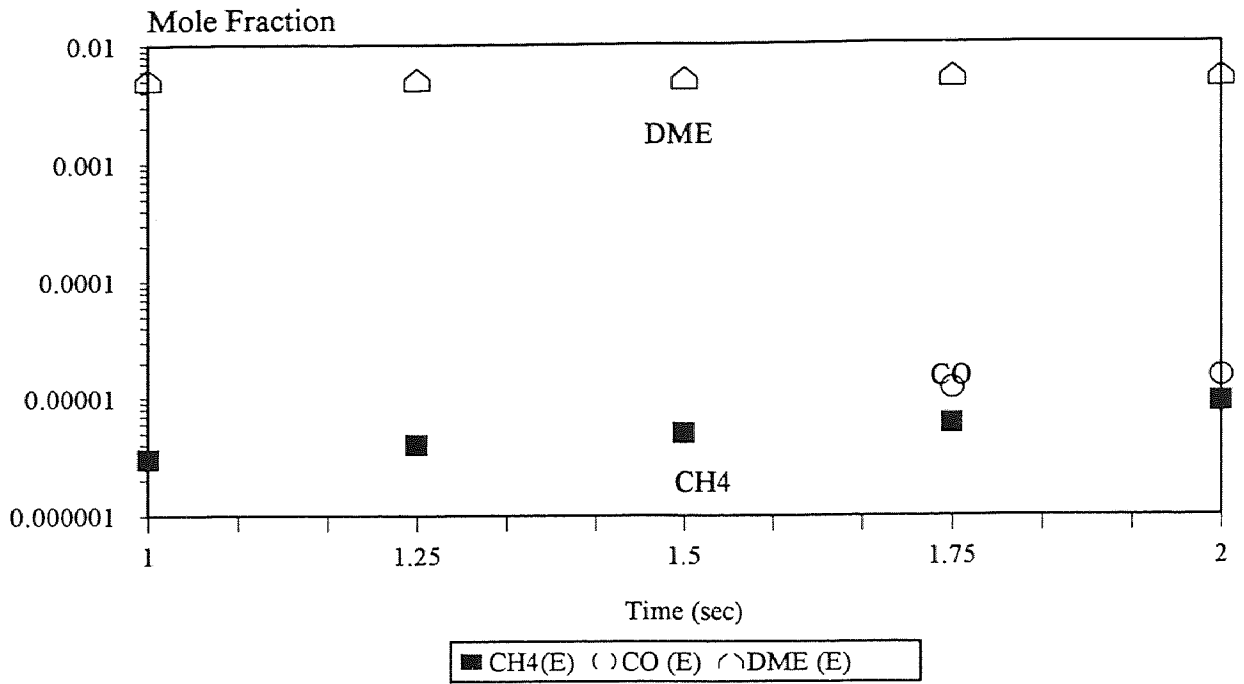
Figure B.1 Experimental Results (Pyrolysis, T=823 K)
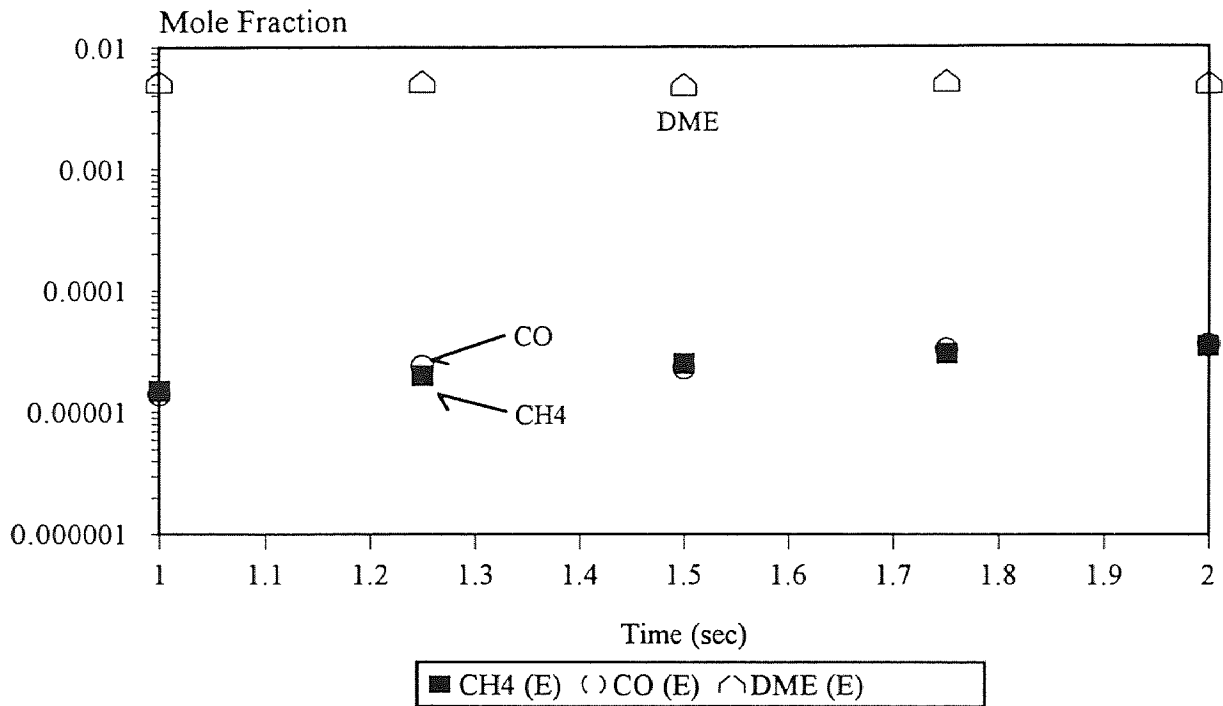
Figure B.2 Experimental Results (Pyrolysis, T=873 K)
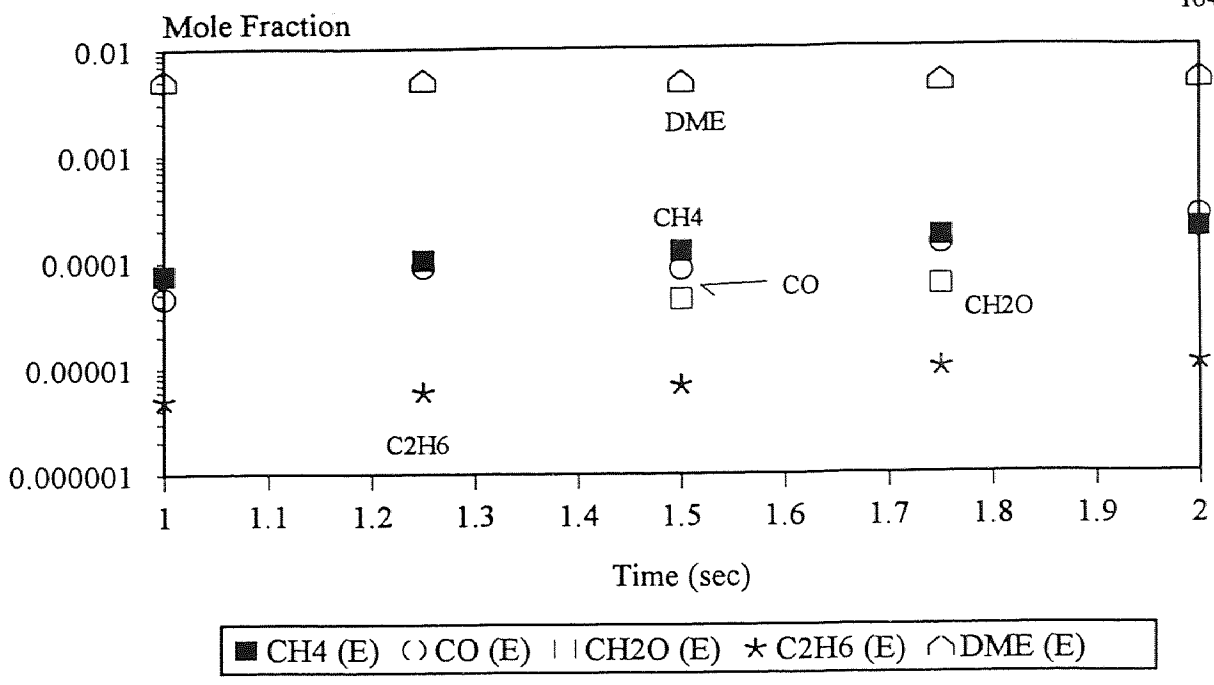
Figure B.3 Experimental Results (Pyrolysis, T=923 K)
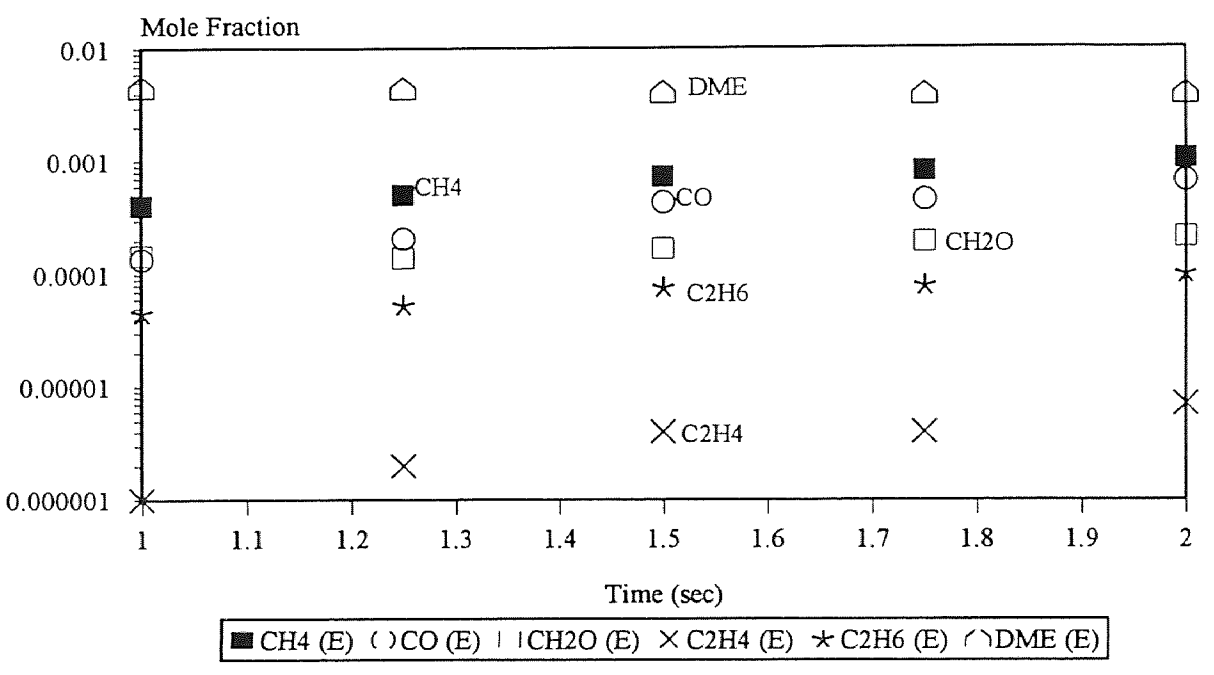
Figure B.4 Experimental Results (Pyrolysis, T=973 K)
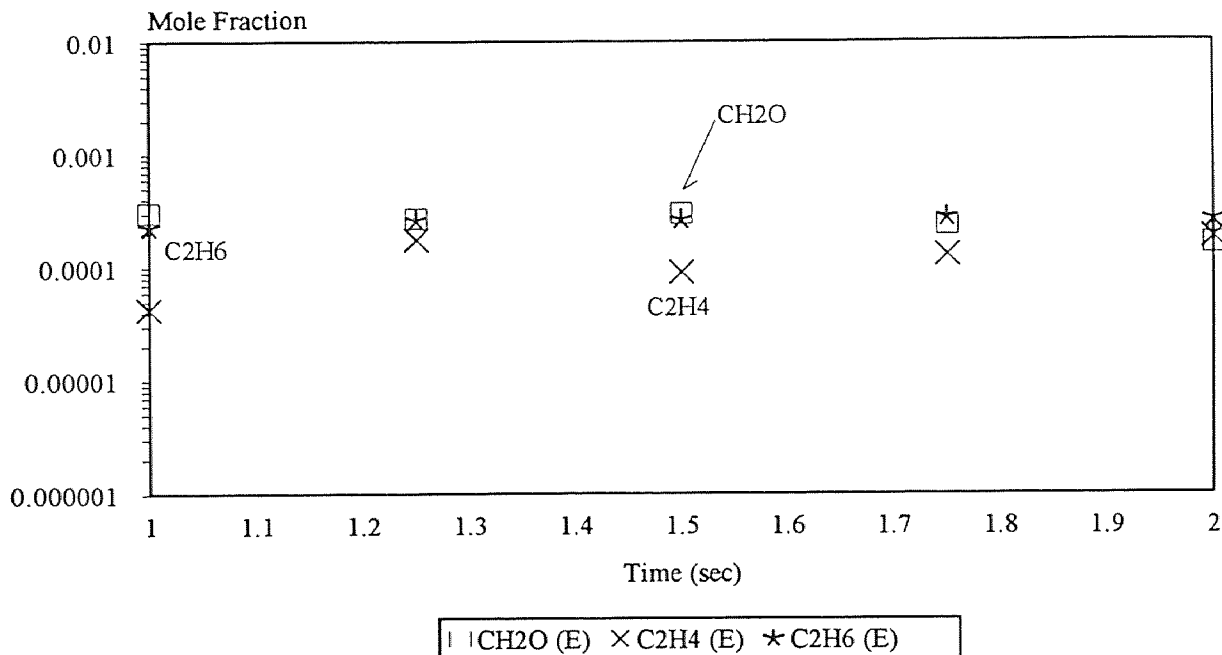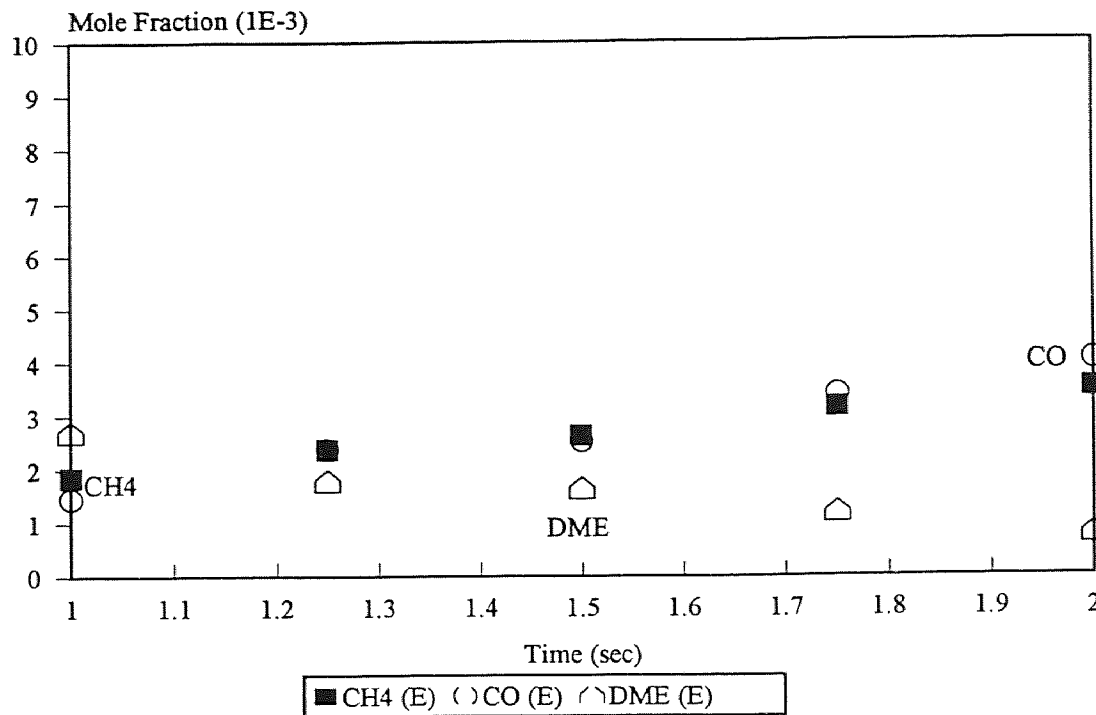
Figure B.5 Experimental Results (Pyrolysis, T=1023 K)
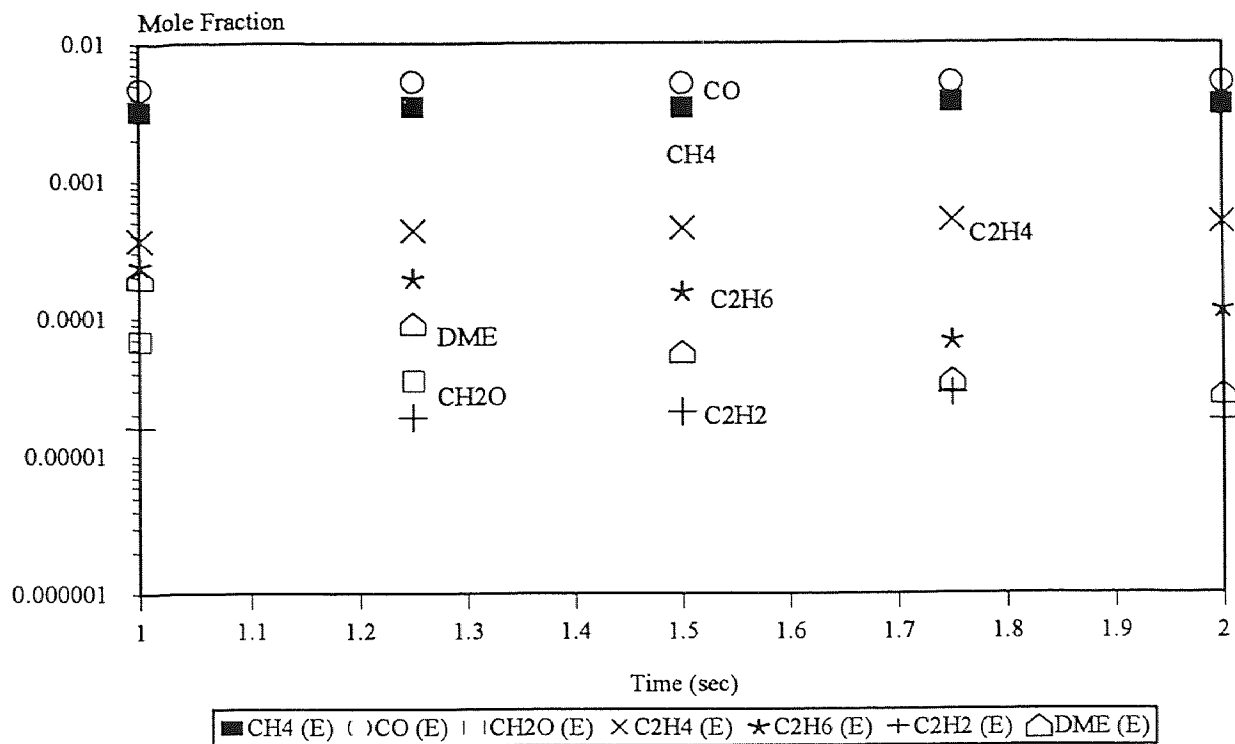
Figure B.6 Experimental Results (Pyrolysis, T=1073 K)
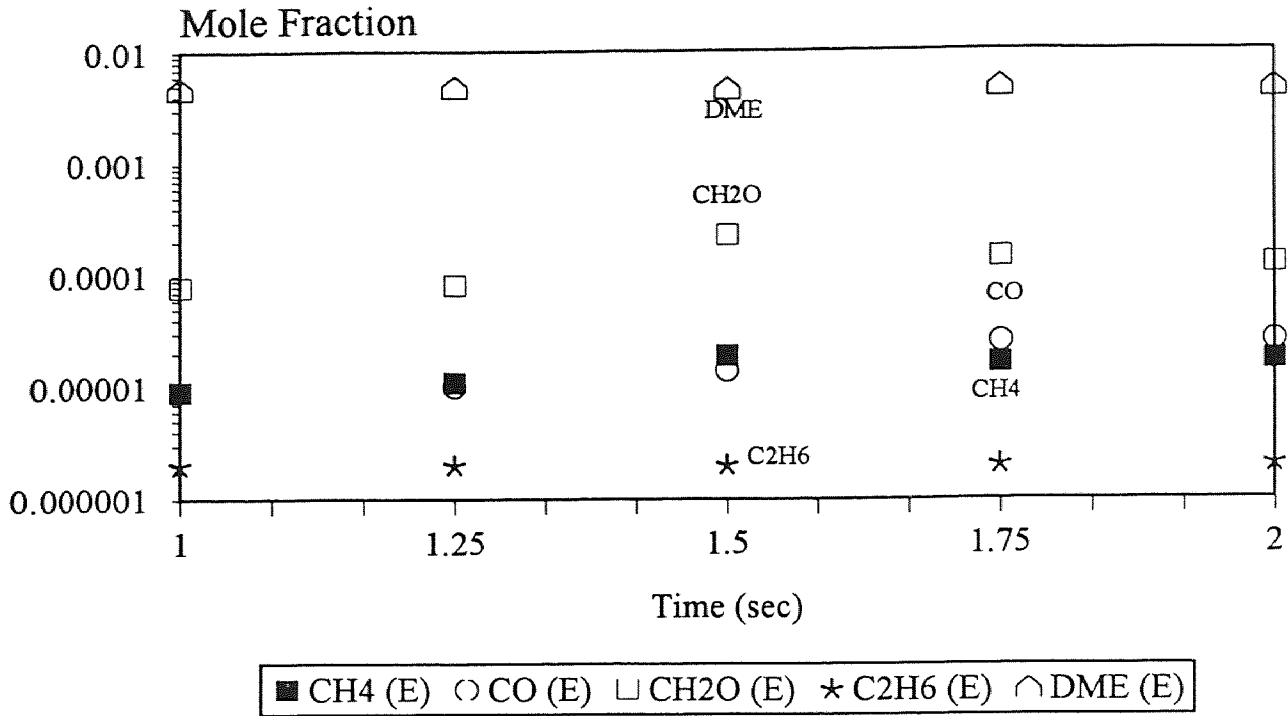
Figure B.7 Experimental Results (Phi=1.5, T=773 K)
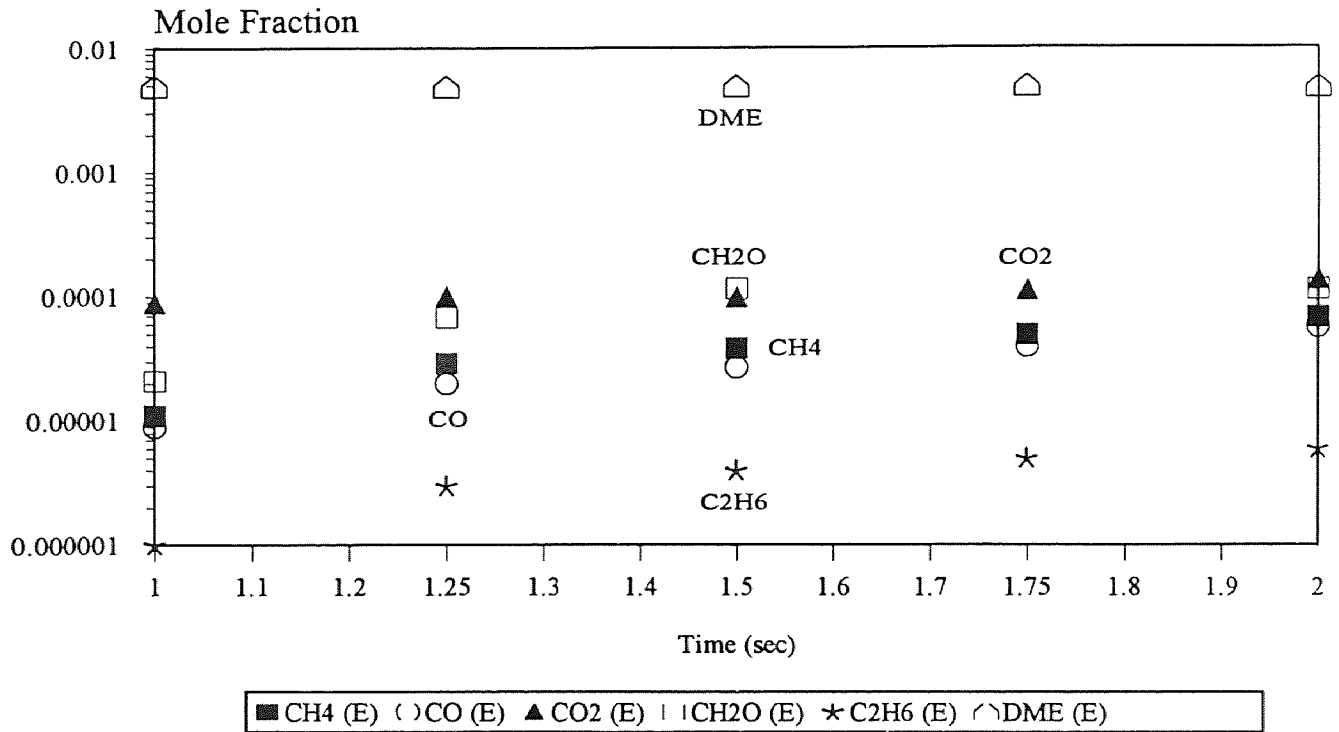
Figure B.8 Experimental Results (Phi=1.5, T=823 K)
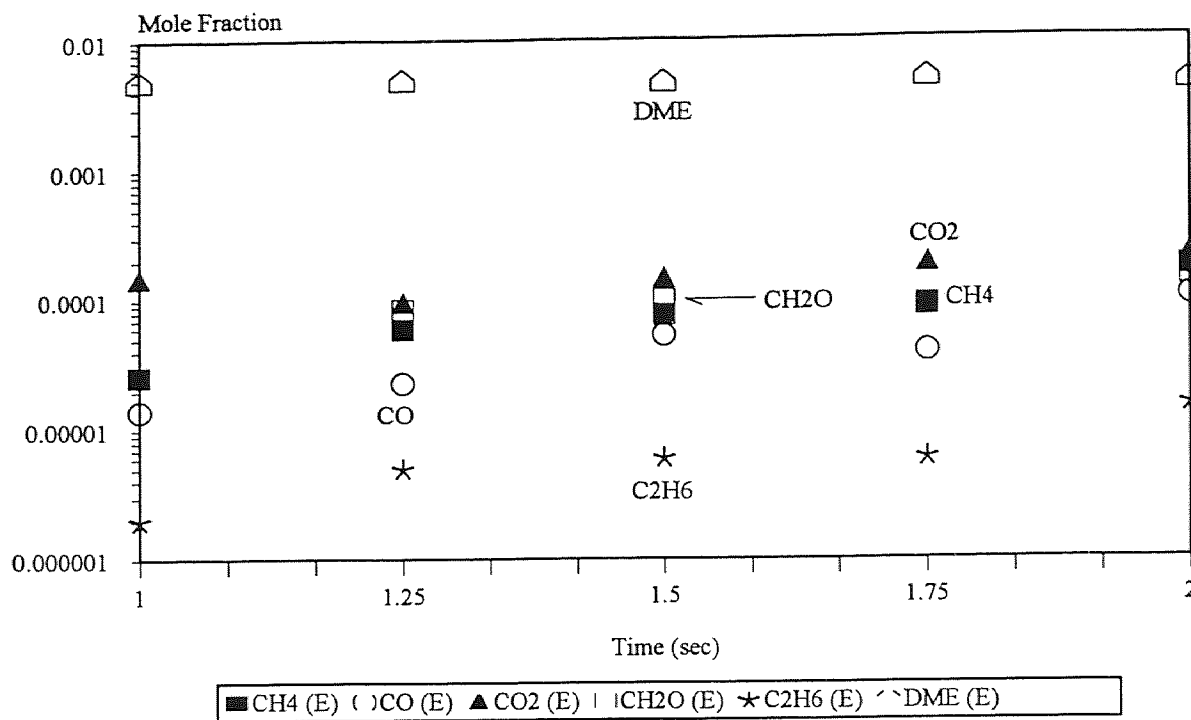
Figure B.9 Experimental Results (Phi=1.5, T=873 K)
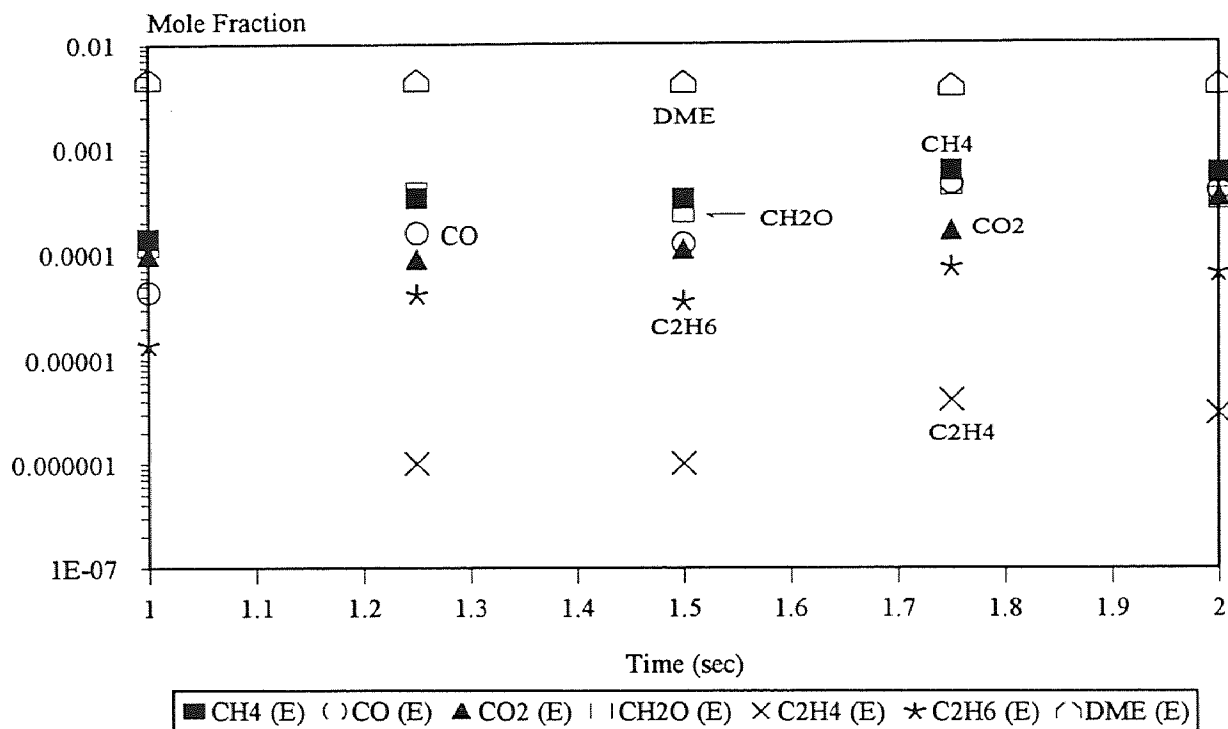
Figure B.10 Experimental Results (Phi=1.5, T=923 K)

Mole Fraction (1E-3)

Mole Fraction
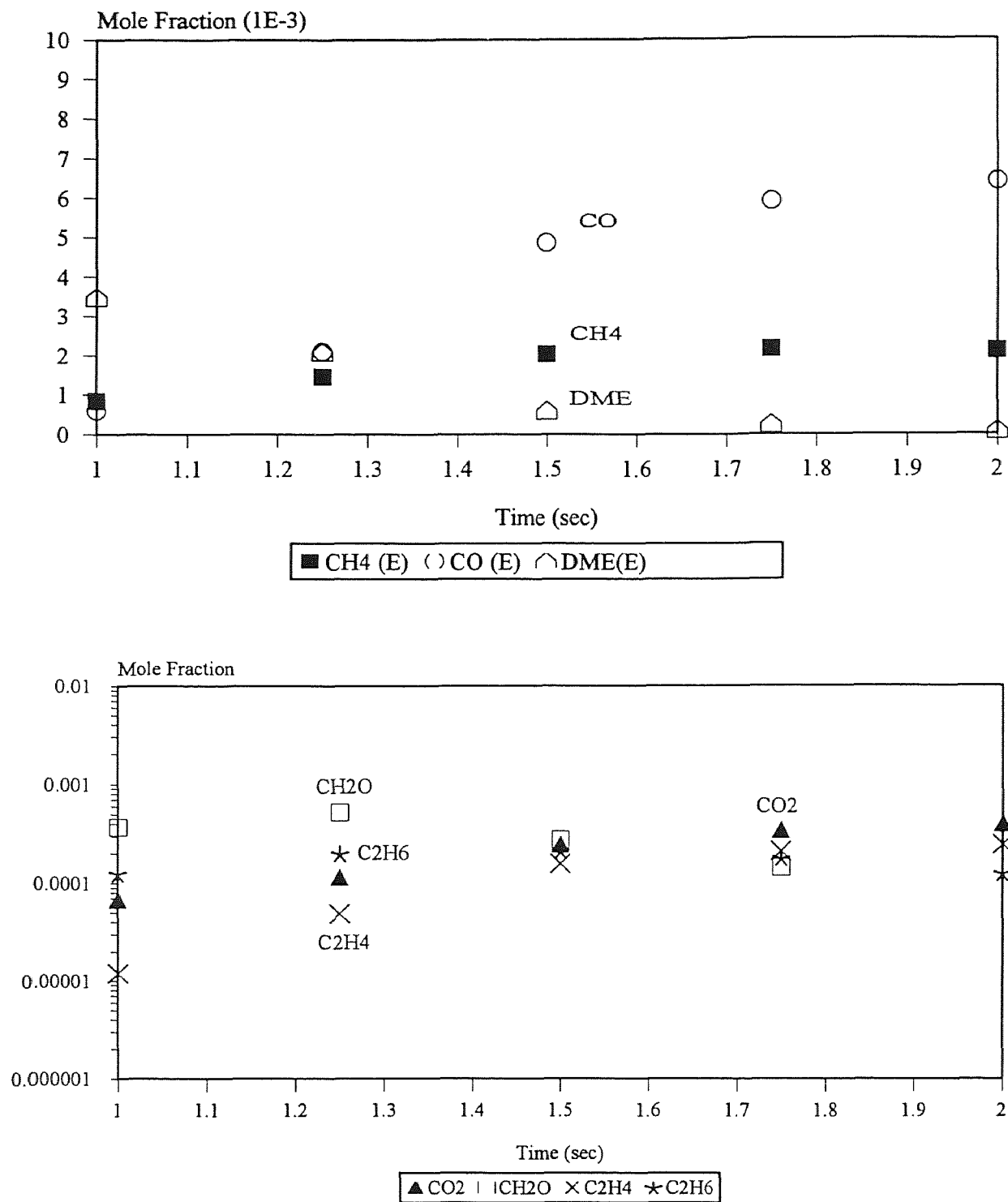
Figure B.11 Experimental Results (Phi=1.5, T=973 K)
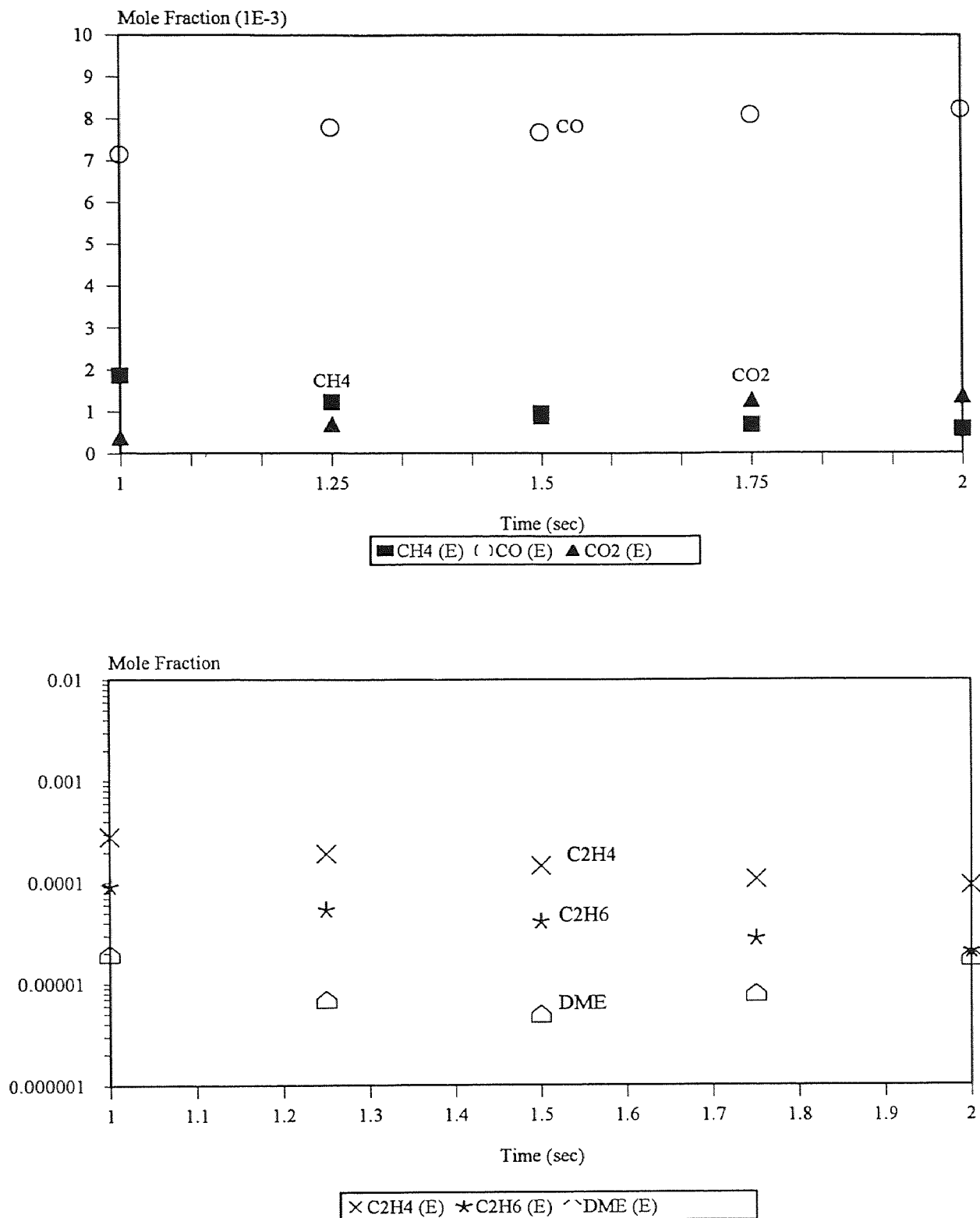
Figure B.12 Experimental Results (Phi=1.5, T=1023 K)
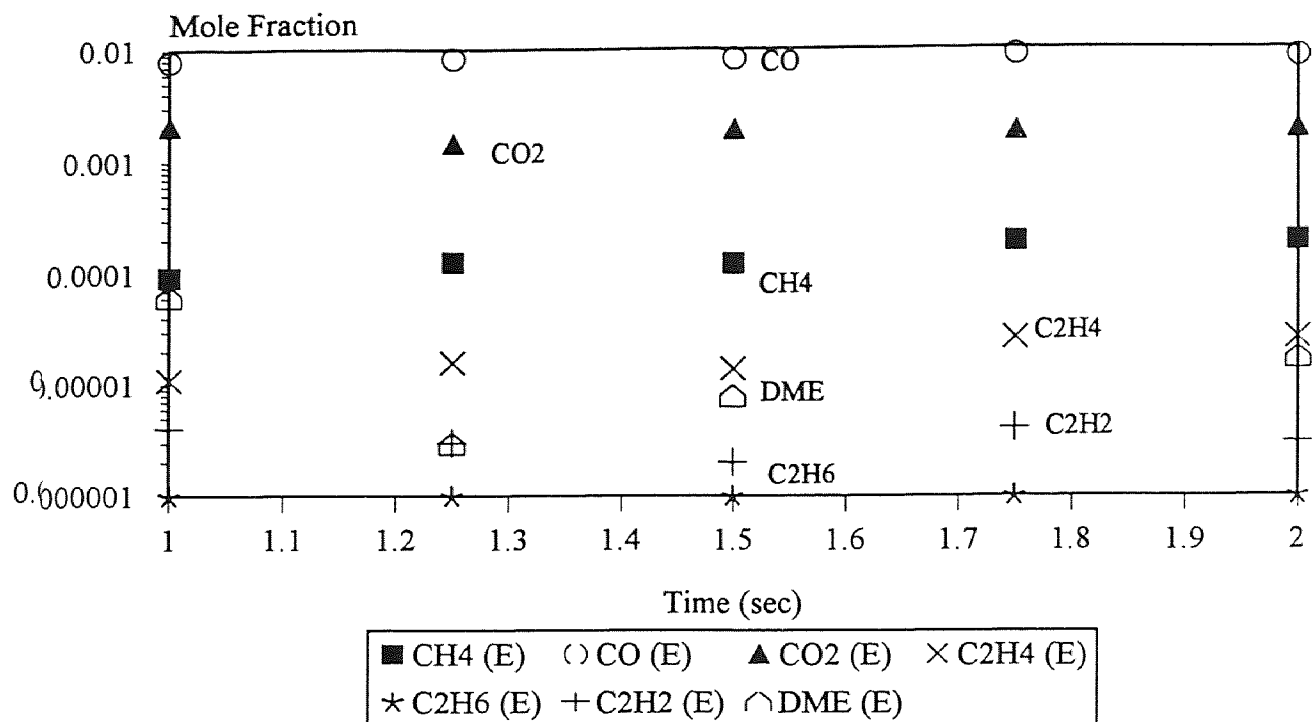
Figure B.13 Experimental Results (Phi=1.5, T=1073 K)
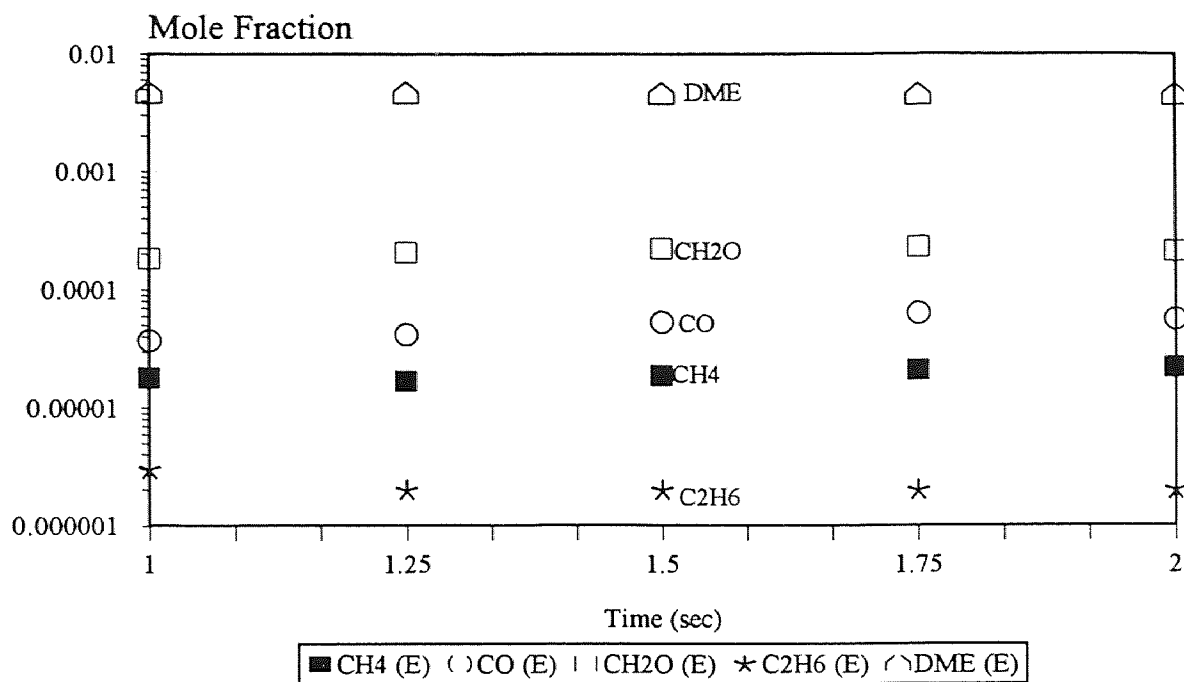
Figure B.14 Experimental Results (Phi=1.0, T=773 K)
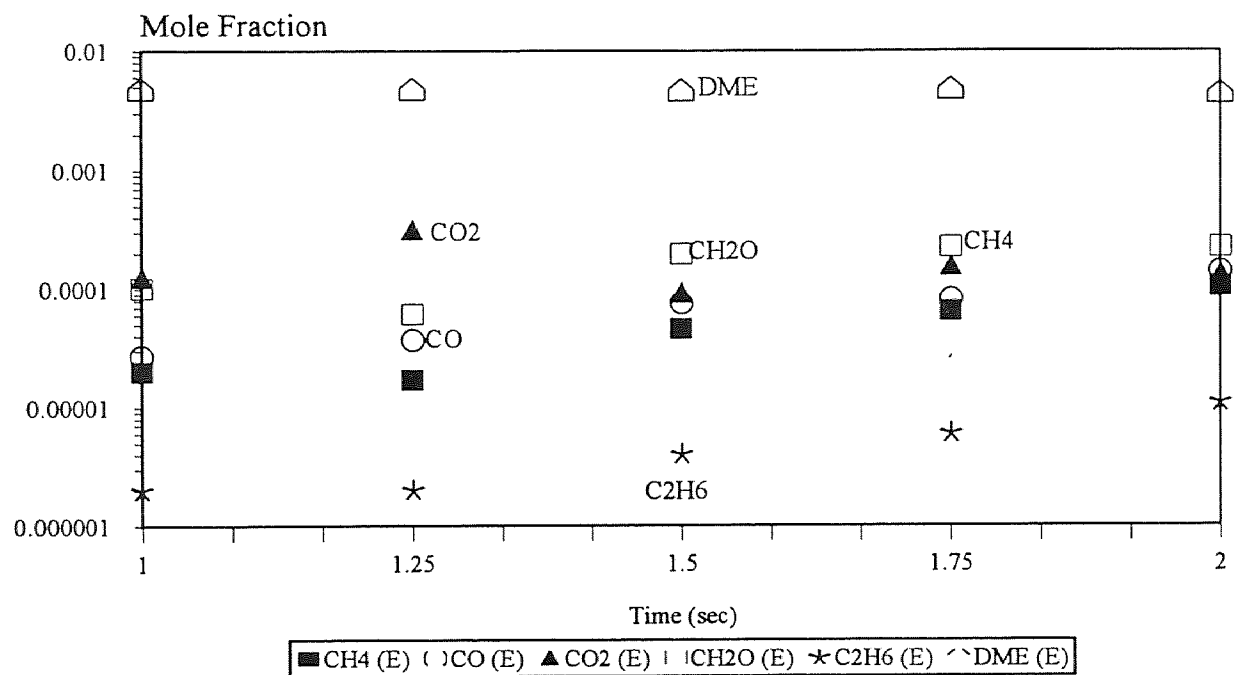
Figure B.15 Experimental Results (Phi=1.0, T=823 K)
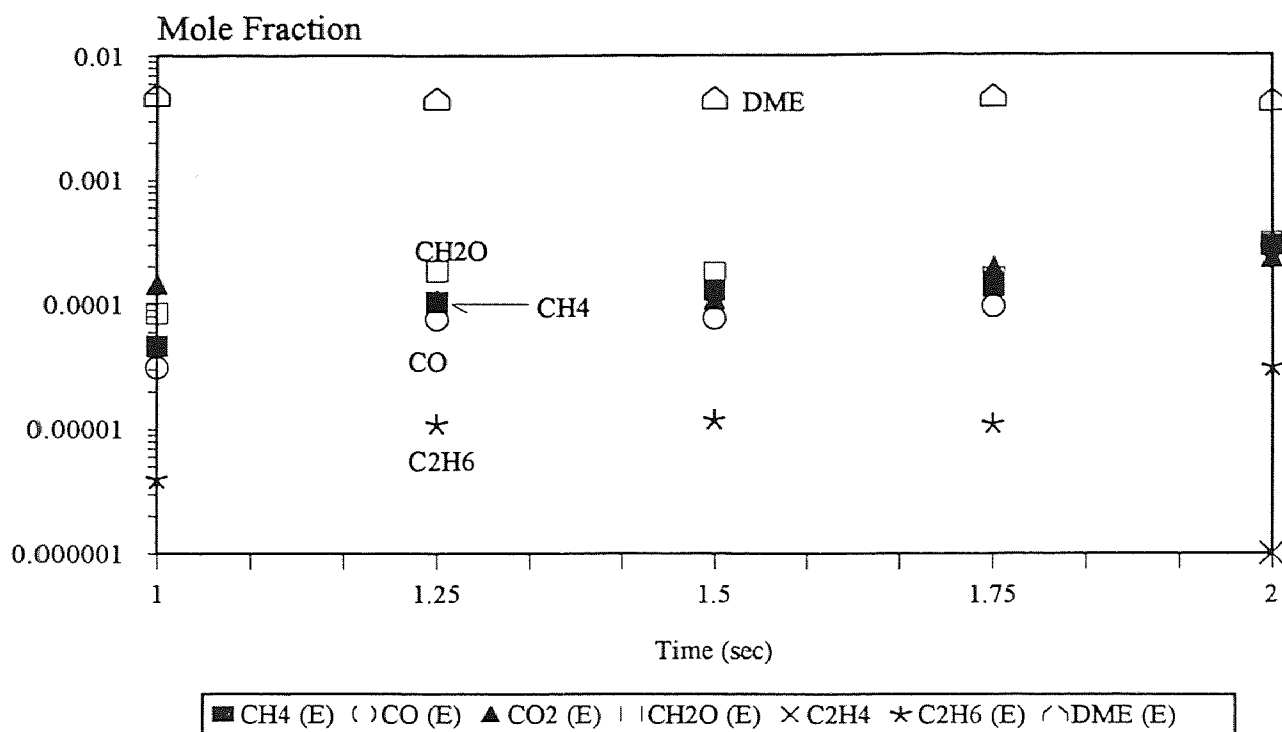
Figure B.16 Experimental Results (Phi=1.0, T=873 K)
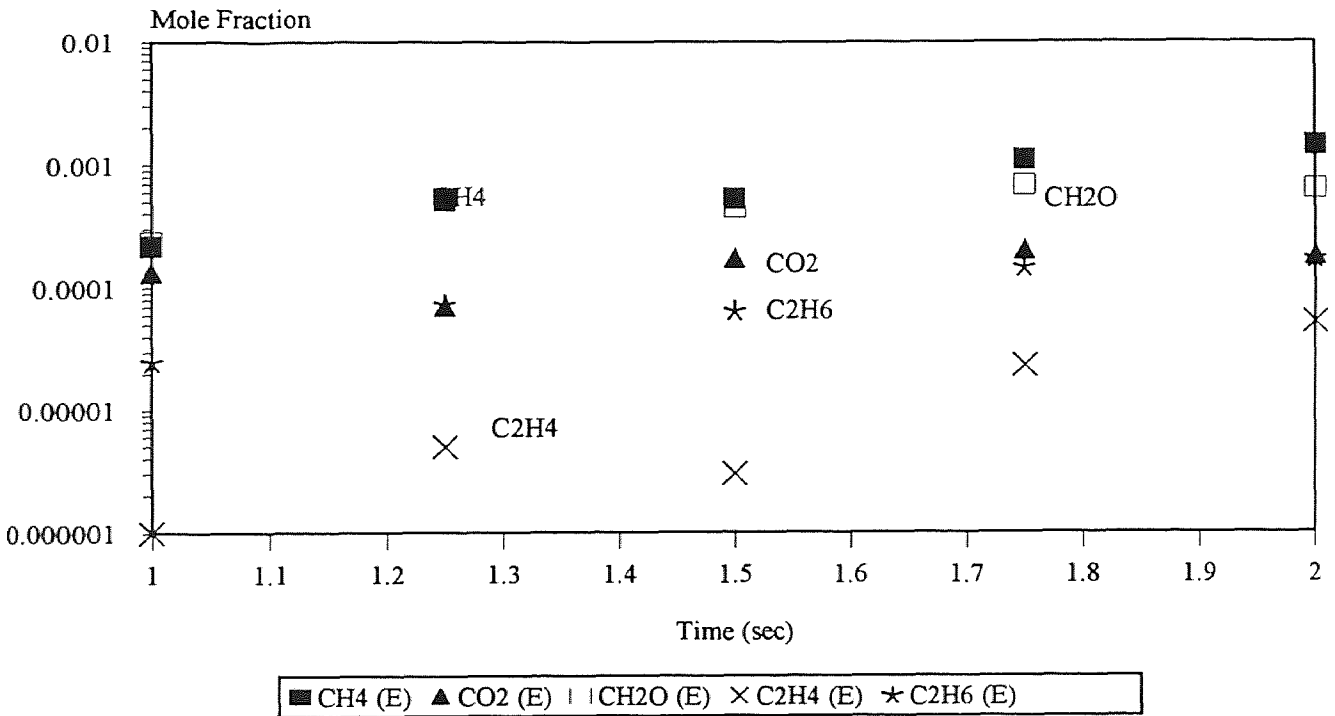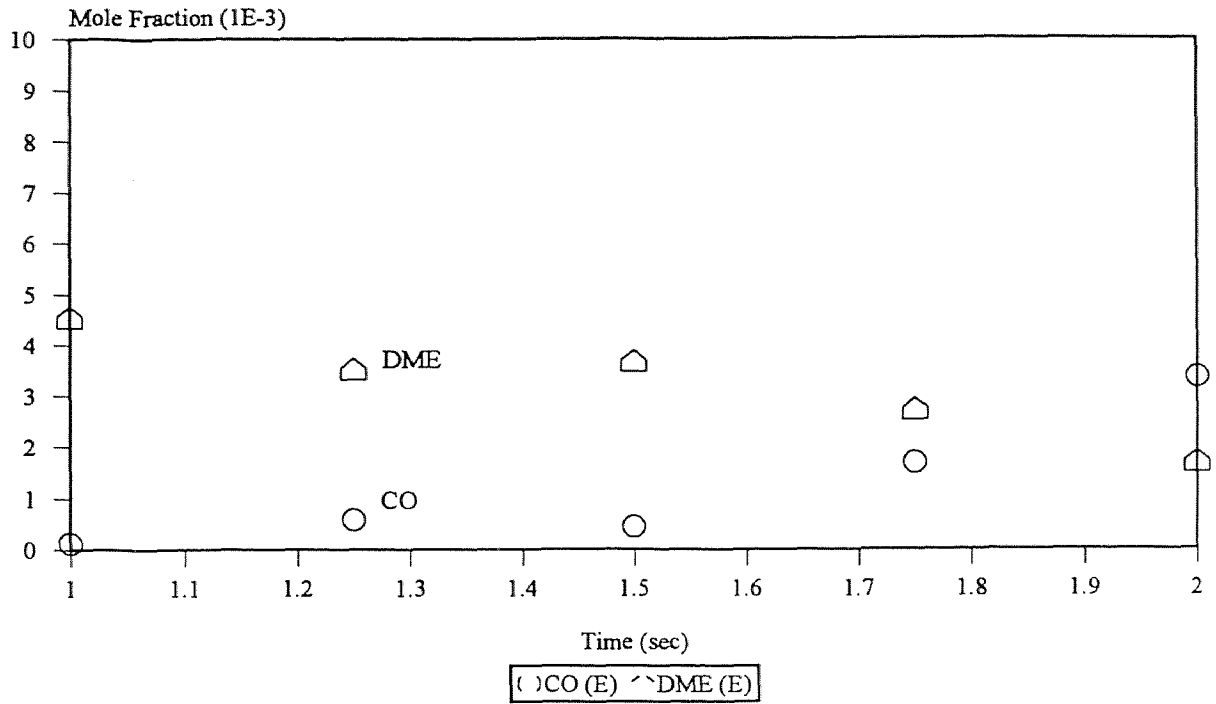
Figure B.17 Experimental Results (Phi=1.0, T=923 K)
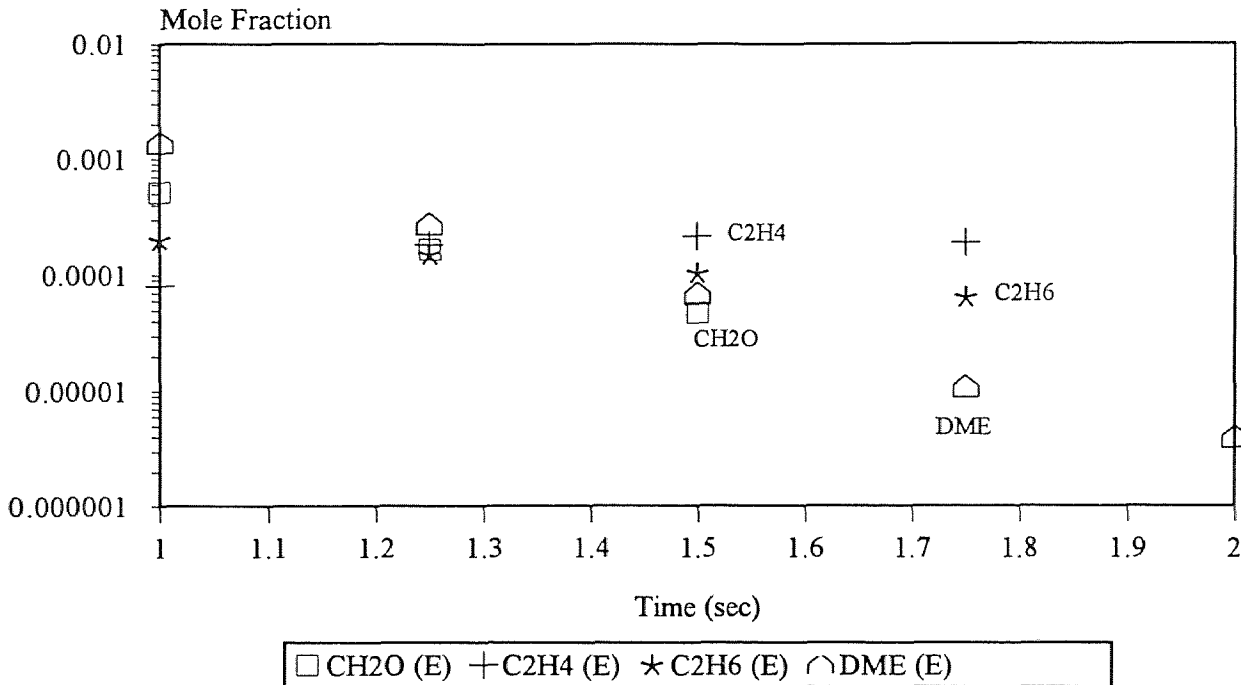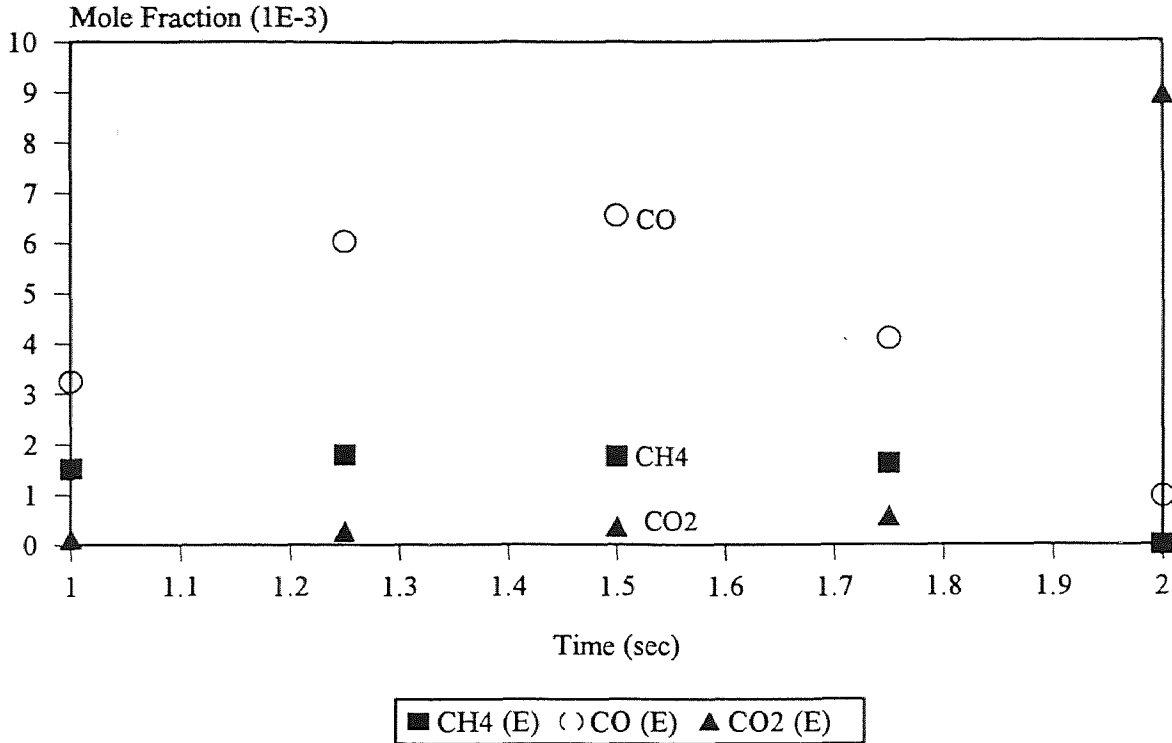
Figure B.18 Experimental Results (Phi=1.0, T=973 K)
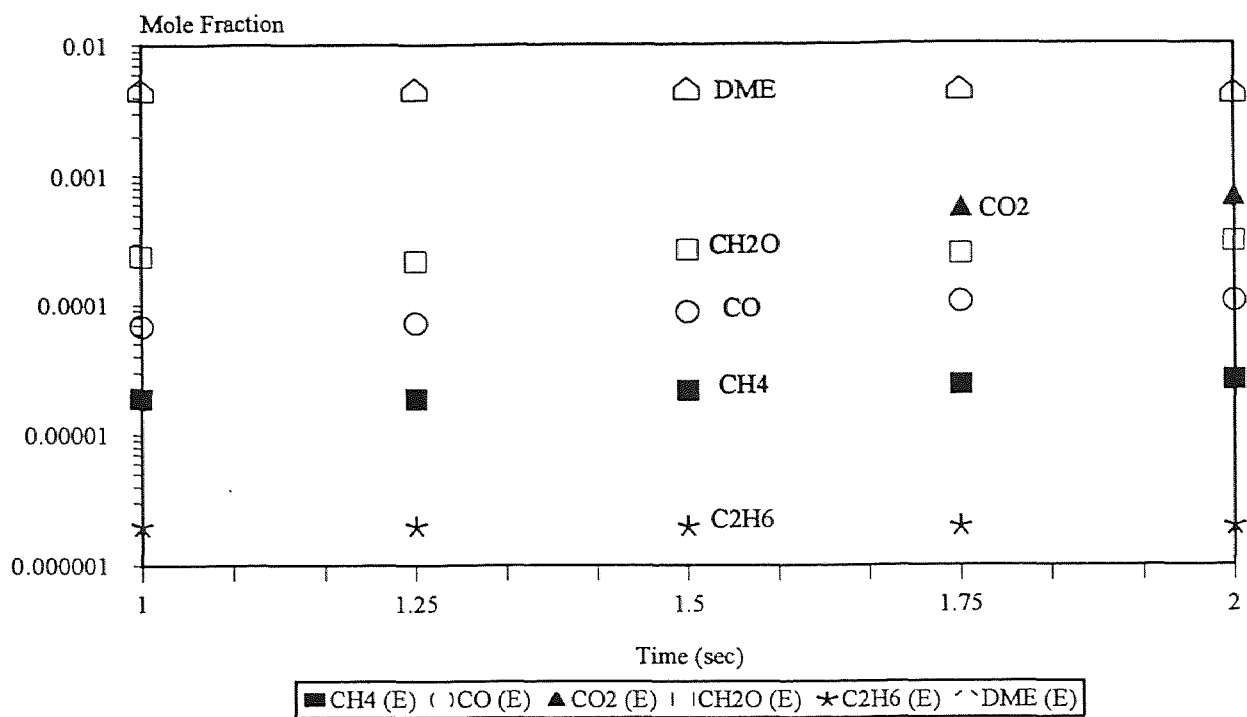
Figure B.19 Experimental Results (Phi=0.75, T=773 K)
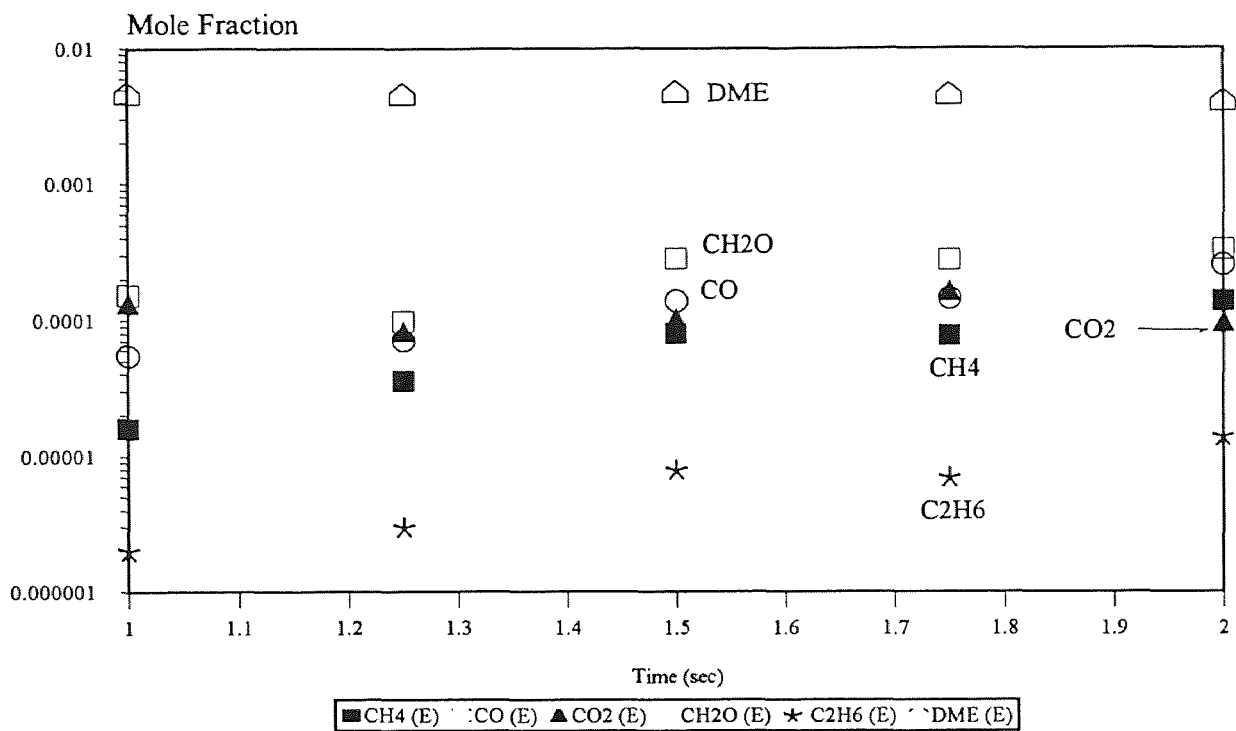
Figure B.20 Experimental Results (Phi=0.75, T=823 K)
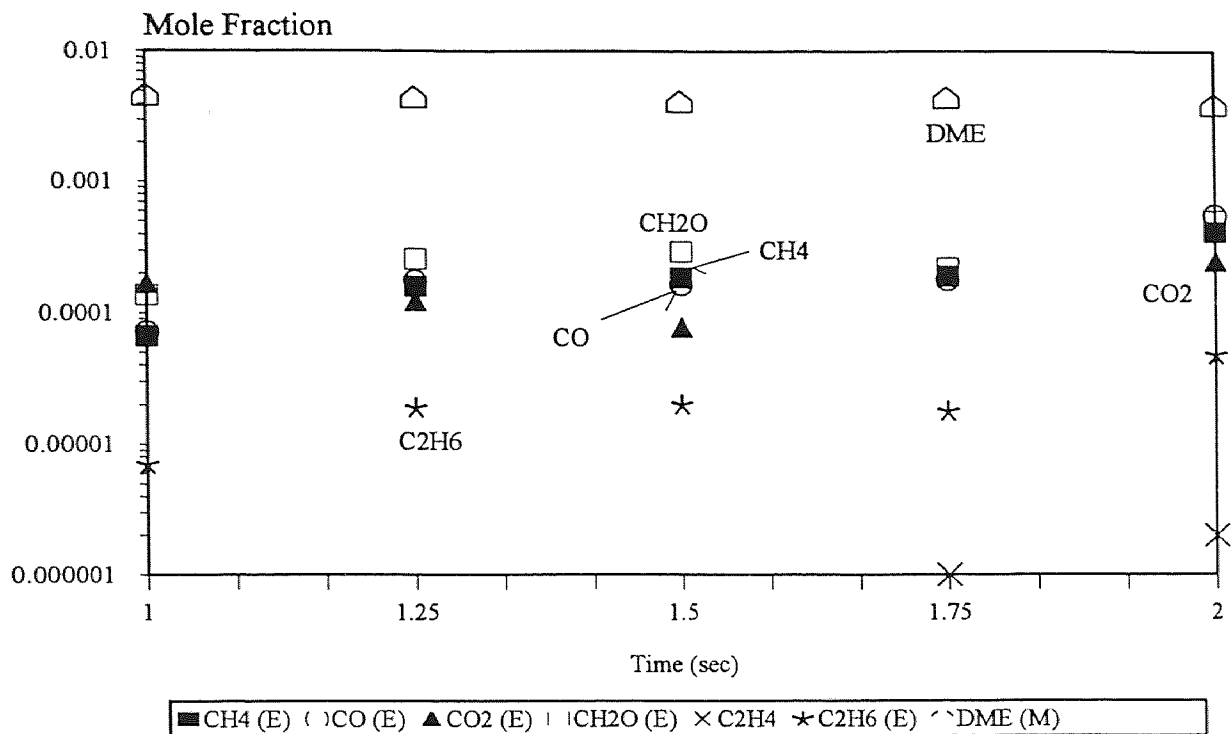
Figure B.21 Experimental Results (Phi=0.75, T=873 K)
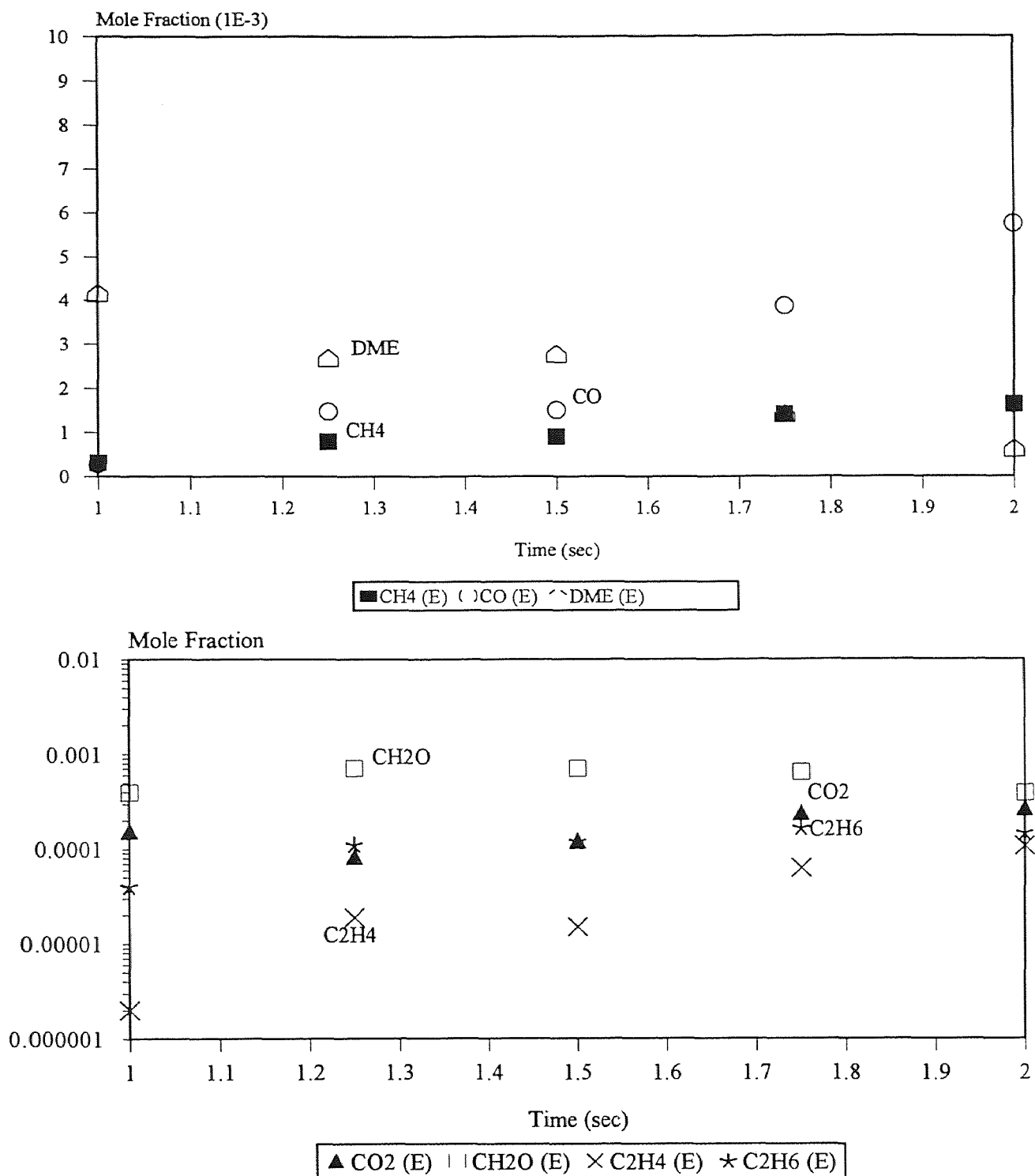
Figure B.22 Experimental Results (Phi=0.75, T=923 K>
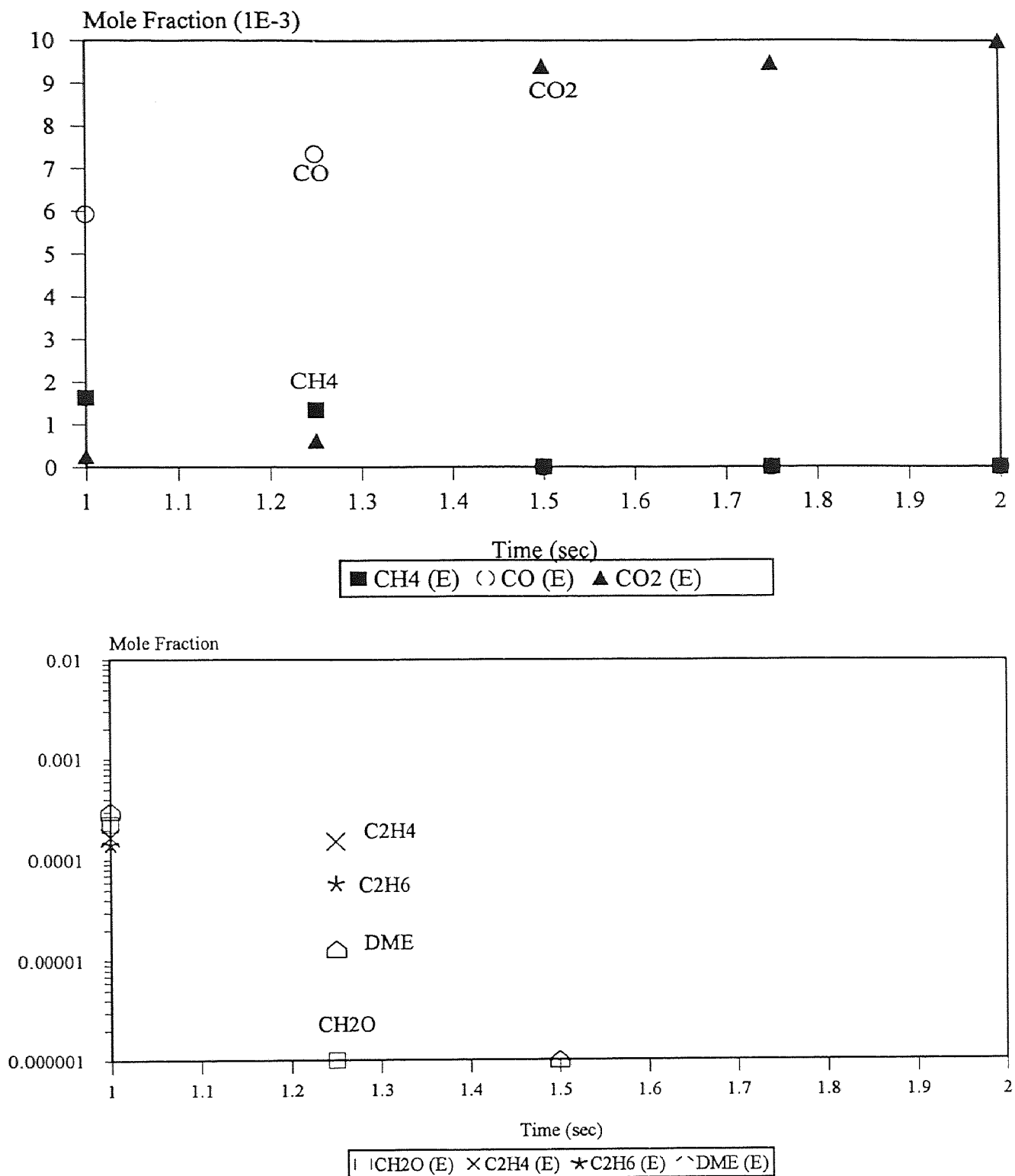
Figure B.23 Experimental Results (Phi=0.75, T=973 K)
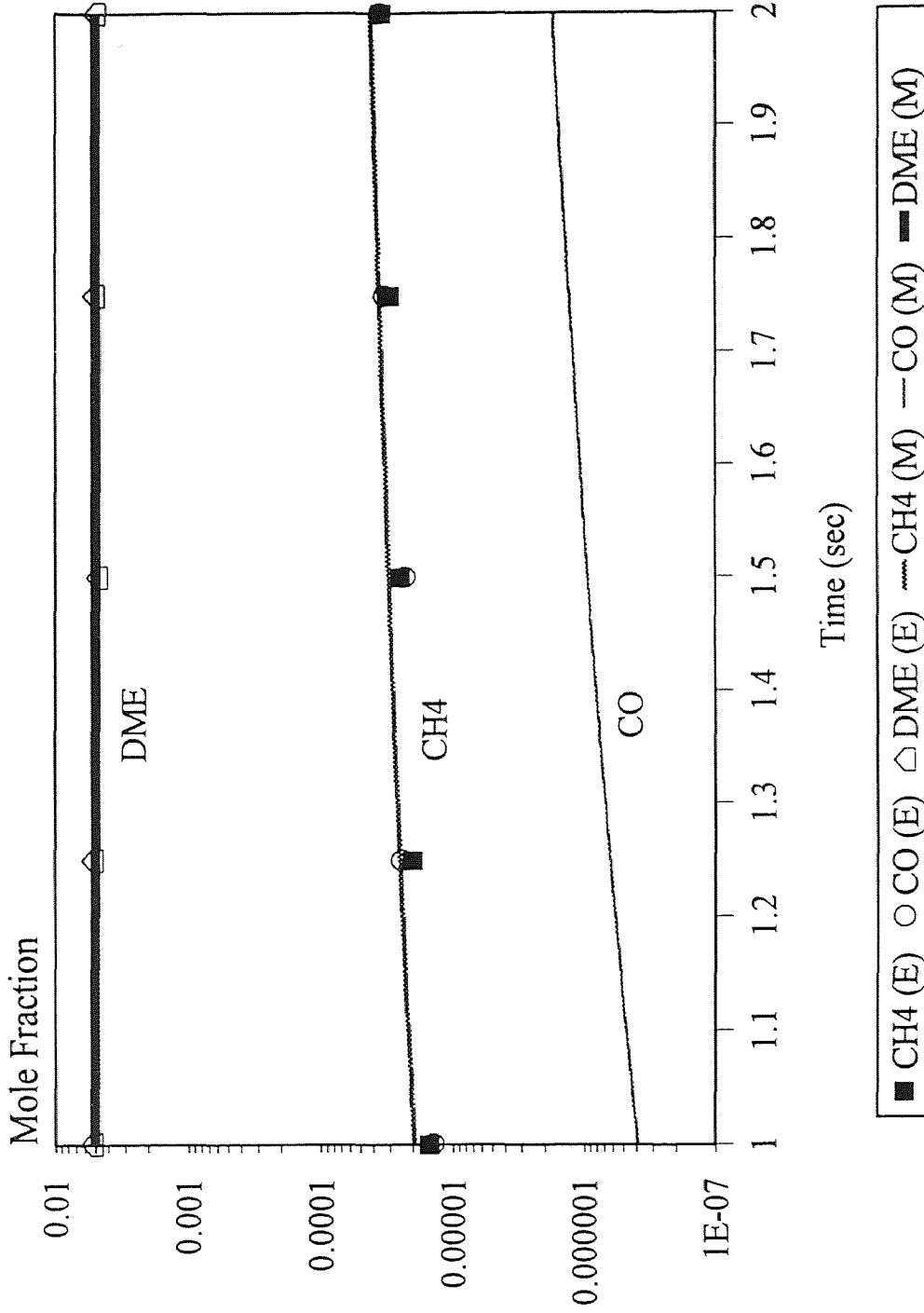
Figure B.24 Modeling Comparison with Experiment (Pyrolysis, T=873 K)
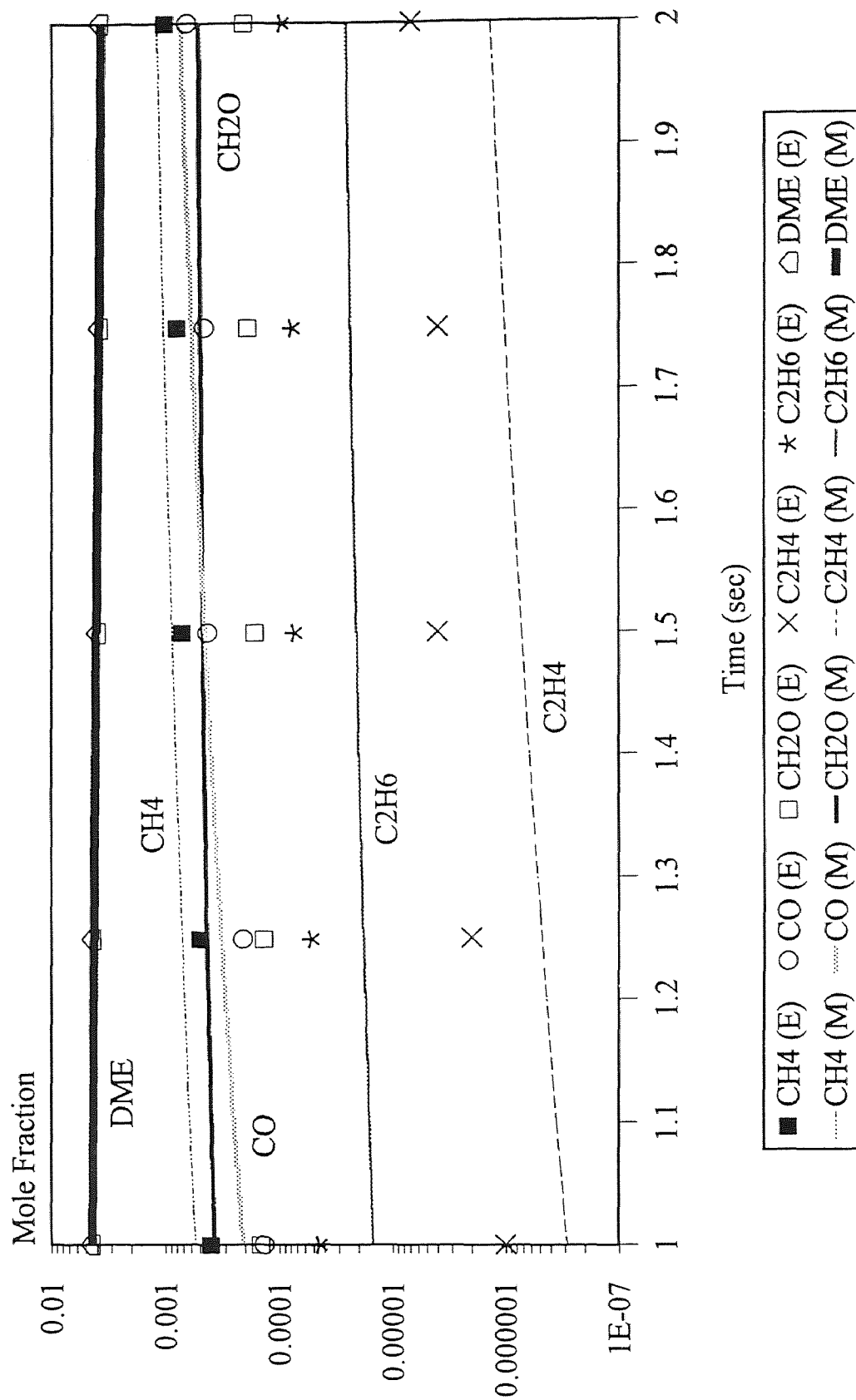
Figure B.25 Modeling Comparison with Experiment (Pyrolysis, T=973 K)
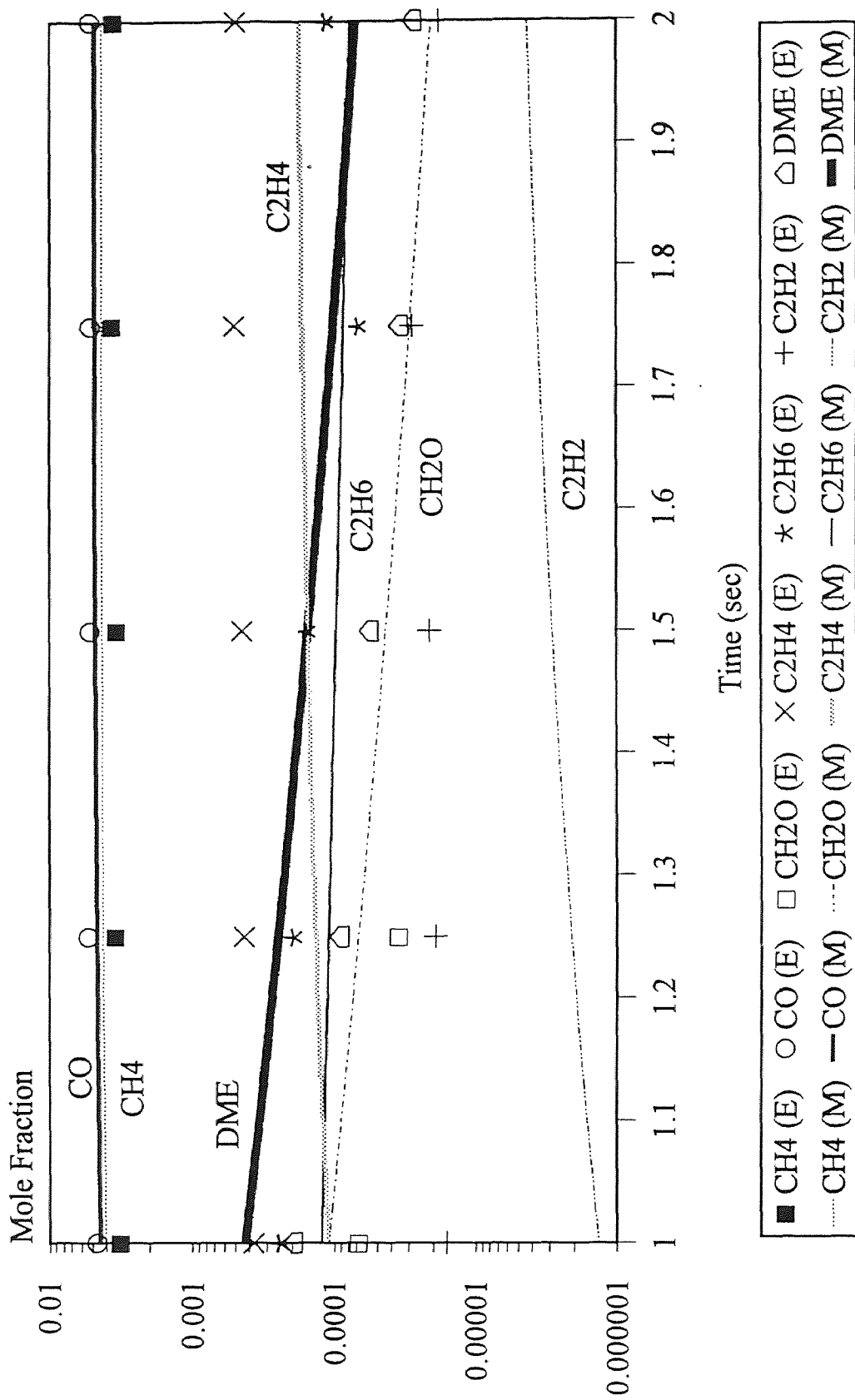
Figure B.26 Modeling Comparison with Experiment (Pyrolysis, T=1073 K)
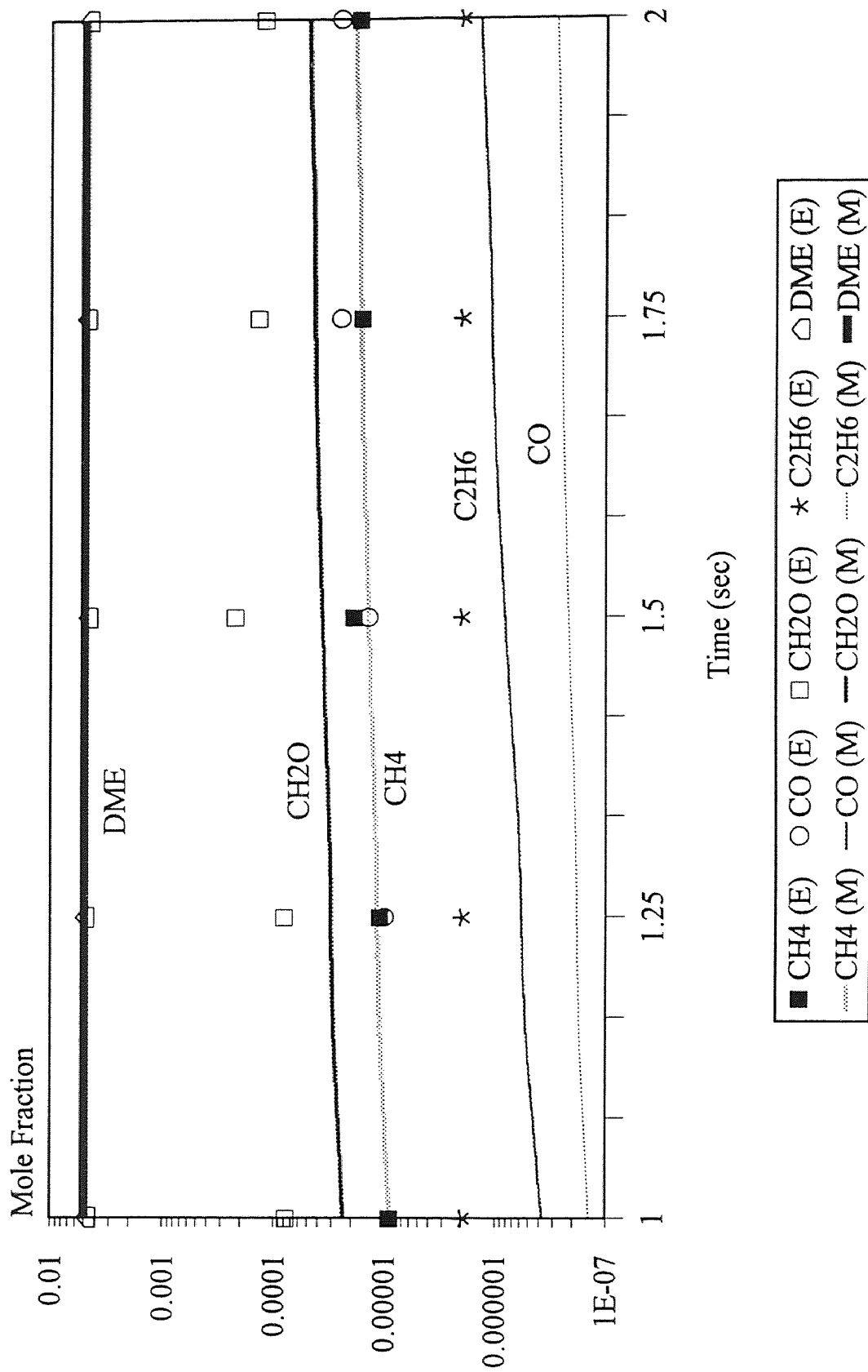
Figure B.27 Modeling Comparison with Experiment (Phi=1.5, T=773 K)
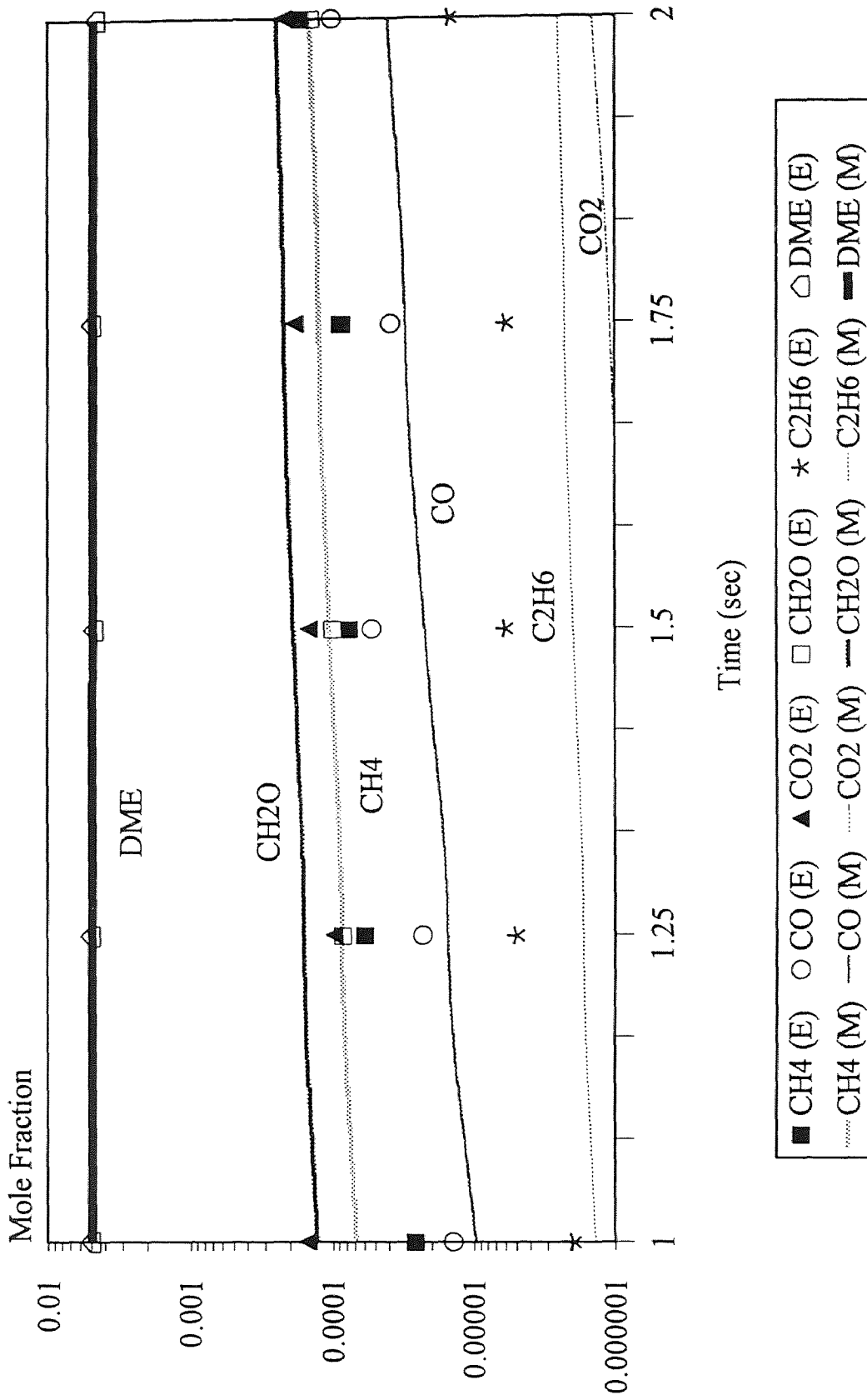
Figure B.28 Modeling Comparison with Experiment (Phi=1.5, T=873 K)
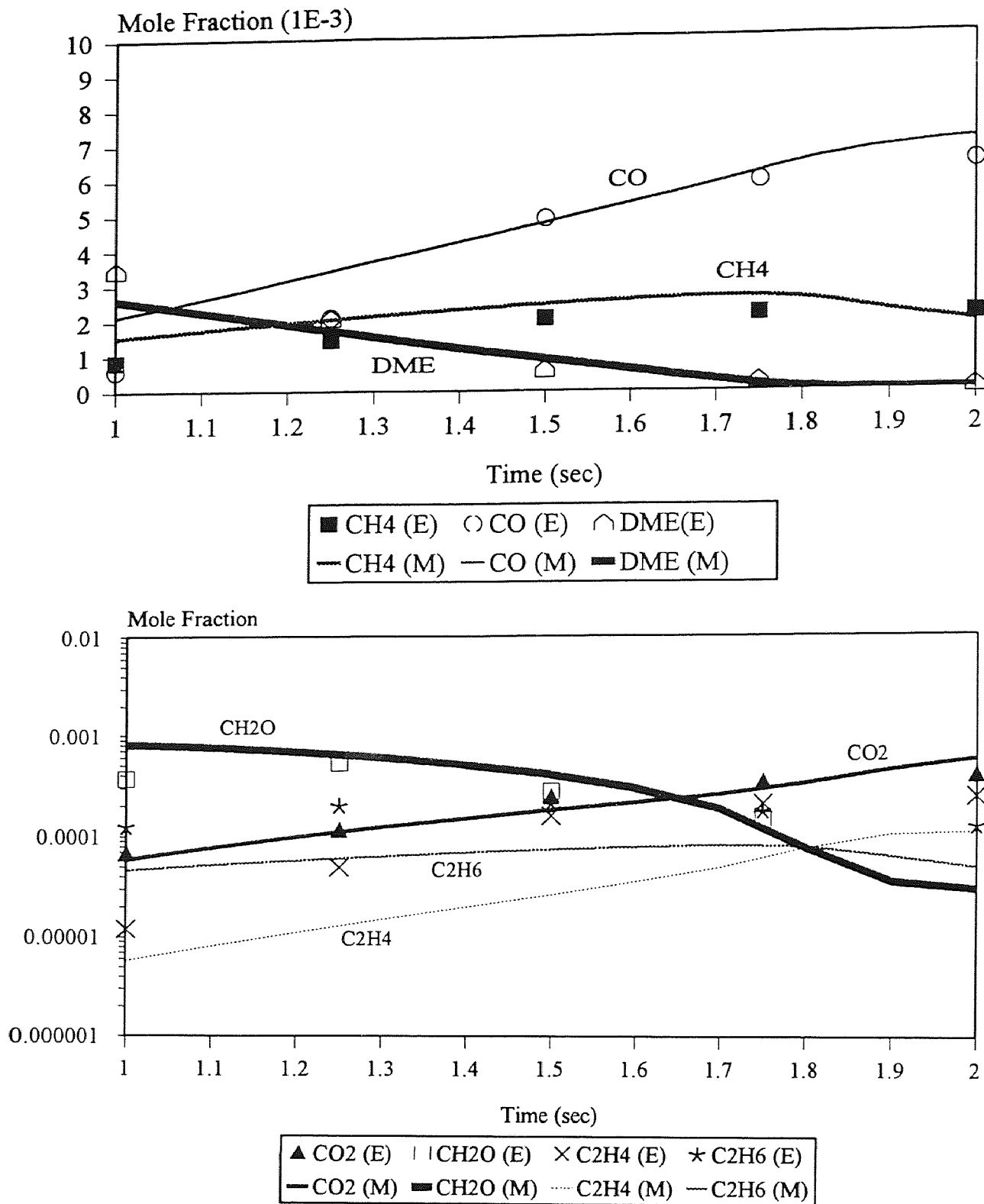
Figure B.29 Modeling Comparison with Experiment (Phi=1.5, T=973 K)
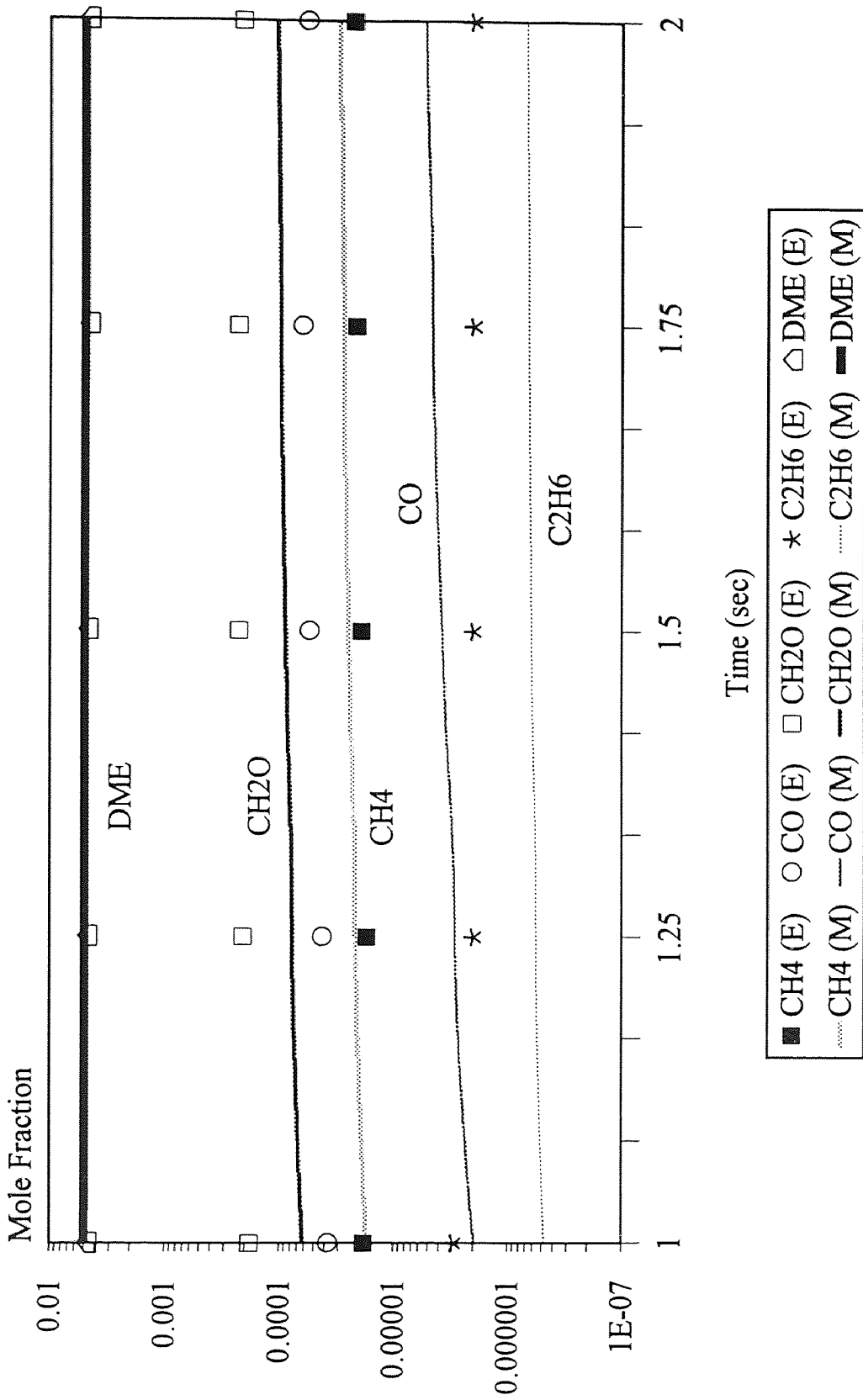
Figure B.30 Modeling Comparison with Experiment (Phi=1.0, T=773 K)
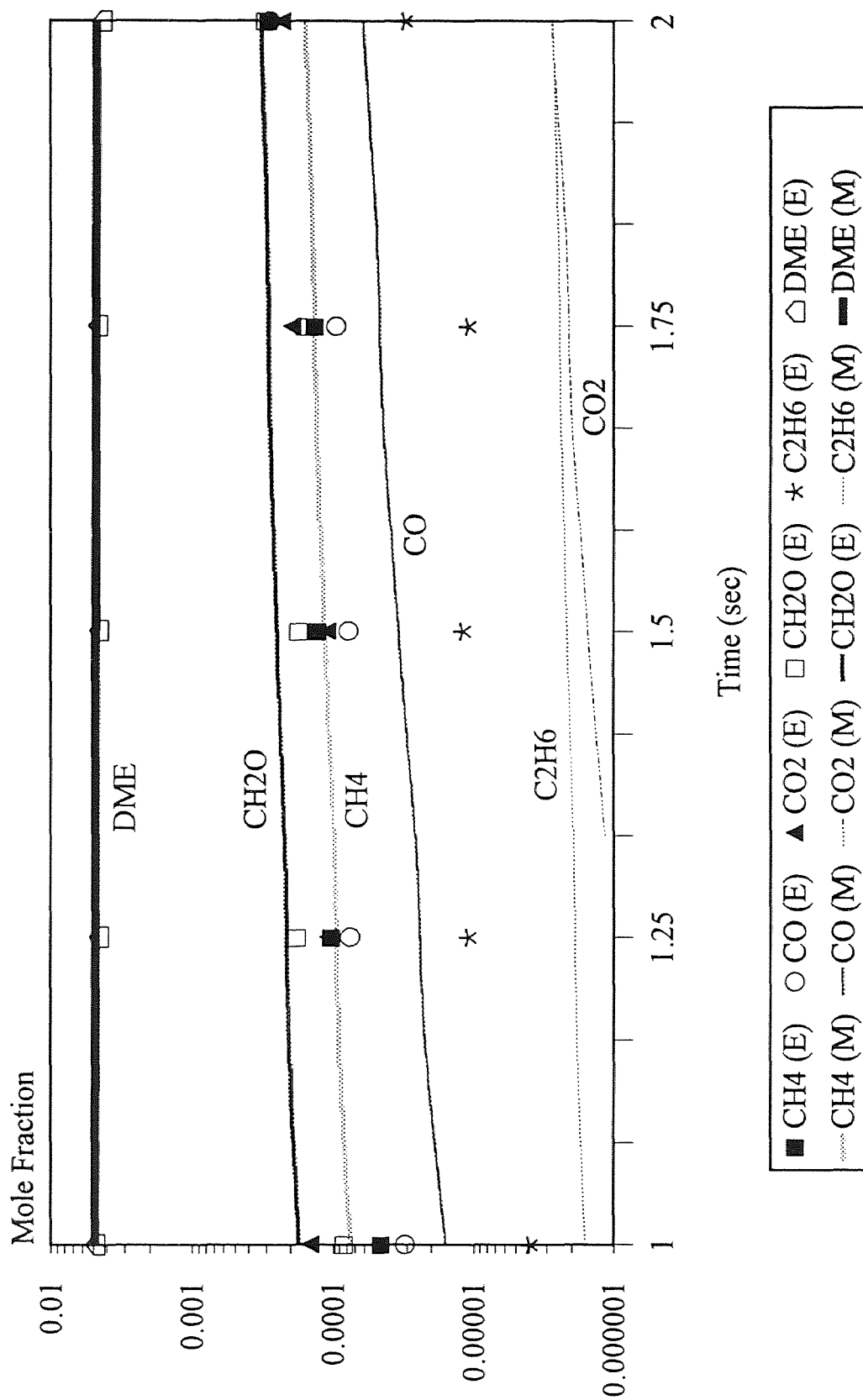
Figure B.31 Modeling Comparison with Experiment (Phi=1.0, T=873 K)
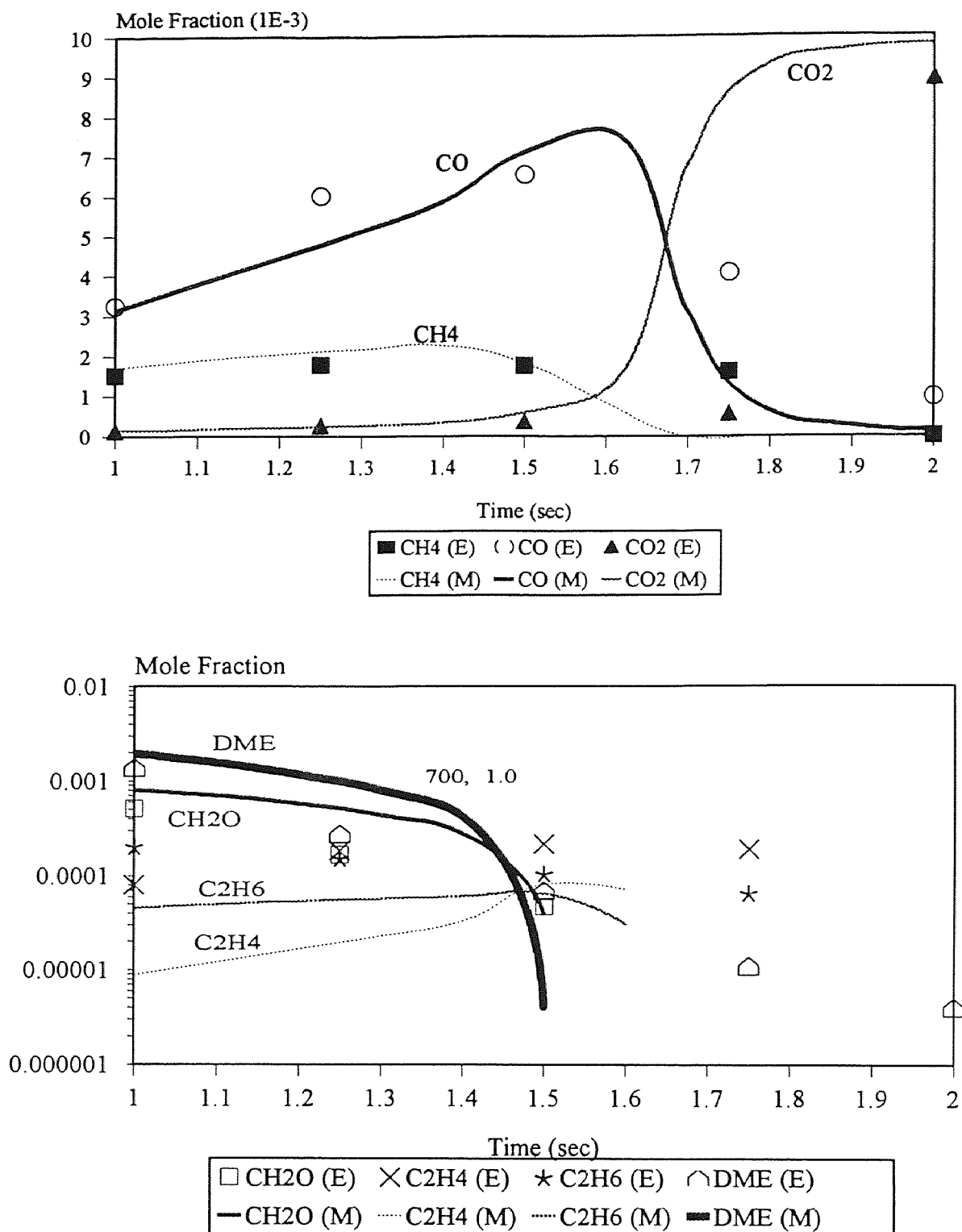
Figure B.32 Modeling Comparison with Experiment (Phi=1.0, T=973 K)
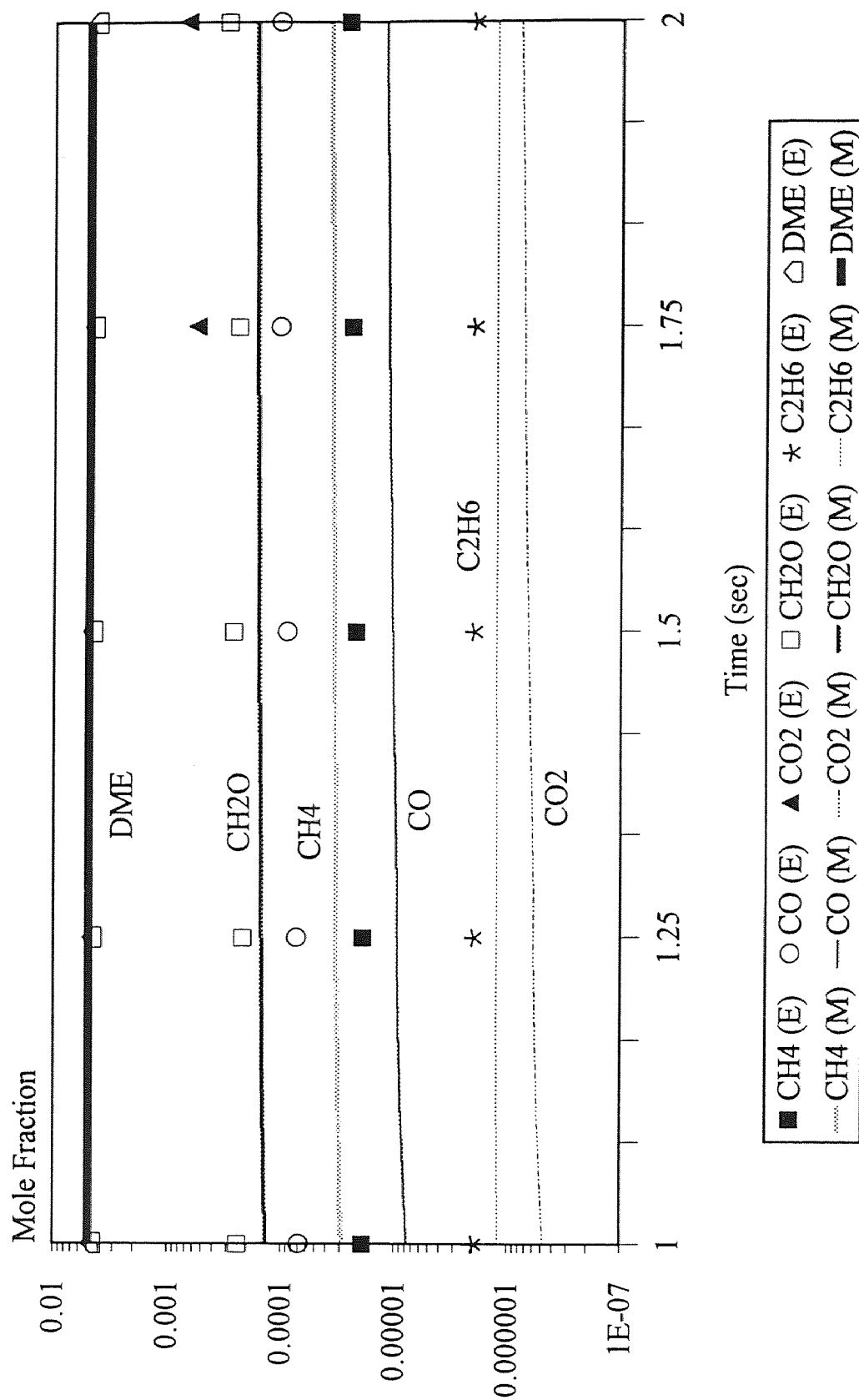
Figure B.33 Modeling Comparison with Experiment (Phi=0.75, T=773 K)

190
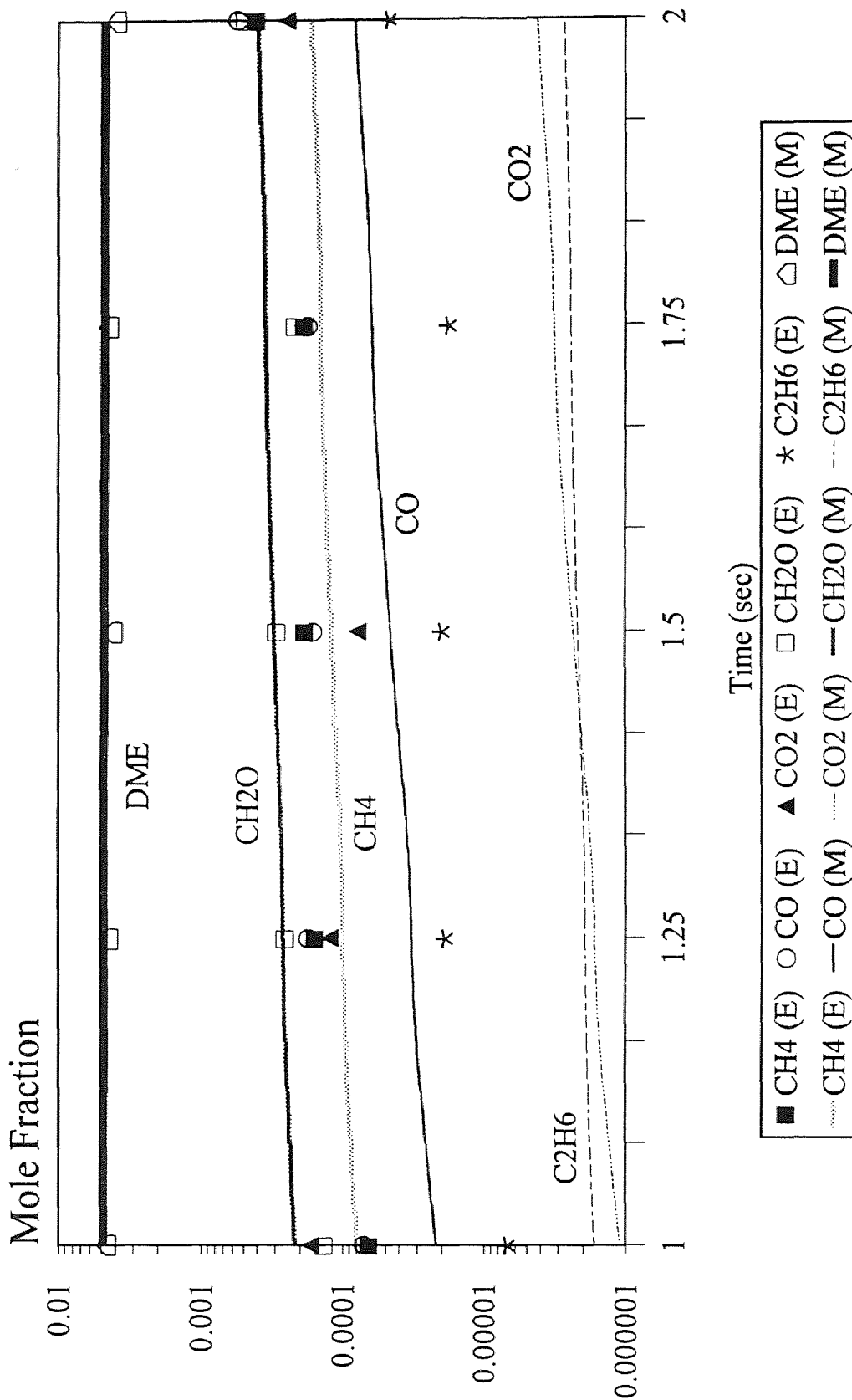
Figure B.34 Modeling Comparison with Experiment (Phi=0.75, T=873 K)
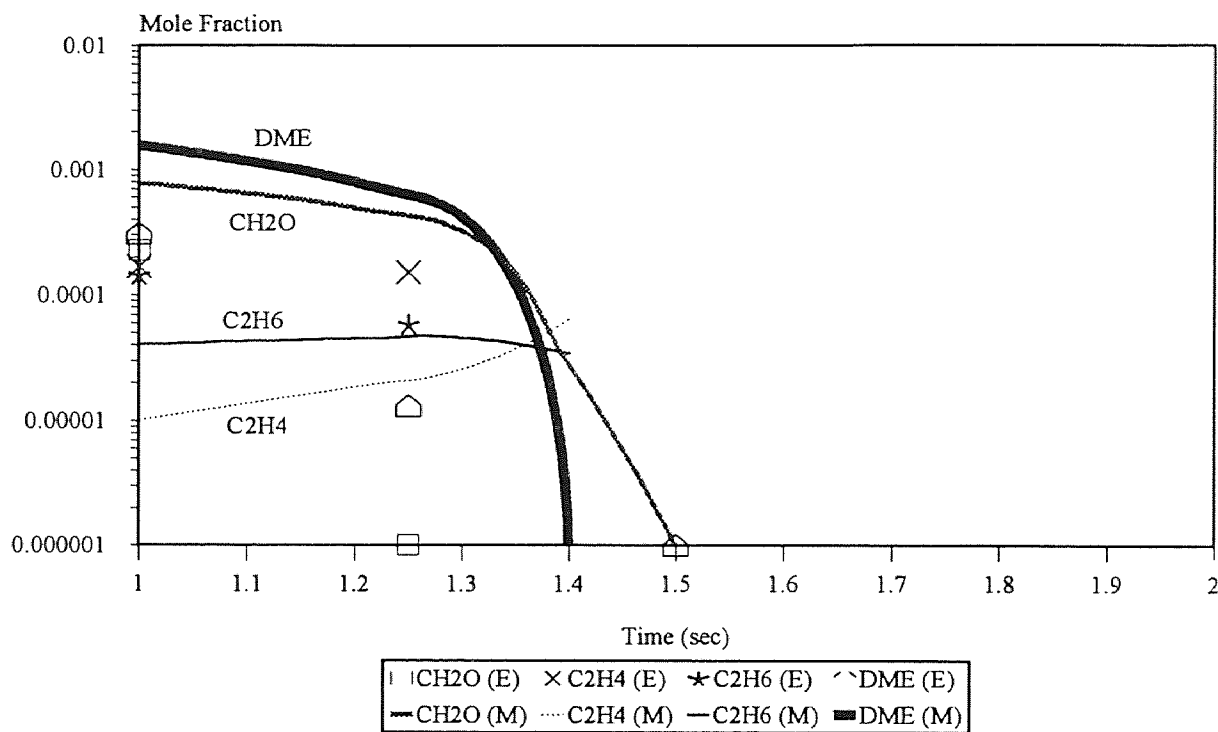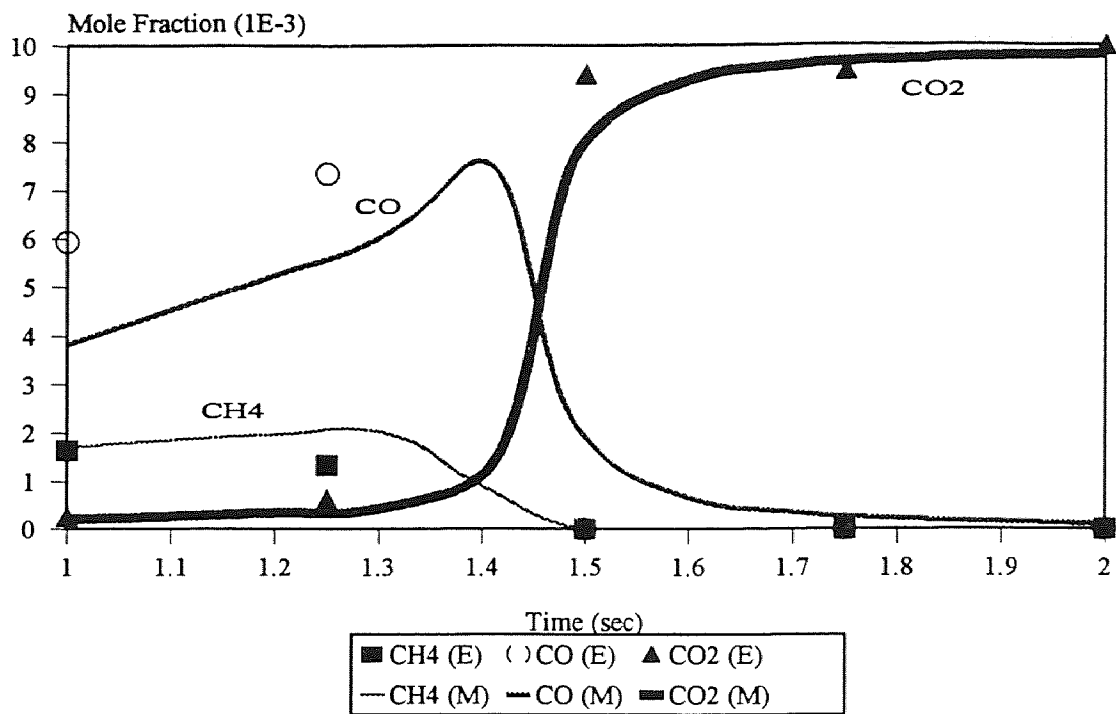
Figure B.35 Modeling Comparison with Experiment (Phi=0.75, T=973 K)

REFERENCES

(1) Sehested, J.; Mogelbelg, T.; Wallington, T. J.; Kaiser, E. W.; Nielsen, O. J. *J. Phys. Chem* **1996**, *100*, 17218 .

(2) Sehested, J.; Sehested, K.; Platz, J.; Egsgaard, H.; Nielsen, O. J. *Int. J. Chem. Kinet.* **1997**, *29*, 627.

(3) Masaki, A.; Tsunashima, S.; Washida, N. *J. Phys. Chem* **1995**, *99*, 13126.

(4) Hoyermann, K.; Nacke, F. "Elementary Reactions of the Methoxymethyl Radical In The Gas Phase"; International Symposium on Combustion, 1996, Napoli, Italy, 505.

(5) Dean, A. M. *J. Phys. Chem.* **1987**, *89*, 4600.

(6) Chang, A. M.; Chiang, H. M.; Bozzelli, J. W.; Dean, A. M., (in process of submittal).

(7) Montgomery, J. A.; Ocherski, J. W.; Petersson, G. A. *J. Chem. Phys.* **1994**, *101*, 5900.

(8) Curtiss, L. A.; Raghavachari, K.; Trucks, G. W.; Pople, J. A. *J. Chem. Phys.* **1991**, *94*, 7221 .

(9) Frisch, M. J.; Trucks, G. W.; Schlegel, H. B.; Gill, P. M. W.; Johnson, B. G.; Robb, M. A.; Cheeseman, R. J.; Keith, T.; Petersson, G. A.; Montgomery, J. A.; Raghavachari, K.; Al-Laham, M. A.; Zakrzewski, V. G.; Ortiz, J. V.; Foresman, J. B.; Cioslowski, J.; Stefanov, B. B.; Nanayakkara, A.; Challacombe, M.; Peng, C. Y.; Ayala, P. Y.; Chen, W.; Wong, M. W.; Andres, J. L.; Replogle, E. S.; Gomperts, R.; Martin, R. L.; Fox, D. J.; Binkley, J. S.; Defrees, D. J.; Baker, J.; Stewart, J. P.; Head-Gordon, M.; Gonzalez, C.; Pople, J. A. Gaussian 94; Gaussian, Inc.: Pittsburgh, PA, 1995.

(10) Pitzer, K. S.; Gwinn, W. *J. Chem. Phys.* **1942**, *10*, 428.

(11) Scott, A. P.; Radom, L. *J. Phys. Chem.* **1996**, *100*, 16502.

(12) Hehre, W. J.; Radom, L.; Schleyer, P. R.; Pople, J. A. *Ab-Initio Molecular Orbital Theory*; John Wiley & Sons: New York, NY, 1986.

(13) Benson, S. W. *Thermochemical Kinetics*; A Wiley-Interscience Publication: New York, NY, 1976.

(14) Westmoreland, P. R. *Combust. Sci. Technol.* **1992**, *82*, 1515.

(15) Bozzelli, B. W.; Dean, A. M.; Ritter, E. R. *Combust. Sci. Technol.* **1991**, *80*, 169.

(16) Dean, A. M. *J. Phys. Chem.* **1985**, *89*, 4500.

(17) Gilbert, R. G.; Smith, S. C. *Theory of Unimolecular and Recombination Reactions.*; Oxford Press: Boston, MA, 1990.

(18) Gilbert, R. G.; Smith, C. S. UNIMOL, 1990.

(19) Gilbert, R. G.; Luther, K.; Troe, J. *Ber. Bunsen-Gas. Phys. Chem.* **1983**, *87*, 169.

(20) Hirschfelder, J. O.; Curtiss, C. F.; Bird, R. B. *Molecular Theory of Gases and Liquids*, 2nd ed.; Wiely: London, England, 1963.

(21) Reid, R. C.; Prausinitz, J. M.; Sherwood, T. K. *The Properties of Gases and Liquids*; McGraw-Hill Co.: New York, NY, 1979.

(22) Westmoreland, P. R.; Howard, J. B.; Longwell, J. P.; Dean, A. M. AICHE Annual Meeting, 1986.

(23) Bozzelli, J. W.; Dean, A. M. *J. Phys. Chem.* **1990**, *94*, 3313.

(24) Bozzelli, J. W.; Dean, A. M. *J. Phys. Chem.* **1993**, *07*, 4427.

(25) Stull, D. R.; Westrum, E. F.; Sinke, G. C. *The Chemical Thermodynamics of Organic Compounds*; Robert E. Krieger Publishing Company: Malabar, FL, 1987.

(26) Tsang, W.; Hampson, R. F. *J. Phys. Chem. Ref. Data* **1986**, *15*, 1087.

(27) Lay, T. H.; Krasnoperov, L. N.; Venanzi, C. A.; Bozzelli, J. W. *J. Phys. Chem.* **1996**, *100*, 8240.

(28) Lay, T. H.; Bozzelli, J. W.; Dean, A. M.; Ritter, E. R. *J. Phys. Chem.* **1995**, *99*, 14514.

(29) Bozzelli, J. W.; Chang, A. Y.; Dean, A. M. *Int. J. Chem. Kint.* **1997**, *29*, 161 .

(30) Atkinson, R.; Baulch, D. I.; Cox, R. A.; Hampson, R. F. J.; Kerr, J. A.; Troe, J. *J. Phys. Chem. Ref. Data* **1992**, *21*, 1125.

(31) Ritter, E.; Bozzelli, J. W. *Int. J. Chem. Kinet.* **1991**, *23*, 767.

(32) Stewart, J. J. P. *J. Comput. Chem.* **1989**, *10*, 209.

(33) *MOPAC: A General Molecular Orbital Package* (QCPE 445): *QCPE Bull.* **1983**, 3, 43. *MOPAC 6.0*: Frank J. Seiler Research Lab., U.S. Airfoece Academy, CO., 1990.

(34) Ing, W.-C. "Reaction Kinetics of Methanol and MTBE Oxidation and Pyrolysis" Ph.D. dissertation, Dep. Chemical Engineering, New Jersey Institute of Technology, January, 1996.

(35) Dean, A. M.; Bozzelli, J. W. *Comb. Chem. Nitro.* **1997**, *1*, 12.

(36) Nash, J. J.; Francisco, J. S. *J. Phys. Chem.* **1998**, *102*, 236.

(37) Baulch, D. L.; Cobos, C. J.; Cox, R. A.; Esser, C.; Frank, P.; Just, T.; Kerr, J. A.; Pilling, M. J.; Troe, J.; Walker, R. W.; Warnatz, J. *J. Phys. Chem. Ref. Data* **1992**, *21*, 411.

(38) Tsan, W. *J. Phys. Chem. Ref. Data* **1987**, *16*, 471.

(39) Allara, D. L.; Shaw, R. *J. Phys. Chem. Ref. Data* **1980**, *9*, 523.

(40) Tsang, W. *J. Phys. Chem. Ref. Data* **1987**, *16*, 471.

(41) Chen, C. J., (in process of submittal).

(42) Kee, R. J.; Miller, J. A.; Jefferson, T. H. CHEMKIN: Fortran Chemical Kinetics Code Package, Sandia Report SAND80-8003. UC-4 Livermore, CA., 1980.

(43) Griener, N. R. *J. Chem. Phys.* **1970**, *53*, 1284.

(44) Atkinson, R.; Perry, R. A.; Pitts, J. N. *J. Chem. Phys.* **1976**, *66*, 1197.

(45) Tully, F. P. *Chem. Phys. Lett.* **1983**, *96*, 148.

(46) Zellner, R.; Lorenz, K. *J. Phys. Chem.* **1984**, *88*, 984.

(47) Sosa, C.; Schlegel, H. B. *J. Am. Chem. Soc.* **1987**, *109*, 4193.

(48) Liu, A.; Mulac, W. A.; Jonah, C. D. *J. Phys. Chem* **1988**, *92*, 3828.

(49) Villa, J.; Gonzalez-Lafont, A.; Lluch, J. M.; Corchado, J. C.; Espinosa-Garcia, J. *J. Chem. Phys.* **1997**, *107*, 7266.

(50) Sosa, C.; Schlegel, H. B. *J. Am. Chem. Soc.* **1986**, *109*, 7007.

(51) Smith, B. J.; Nguyen, M. T.; Bouma, W. J.; Radom, L. *J. Am. Chem. Soc.* **1991**, *113*, 6452.

(52) Meagher, J. F.; Heicklen, J. *J Phys. Chem.* **1976**, *80*, 1645.

(53) Lloyd, A. C.; Darnall, K. R.; Winer, A. M.; Pitts, J. M. *J. Phys. Chem.* **1976**, *80*, 789.

(54) Bartels, M.; Hoyermann, K.; Sievert, R. "Elementary Reactions in the Oxidation of Etylene"; International Symposium on Combustion, 1982, Haifa, Israel, 61.

(55) Liu, A.; Jonah, C. D.; Mulac, W. A. *Radiat. Phys. Chem* **1989**, *34*, 687.

(56) Smith, I. W. M.; Zellner, R. *J. Chem. Soc. Faraday Trans. (2)* **1973**, *69*, 1617.

(57) Mozurkewich, M.; Benson, S. W. *J. Phys. Chem.* **1984**, *88*, 6429.

(58) Howard, C. J. *J.Chem. Phys.* **1976**, *65*, 4771.

(59) Diau, E. W.-G.; Lee, Y.-P. *J. Chem. Phys* **1992**, *96*, 377.

(60) Pastrana, A. V.; Carr, J. R. W. *J. Phys. Chem.* **1975**, *79*, 765.

(61) Morris, E. D.; Stedman, D. H.; Niki, H. *J.Am. Chem. Soc.* **1971**, *93*, 3570.

(62) Bradley, J. N.; Hack, W.; Hoyermann, K.; Wagner, H. G. *J. Chem. Soc. Faraday Trans. (1)* **1973**, *69*, 1889.

(63) Kuo, C.-H.; Lee, Y.-P. *J. Phys. Chem.* **1991**, *95*, 1253.

(64) Overend, R.; Paraskevopoulos, G. *J. Chem. Phys.* **1977**, *67*, 674.

(65) Stull, D. R.; Prophet, H. *JANAF Thermochemical Tables*; U. S. Government Printing Office: Washington D. C., 1971; Vol. NSRDS-NBS 37.

(66) Petersson, G.; Schwartz, M. personal communication, Jan-Mar. 1998.

(67) Eckart, C. *Phys. Rev.* **1930**, *35*, 1203.

(68) Turecek, F.; Cramer, C. J. *J. Am. Chem. Soc.* **1995**, *117*, 12243.

(69) William, L. H.; Schlegel, H. B.; Balbyshev, V.; Page, M. *J. Phys. Chem.* **1996**, *100*, 5354.

(70) Liu, A.-D.; Mulac, W. I.; Jonah, C. D. *Int. J. Chem. Kinet* **1987**, *19*, 25.

(71) Atri, M. G.; Baldwin, R. R.; Evans, G. A.; Walker, R. W. *J. Chem. Soc. Faraday Trans.* **1978**, *1*, 366.

(72) Koert, D.; Pitz, W.; Bozzelli, J. W.; Cernanzky, N. "Chemical Kinetic Modeling of High-Pressure Oxidation and Comparison to Experimental Results"; International Symposium on Combustion, 1996, Napoli, Italy, 633.

(73) Boyd, S. L.; Boyd, R. J.; Ross, L.; Barclay, R. C. *J. Am. Chem. Soc.* **1990**, *112*, 5724.

(74) Lay, T. H.; Bozzelli, J. W.; Seinfeld, J. H. *J. Phys. Chem.* **1996**, *100*, 6543.

(75) Atkinson, R. *J. Phys. Chem. Ref. Data* **1991**, *20*, 459.

(76) Atkinson, R.; Tuazon, E. C.; AschMann, S. M. *Environ. Sci. Technol.* **1995**, *29*, 1860.

(77) Dorofeeva, O. V. *Thermochemica Acta* **1992**, *194*, 9.

(78) Dorofeeva, O. V. *Thermochemica Acta* **1992**, *194*, 121.

(79) Pedley, J. B.; Naylor, R. D.; Kirby, S. P. *Thermochemical Data of Organic Compounds, 2nd Ed*; Chapman and Hall: London, 1986.

(80) Coolidge, M. B.; Marlin, J. E.; Stewart, J. J. P. *J. Comput. Chem.* **1991**, *12*, 948.

(81) Cohen, N.; Benson, S. W. *Chem. Rev.* **1993**, *93*, 2419.

(82) Luo, Y.-R.; Holmes, J. L. *J. Phys. Org. Chem.* **1994**, *7*, 403.

(83) Holmes, J. L.; Lossing, F. P. *J. Am. Chem. Soc.* **1982**, *104*, 2648.

(84) Cox, J. D.; Pilcher, G. *Thermochemistry of Organic and Organometallic Compounds*; Academic Press: New York, NY, 1970.

(85) Jungkamp, T. P. W.; Seinfeld, J. H. *Chem. Phys. Letters* **1996**, *257*, 15.

(86) Pickett, H. M.; Strauss, H. L. *J. Chem. Phys.* **1970**, *53*, 376.

(87) Vacek, G.; Galbraith, J. M.; Yamaguchi, Y.; Schaefer, H. F. *J. Phys. Chem.* **1994**, *35*, 8660.

(88) Yu, T.; Mebel, A. M.; Lin, M. C. *J. Phys. Org. Chem.* **1995**, *8*, 47.

(89) Berkowitz, J.; Ellison, G. B.; Gutman, D. *J. Phys. Chem.* **1994**, *98*, 2744.

(90) Benson, S. W. *Int. J. Chem. Kinet.* **1996**, *28*, 665.

PART II

THERMODYNAMIC STUDIES ON HYDROFLUOROCARBONS (HFC'S) USING *AB INITIO* CALCULATION METHODS

Overview

Thermodynamic properties ($\Delta H_f^\circ{}_{298}$, $S^\circ{}_{298}$ and $C_p(T)$'s, ($300 \leq T/K \leq 1500$)), of two to four carbon fluorinated hydrocarbons, groups for group additivity and interaction terms are calculated in this part.

Chlorofluorocarbons (CFCs) are being replaced by hydrofluorocarbons (HFCs) and hydrochlorofluorocarbons(HCFCs) because of their non or less adverse effects on the stratospheric ozone layer. Examples includes HFC-134a (CH_2FCF_3), a replacement for CFC-12 (CF_2Cl_2) in domestic refrigeration and automobile air conditioning units, and HFC-227ea (CF_3CFHCF_3), replacements for Halon 1301 (CF3Br) as fire suppressants and for CFC114 (CF_2ClCF_2Cl) as refrigerant.

Thermodynamic properties for these fluorinated carbons are necessary for kinetic and thermodynamic studies needed to analyze their chemical reactions in atmospheric, in combustion environments and to evaluate effects of the fluorocarbon molecule on global warming. The thermodynamic properties are also important for use in refrigeration systems. Thermodynamic properties for fluorinated carbon groups are also of value since these values allow the estimate of accurate thermodynamic properties on higher molecular weight fluorocarbons in an economical way. Errors caused by group additivity, which gives accurate estimation for hydrocarbons, are large for halocarbons. These errors are corrected using fluorine-fluorine interaction terms and methyl-fluorine gauche interaction term developed in this study.

Thermodynamic properties for nine fluoroethanes, fluoroethane, 1,1- and 1,2-difluoroethane, 1,1,1- and 1,1,2-trifluoroethane, 1,1,1,2- and 1,1,2,2-tetrafluoroethane, pentafluoroethane, and hexafluoroethane, and nine fluoropropanes, 1-fluoropropane, 1,1- and 1,2-difluoropropane, 1,1,1- and 1,1,2-trifluoropropane, 1,1,1,2- and 1,1,2,2-tetrafluoropropane, 1,1,1,2,2-pentafluoropropane, and 2-methyl,2-fluoropropane are estimated using *ab initio* methods. Geometries, frequencies, and rotational barriers for above compounds are also calculated.

Thermodynamic properties for fluorocarbon groups, C/C/H2/F, C/C/H/F2, C/C/F3, C/C2/H/F, C/C2/F2 and C/C3/F for fluoroalkanes, CD/H/F and CD/F2 for fluoroalkenes, and CT/F for fluoroalkynes are estimated using above *ab initio* determined thermodynamic properties and literature data.

Thermodynamic properties for interaction terms, F/F, 2F/F, 2F/2F, 3F/F, 3F/2F and 3F/3F for fluoroalkanes, F//F, 2F//F and 2F//2F for fluoroalkenes, and F///F for fluoroalkyne are estimated using above groups and selected fluorinated compounds. The methyl-fluorine gauche interaction term is needed as well as fluorine-fluorine interaction terms to calculate accurate thermodynamic properties using group additivity methods.

CHAPTER 6

AB INITIO CALCULATIONS AND INTERNAL ROTOR: CONTRIBUTION FOR THERMODYNAMIC PROPERTIES S°$_{298}$ AND C$_P$(T)'S (300 ≤ T/K ≤ 1500): GROUP ADDITIVITY FOR FLUOROETHANES

6.1 Introduction

Ab initio calculations are performed on nine fluorinated ethane compounds, CH_3CH_2F,

CH_2FCH_2F, CH_3CHF_2, CH_2FCHF_2, CH_3CF_3, CHF_2CHF_2, CH_2FCF_3, CHF_2CF_3 and

CF_3CF_3, and thermodynamic properties (S°$_{298}$ and C$_p$(T)'s 300 ≤ T/K ≤ 1500) are

calculated. A number of studies on thermodynamic property data have been reported for

these species by experiment and *ab initio* calculations. Chen et al. [1] studied and

recommended thermodynamic properties ($\Delta H_f°_{298}$, S°$_{298}$ and C$_p$(T) for 0 K to 1500 K) for

six fluoroethanes in which at least one of the internally rotating groups is a symmetric

top. Zachariah et al. reported thermochemical data on about 100 closed and open shelled

fluorocarbon species using BAC-MP4 method [2]. Chen et al. studied the structures,

moments of inertia and frequencies at the RHF/6-31G* level of theory, and barriers for

internal rotation at the MP4/6-311G**//6-31G* level of theory, and estimated

thermodynamic properties and functions of 1,1,2-trifluoroethane and 1,1,2,2-

tetrafluoroethane [3]. Berry et al reported enthalpies of formation ($\Delta H_f°_{298}$) for ethane and

the complete series of fluoroethanes, $C_2H_xF_{6-x}$, x=0 to 5 by *ab initio* G2, G2(MP2), CBS-

4 and CBS-Q quantum mechanical protocols and the parameterized BAC-MP4 procedure

[4]. Marshall et al. have reported C-H bond dissociation enthalpies at 298 K for a variety

of C_1 -C_4 hydrofluorocarbons using MP2/6-311+G(3df,2p)//MP2/6-31G(d) level of

theory and isodesmic reactions [5]. These *ab initio* studies are quite valuable, however it is

difficult to extend these beyond 3 to 4 carbon species and a method is needed to accurately estimate thermodynamic properties of fluoro and other halogenated species.

The group additivity method [6], which is an easy, inexpensive and accurate calculation for hydrocarbons and oxygenated hydrocarbons[7], is not accepted as accurate for these fluorocarbons where average errors are several kcal/mol with maximum errors exceeding 5 kcal/mol. Accuracy of conventional group additivity method is unacceptable by the standards set by the above research studies.

In this study RHF/6-31G* and MP2/6-31G* calculations are applied on nine HFCs, CH_3CH_2F, CH_2FCH_2F, CH_3CHF_2, CH_2FCHF_2, CH_3CF_3, CHF_2CHF_2, CH_2FCF_3, CHF_2CF_3 and CF_3CF_3 to obtain potential barriers for internal rotations. Standard entropy (S°_{298}) and heat capacities $(C_p(T)$, $300 \leq$ T/K $\leq 1500)$ are calculated using the rigid-rotor-harmonic-oscillator approximation based on the information obtained from the *ab initio* studies. Enthalpies of formation $(\Delta H_f^{\circ}{}_{298})$ for CH_3CH_2F, CH_3CHF_2, CH_3CF_3, CH_2FCF_3, CHF_2CF_3, CF_3CF_3 are adopted from the literature study evaluation of Chen et al.[1], $\Delta H_f^{\circ}{}_{298}$ value for CH_2FCH_2F is adopted from Bond Additivity Correction-MP4 (BAC-MP4) *ab initio* calculation [2,8], and $\Delta H_f^{\circ}{}_{298}$ of CH_2FCHF_2 and CHF_2CHF_2 are average values of Lacher et al.[9] and Chen et al.[3].

Group values are estimated for C/C/F/H2, C/C/F2/H and C/C/F3 based on the selected molecules, CH_3CH_2F, CH_3CHF_2 and CH_3CF_3, where there are no fluorine atoms on the carbon adjacent to the carbon containing the fluorine atom(s). Group additivity corrections (fluorine interaction terms) are determined for F/F, 2F/F, 3F/F, 2F/2F, 3F/2F and 3F/3F. Consider 1,1-difluoroethane with groups C/C/F2/H and C/C/H3, and 1,2-difluoroethane with groups C/C/F/H2 and C/C/F/H2. For 1,1-difluoroethane, the

C/C/F2/H group data includes steric, electronic and polar effects of the two fluorine atoms, but the C/C/F/H2 groups on 1,2-difluoroethane do not include steric, electronic and polar effects resulting from F -F interactions on the adjacent carbons. Interaction groups are developed to account for these effects. The use of a modified group additivity for the properties of C_1 to C_n fluorocarbons is valuable and the tabulated data and databases allow easy estimation of the thermodynamic property data for a large number of fluorocarbons.

6.2 Calculation Methods

6.2.1 Thermodynamic Properties (Standard Entropy ($S°_{298}$) and Heat Capacities ($C_p(T)$, 300≤ T/K ≤ 1500) Using *ab initio* Calculations

All *ab initio* calculations are performed using the Gaussian94[10] system of programs on a DEC Alpha 200 work station. Equilibrium and saddle-point geometries are completely optimized using the closed shell restricted Hartree-Fock (RHF) method and second-order Møller-Plesset (MP2) perturbation theory with analytical gradients with the 6-31G* basis set (HF/6-31G* and MP2/6-31G*).

Energies for equilibrium structures and saddle-point structures between rotational conformers are calculated at the MP2/6-31G* level of theory. Vibrational frequencies are calculated for all rotational conformers and saddle-points using analytical second derivatives at the HF/6-31G* level. Zero point vibrational energies (ZPVE) are scaled by the factor of 0.89 as recommended[11] because of the systematic overestimation of the HF-SCF determined harmonic vibrational frequencies by about 10 %.

The scaled harmonic vibrational frequencies from the HF6-31G* level of calculations and the moments of inertia of molecular structures optimized at MP2/6-31G* are used to calculate the $S°_{298}$ and $C_p(T)$.

6.2.2 Calculation of Hindered Rotational Contribution to Thermodynamic Parameters

A technique for the calculation of thermodynamic functions from hindered rotations with arbitrary potentials has been developed.

The technique employs expansion of the hindrance potential in a Fourier series, calculation of the Hamiltonian matrix in the basis of the wave functions of free internal rotation and subsequent calculation of energy levels by direct diagonalization of the Hamiltonian matrix. The torsional potential calculated at discrete torsional angles is represented by a truncated Fourier series. All potential curves of rotational barrier vs. dihedral angle are fit by a cosine curve. The specific fit function

for CH_2FCH_2F, CHF_2CH_2F and CHF_2CHF_2 is

$$V(\emptyset) = a_0 + a_1\cos(\emptyset) + a_2\cos(2\emptyset) + a_3\cos(3\emptyset) \qquad \text{---------- (1)}$$

for CH_2FCH_3, CHF_2CH_3, CF_3CH_3, CF_3CH2F, CF_3CHF2 and CF_3CF_3 is

$$V(\emptyset) = a_0 + a_3\cos(3\emptyset). \qquad \text{---------- (2)}$$

Values of the coefficients a_i are calculated to provide the minimum and maxima of the torsional potentials with allowance of a shift of the theoretical extrema angular positions.

Evaluation of the matrix elements of individual cosine terms in the basis of the free rotor wave functions is straightforward. The terms $\cos(m\emptyset)$ induce transitions with $\Delta K = \pm m$, where K is the rotational quantum number. Moreover, the matrix element does not

depend on K, which leads to a simple form of the hamiltonian matrix. The matrix has a band structure and consists of diagonal terms that are equal to those of the free rotor and subdiagonals of constant values that correspond to a different terms in the potential expansion.

The Hamiltonian matrix is then truncated to the size of $2 K_{max} + 1$, where K_{max} is the maximum rotational quantum number considered. The choice of the size of the truncated matrix is made by checking the independence of the thermodynamic properties calculated on K_{max}. The truncated matrix (in reduced dimensionless form) is diagonalized and the eigenvalues are used to calculate the partition function, entropy, heat capacity and etc. This is accomplished using direct summation over the calculated energy levels according to standard expressions of statistical thermodynamics[12].

6.2.3 Group Values and Group Additivity Correction Term Estimation

Selection (definition) of the initial groups is critical to development of a group additivity scheme for accurate property estimation. We develop a new set of groups for fluorocarbon alkane groups derived from use of thermodynamic property data on molecules where there are only hydrogen atoms on the carbons which are adjacent to the carbon atom bonded to fluorines. The properties of the C/C/F/H2, C/C/F2/H, of C/C/F3 groups, for example, are derived from fluoroethane (CH_2FCH_3); 1,1-difluoroethane (CHF_2CH_3); 1,1,1-trifluoroethane (CF_3CH_3), respectively. There are no fluorines, other halogens, or bulky groups/fragments on the carbon atoms adjacent to the carbon atoms

containing the fluorine(s) in the defining group. $H_f°_{298}$ and $C_p(T)$ of C/C/F/H2 are

calculated based on:

$$(CH_3CH_2F) = (C/C/H3) + (C/C/F/H2) \quad\quad\quad \text{--------- (3)}$$

$S°_{298}$ of C/C/F/H2 is calculated based on:

$$(CH_3CH_2F) = (C/C/H3) + (C/C/F/H) - R \ln(\sigma) \quad\quad\quad \text{--------- (4)}$$

where R=1.987 cal/mol-K, and σ is symmetry number, which is 3 for CH_3CH_2F. The

group values of C/C/F2/H and C/C/F3 are also estimated in the same manner.

Thermodynamic properties of fluoroethanes with no fluorine on the carbon atoms

adjacent to a carbon with fluorine are now accurately predicted; but an adjustment needs

to be made for fluoroethane species where there are fluorine atoms on an adjacent carbon,

such as 1,2-difluoroethane, or 1,1,2-trifluoroethane. This adjustment comes in the form

of an interaction term to count the total number of fluorine atoms on each of the two

adjacent carbon atoms. No interaction term is needed when there are no fluorine(s) on

adjacent carbons.

Assumption is based on the known accuracy and validity of group additivity for

hydrocarbon and oxyhydrocarbons with gauche interactions [6,7]. Conventional group

additivity does not, however, work for fluorocarbons or other halocarbons. Group

additivity does not incorporate effects of non-next nearest neighbors. Consider the two

molecules 1,1-difluoroethane and 1,2-difluoroethane and the groups that are used to

estimate the respective properties.

Compound	1,1-difluoroethane CHF_2-CH_3	1,2-difluoroethane CH_2FCH_2F
Groups	C/C/F2/H	C/C/F/H2
	C/C/H3	C/C/F/H2

In the 1,1-difluoroethane isomer, the C/C/F2/H group knows and incorporates polar, electronic and steric interactions between the two fluorines as well as adjacent hydrogens and carbons. In the 1,2-difluoroethane isomer, C/C/F/H2 groups do not recognize or incorporate any interactions (polar, steric, etc.) between the two fluorines.

Groups and a limited set of interaction terms which can be used with Benson type group additivity scheme for calculation of the thermodynamic properties of multi-fluoro alkanes are defined and developed in this chapter.

The interaction values between fluorines attached to two adjacent carbons (F/F, 2F/F, 3F/F, 2F/2F, 3F/2F and 3F/3F) are calculated from differences between the defined fluorinated hydrocarbon group values and thermodynamic properties of the parent compounds. For example, $H_f°_{298}$ and $C_p(T)$ for the F/F interaction are estimated by:

$$(CH_2FCH_2F) = (C/C/F/H2) \times 2 + (F/F) \qquad \text{---------- (5)}$$

$S°_{298}$ for the F/F interaction is calculated by:

$$(CH_2FCH_2F) = (C/C/F/H2) \times 2 - R \ln(\sigma) + (F/F) \qquad \text{---------- (6)}$$

where $R=1.987$ cal K^{-1} mol^{-1} and $\sigma = 2$ for CH_2FCH_2F

Other interaction values are also estimated in the same manner.

6.3 Results and Discussion

6.3.1 Rotational Barriers

The barriers for internal rotations are calculated as the difference between the total energy of each conformation and that of the global equilibrium plus the scaled ZPVE difference (see Table 6.2). The curves are fit by a truncated Fourier series (1) and (2).

Table 6.1 Vibrational Frequencies^a (v cm^{-1})

Species	v1^b	v2	v3	v4	v5	v6	v7	v8	v9	v10	v11	v12	v13	v14	v15	v16	v17	v18
CH$_3$CH$_2$F	274	440	878	972	1169	1240	1310	1422	1547	1588	1627	1645	1683	3212	3242	3274	3280	3301
CH$_2$FCH$_2$F	150	348	541	956	1002	1212	1231	1251	1383	1425	1563	1607	1658	1662	3242	3258	3299	3313
CH$_3$CHF$_2$	258	408	503	614	948	1072	1254	1283	1298	1540	1558	1603	1630	1633	3229	3302	3306	3324
CH$_2$FCHF$_2$	128	263	462	522	627	1003	1211	1245	1260	1292	1386	1492	1570	1632	1664	3274	3327	3344
CH$_3$CF$_3$	251	392	392	585	585	646	908	1095	1095	1415	1415	1430	1601	1627	1627	3246	3330	3330
CHF$_2$CHF$_2$	96	220	390	455	533	585	679	1225	1257	1276	1286	1304	1463	1526	1556	1657	3343	3353
CH$_2$FCF$_3$	117	233	382	446	578	594	723	928	1098	1234	1344	1363	1460	1472	1622	1663	3286	3348
CHF$_2$CF$_3$	81	225	263	393	455	565	626	634	791	962	1266	1309	1363	1407	1483	1551	1641	3354
CF$_3$CF$_3$	70	230	230	378	415	415	564	564	674	674	774	888	1243	1426	1426	1434	1434	1627

^{a} Non-scaled, Frequencies are calculated at the HF/6-31G* level of theory.
^{b} Torsional Frequencies, these frequencies are not included in the calculation of thermodynamic properties.

Figure 6.1 shows rotational barrier diagrams for CH$_3$CH$_2$F, CH$_3$CHF$_2$ and CH$_3$CF$_3$, with rotational barriers 4.05, 4.13 and 4.07 kcal/mol respectively. Figure 6.2 shows the diagrams for CH$_2$FCF$_3$, CHF$_2$CF$_3$ and CF$_3$CF$_3$ with barriers 4.43, 3.90 and 3.95 kcal/mol respectively. These curves are also represented by truncated Fourier series. Table 6.6 lists the coefficients of the respective Fourier series. Table 6.2 shows the comparison of calculated and experimentally determined rotational barriers. The rotational barriers estimated by Chen et al. [1] are 3.306, 3.215, 3.167, 4.428, 4.338, 4.300 kcal/mol respectively. The rotational barrier of CH$_3$CHF$_2$ is also experimentally investigated by Villaman et al. using waveguide microwave Fourier transform spectrometer (MWFT)[13]. Their result is 3.32 kcal/mol. Our result, see column note c, Table 6.2, shows barriers 0.4 to 0.5 kcal/mol higher than Chen et al. and Villamanan et al.'s result. The rotational barrier for CH$_2$FCF$_3$, CHF$_2$CF$_3$ and CF$_3$CF$_3$ are also experimentally determined as 4.20 kcal/mol by Danti et al.[14], as 3.40 kcal/mol by Eltayeb et al.[15], as 3.67 kcal/mol by Gallaher et al.[16] respectively. Our result for CHF$_2$CF$_3$ is 0.4 kcal/mol higher, while

Table 6.2 Barriers for Internal Rotations and Zero-Point Vibrational Energies

Species[a]	MP2/6-31G**// HF/6-31G* (Hartree)	ZPVE (kcal/mol)	Rotational Barrier[b] (kcal/mol)	Rotational Barrier[c] torsion frequency in ZPVE (kcal/mol)	Other Studies (kcal/mol)
CH_3CH_2F S	-178.50873	45.897	0.000	0.000	
CH_3CH_2F E	-178.50247	45.645	4.049	3.700	3.306[d]
CH_2FCH_2F Sa	-277.51800	41.613	0.193	0.186	
CH_2FCH_2F Sg	-277.51828	41.601	0.000	0.000	
CH_2FCH_2F El	-277.51290	41.400	3.391	3.200	
CH_2FCH_2F Eh	-277.50559	41.570	8.126	7.935	
CH_3CHF_2 S	-277.54340	41.117	0.000	0.000	
CH_3CHF_2 E	-277.53697	40.857	4.130	3.800	3.215[d] 3.32[f] 2.88[j] 2.61[k]
CH_2FCHF_2 Sa	-376.54957	36.743	0.000	0.000	
CH_2FCHF_2 Sg	-376.54699	36.766	1.651	1.643	
CH_2FCHF_2 El	-376.54435	36.567	3.280	3.120	
CH_2FCHF_2 Eh	-376.54005	36.693	6.095	5.932	5.61[e]
CH_3CF_3 S	-376.58731	35.695	0.000	0.000	
CH_3CF_3 E	-376.58094	35.426	4.073	3.754	3.167[d]
CHF_2CHF_2 Sa	-475.57814	31.744	0.000	0.000	
CHF_2CHF_2 Sg	-475.57554	31.818	1.709	1.697	
CHF_2CHF_2 El	-475.57158	31.769	4.258	4.136	
CHF_2CHF_2 Eh	-475.56672	31.875	7.403	7.281	7.11[e]
CH_2FCF_3 S	-475.58999	31.295	0.000	0.000	
CH_2FCF_3 E	-475.58303	31.195	4.432	4.283	4.428[d] 4.20[g] 4.23[j] 3.73[k]
CHF_2CF_3 S	-574.61543	26.266	0.000	0.000	
CHF_2CF_3 E	-574.60942	26.296	3.899	3.796	4.338[d] 3.40[h] 4.04[j] 3.45[k]
CF_3CF_3 S	-673.65238	20.677	0.000	0.000	
CF_3CF_3 E	-673.64631	20.740	3.954	3.865	4.300[d] 3.67[i] 4.11[j] 3.62[k]

[a] S at the end of species stands for "staggered", E stands for "eclipsed",
Sa stands for "anti staggered", Sg stands for "gauche staggered"
El stands for "eclipsed low", whose energy barrier is lower than the other
eclipsed position, Eh stands for "eclipsed high", whose energy
barrier is higher than the other eclipsed position. See Figure 1 for definition
of geometric nomenclature.

[b] Rotational barriers are calculated as the difference in total energies plus
scaled (0.89) zero-point vibrational energies. The corresponding torsional
frequency is excluded in the calculation of ZPVE.

[c] Rotational barriers are calculated as the difference in total energies plus
scaled (0.89) zero-point vibrational energies, where the corresponding torsional
frequency is included in the ZPVE for comparison to other studies.

[d] reference [1]. [e] MP4/6-311G**//6-31G*[3]. [f] reference [13]. [g] reference [14]. [h] reference [15].
[i] reference [16]. [j] MP2/6-311++G(3df,3p)//MP2/6-31G(d,p) method. ZPVE is included[17].

[k] MP2/6-311++G(3df,3p)//MP2/6-31G(d,p) method. ZPVE and thermal correction are included[17].

CH$_2$FCF$_3$ and CF$_3$CF$_3$ are in good agreement with the experimental results. Parra et al. recently reported rotational barrier heights of CH$_3$CHF$_2$, CH$_2$FCF$_3$, CHF$_2$CF$_3$ and CF$_3$CF$_3$ including ZPVE's and thermal corrections, using B3LYP and MP2 calculation methods with various basis sets[17]. Torsion modes were considered as harmonic oscillators in their report[17]. The values shown in Table 6.2 are MP2/6-4311++G(3df,3p) single point calculations with optimized geometry of MP2/6-31G(d,p). The comparison of rotational barriers with and without thermal correction for CH$_2$FCF$_3$, CHF$_2$CF$_3$ and CF$_3$CF$_3$ shows that thermal corrections decrease the barrier height by the factor of 0.5 cal/mol-K. The differences between this study and their results are within 0.2 cal/mol-K, except CH$_3$CHF$_2$, which has a 1.25 cal/mol-K higher value in this analysis.

Figure 6.3 shows the rotational barrier diagram for CH$_2$FCH$_2$F. The barriers at MP2/6-31G* level are 8.13 and 3.39 kcal/mol, which are the highest rotational barrier among nine fluorinated hydrocarbons. The calculation also shows that the gauche conformer is more stable than the anti conformer by 0.193 kcal/mol. An earlier report[18], using MP2/6-31G** basis set, also indicated that gauche conformer is 0.15 kcal/mol lower than anti conformer, 6-311++G* level calculation resulted in similar difference of 0.197 kcal/mol [19].

Figure 6.4 shows the rotational barrier diagrams for CH$_2$FCHF$_2$. The barriers are determined to be 6.09 and 3.28 kcal/mol, where Chen et al. estimated as 5.61 and 2.80 kcal/mol respectively using MP4/6-311G**//6-31G*[3]. Our estimation result is approximately 0.5 kcal/mol higher than Chen et al.'s. Figure 6.5 shows the rotational barrier diagrams for CHF$_2$CHF$_2$. The barriers are determined to be 7.40 and 4.26
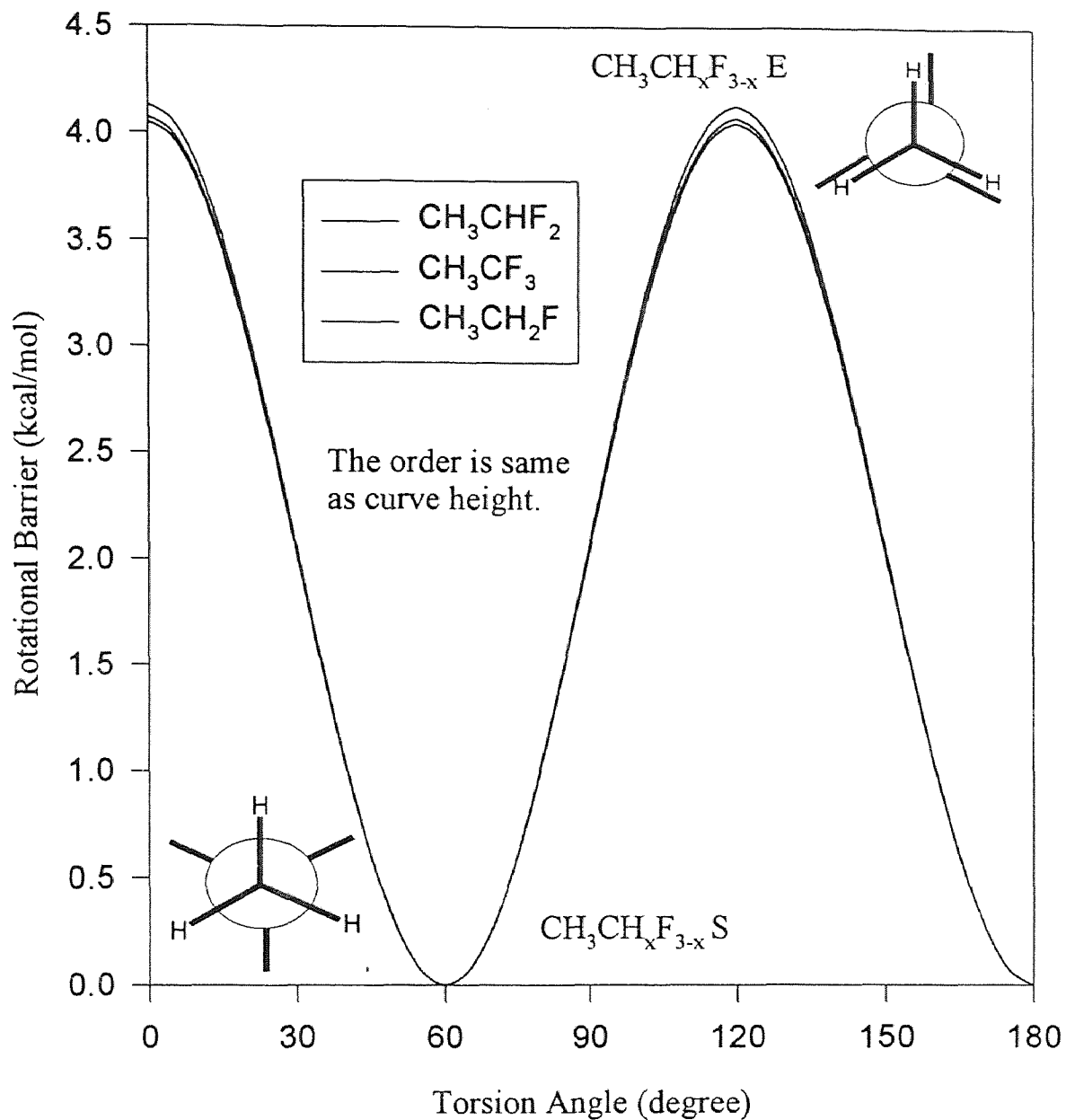
Figure 6.1 Potential Barriers for Internal Rotations about C-C bonds of CH_3CH_2F, CH_3CHF_2, and CH_3CF_3
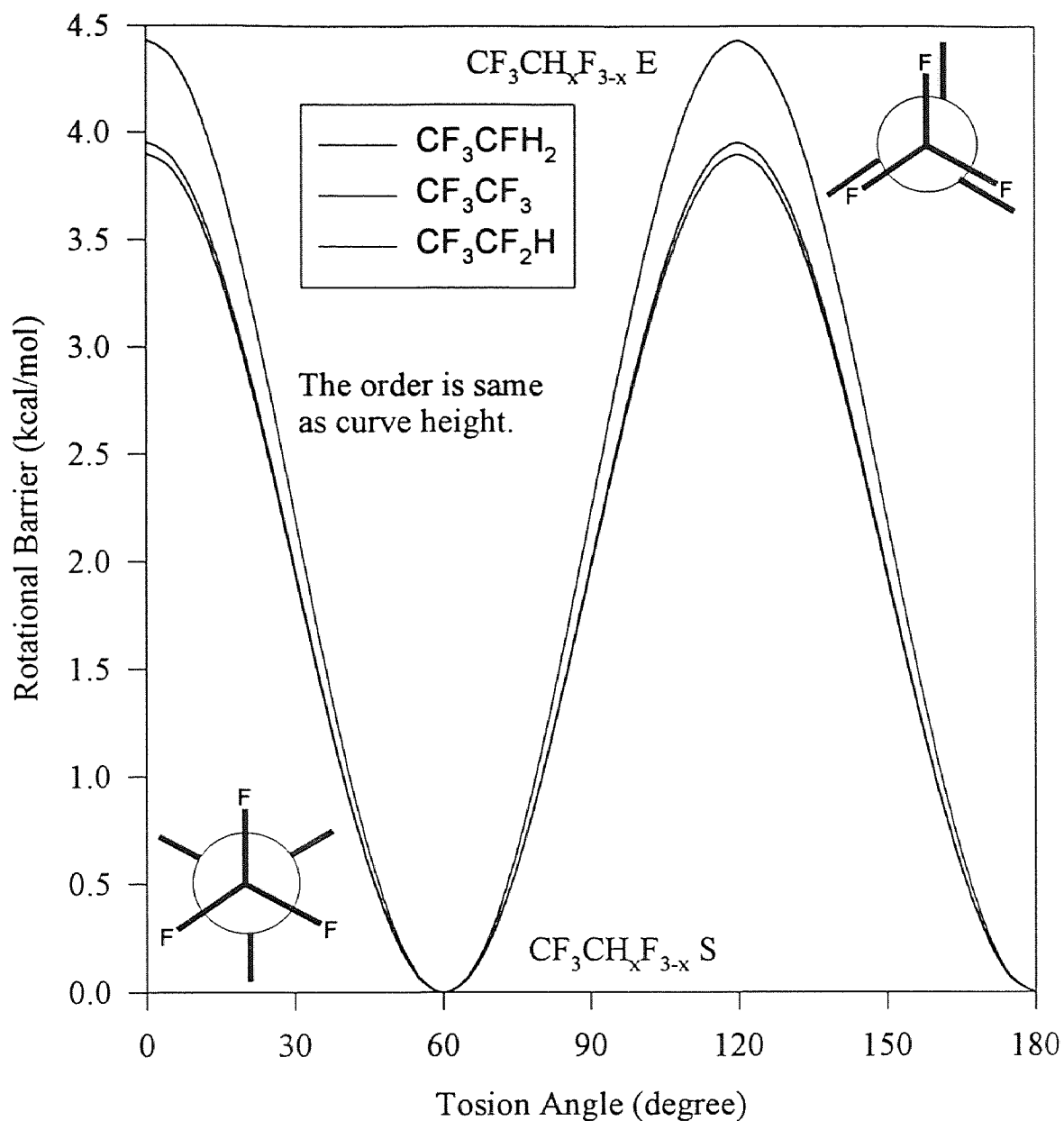
Figure 6.2 Potential Barriers for Internal Rotations about C-C bonds of CF_3CH_2F, CF_3CHF_2, and CF_3CF_3
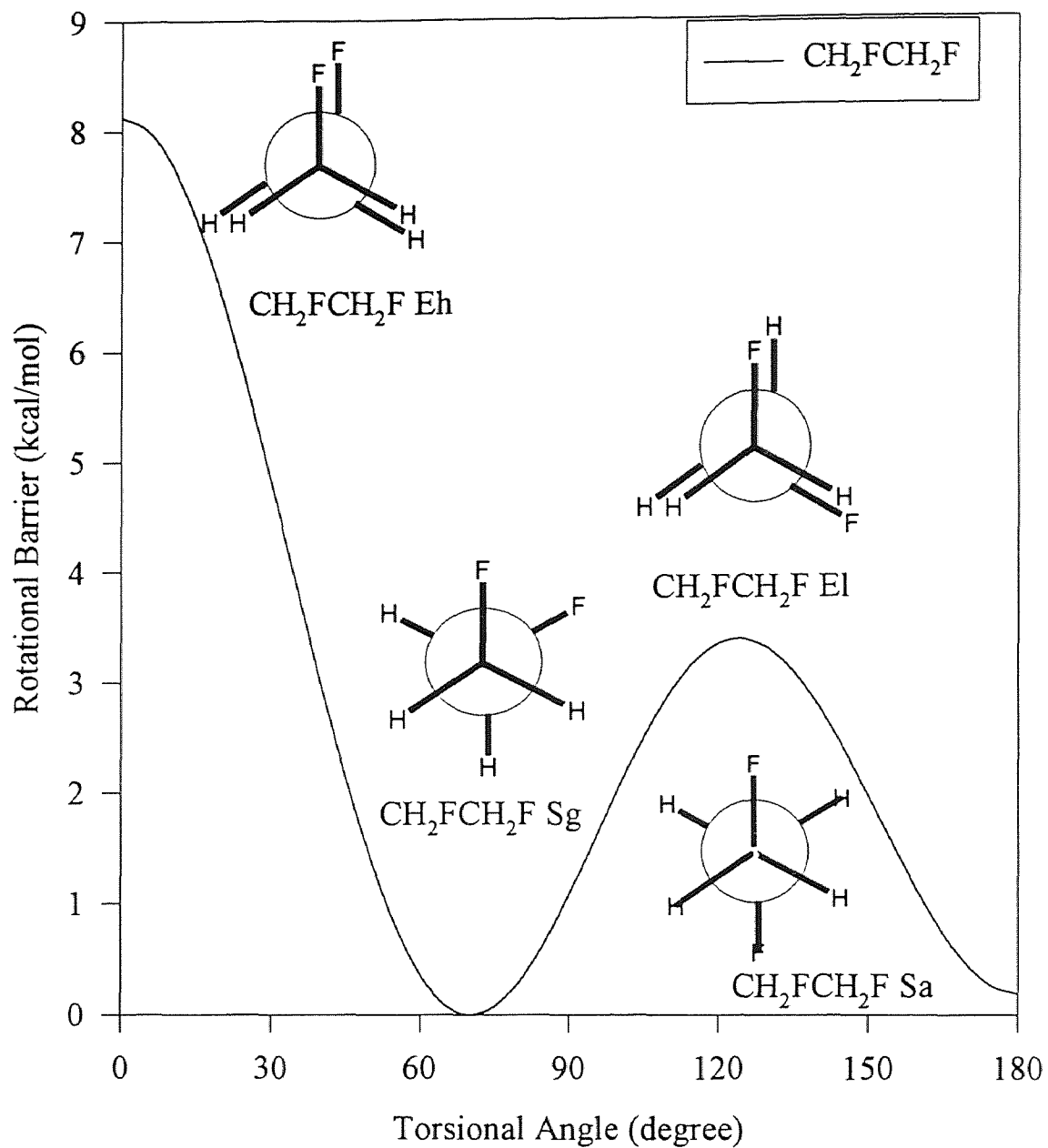
Figure 6.3 Potential Barriers for Internal Rotations about C-C bonds of CH_2FCH_2F
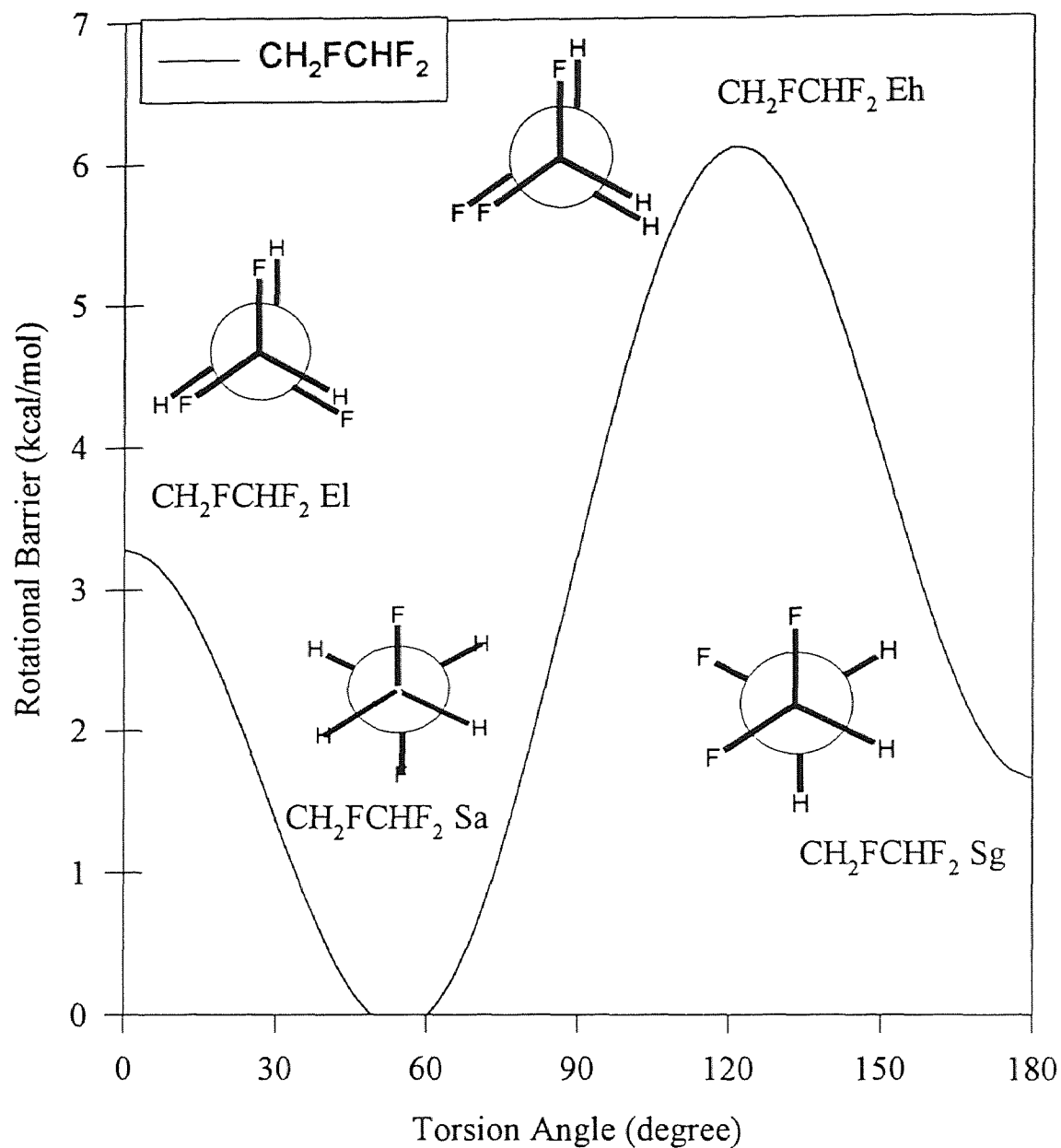
Figure 6.4 Potential Barriers for Internal Rotations about C-C bonds of CH$_2$FCHF$_2$
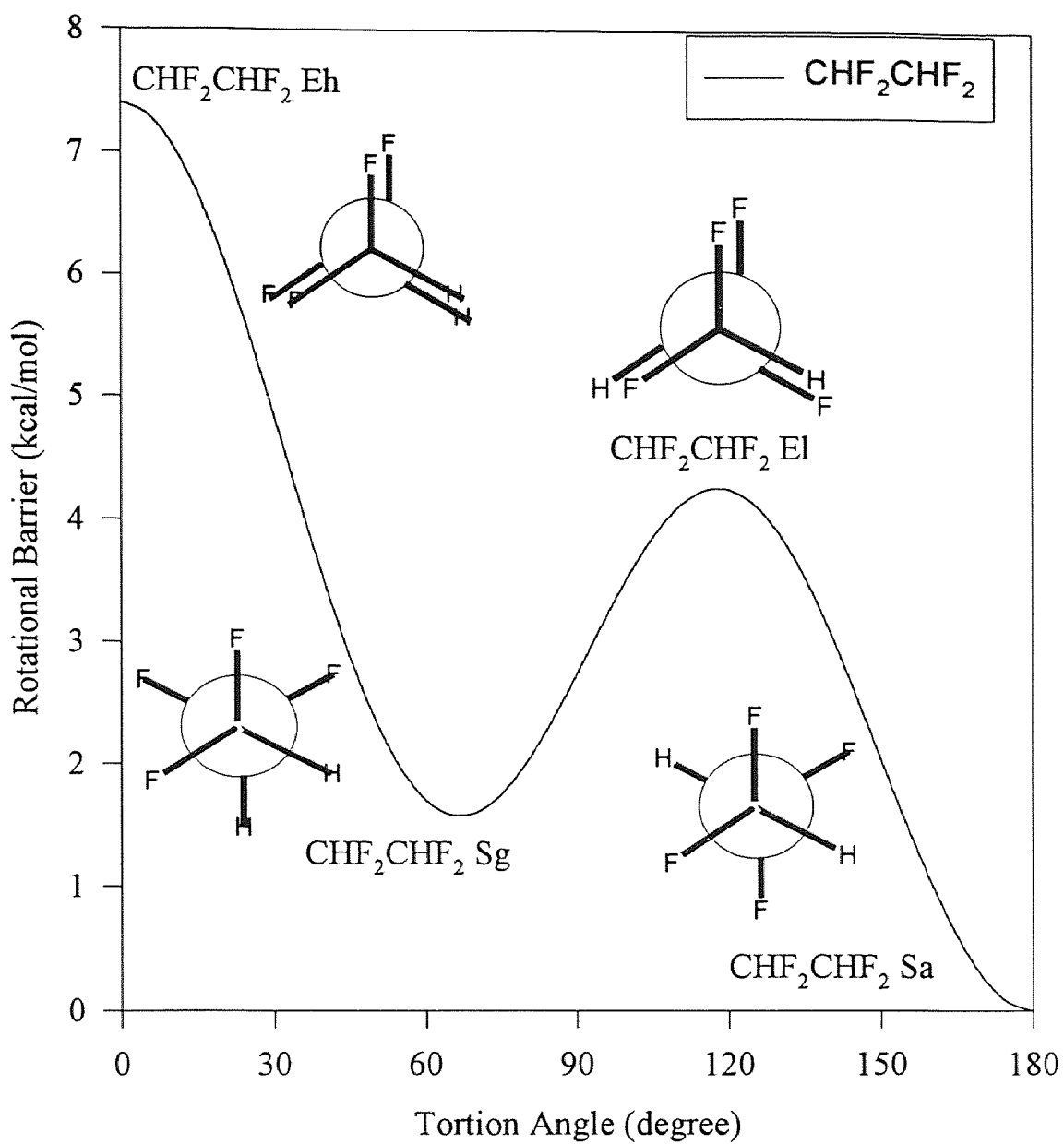
**Figure 6.5 Potential Barriers for Internal Rotations
about C-C bonds of CHF₂CHF₂**

Table 6.3 Rotational Constants[a]

Species	Ia	Ib	Ic
CH_3CH_2F	36.752	9.534	8.351
CH_2FCH_2F	17.520	5.176	4.505
CH_3CHF_2	9.720	9.096	5.271
CH_2FCHF_2	9.335	3.725	2.875
CH_3CF_3	5.641	5.286	5.286
CHF_2CHF_2	5.253	3.222	2.115
CH_2FCF_3	5.492	2.866	2.826
CHF_2CF_3	3.782	2.481	2.055
CF_3CF_3	2.913	1.894	1.894

[a] Unit in GHz

kcal/mol, where Chen et al. estimated 7.11 and 3.90 kcal/mol respectively using MP4/6-311G**//6-31G*[3]. Our estimation is approximately 0.3 kcal/mol higher than Chen et al.

6.3.2 Entropy ($S°_{298}$)

Table 6.4 lists the calculation results and comparisons with previous *ab initio* calculations and experimental data. The calculation at the MP2/6-31G*//HF/6-31G* level gives good agreement for $S°_{298}$ of CH_3CH_2F, CH_3CHF_2 and CH_3CF_3 with experimentally determined data [20] and the literature study [1]. The value for CH_2FCH_2F is 0.67 cal/mol K higher than suggested value by Burgess et al. [8]. Their estimations are based on vibrational frequencies and moments of inertia from their *ab initio* calculations. The value for CH_2FCHF_2 shows good agreement with the suggested value by Burgess et al. [8], but overestimates by 0.60 cal/mol K the value from MP4/6-31G** level *ab initio* calculation [3]. Our $S°_{298}$ for CHF_2CHF_2 has a slightly larger difference, 1.16 cal/mol higher, than Burgess et al.'s reported value [8]. We are 0.60 cal/mol-K above the MP4/6-31G** level *ab initio* calculation [3]. Burgess et al. only indicate that standard state $S°_{298}$ and $C_p(T)$

were computed based on vibrational frequencies and moments of inertia from their *ab initio* calculations. We do not know if they made any attempt to incorporate a contribution for internal rotation. Our values for CH_2FCF_3, CHF_2CF_3 and CF_3CF_3 are higher by 0.64, 0.45 and 0.55 cal/mol K respectively compared to the values from the literature estimation [1]. Ideal gas thermodynamic functions $S°_{298}$ and $C_p(T)$ in the temperature range 0 - 1500 K and 1 atm pressure are calculated in Chen et al.'s work[3], by

Table 6.4 Ideal Gas Phase Thermodynamic Properties[a]

Species and Symmetry #		$H_f°_{298}$	$S°_{298}$ [b]	C_{p300} [b]	C_{p400}	C_{p500}	C_{p600}	C_{p800}	C_{p1000}	C_{p1500}
CH_3CH_2F	TVR [c]		61.432	12.203	15.500	18.715	21.565	26.157	29.575	34.784
(3)	Internal Rotor [d]		3.976	2.022	2.190	2.202	2.126	1.898	1.690	1.372
	Total		63.225[e]	14.225	17.690	20.917	23.691	28.055	31.265	36.156
	Stull et. al.[f]	-62.50	63.22	14.17	17.57	20.12	23.44	27.76	30.98	
	Chen et. al.[g]	-62.90	63.34	14.28	17.71	20.86	23.56	27.82	31.00	35.9
CH_2FCH_2F	TVR		65.365	13.614	17.183	20.532	23.403	27.845	31.017	35.689
(2)	Internal Rotor		5.565	2.257	2.266	2.194	2.094	1.899	1.743	1.482
	Total		69.553	15.871	19.449	22.726	25.497	29.744	32.760	37.171
	Zachariah et. al.[h] & Burgess et. al.[i]	-103.70	68.88	16.22		22.74		29.71	33.03	37.12
CH_3CHF_2	TVR		65.528	14.344	17.873	21.106	23.865	28.141	31.214	35.774
(3)	Internal Rotor		3.993	2.021	2.193	2.212	2.142	1.918	1.709	1.386
	Total		67.338	16.365	20.066	23.318	26.007	30.059	32.923	37.160
	Stull et. al.[f]	-118.00	67.52	16.31	19.93	23.07	25.68	29.69	32.56	
	Chen et. al.[g]	-119.70	67.50	16.31	19.93	23.08	25.70	29.70	32.57	36.9
CH_2FCHF_2	TVR		69.316	15.889	19.600	22.925	25.691	29.813	32.644	36.674
(1)	Internal Rotor		5.182	2.628	2.730	2.687	2.575	2.296	2.037	1.588
	Total		74.498	18.517	22.330	25.612	28.266	32.109	34.681	38.262
	Lacher et. al.[j] & Burgess et. al.[i]	-158.89	74.50	18.00		25.70		31.90	34.40	38.22
	Chen, Paddison,& Tschuikow-Roux[k]	-156.80	73.90	18.49	22.33	25.59	28.22	32.01	34.56	38.18
CH_3CF_3	TVR		68.932	16.905	20.695	23.901	26.513	30.384	33.053	36.882
(9)	Internal Rotor		4.022	2.032	2.198	2.210	2.134	1.906	1.697	1.377
	Total		68.589	18.937	22.893	26.111	28.647	32.290	34.750	38.259
	Stull et. al.[f]	-178.20	68.66	18.83	22.75	25.90	28.38	31.98	34.45	
	Chen et. al.[g]	-178.20	68.67	18.84	22.75	25.90	28.38	31.98	34.44	38.0

Table 6.4 Ideal Gas Phase Thermodynamic Properties[a] (cont'd)

Species and Symmetry #		Hf°298	S°298[b]	Cp300[b]	Cp400	Cp500	Cp600	Cp800	Cp1000	Cp1500
CHF2CHF2	TVR		72.809	18.190	22.032	25.330	27.992	31.804	34.300	37.689
(2)	Internal Rotor		4.963	3.783	3.642	3.284	2.924	2.372	2.012	1.535
	Total		76.395	21.973	25.674	28.614	30.916	34.176	36.312	39.224
	Zachariah et. al.[h] & Burgess et. al.[i]	-211.10	75.24	20.37		27.55		33.76	35.99	39.03
	Chen, Paddison,& Tschuikow-Roux[k]	-209.10	75.80	22.21	25.97	28.82	31.03	34.18	36.27	39.15
CH2FCF3	TVR		72.522	18.440	22.382	25.672	28.294	32.027	34.469	37.784
(3)	Internal Rotor		5.885	2.208	2.313	2.321	2.252	2.024	1.800	1.413
	Total		76.224	20.648	24.695	27.993	30.546	34.051	36.269	39.197
	Chen et. al.[g]	-214.10	75.58	20.70	24.90	28.23	30.76	34.20	36.36	39.3
CHF2CF3	TVR		75.957	20.747	24.794	28.048	30.566	33.998	36.115	38.799
(3)	Internal Rotor		6.436	2.267	2.332	2.284	2.169	1.902	1.679	1.335
	Total		80.210	23.014	27.126	30.332	32.735	35.900	37.794	40.134
	Chen et.al.[g]	-264.00	79.76	22.97	27.20	30.50	32.94	36.12	37.98	40.3
CF3CF3	TVR		79.026	23.472	27.673	30.849	33.203	36.235	37.960	39.926
(18)	Internal Rotor		6.602	2.266	2.334	2.291	2.181	1.915	1.688	1.308
	Total		79.885	25.738	30.007	33.140	35.384	38.150	39.648	41.234
	Stull et.al.[f]	-321.00	79.37	25.53	29.99	33.26	35.54	38.32	39.78	
	Chen et.al.[g]	-320.90	79.30	25.520	30.010	33.290	35.600	38.400	39.870	41.4

[a] Thermodynamic properties are referred to a standard state of an ideal gas of pure enantiometer at 1 atm. One torsional frequency is excluded in the calculations of entropies and heat capacities. Instead, an exact contribution from hindered rotations about the C-C is included. See text. [b] Units in cal/mol-K. [c] The sum of contributions from translations, external rotations and vibrations. [d] Contribution from internal rotation about C-C bond. [e] Symmetry number is taken into account (-R x ln (number of symmetry)) [f] reference [20]. [g] reference [1]. [h] reference [2]. [i] reference [8]. [j] reference [9]. [k] reference [3]. standard methods of statistical thermodynamics on the basis of the rigid rotor-harmonic oscillator model. The reduced moments of inertia, I_r, for internal rotation of unsymmetrical groups are calculated on the basis of the formulation of Pitzer [21].

6.3.3 Heat Capacities (Cp(T)'s 300≤T/K≤1500)

Table 6.4 also lists the $C_p(T)$ calculation results and comparisons with previous *ab initio* calculations and experimental data. Overall the calculation results are in good agreement with the experimental data for $C_p(T)$ and other *ab initio* calculations. The trends are similar to those for $S°_{298}$; we estimate slightly higher values relative to the suggested

values by Burgess et. al [8] for CHF_2CHF_2, but have good agreement with *ab initio*
calculations of Chen et al. [3].

Table 6.7 lists the torsion frequencies of nine fluoroethanes and compares the
torsion contribution to $S°_{298}$ using the scaled torsion frequencies[11] versus our rigid-rotor-
harmonic-oscillator approximation. The contribution from a torsion frequency calculation
is about 2 cal/mol-K lower in each case, with one exception CHF_2CHF_2 which is only
1.195 cal/mol-K lower. A comparison for heat capacity at 300 K is shown in Table 6.8.
The $C_p(300 K)$ contribution is approximately 0.2 to 0.3 cal/mol-K lower in the torsion
calculation. The $C_p(300 K)$ difference for CHF_2CHF_2 is more significant (1.823 cal/mol-
K).

**Table 6.5 Comparison of Heats of Formation by
G2(MP2)[BAC][a] with Previous Study[b]**

Compounds	G2(MP2)[BAC]	Previous Study
CH_3CH_2F	-64.5	-62.9[c]
CH_2FCH_2F	-105.9	-103.7[d]
CH_3CHF_2	-119.3	-119.7[c]
CH_2FCHF_2	-158.5	-158.9[d]
CH_3CF_3	-178.5	-178.2[c]
CHF_2CHF_2	-209.1	-211.1[d]
CH_2FCF_3	-215.6	-214.1[c]
CHF_2CF_3	-264.3	-264.0[c]
CF_3CF_3	-319.2	-320.9[c]

[a] reference [4]. [b] Unit in kcal/mol.
[b] reference [1]. [c] reference [8]

Table 6.6 Coefficients of Truncated Fourier Series Representation Expansions for Internal Rotation Potentials[a]

Rotors	a_0	a_1	a_2	a_3
CH_3-CH_2F	2.025			2.025
CH_2F-CH_2F	2.622	1.648	1.537	2.319
CH_3-CHF_2	4.130			4.130
CH_2F-CHF_2	2.854	-1.488	-0.387	2.304
CH_3-CF_3	2.037			2.037
CHF_2-CHF_2	3.223	1.618	0.4787	2.083
CH_2F-CF_3	2.216			2.216
CHF_2-CF_3	1.900			1.900
CF_3-CF_3	1.977			1.977

Values of rotational barriers computed at the HF/6-31G*//MP2/6-31G* level of theory are used to calculate the coefficients. Equation (1) and (2) in text. See text. [a] Unit in kcal/mol

Table 6.7 Torsion Frequencies and Comparison of Their Contribution for Entropies $S°_{298}$ Using Torsion Frequencies and Rigid-Rotor-Harmonic-Oscillator Approximation

Species	Torsion Frequency (cm^{-1})	$S°_{298}$ from Torsion Frequency (cal/mol-K)	$S°_{298}$ from Rigid-rotor-harmonic-oscillator approximation (This Study) (cal/mol-K)
CH_3CH_2F	274.4	1.772	3.976
CH_2FCH_2F	150.0	2.895	5.565
CH_3CHF_2	258.1	1.881	3.993
CH_2FCHF_2	127.9	3.202	5.182
CH_3CF_3	251.4	1.929	4.022
CHF_2CHF_2	95.68	3.768	4.963
CH_2FCF_3	117.4	3.369	5.885
CF_2HCF_3	80.85	4.099	6.436
CF_3CF_3	69.83	4.388	6.602

Table 6.8 Torsion Frequencies and Comparison of Their Contribution for Heat Capacities C_{p300} Using Torsion Frequencies and Rigid-Rotor-Harmonic-Oscillator Approximation

Species	Torsion Frequency (cm-1)	C_{p300} from Torsion Frequency (cal/mol/K)	C_{p300} from Rigid-rotor-harmonic-oscillator approximation (This Study) (cal/mol/K)
CH_3CH_2F	274.4	1.775	2.022
CH_2FCH_2F	150.0	1.921	2.257
CH_3CHF_2	258.1	1.798	2.021
CH_2FCHF_2	127.9	1.938	2.628
CH_3CF_3	251.4	1.807	2.032
CHF_2CHF_2	95.68	1.96	3.783
CH_2FCF_3	117.4	1.946	2.208
CF_2HCF_3	80.85	1.967	2.267
CF_3CF_3	69.83	1.972	2.266

6.3.4 Group Additivity Values

Thermodynamic properties of fluorinated hydrocarbon groups are listed in Table 6.9.

Enthalpies of formations of CH_3CH_2F, CH_3CHF_2, CH_3CF_3, CH_2FCF_3, CHF_2CF_3, CF_3CF_3

are adopted from the literature study [1], values for CH_2FCH_2F is adopted from BAC-MP4

ab initio calculations [2,8], and averages between the values of Lacher et al.[9] and those of

Chen et al.[3] are adopted for $\Delta H_f{}^{\circ}{}_{298}$ of CH_2FCHF_2 and CHF_2CHF_2. Values for the $S^{\circ}{}_{298}$

and $C_p(T)$ are from this work. The enthalpies of formations of the *ab initio* / bond

additivity correction study of Berry et al. [4] is also listed for comparison [4]. The

G2(MP2)[BAC] method is chosen among his several calculation methods, G2[BAC],

CBS-4 and CBS-Q. The G2(MP2)[BAC] calculations of Berry et al. give enthalpies of

formation that are consistently lower by 1 to 2 kcal/mol than the recommended values of

Chen et al.[1] and Burgess et al.[8]. Table 6.5 shows the comparison of $\Delta H_f{}^{\circ}{}_{298}$ values for

all nine species.

The group values for $\Delta H_f{}^{\circ}{}_{298}$ and $S^{\circ}{}_{298}$ of C/C/H3 is taken from existing literature

value [7] and is -10.0 Kcal/mol and 30.41 cal/mol-K respectively. Group values for

enthalpy of formation are -52.9, -109.7 and -168.2 kcal/mol for C/C/F/H2, C/C/F2/H and

C/C/F3 respectively. Group values for $S^{\circ}{}_{298}$ are 35.00 39.11 and 42.55 cal/mol-K

respectively. These numbers are derived from thermodynamic properties of fluoroethane

(CH_2FCH_3); 1,1-difluoroethane (CHF_2CH_3); 1,1,1-trifluoroethane (CF_3CH_3) and those of

C/C/H3 group [7]. The $\Delta H_f{}^{\circ}{}_{298}$ decrease and the $S^{\circ}{}_{298}$ increase with increased number of

fluorines.

Table 6.9 Thermodynamic Properties of Fluorine Groups and Their Corrections

Groups	$H_{f\,298}^{\circ}$ [a]	S_{298}° [b]	C_{p300} [b]	C_{p400}	C_{p500}	C_{p600}	C_{p800}	C_{p1000}	C_{p1500}
C/C/H3[c]	-10.0	30.41	6.19	7.84	9.4	10.79	13.02	14.77	17.58
C/C/F/H2	-52.9	35.00	8.04	9.85	11.52	12.9	15.04	16.5	18.58
C/C/F2/H	-109.7	39.11	10.18	12.23	13.92	15.22	17.04	18.15	19.58
C/C/F3	-168.2	42.55	12.75	15.05	16.71	17.86	19.27	19.98	20.68
Correction	$H_{f\,298}^{\circ}$ [a]	S_{298}° [b]	C_{p300} [b]	C_{p400}	C_{p500}	C_{p600}	C_{p800}	C_{p1000}	C_{p1500}
F/F	2.1	0.92	-0.21	-0.25	-0.31	-0.3	-0.34	-0.24	0.01
F/2F	4.8	0.38	0.3	0.25	0.17	0.15	0.03	0.03	0.1
F/3F	7.0	0.85	-0.14	-0.2	-0.24	-0.21	-0.26	-0.21	-0.06
2F/2F	9.3	-0.45	1.61	1.21	0.77	0.48	0.09	0.01	0.06
2F/3F	13.9	0.73	0.08	-0.15	-0.3	-0.34	-0.41	-0.34	-0.13
3F/3F	15.5	0.54	0.24	-0.09	-0.28	-0.34	-0.39	-0.31	-0.13

[a] Units in kcal/mol. [b] Units in cal/mol-K. [c] reference [7].

6.3.5 Interaction Terms

Interaction term values are also listed in Table 6.9. The group additivity corrections for

enthalpy are: 2.1, 4.8, 7.0, 9.3, 13.9 and 15.5 kcal/mol for F/F, F/2F, F/3F, 2F/2F, 2F/3F

and 3F/3F respectively. Interaction values for S_{298}° and $C_p(T)$ are small and less

significant. These values are calculated by the defined fluorinated hydrocarbon group

values and thermodynamic properties of the parent compounds. The correction values

for enthalpies of formation increase as the number of fluorine atoms increase. It is

important to note that the interaction terms for $\Delta H_{f\,298}^{\circ}$ and S_{298}° between F/3F and 2F/2F

are different, even though the interaction is between same number of fluorines. These

two molecules also have the same number of F/F gauche interactions in the most stable

configurations of the two isomers. The F/3F and 2F/2F interaction terms for enthalpy of

formation correction are 7.0 kcal/mol and 9.3 kcal/mol respectively. The S_{298}° correction

terms are 0.85 and -0.45 cal/mol-K respectively. Table 6.10 shows groups and

interaction terms which are necessary to obtain the thermodynamic properties using this

modified group additivity method reported in this chapter.

Table 6.10 Composition of Groups and Interaction Terms for 9 Fluoroethanes

Compounds	CH_3CH_2F	CH_2FCH_2F	CH_3CHF_2	CH_2FCHF_2	CH_3CF_3	CHF_2CHF_2	CH_2FCF_3	CHF_2CF_3	CF_3CF_3
Group 1	C/C/H3	C/C/F/H2	C/C/H3	C/C/F/H2	C/C/H3	C/C/F2/H	C/C/F/H2	C/C/F2/H	C/C/F3
Group2	C/C/F/H2	C/C/F/H2	C/C/F2/H	C/C/F2/H	C/C/F3	C/C/F2/H	C/C/F3	C/C/F3	C/C/F3
Interaction	----	F-F	----	F-2F	----	2F-2F	F-3F	2F-3F	3F-3F

6.4 Summary

Ab initio calculations are performed on nine fluorinated hydrocarbons using the Gaussian 94[10] system of programs at the RHF/6 -31G* and MP2/6-31G* levels of theory.

Thermodynamic properties ($\Delta H_f^\circ{}_{298}$, $S^\circ{}_{298}$ and $C_p(T)$, $300 \leq T/K \leq 1500$) for group values of C/C/F/H2, C/C/F2/H and C/C/F3 are defined and a set of interaction terms F/F, F/2F, F/3F, 2F/2F, 2F/3F and 3F/3F are derived for use with our proposed modified group additivity. The interactions between fluorines on adjacent carbons are strong with enthalpy corrections : 2.1, 4.8, 7.0, 9.3, 13.9 and 15.5 kcal/mol for F/F, F2F, F/3F, 2F/2F, 2F/3F and 3F/3F respectively.

Results on $S^\circ{}_{298}$ at RHF/6-31G*//MP2/6-31G* level of calculation with direct integration over energy levels of the exact potential energy curve of the rotational barriers show slightly higher values for most HFCs in this study compared with previously determined thermodynamic properties and different level *ab initio* calculations[1,2,3,20]. Values of group additivity correction terms increase significantly with an increased number of adjacent fluorines for the enthalpies of formation. Small group additivity corrections are needed for $S^\circ{}_{298}$ and $C_p(T)$.

CHAPTER 7

THERMODYNAMIC PROPERTIES
($\Delta H_F^\circ{}_{298}$, $S^\circ{}_{298}$ AND $C_P(T)$'S $300 \leq T/K \leq 1500$)
OF FLUORINATED PROPANES

7.1 Introduction

Thermodynamic properties ($\Delta H_f^\circ{}_{298}$, $S^\circ{}_{298}$ and $C_p(T)$'s ($300 \leq T/K \leq 1500$)) plus

frequencies, geometries and internal rotational barriers for eight fluorinated propane

compounds, 1-fluoropropane, 1,1- and 1,2-difluoropropane, 1,1,1- and 1,1,2-

trifluoropropane, 1,1,1,2- and 1,1,2,2-tetrafluoropropane and 1,1,1,2,2-

pentafluoropropane are reported in this study.

A number of theoretical and experimental studies on thermodynamic properties

($\Delta H_f^\circ{}_{298}$, $S^\circ{}_{298}$ and $C_p(T)$'s $300 \leq T/K \leq 1500$), frequencies and internal rotational barrier

for fluorinated ethane compounds have been reported. However, literature data on the

estimation of thermodynamic properties for fluorinated propane compounds is limited to ;

1-fluoropropane, 2-fluoropropane and 2,2-difluoropropane[20,22].

7.2 Method

7.2.1. Enthalpies of Formation ($\Delta H_f^\circ{}_{298}$) Calculations

The $\Delta H_f^\circ{}_{298}$ are estimated using the G2MP2 composite calculation method and isodesmic

reactions. All *ab initio* calculations are performed using the Gaussian94[10] system of

programs. ZPVE's and thermal corrections to 298.15 K are obtained with scaled

frequencies, 0.8929, as widely used in theoretical thermochemical calculation[23] for

frequencies determined at the HF/6-31G(d) level of theory. The general formula of

isodesmic reaction to calculate $\Delta H_f^\circ{}_{298}$ of fluorinated propane is:

$$CH_{(3-x)}F_xCH_{(2-y)}F_yCH_{(3-z)}F_z + CH_3CH_3 \rightarrow CH_3CH_{(2-y)}F_yCH_3 + CH_{(3-x)}F_xCH_{(3-z)}F_z$$

$$----------(1)$$
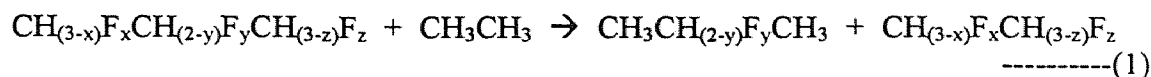
where

$0 \leq x, z \leq 3$

$0 \leq y \leq 2$

The method of isodesmic reactions relies upon the similarity of bonding

environment in the reactants and products that leads to cancellation of systematic errors

in the *ab initio* MO calculations[11]. The basic requirement of the isodesmic reaction is

bond type conservation, where the number of each formal chemical bond type is

conserved in the reaction. An isodesmic reaction will lead to more accurate results if

groups are conserved in the reaction scheme[24]. This results because interactions of next-

nearest-neighbor atoms in reactants and products are conserved in addition to bond types.

Since $\Delta H_f^\circ{}_{298}$ for CH_3CH_3, $CH_3CH_2CH_3$ and $CH_{(3-x)}F_xCH_{(3-z)}F_z$ are well

known[1,20,22], and those for CH_3CFHCH_3 and $CH_3CF_2CH_3$ are also reported[22], the

remaining compound, $CH_{(3-x)}F_xCH_{(2-y)}F_yCH_{(3-z)}F_z$, in reaction (1) can be accurately

estimated from the calculated $\Delta H^\circ{}_{rxn,298}$. For example, 1-fluoropropane is estimated by

the isodesmic reaction:

$$CH_2FCH_2CH_3 + CH_3CH_3 \rightarrow CH_3CH_2CH_3 + CH_2FCH_3 \qquad\qquad ----------(2)$$
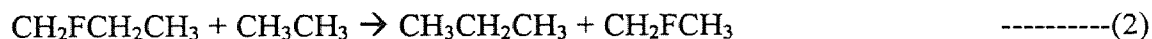
G2MP2 composite calculations are performed for all of four compounds in reaction (2), and enthalpy of reaction ($\Delta H_{f\ rxn,298}^{\circ}$) is calculated. The evaluated literature data for the $\Delta H_{f\ 298}^{\circ}$ are substituted for CH_3CH_3, $CH_3CH_2CH_3$ and CFH_2CH_3, then the $\Delta H_{f\ 298}^{\circ}$ of $CFH_2CH_2CH_3$ is calculated. Seven additional fluorinated propanes are calculated in the same manner. Isodesmic reaction (1) is suggested as a general isodesmic reaction scheme for estimation of fluorocarbons and other halocarbons.

7.2.2 Standard Entropy (S_{298}°) and Heat Capacities ($C_p(T)$'s, $300 \leq T/K \leq 1500$) and Hindered Rotation Contribution to Thermodynamic Parameters

Harmonic vibrational frequencies calculated at the HF6-31G(d) level of theory and the moments of inertia from molecular structures optimized at MP2/6-31G(d) are used to calculate the S_{298}° and $C_p(T)$'s.

Since a technique for the calculation of thermodynamic functions from hindered rotations with arbitrary potentials has been previously reported[24-26], only a summary of the method is described. The technique employs expansion of the hindrance potential in a Fourier series, calculation of the Hamiltonian matrix in the basis of the wave functions of free internal rotation and subsequent calculation of energy levels by direct diagonalization of the Hamiltonian matrix. The torsional potential calculated at discrete torsional angles is represented by a truncated Fourier series. All potential curves of rotational barrier vs. dihedral angle are fit by a truncated Fourier series:

$$V(\emptyset) = a_0 + a_1\cos(\emptyset) + a_2\cos(2\emptyset) + a_3\cos(3\emptyset) + b_1\sin(\emptyset) + b_2\sin(2\emptyset) + b_3\sin(3\emptyset) \qquad (3)$$

where values of the coefficients a_i are calculated to provide the minimum and maxima of the torsional potentials with allowance of a shift of the theoretical extrema angular positions.

The Hamiltonian matrix is then truncated to the size of $2 K_{max} + 1$, where K_{max} is the maximum rotational quantum number considered. The truncated matrix (in reduced dimensionless form) is diagonalized, and the eigenvalues are used to calculate the partition function, entropy, heat capacity and etc. This is accomplished using direct summation over the calculated energy levels according to standard expressions of statistical thermodynamics[12].

7.3 Results and Discussion

7.3.1 Geometries

Figures 7.1 to 7.8 present MP2(full)/6-31G(d) determined geometries. Figure 7.1 presents a distance matrix as well as major bond lengths and the bond angles $\angle C_1$-C_2-C_3. The methyl-F gauche conformation consistently shows lower energy than anti staggered conformation. This is evaluated as F-H attractive interaction between fluorine connected to C_1 and hydrogen connected to C_3, but there is not strong evidence for it. The bond lengths between fluorine connected to C_1 and hydrogens connected to C_3 are 2.569, 3.295 and 3.883 Å.

The evaluated bond lengths for C_1-C_2 in 1-fluoropropane, 1,1-difluoropropane 1,1,1-trifluoropropane show that an increase in fluorine number at the C_1 carbon site causes a decrease in the C_1-C_2 bond length. The evaluation of the bond length for C_1-C_2 and C_2-C_3 in 2-fluoropropane and 2,2-difluoropropane also shows that an increase of
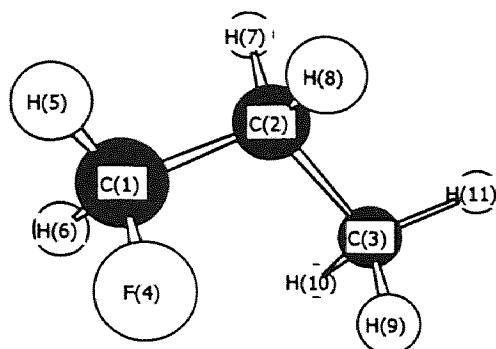
Distance Matrix

	C1	C2	C3	F4	H5	H6	H7	H8	H9	H10	H11
C1	0										
C2	1.512694	0									
C3	2.522071	1.525067	0								
F4	1.40246	2.378353	2.895505	0							
H5	1.094728	2.172676	3.483047	2.024092	0						
H6	1.095583	2.166498	2.781375	2.02326	1.783083	0					
H7	2.127947	1.096923	2.169753	3.312214	2.477985	2.501544	0				
H8	2.129557	1.095177	2.163015	2.634413	2.469521	3.055638	1.761658	0			
H9	2.763891	2.160288	1.091562	2.569485	3.769508	3.111343	3.073018	2.515453	0		
H10	2.794142	2.171006	1.094523	3.295208	3.804297	2.606271	2.519009	3.076045	1.769504	0	
H11	3.473644	2.17384	1.093004	3.883398	4.322807	3.790691	2.524472	2.502642	1.77189	1.769604	0

Major Bond Lengths and Angle

Bond	Length (Å)
$C_1 - C_2$	1.513
$C_2 - C_3$	1.525
$C_1 - F$	1.402
$C_1 - H$	1.095
$C_1 - H$	1.096
$C_2 - H$	1.097
$C_2 - H$	1.095
$C_3 - H$	1.092
$C_3 - H$	1.095
$C_3 - H$	1.093
Bond	Angle (degree)
$C_1 - C_2 - C_3$	112.2

Figure 7.1 1-Fluoropropane Geometry

fluorine number at the C_2 carbon site causes a decrease in the C_1-C_2 and C_2-C_3 bond

lengths. The C_1-C_2 and C_2-C_3 bond lengths in propane, 1-fluoropropane and
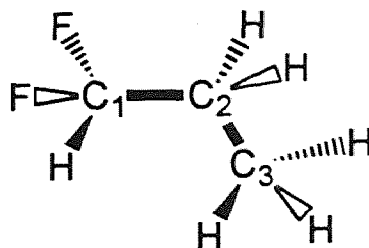
Major Bond Lengths and Angle

Bond	Length (Å)
$C_1 - C_2$	1.505
$C_2 - C_3$	1.525
$C_1 - F$	1.378
$C_1 - F$	1.378
$C_1 - H$	1.094
$C_2 - H$	1.095
$C_2 - H$	1.095
$C_3 - H$	1.092
$C_3 - H$	1.092
$C_3 - H$	1.092
Bond	Angle (degree)
$C_1 - C_2 - C_3$	112.2

Figure 7.2 1,1-Difluoropropane Geometry

2,2-difluoropropane are 1.528, 1.5156 and 1.5078 Å respectively, where the geometries

are not shown.   Figure 7.3, 7.7, 7.8 also support this observation and show the bond

length between C_2 and C_3 decreases with increase in number of fluorine(s) at C_2 where no

fluorine is on C_3. Figures 7.1 to 7.3 show that the number of fluorines connected to C_1

does not significantly affect to the bond length of C_2-C_3. On the other hand, the

interaction between the fluorine(s) on the C_1 with fluorine(s) and the methyl bonded to C

$_2$ causes an increase in the C_1-C_2 bond length.
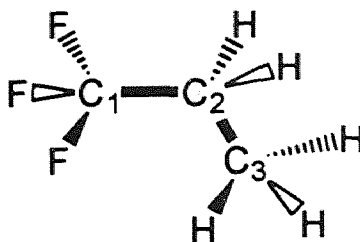
Major Bond Lengths and Angle

Bond	Length (Å)
$C_1 - C_2$	1.502
$C_2 - C_3$	1.525
$C_1 - F$	1.354
$C_1 - F$	1.356
$C_1 - F$	1.356
$C_2 - H$	1.093
$C_2 - H$	1.093
$C_3 - H$	1.092
$C_3 - H$	1.092
$C_3 - H$	1.092
Bond	Angle (degree)
$C_1 - C_2 - C_3$	112.4

Figure 7.3 1,1,1-Trifluoropropane Geometry

The bond length between carbon and fluorine decreases with increase in fluorine number on the same carbon. The bond lengths between C_1 and F are 1.402, 1.378 and 1.356 Å for 1-fluoropropane, 1,1-difluoropropane and 1,1,1-trifluoropropane respectively. All C-H bond lengths are more than 0.01 Å longer than normal C-H bond length in hydrocarbons.

The bond angle $\angle C_1-C_2-C_3$ is also listed in each figure. Interactions between the fluorines connected to different carbons show only slight affects on the bond angle $\angle C_1-C_2-C_3$. The interaction between the fluorines connected to same carbon also appears to have no significant effect on the $\angle C_1-C_2-C_3$ bond angle.
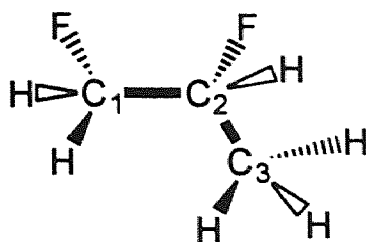
Major Bond Lengths and Angle

Bond	Length (Å)
$C_1 - C_2$	1.515
$C_2 - C_3$	1.509
$C_1 - F$	1.398
$C_1 - H$	1.093
$C_1 - H$	1.094
$C_2 - F$	1.406
$C_2 - H$	1.095
$C_3 - H$	1.092
$C_3 - H$	1.093
$C_3 - H$	1.092
Bond	Angle (degree)
$C_1 - C_2 - C_3$	113.3

Figure 7.4 1,2-Difluoropropane Geometry
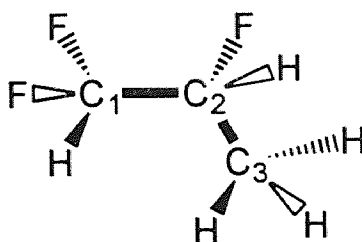
Major Bond Lengths and Angle

Bond	Length (Å)
$C_1 - C_2$	1.513
$C_2 - C_3$	1.509
$C_1 - F$	1.368
$C_1 - F$	1.374
$C_1 - H$	1.093
$C_2 - F$	1.401
$C_2 - H$	1.095
$C_3 - H$	1.092
$C_3 - H$	1.090
$C_3 - H$	1.091
Bond	Angle (degree)
$C_1 - C_2 - C_3$	113.2

Figure 7.5 1,1,2-Trifluoropropane Geometry
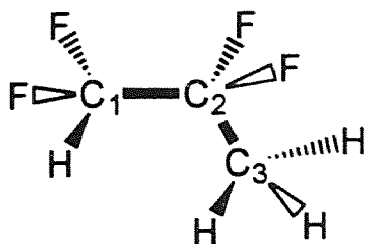
Major Bond Lengths and Angle

Bond	Length (Å)
$C_1 - C_2$	1.519
$C_2 - C_3$	1.499
$C_1 - F$	1.366
$C_1 - F$	1.366
$C_1 - H$	1.092
$C_2 - F$	1.375
$C_2 - F$	1.345
$C_3 - H$	1.091
$C_3 - H$	1.090
$C_3 - H$	1.090
Bond	Angle (degree)
$C_1 - C_2 - C_3$	115.5

Figure 7.6 1,1,2,2-Tetrafluoropropane Geometry
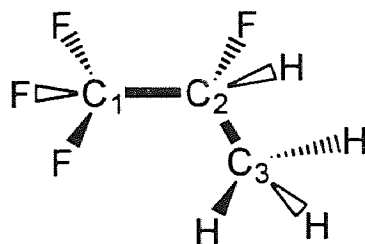
Major Bond Lengths and Angle

Bond	Length (Å)
$C_1 - C_2$	1.515
$C_2 - C_3$	1.509
$C_1 - F$	1.346
$C_1 - F$	1.348
$C_1 - F$	1.355
$C_2 - F$	1.394
$C_2 - H$	1.095
$C_3 - H$	1.092
$C_3 - H$	1.091
$C_3 - H$	1.091
Bond	Angle (degree)
$C_1 - C_2 - C_3$	112.9

Figure 7.7 1,1,1,2-Tetrafluoropropane Geometry
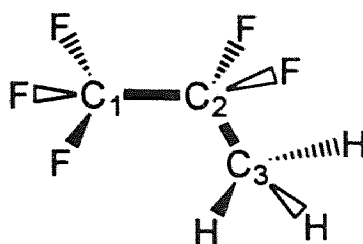
Major Bond Lengths and Angle	
Bond	Length (Å)
$C_1 - C_2$	1.528
$C_2 - C_3$	1.500
$C_1 - F$	1.348
$C_1 - F$	1.340
$C_1 - F$	1.348
$C_2 - F$	1.369
$C_2 - F$	1.369
$C_3 - H$	1.091
$C_3 - H$	1.090
$C_3 - H$	1.090
Bond	Angle (degree)
$C_1 - C_2 - C_3$	114.8

Figure 7.8 1,1,1,2,2-Pentafluoropropane Geometry

7.3.2 Frequencies

Table 7.1 lists the HF/6-31G(d) determined frequencies of fluorinated propane

compounds: 1-fluoropropane, 1,1-difluoropropane, 1,2-difluoropropane, 1,1,1-

trifluoropropane, 1,1,2-trifluoropropane, 1,1,2,2-tetrafluoropropane, 1,1,1,2-

tetrafluoropropane, 1,1,1,2,2-pentafluoropropane. The first two numbers in Table 7.1 are

torsional frequencies which are excluded from S°_{298} and $C_p(T)$ calculations. The first

number is the torsional frequency for C_1 and C_2. The interaction between fluorine(s)

connected to C_1 with fluorine(s) and C_3 connected to C_2 lowers the torsional frequencies.

The second number is the torsional frequency for C_2 and C_3. Since there is no fluorine -

fluorine or carbon - fluorine interaction between the C_2 and C_3 groups, the difference

from normal hydrocarbon torsion for the torsional frequencies for C_2 and C_3 is small.

Table 7.1 Vibrational Frequencies[a] (ν cm^{-1})

Species	CH$_2$FCH$_2$CH$_3$	CHF$_2$CH$_2$CH$_3$	CF$_3$CH$_2$CH$_3$	CH$_2$FCHFCH$_3$	CHF$_2$CHFCH$_3$	CHF$_2$CF$_2$CH$_3$	CF$_3$CFHCH$_3$	CF$_3$CF$_2$CH$_3$
ν1	152*	119*	111*	128*	94*	93*	84*	76*
ν2	243*	236*	234*	242*	237*	225*	230*	229*
ν3	337	271	244	274	262	249	244	235
ν4	518	414	395	409	276	263	269	248
ν5	838	541	444	475	418	389	364	360
ν6	932	738	583	527	492	389	448	383
ν7	1003	861	593	919	615	527	513	398
ν8	1070	928	676	1018	738	558	588	483
ν9	1181	1071	869	1061	917	594	629	551
ν10	1233	1132	880	1191	1054	703	731	644
ν11	1293	1209	1064	1233	1130	870	878	651
ν12	1395	1283	1160	1268	1247	1084	1012	689
ν13	1424	1289	1178	1297	1255	1097	1137	847
ν14	1520	1418	1350	1379	1264	1257	1235	1033
ν15	1567	1531	1350	1478	1322	1285	1273	1093
ν16	1582	1556	1426	1529	1483	1354	1342	1260
ν17	1626	1565	1471	1580	1522	1365	1388	1376
ν18	1642	1582	1558	1589	1560	1436	1463	1381
ν19	1653	1627	1576	1634	1580	1541	1512	1398
ν20	1677	1645	1629	1641	1595	1574	1575	1424
ν21	3201	1656	1644	1680	1635	1602	1587	1568
ν22	3207	3220	1657	3219	1649	1628	1636	1584
ν23	3233	3225	3225	3261	3232	1646	1648	1628
ν24	3244	3258	3245	3263	3271	3244	3234	1642
ν25	3266	3287	3282	3291	3303	3323	3288	3246
ν26	3286	3301	3292	3303	3318	3333	3309	3327
ν27	3290	3313	3304	3319	3335	3348	3318	3334

[a] Non-scaled. Frequencies are calculated at the HF/6-31G* level of theory.
* Torsional frequencies. These frequencies are not included in the calculation of entropies S$°_{298}$'s and heat capacities C$_p$(T)'s.

7.3.3 Enthalpies of Formation ($\Delta H_f°_{298}$)

G2MP2 determined total energies for the eight compounds and the $\Delta H_f°_{298}$ from the

literature are tabulated in Table 7.2 and 7.3 respectively. The $\Delta H_f°_{298,rxn}$ for (2) is

calculated using G2MP2 determined total energies.

$CH_3CH_2CH_3 + CFH_2CH_3 - (CFH_2CH_2CH_3 + CH_3CH_3) = -0.02$ kcal/mol

The $\Delta H_f^{\circ}{}_{298}$ of 1-fluoropropane is calculated using the known $\Delta H_f^{\circ}{}_{298}$ for ethane, propane and fluoroethane, with the calculated $\Delta H_f^{\circ}{}_{298,rxn}$. The calculation results in a value of -67.46 kcal/mol as shown in Table 7.7. Literature values[20,22] are also listed in Table 7.7. Our result is between and in good agreement with the literature values. The $\Delta H_f^{\circ}{}_{298}$ of the seven remaining compounds are calculated in the same manner and listed in Table 7.7.

7.3.4 Rotational Barriers

Barriers for internal rotations are calculated as the difference between the total energy of each conformation and that of the global equilibrium plus the scaled ZPVE difference (see Table 7.4). The curves are fit by a truncated Fourier series (3). Table 7.6 lists the coefficients of the respective Fourier series.

Figure 7.9 shows the calculated rotational barriers for 1-fluoropropane. Solid and broken lines in Figure 7.9 to 7.16 show rotational barriers for C_1-C_2 and C_2-C_3 respectively for the eight fluoro propanes. The C-F eclipsed conformation for C_1-C_2 in 1-fluoropropane has highest rotational barrier, which is 5.09 kcal/mol. The C-F gauche staggered conformation is more stable than C-F anti staggered conformation. Since this rotational barrier curve is symmetric with respect to zero torsion angle (F-C_1-C_2-C_3), it can be fit by a cosine series. The calculated rotational barrier for C_2-C_3 is 3.28 kcal/mol, and the rotational barrier curves of C_2-C_3 for all eight compounds can be fit by using only a_0 and a_3 in a truncated Fourier series.
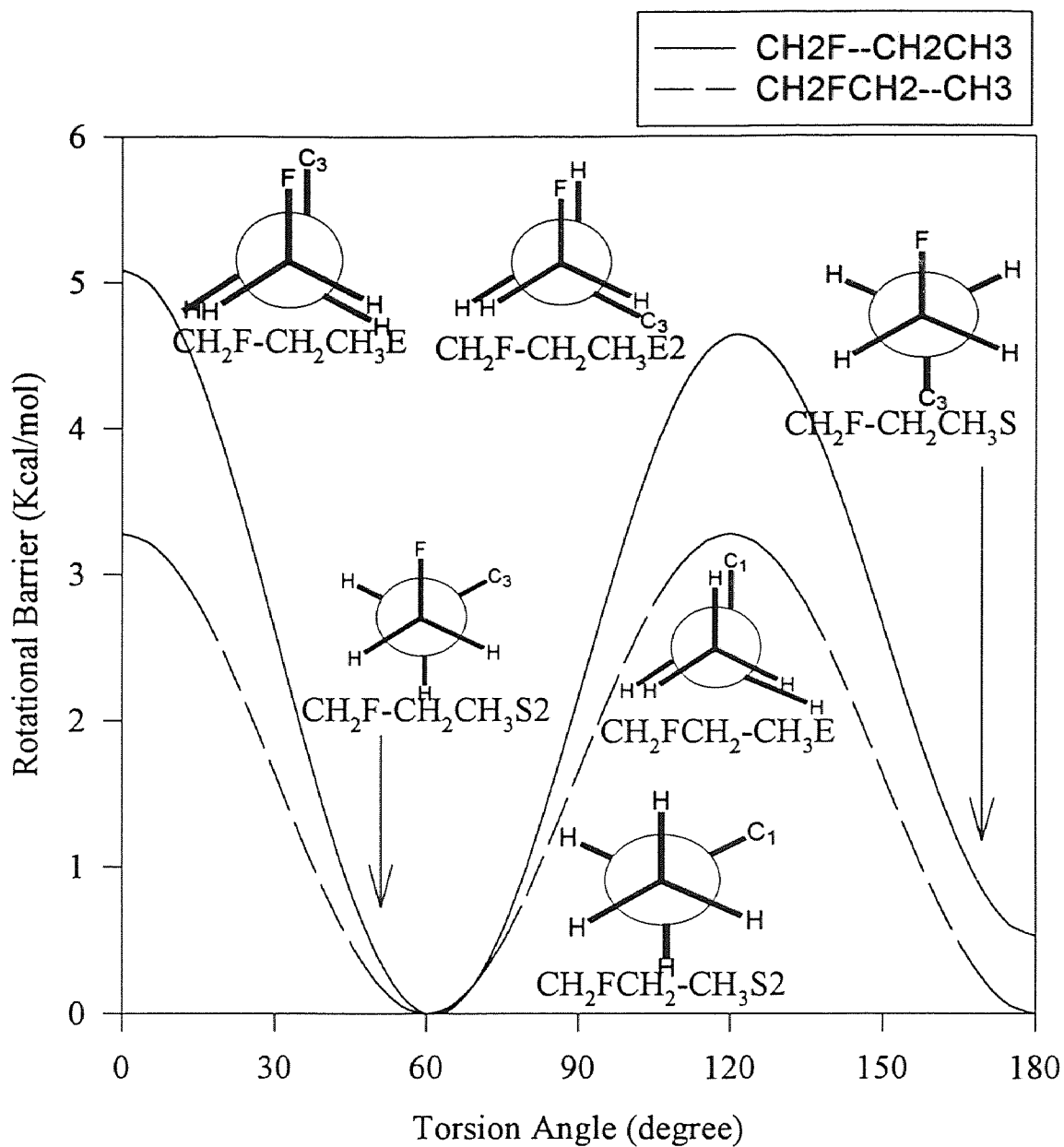
Figure 7.9 Potential Barriers for Internal Rotations about C1-C2 and C2-C3 bonds of CH$_2$F-CH$_2$-CH$_3$

Table 7.2 G2MP2 Total Energy

Species	Total Energy[a]
CH_3CH_3	-79.624450
CH_2FCH_3	-178.775279
CHF_2CH_3	-277.942239
CF_3CH_3	-377.116202
$CH_3CH_2CH_3$	-118.847504
$CFH_2CH_2CH_3$	-217.998301
$CF_2HCH_2CH_3$	-317.165109
$CF_3HCH_2CH_3$	-416.339752
CH_3CHFCH_3	-218.006412
$CH_3CF_2CH_3$	-317.177527
CFH_2CFHCH_3	-317.152673
$CF_2HCFHCH_3$	-416.316634
$CF_2HCF_2CH_3$	-515.480011
CF_3CFHCH_3	-515.487735
$CF_3CF_2CH_3$	-614.650639

[a] ZPVE's and thermal corrections to 298 K are included. Unit in Hartree

Table 7.3 Enthalpy of Formation $\Delta H_f°_{298}$ Literature Values for Use in Isodesmic Reactions

Species	$\Delta H_f°_{298}$ (kcal/mol)
CH_3CH_3	-20.24[a]
CH_2FCH_3	-62.90[b]
CHF_2CH_3	-119.70[b]
CF_3CH_3	-178.20[b]
$CH_3CH_2CH_3$	-24.82[a]
CH_3CHFCH_3	-70.15[c]
$CH_3CF_2CH_3$	-124.88[c]

[a] reference [20]. [b] reference [1].
[c] reference [22].

Table 7.4 Barriers for Internal Rotors and ZPVE

Compound & Rotor[a]	MP2/6-31G*[b]	ZPVE[b] (Non scaled)	Total Energy[b, c]	Rotational Barrier Height (kcal/mol)
CH_2F-CH_2CH_3S	-217.6741723	0.1037922	-217.581783	0.53
CH_2F-CH_2CH_3S2	-217.6751056	0.1039213	-217.5826243	0.00
CH_2F-CH_2CH_3E	-217.6673272	0.1039412	-217.5745181	5.09
CH_2F-CH_2CH_3E2	-217.6677755	0.1036402	-217.5752352	4.64
CH_2F-CH_2CH_3S2	-217.6751056	0.1039213	-217.5828086	0.00
CH_2FCH_2-CH_3E3	-217.6700916	0.1036050	-217.5775827	3.28
CHF_2-CH_2CH_3S	-316.7095848	0.096176	-316.6239599	0.01
CHF_2-CH_2CH_3S2	-316.7098676	0.096312	-316.6241122	0.000
CHF_2-CH_2CH_3E	-316.7023192	0.096210	-316.6164133	4.83
CHF_2-CH_2CH_3E2	-316.7024861	0.095992	-316.6167748	4.60
CHF_2CH_2-CH_3S2	-316.7098676	0.096312	-316.6243504	0.00
CHF_2CH_2-CH_3E	-316.7054497	0.095985	-316.6197447	2.89
CF_3-CH_2CH_3S	-415.7537611	0.087572	-415.6757945	0.00
CF_3-CH_2CH_3E	-415.7465738	0.087481	-415.668462	4.60
CF_3CH_2-CH_3S	-415.7537611	0.087572	-415.6760435	0.00
CF_3CH_2-CH_3E	-415.7494645	0.087286	-415.6715268	2.83
CH_2F-$CHFCH_3S$	-316.6924925	0.096040	-316.6069966	0.68
CH_2F-$CHFCH_3S2$	-316.6932926	0.096211	-316.6076307	0.28
CH_2F-$CHFCH_3S3$	-316.693671	0.096155	-316.6080739	0.00
CH_2F-$CHFCH_3E$	-316.6807383	0.096094	-316.594936	8.24
CH_2F-$CHFCH_3E2$	-316.687754	0.096089	-316.6019561	3.84
CH_2F-$CHFCH_3E3$	-316.6873161	0.095903	-316.6016843	4.01
CH_2F-$CHFCH_3S3$	-316.693671	0.096155	-316.608306	0.00
CH_2FCHF-CH_3E	-316.6879687	0.095820	-316.602411	3.55

Table 7.4 Barriers for Internal Rotors and ZPVE (cont'd)

Compound & Rotor[a]	MP2/6-31G*[b]	ZPVE[b] (Not scaled)	Total Energy[b, c]	Rotational Barrier (kcal/mol)
CHF_2-$CHFCH_3$S	-415.7224941	0.088335	-415.6438083	1.88
CHF_2-$CHFCH_3$S2	-415.7255443	0.088400	-415.6468032	0.00
CHF_2-$CHFCH_3$S3	-415.7249126	0.088424	-415.6461506	0.41
CHF_2-$CHFCH_3$E	-415.714511	0.088500	-415.6354894	7.10
CHF_2-$CHFCH_3$E2	-415.7199746	0.088282	-415.6411476	3.55
CHF_2-$CHFCH_3$E3	-415.715448	0.088296	-415.6366085	6.40
$CHF_2CHF\_CH_3$S2	-415.7255443	0.088400	-415.6470945	0.00
CHF_2CHF-CH_3E	-415.7169994	0.087998	-415.638426	5.44
CHF_2-CF_2CH_3S	-514.7558364	0.079670	-514.6848668	2.21
CHF_2-CF_2CH_3S2	-514.7593602	0.079688	-514.6883944	0.00
CHF_2-CF_2CH_3E	-514.7465394	0.079732	-514.6753467	8.19
CHF_2-CF_2CH_3E2	-514.7511448	0.079756	-514.6799307	5.31
CHF_2CF_2-CH_3S2	-514.7593602	0.079688	-514.6886642	0.00
CHF_2CF_2-CH_3E	-514.7500985	0.079283	-514.6793067	5.87
CF_3-$CHFCH_3$S	-514.7658002	0.079590	-514.694906	0.00
CF_3-$CHFCH_3$E	-514.7582466	0.079642	-514.6871343	4.88
CF_3CHF-CH_3S	-514.7658002	0.079590	-514.6952013	0.00
CF_3CHF-CH_3E	-514.7607031	0.079273	-514.6899202	3.31
CF_3-CF_2CH_3S	-613.7963452	0.070823	-613.7332628	0.00
CF_3-CF_2CH_3E	-613.7888293	0.070949	-613.7254789	4.88
CF_3CF_2-CH_3S	-613.7963452	0.070823	-613.7335734	0.00
CF_3CF_2-CH_3E	-613.7909119	0.070460	-613.7279982	3.50

[a] See Figure 9 to 16 for definition of geometric nomenclature. [b] Unit in Hartree
[c] Scaled ZPVE are included. The corresponding torsional frequencies are excluded.

Table 7.5 Rotational Constants[a]

Species	Ia	Ib	Ic
$CH_2FCH_2CH_3$	14.639	5.175	4.351
$CHF_2CH_2CH_3$	7.124	4.118	3.437
$CF_3CH_2CH_3$	5.349	2.789	2.759
$CH_2FCHFCH_3$	8.152	3.624	2.731
CHF_2CHFCH_3	4.962	2.798	2.473
$CHF_2CF_2CH_3$	3.511	2.374	2.022
CF_3CHFCH_3	3.614	2.431	1.994
$CF_3CF_2CH_3$	2.777	1.871	1.847

[a]Unit in GHz

Table 7.6 Coefficients of Truncated Fourier Series Representation
Expansions for Internal Rotational Potentials

Species	a_0	a_1	a_2	a_3	b_1	b_2	b_3
$CH_2F-CH_2CH_3$	2.482	-0.026	0.326	2.306	0.000	0.000	0.000
$CH_2FCH_2-CH_3$	1.640	0.000	0.000	1.640	0.000	0.000	0.000
$CHF_2-CH_2CH_3$	2.410	-0.044	-0.108	2.346	0.000	0.000	0.000
$CHF_2CH_2-CH_3$	1.445	0.000	0.000	1.445	0.000	0.000	0.000
$CF_3-CH_2CH_3$	2.301	0.000	0.000	2.301	0.000	0.000	0.000
$CF_3CH_2-CH_3$	1.417	0.000	0.000	1.417	0.000	0.000	0.000
$CH_2F-CHFCH_3$	2.841	1.599	1.281	2.523	-0.164	-0.066	0.000
$CH_2FCHF-CH_3$	1.777	0.000	0.000	1.777	0.000	0.000	0.000
$CHF_2-CHFCH_3$	3.263	0.925	0.493	2.419	-1.296	0.349	0.357
$CHF_2CHF-CH_3$	2.720	0.000	0.000	2.720	0.000	0.000	0.000
$CHF_2-CF_2CH_3$	3.892	1.733	0.202	2.361	0.000	0.000	0.000
$CHF_2CF_2-CH_3$	2.936	0.000	0.000	2.936	0.000	0.000	0.000
$CF_3-CHFCH_3$	2.439	0.000	0.000	2.439	0.000	0.000	0.000
$CF_3CHF-CH_3$	1.657	0.000	0.000	1.657	0.000	0.000	0.000
$CF_3-CF_2CH_3$	2.442	0.000	0.000	2.442	0.000	0.000	0.000
$CF_3CF_2-CH_3$	1.750	0.000	0.000	1.750	0.000	0.000	0.000

Figure 7.10 shows the rotational barriers for 1,1-difluoropropane. The curves are similar in form to 1-fluoropropane. C-F eclipsed conformation has highest rotational barrier, which is 4.83 kcal/mol. The dual C-F gauche staggered conformation is more stable than the single C-F gauche staggered conformation. The rotational barrier for C_2-C_3 is 2.89 kcal/mol.

Figure 7.11 shows the rotational barriers for 1,1,1-trifluoropropane. The rotational barriers are 4.60 and 2.83 kcal/mol for C_1-C_2 and C_2-C_3 respectively.

Figure 7.12 shows the rotational barriers for 1,2-difluoropropane. The F-F eclipsed conformation for C_1-C_2 has highest rotational barrier, which is 8.24 kcal/mol. This rotational barrier is also the highest among eight fluorinated propane compounds. This trend is also seen in our previous study on fluorinated ethanes[26], where F-F eclipsed conformation for 1,2-difluoroethane shows the highest rotational barrier among nine fluorinated ethane compounds. The F-C gauche conformation shows the most stable conformation. The rotational barrier for C_2-C_3 is 3.55 kcal/mol.

Figure 7.13 shows the rotational barrier for 1,1,2-trifluoropropane. The F-C eclipsed conformation for C_1-C_2 has highest rotational barrier, which is 7.10 kcal/mol. The single F-F, dual C-F gauche conformation is the most stable. The rotational barrier for C_2-C_3 is 5.44 kcal/mol.

Figure 7.14 shows the rotational barrier for 1,1,2,2-tetrafluoropropane. The dual F-F eclipsed conformation for C_1-C_2 has the highest rotational barrier, which is 8.19 kcal/mol. The dual C-F gauche conformation shows the most stable conformation. The rotational barrier for C_2-C_3 is 5.87 kcal/mol.
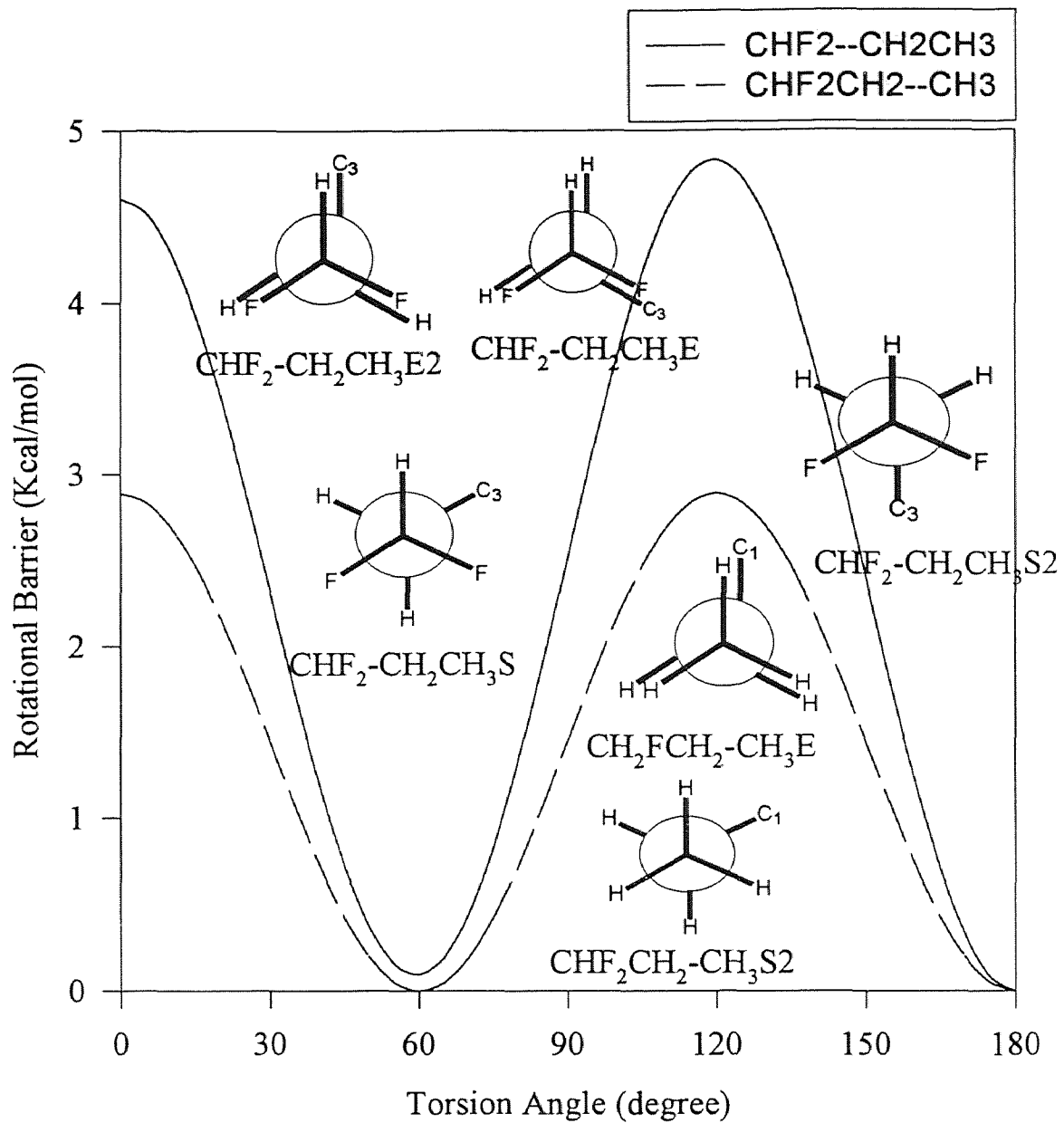
Figure 7.10 Potential Barriers for Internal Rotations about
C1-C2 and C2-C3 bonds of CHF_2-CH_2-CH_3
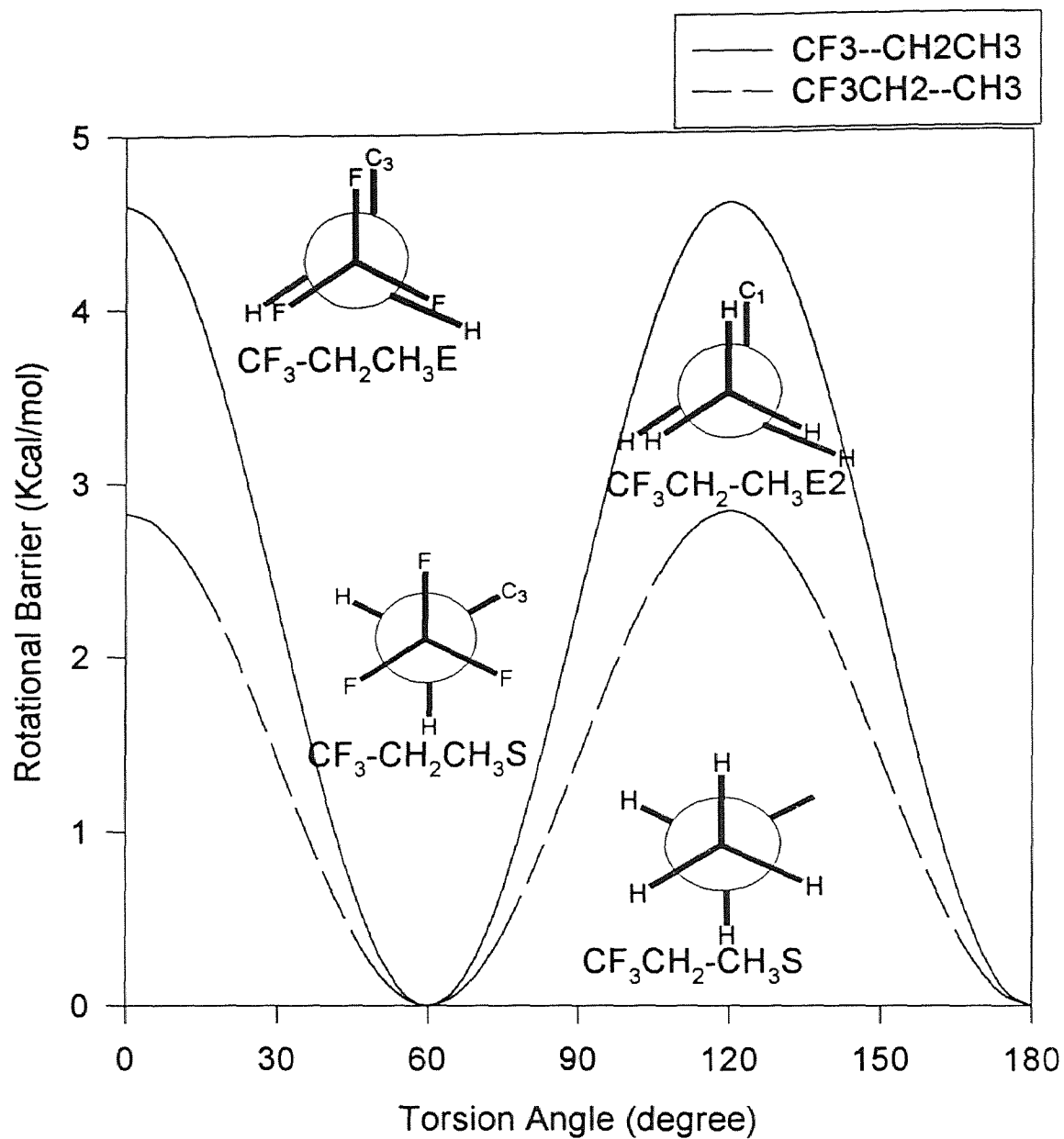
Figure 7.11 Potential Barriers for Internal Rotations about
C1-C2 and C2-C3 bonds of CF_3-CH_2-CH_3
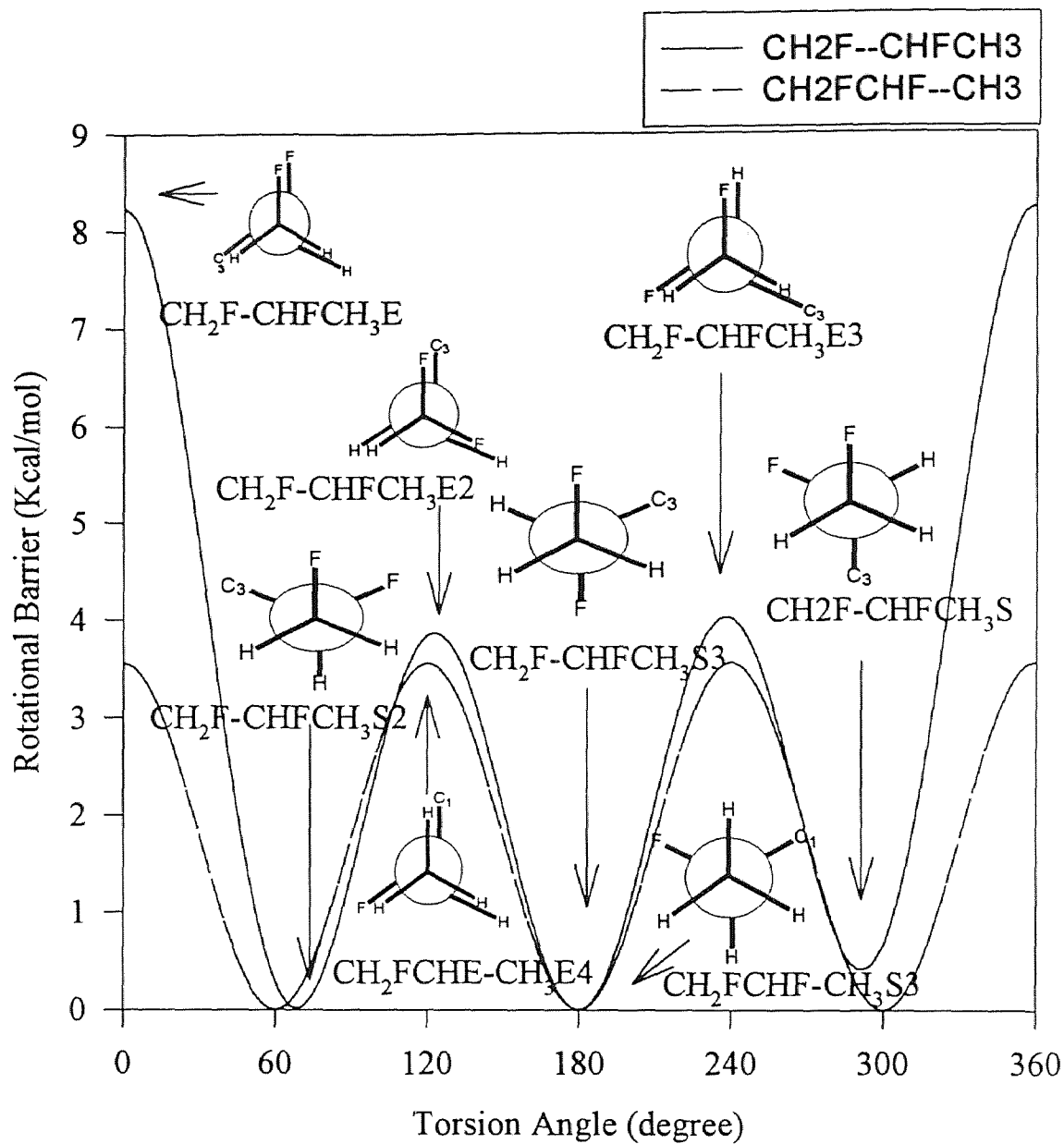
Figure 7.12 Potential Barriers for Internal Rotations about C1-C2 and C2-C3 bonds of CH_2F-CHF-CH_3
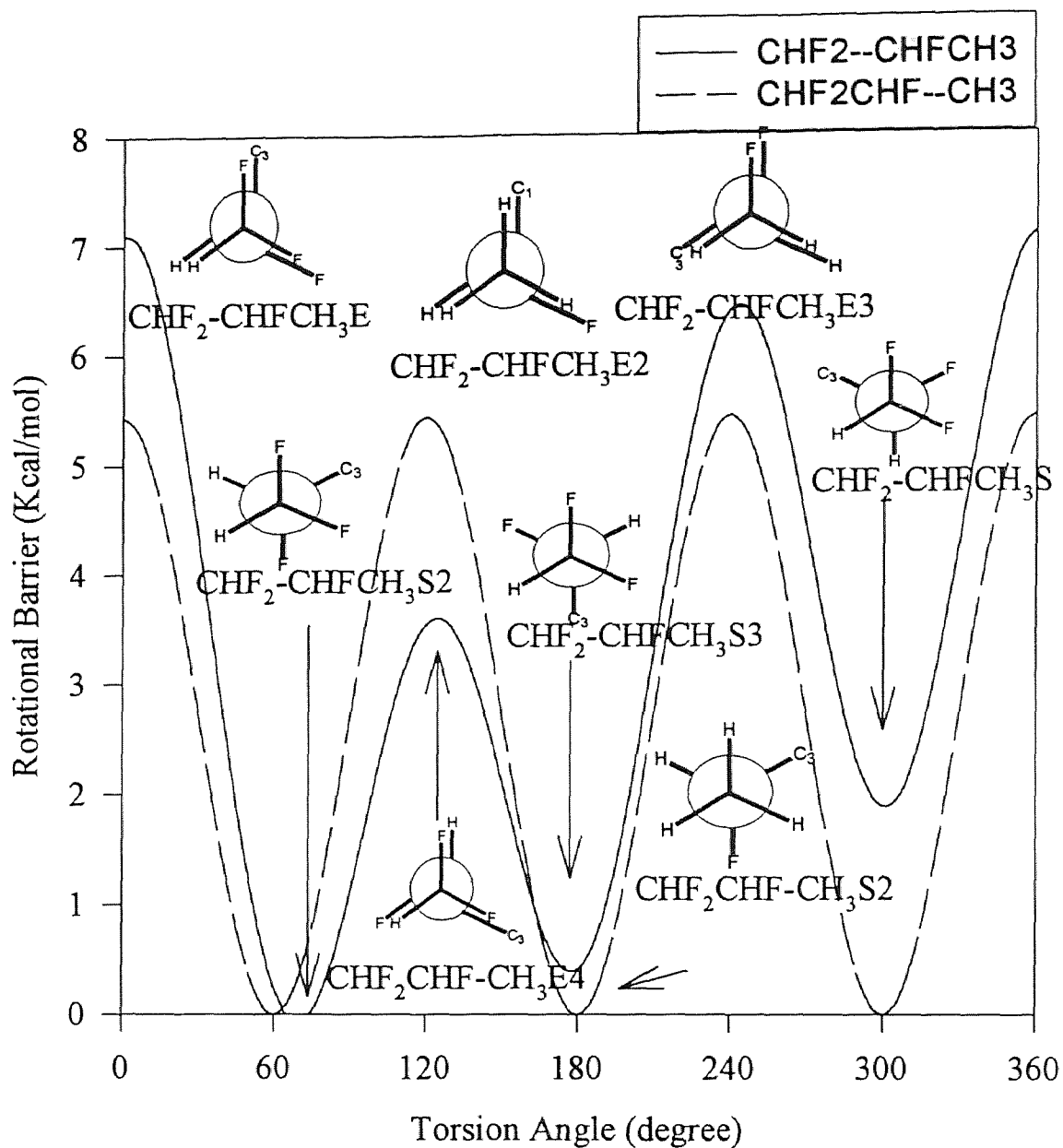
Figure 7.13 Potential Barriers for Internal Rotations about
C1-C2 and C2-C3 bonds of CHF_2-CHF-CH_3
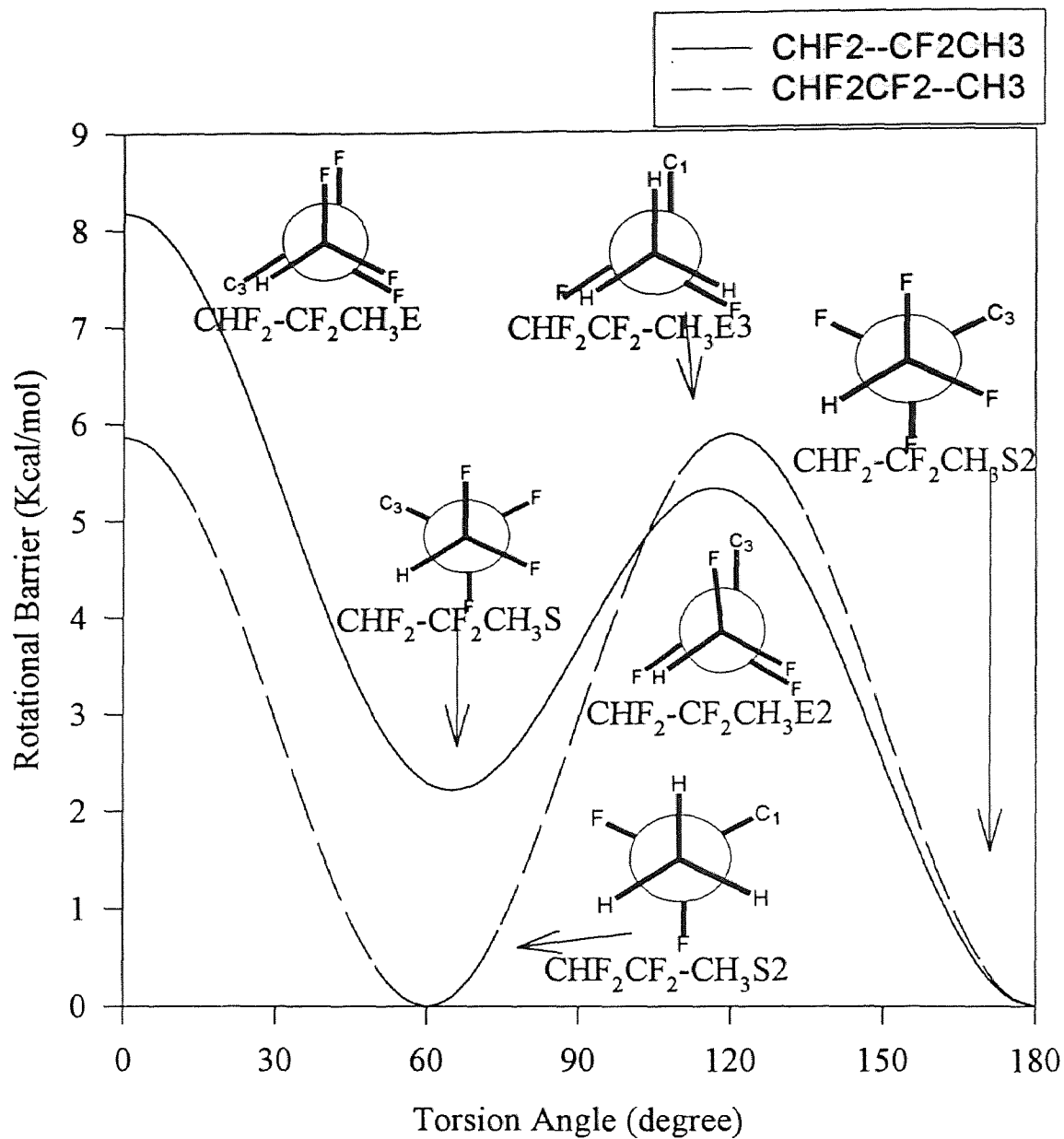
Figure 7.14 Potential Barriers for Internal Rotations about C1-C2 and C2-C3 bonds of CHF_2-CF_2-CH_3
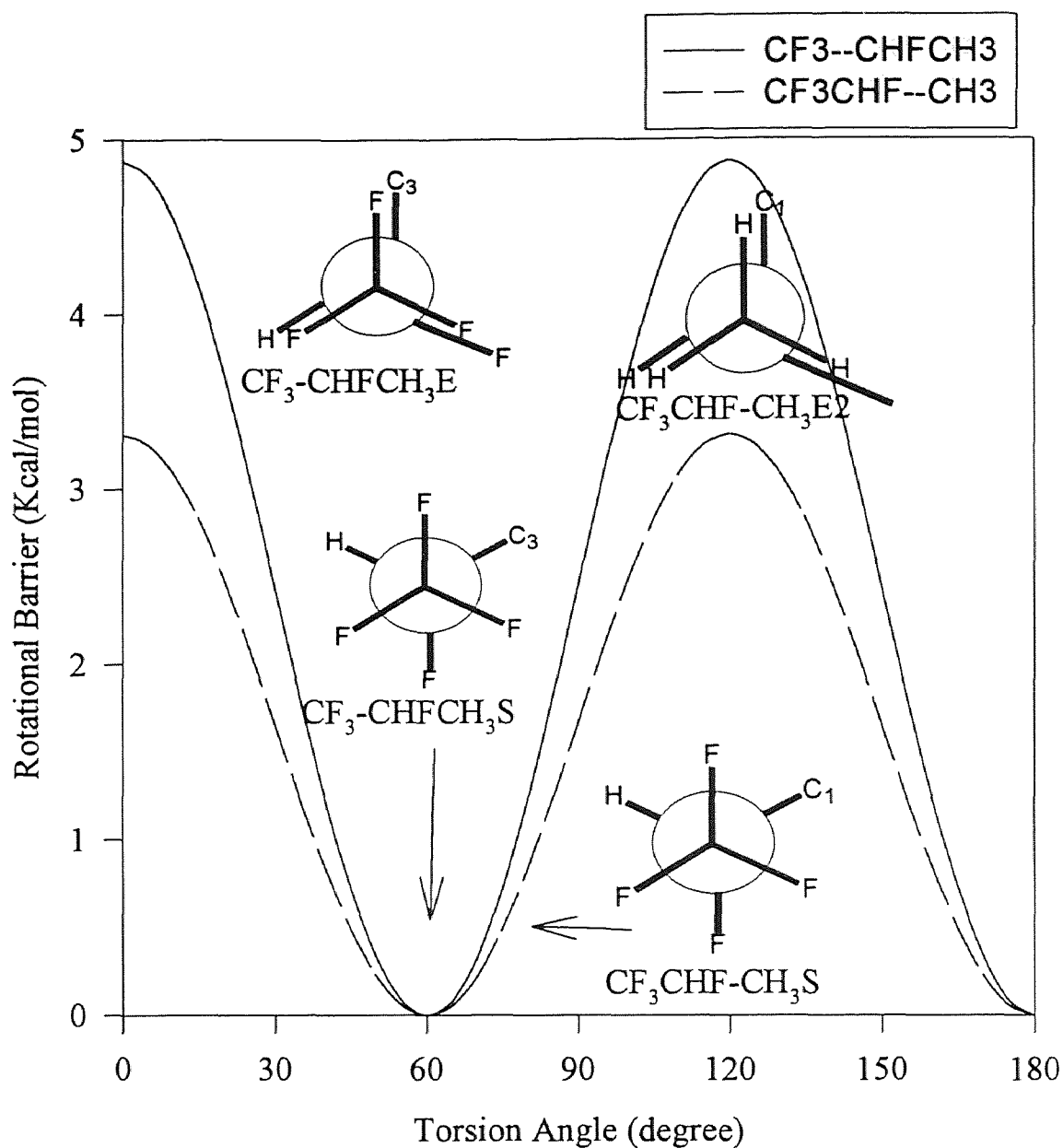
Figure 7.15 Potential Barriers for Internal Rotations about
C1-C2 and C2-C3 bonds of CF_3-CFH-CH_3
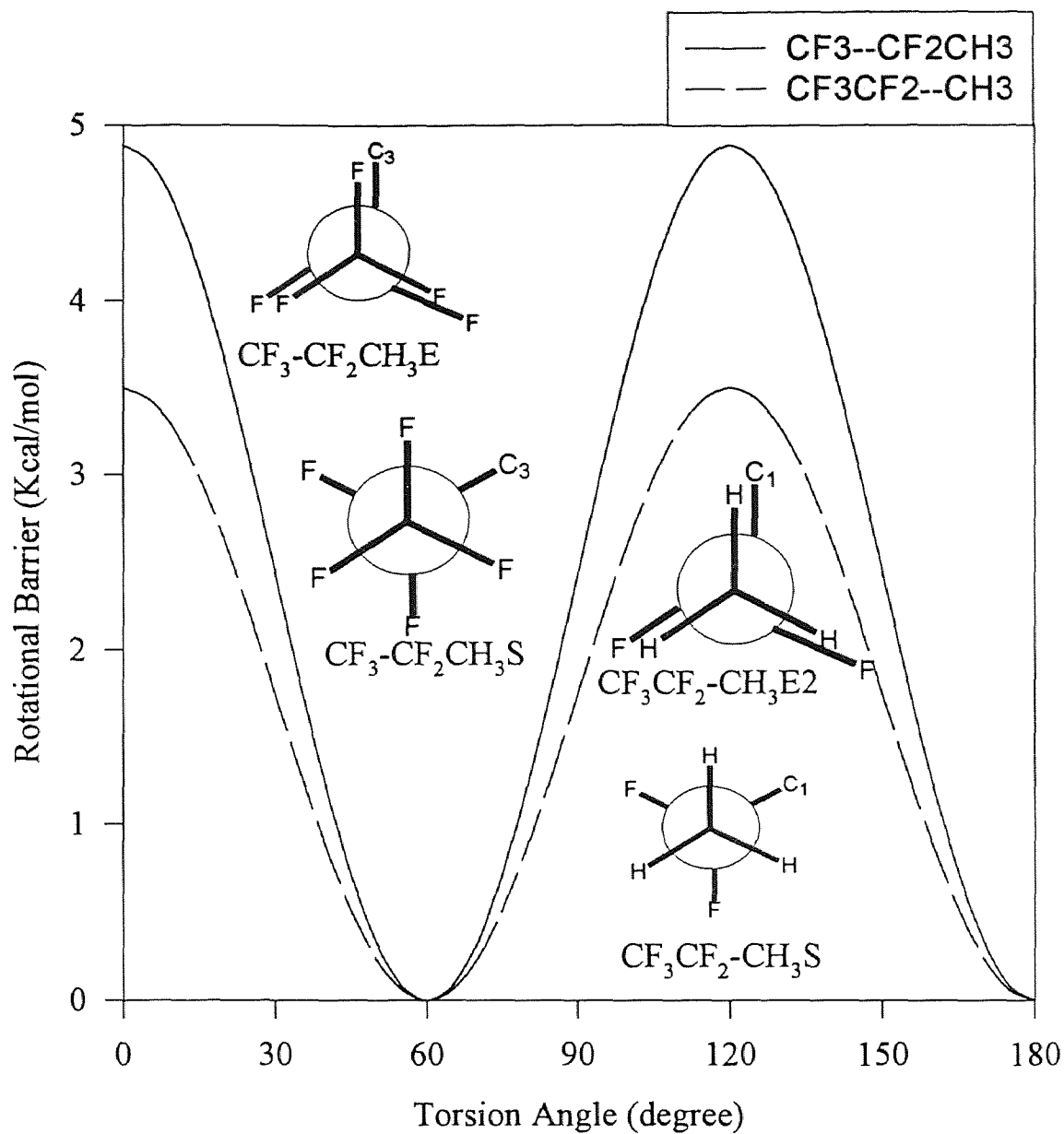
Figure 7.16 Potential Barriers for Internal Rotations about
C1-C2 and C2-C3 bonds of CF_3-CF_2-CH_3

Figure 7.15 and 7.16 shows the rotational barrier for 1,1,1,2-tetrafluoropropane and 1,1,1,2,2-pentafluoropropane respectively. The rotational barriers are 4.88 and 3.31 kcal/mol for C_1-C_2 and C_2-C_3 respectively for 1,1,1,2-tetrafluoropropane. The rotational barriers are 4.88 and 3.50 kcal/mol for C_1-C_2 and C_2-C_3 respectively for 1,1,1,2,2-pentafluoropropane.

7.3.5 Standard Entropy ($S°_{298}$) and Heat Capacities ($C_p(T)$'s, $300 \leq T/K \leq 1500$)

Standard entropy ($S°_{298}$) and heat capacities ($C_p(T)$'s, $300 \leq T/K \leq 1500$) are listed in Table 7.7. TVR indicates sum of contributions from translations, external rotations and vibrations. Internal rotor 1 and internal rotor 2 indicate contributions for the $S°_{298}$ and $C_p(T)$'s from internal rotation about C_1-C_2 and C_2-C_3 respectively. The literature values for 1-fluoropropane are also shown in Table 7.7[20,22]. The calculated $S°_{298}$ is 0.55 cal/mol-K higher values than the literature value. The calculated $C_p(T)$'s also show 0 to 0.4 cal/mol-K higher values than the literature data.

Table 7.7 Ideal Gas Phase Thermodynamic Properties[a]

Species and Symmetry #		$H_{f\,298}$[b]	$S°_{298}$[c]	C_{p300}[c]	C_{p400}	C_{p500}	C_{p600}	C_{p800}	C_{p1000}	C_{p1500}
$CFH_2CH_2CH_3$	TVR[d]		63.73[g]	15.16	20.10	24.82	28.96	35.57	40.44	47.83
(3)	Internal Rotor 1[e]		5.38	2.41	2.45	2.43	2.35	2.11	1.87	1.48
	Internal Rotor 2[f]		4.28	2.13	2.19	2.10	1.96	1.70	1.51	1.26
	Total	-67.46	73.39	19.70	24.74	29.35	33.27	39.38	43.82	50.57
	Frenkel et. al.[h]	-67.83	72.84	19.71	24.65	29.18	33.02	39.04	43.42	
	Stull et. al.[i]	-67.20	72.84	19.83	24.55	28.99	32.82	38.88	43.37	
$CHF_2CH_2CH_3$	TVR[d]		67.31	17.29	22.45	27.18	31.23	37.52	42.06	48.81
(3)	Internal Rotor 1[e]		5.75	2.19	2.30	2.33	2.28	2.08	1.86	1.46
	Internal Rotor 2[f]		4.45	2.16	2.14	2.00	1.84	1.58	1.41	1.20
	Total	-123.67	77.51	21.64	26.89	31.51	35.35	41.18	45.33	51.47

Table 7.7 Ideal Gas Phase Thermodynamic Properties[a] (cont'd)

Species and Symmetry #		$H_f°_{298}$[b]	$S°_{298}$[c]	C_{p300}[c]	C_{p400}	C_{p500}	C_{p600}	C_{p800}	C_{p1000}	C_{p1500}
$CF_3CH_2CH_3$	TVR[d]		68.43	19.97	25.33	30.01	33.90	39.78	43.91	49.92
(9)	Internal Rotor 1[e]		5.89	2.19	2.31	2.33	2.27	2.06	1.84	1.43
	Internal Rotor 2[f]		4.47	2.16	2.13	1.98	1.82	1.57	1.40	1.20
	Total	-183.09	78.79	24.32	29.77	34.32	37.99	43.41	47.15	52.55
$CH_2FCHFCH_3$	TVR[d]		67.98	17.61	22.62	27.29	31.30	37.55	42.06	48.80
(3)	Internal Rotor 1[e]		5.58	2.50	2.44	2.35	2.23	2.01	1.83	1.51
	Internal Rotor 2[f]		4.18	2.10	2.20	2.15	2.03	1.77	1.57	1.30
	Total	-109.95	77.74	22.21	27.26	31.79	35.56	41.33	45.46	51.61
CHF_2CHFCH_3	TVR[d]		71.27	19.75	24.96	29.63	33.56	39.51	43.70	49.79
(3)	Internal Rotor 1[e]		5.36	2.89	2.88	2.79	2.65	2.36	2.08	1.56
	Internal Rotor 2[f]		3.72	1.86	2.09	2.21	2.25	2.15	1.98	1.60
	Total	-164.86	80.35	24.50	29.93	34.63	38.46	44.02	47.76	52.95
$CHF_2CF_2CH_3$	TVR[d]		74.59	22.59	27.92	32.49	36.22	41.74	45.51	50.88
(3)	Internal Rotor 1[e]		4.48	3.51	3.87	3.78	3.50	2.88	2.38	1.67
	Internal Rotor 2[f]		7.08	2.33	2.23	2.05	1.86	1.56	1.33	0.94
	Total	-214.74	82.72	27.92	33.84	38.46	41.97	46.82	49.94	54.14
CF_3CHFCH_3	TVR[d]		72.14	22.41	27.82	32.43	36.20	41.75	45.54	50.92
(9)	Internal Rotor 1[e]		6.20	2.18	2.30	2.34	2.30	2.10	1.86	1.35
	Internal Rotor 2[f]		4.29	2.13	2.19	2.11	1.97	1.71	1.52	1.26
	Total	-221.57	82.63	26.72	32.31	36.88	40.47	45.56	48.92	53.53
$CF_3CF_2CH_3$	TVR[d]		75.45	25.27	30.76	35.27	38.85	43.97	47.56	52.01
(9)	Internal Rotor 1[e]		6.38	2.19	2.30	2.34	2.30	2.09	1.82	1.26
	Internal Rotor 2[f]		4.23	2.11	2.20	2.14	2.02	1.76	1.56	1.29
	Total	-271.14	86.06	29.57	35.26	39.75	43.17	47.82	50.94	54.56

[a] Thermodynamic properties are referred to a standard state of an ideal gas of pure enantiometer at 1 atm. Torsional frequencies are excluded in the calculations of entropies and heat capacities. Instead, an exact contribution from hindered rotations about the C-C is included. See text. [b] Units in kcal/mol. [c] Units in cal/mol-K. [d] Sum of contributions from translations, external rotations and vibrations.
[e] Contribution from internal rotation about C1 - C2 bond. [f] Contribution from internal rotation about C2 - C3 bond. [g] Symmetry number is taken into account (-R x ln (number of symmetry)). [h] reference [22]. [i] reference [20].

7.4 Summary

Thermodynamic properties ($\Delta H_f^\circ{}_{298}$, $S^\circ{}_{298}$ and $C_p(T)$'s ($300 \leq T/K \leq 1500$)) for 1-fluoropropane, 1,1-difluoropropane, 1,2-difluoropropane, 1,1,1-trifluoropropane, 1,1,2-trifluoropropane, 1,1,2,2-tetrafluoropropane, 1,1,1,2-tetrafluoropropane, 1,1,1,2,2-pentafluoropropane are calculated. The $\Delta H_f^\circ{}_{298}$ for the above eight compounds are estimated using the G2MP2 composite calculation methods and isodesmic reactions. Lowest energy geometries correspond to the maximum number of C-F gauche conformations. A general isodesmic reaction scheme for fluorinated propane compounds is presented and suggested for other fluorocarbons. $S^\circ{}_{298}$ and $C_p(T)$'s are estimated using scaled HF/6-31G(d) determined frequencies and MP2/6-31G(d) determined geometries. Hindered internal rotational contributions for $S^\circ{}_{298}$ and $C_p(T)$'s are calculated using the rigid-rotor-harmonic oscillator approximation with direct integration over energy levels of the intramolecular rotation potential energy curve. Rotational barrier heights are reported for both C_1-C_2 and C_2-C_3 internal rotors. The calculated thermodynamic properties ($\Delta H_f^\circ{}_{298}$, $S^\circ{}_{298}$ and $C_p(T)$'s ($300 \leq T/K \leq 1500$)) for 1-fluoropropane are compared with literature value and shown to be in good agreement.

CHAPTER 8

THERMODYNAMIC PROPERTIES
($\Delta H_F^{\circ}{}_{298}$, $S^{\circ}{}_{298}$ AND $C_P(T)$'S, $300 \leq T/K \leq 1500$), GROUP ADDITIVITY AND INTERACTION TERMS FOR FLUORINATED ALKANES, ALKENES AND ALKYNES

8.1 Introduction

Thermodynamic properties for the fluorinated ethane groups, C/C/F/H2, C/C/F2/H and C/C/F3 and interaction terms F/F, F2/F, F2/F2, F3/F, F3/F2 and F3/F3 are reported in Chapter 6. Group values, C/C3/F, C/C2/F/H and C/C2/F2 for fluoroalkanes beyond ethane, CD/F/H and CD/F2 for alkenes, and CT/F for alkyne, and interaction terms F//F, 2F//F and 2F//2F for fluoroalkenes, F///F for fluoroalkyne, plus Gauche interaction between methyl group and fluorine are desired to allow application of our modified group additivity method to more fluoro carbons. Conventional group additivity, which gives accurate calculation results for hydrocarbons and oxygenated hydrocarbons[7], is not appropriate for use of fluorocarbons where average errors on fluoroethanes are several kcal/mol with maximum errors in excess of 5 kcal/mol. These errors are dramatically reduced by using a modified group additivity which uses redefined group values and incorporates interaction terms[26].

Group values are estimated for C/C2/F/H, C/C2/F2, C/C3/F, CD/F/H, CD/F2 and CT/F based on the selected molecules, CH_3CFHCH_3, $CH_3CF_2CH_3$, $(CH_3)_3CF$, $CFHCH_2$, CF_2CH_2 and CFCH, where there are no fluorine atoms on the carbon adjacent to the carbon containing the fluorine atom(s).

Group additivity interaction terms are determined for F//F, 2F//F, 2F//2F and F///F, where "//" and "///" indicate group additivity corrections for fluorinated ethylenes and

250

acetylene respectively. Consider 1,1- and 1,2-difluoroethylene with CD/F2 and CD/F/H and two CD/F/H groups respectively. The CD/F2 group values include steric, electronic and polar effects of the two fluorine atoms, but the two CD/F/H groups on 1,2-difluoroethylene do not include steric, electronic, and polar effects resulting from F-F interactions on the adjacent carbons. Interaction groups are developed to account for these effects in order to improve prediction abilities of group additivity. The use of a modified group additivity for the properties of C_1 to C_n fluorocarbons is valuable and the tabulated data and database will allow more accurate estimation of thermodynamic property data for a large number of fluorocarbons.

Group additivity calculations are shown to be more accurate if F-CH3 gauche interaction terms are incorporated, especially in $S°_{298}$ calculation on fluorocarbons which include three or more carbons.

$\Delta H_f°_{298}$ for 1,2-difluoroethane, 1,1,2-trifluoroethane, 1,1,2,2-tetrafluoroethane, 1,1,1,2-tetrafluoroethane, and pentafluoroethane are estimated using G2MP2 calculations and isodesmic reactions, and new F/F, 2F/F, 2F/2F, 3F/F, and 3F/2F group additivity interactions are presented.

8.2 Calculation Method

8.2.1 *ab initio* Calculations for Thermodynamic Properties Estimation of 2 fluoro,2-methylpropane

The G2MP2 composite calculation method is performed on 2-fluoro,2-methylpropane and 2-fluoropropane to estimate thermodynamic properties ($\Delta H_f°_{298}$, $S°_{298}$, and $C_p(T)$'s $(300 \leq T/K \leq 1500)$). All *ab initio* calculations are performed using the Gaussian94[10] system of program. Thermodynamic properties for 1-fluoropropane, which is estimated

in a previous chapter, and those of 2-fluoropropane are used to evaluate the accuracy of

calculation for thermodynamic properties of 2-fluoro,2-methylpropane.

Enthalpy of Formation ($\Delta H_f°_{298}$) Calculations

$\Delta H_f°_{298}$ are estimated using G2MP2 calculations and following isodesmic reactions.

For 1-fluoropropane

$$CH_2FCH_2CH_3 + CH_3CH_3 \rightarrow CH_3CH_2CH_3 + CFH_2CH_3 \qquad \text{---------(1)}$$

For 2-fluoropropane

$$CH_3CFHCH_3 + CH_3CH_3 \rightarrow CH_3CH_2CH_3 + CFH_2CH_3 \qquad \text{---------(2)}$$

For 2-methyl,2-fluoropropane

$$(CH_3)_3CF + CH_3CH_2CH_3 \rightarrow (CH_3)_3CH + CH_3CFHCH_3. \qquad \text{---------(3)}$$
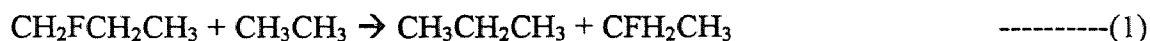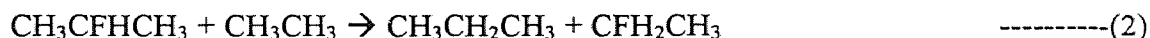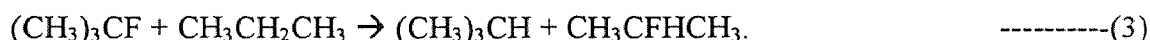
The principle of isodesmic reaction is explained in previous studies[11,24,26,27].

The basic requirement of the isodesmic reaction is bond type conservation, where the

number of each formal chemical bond type is conserved in the reaction[24]. An isodesmic

reaction will lead to more accurate results if groups are conserved in the reaction scheme,

because next nearest neighbor interactions are then conserved. Reaction (1), (2), and (3)

have the following properties: reaction (1) conserves both bond type and groups, while

reaction (2) and (3) conserves only bond type.

ab initio calculations with ZPVE and thermal correction are performed for the four

compounds in reaction (1), and $\Delta H_f°_{rxn,298}$ is calculated. Known enthalpies of formation

are substituted for CH_3CH_3, $CH_3CH_2CH_3$, and CFH_2CH_3, and $CFH_2CH_2CH_3$ enthalpy of

formation is then calculated from these values and the calculated $\Delta H_f°_{298,rxn}$. $\Delta H_f°_{298}$ for

2-difluoropropane and 2-methyl,2-fluoropropane are calculated in the same manner.

Standard Entropy (S°₂₉₈) and Heat Capacity (C_p(T)'s, 300≤T/K ≤1500) Calculations

Harmonic vibrational frequencies calculated at the HF6-31G(d) level of theory and moments of inertia on molecular structures optimized at MP2/6-31G(d) are used in the calculation of the $S°_{298}$ and $C_p(T)$'s.

A technique for the calculation of thermodynamic functions from hindered rotations with arbitrary potentials has been explained previously[24-27]. All potential curves of rotational barrier vs. dihedral angle are fit by a truncated Fourier series:

$$V(\emptyset) = a_0 + a_1\cos(\emptyset) + a_2\cos(2\emptyset) + a_3\cos(3\emptyset) \qquad \text{---------- (4)}$$

where values of the coefficients a_i are calculated to provide the minimum and maxima of the torsional potentials with allowance of a shift of the theoretical extrema angular positions.

8.2.2 *ab initio* Calculations for Enthalpies of Formations ($\Delta H_f°_{298}$) Estimation of Five Fluorinated Ethanes

The enthalpies of formation of 1,1-difluoroethane, 1,1,2-trifluoroethane, 1,1,2,2-tetrafluoroethane, 1,1,1,2-tetrafluoroethane, and pentafluoroethane are calculated using the following isodesmic reactions and existing literature values of ethane, 1-fluoroethane, 1,1-difluoroethane, and 1,1,1-trifluoroethane. These enthalpies of formations are used to further evaluate the enthalpies of formation for fluorine-fluorine interaction terms, F/F 2F/F, 2F/2F, 3F/F, and 3F/2F.

For 1,1-difluoroethane

$$CH_2FCH_2F + C_2H_6 \rightarrow CH_2FCH_3 + CH_2FCH_3 \qquad \text{---------- (5)}$$

For 1,1,2-trifluoroethane

$$CHF_2CH_2F + C_2H_6 \rightarrow CHF_2CH_3 + CH_2FCH_3 \qquad \text{---------- (6)}$$

For 1,1,2,2-tetrafluoroethane

$$CHF_2CHF_2 + C_2H_6 \rightarrow CHF_2CH_3 + CHF_2CH_3 \qquad \text{---------- (7)}$$

For 1,1,1,2-tetrafluoroethane

$$CF_3CH_2F + C_2H_6 \rightarrow CF_3CH_3 + CH_2FCH_3 \qquad \text{---------- (8)}$$

For 1,1,1,2,2-pentafluoroethane

$$CF_3CH_2F + C_2H_6 \rightarrow CF_3CH_3 + CH_2FCH_3 \qquad \text{---------- (9)}$$

8.2.3 Group and F-F Interaction Value Estimation

Selection (definition) of the initial groups is critical to development of a group additivity scheme for accurate property estimation. 2-fluoro,2-methylpropane, 2-fluoropropane, and 2,2-difluoropropane are chosen to derive the groups value of C/C3/F, C/C2/F/H and C/C2/F2 respectively. There are only hydrogen atoms on the end carbons adjacent to carbon bonded to fluorine(s). Fluoroethylene, 1,1-difluoroethylene, and fluoroacetylene, are chosen to derive the groups CD/F/H, CD/F2, and CT/F respectively, again there are only hydrogen atoms on the carbons adjacent to the carbon atom bonded to fluorines.

$H_f°_{298}$ and $C_p(T)$'s of C/C2/F/H are calculated based on:

$$(CH_3CFHCH_3) = (C/C/H3) \times 2 + (C/C2/F/H) \qquad \text{---------- (10)}$$

$S°_{298}$ of C/C2/F/H is calculated based on:

$$(CH3CFHCH_3) = (C/C/H3) \times 2 + (C/C2/F/H) - R \ln(\sigma) \qquad \text{---------- (11)}$$

where R=1.987 cal/mol-K, and σ is symmetry number, which is 9 for CH_3CHFCH_3.

Group values of C/C3/F, C/C2/F2, CD/F/H, CD/F2, and CT/F are estimated in the same manner.

Thermodynamic properties of fluoroethanes with no fluorine on the carbon atoms adjacent a carbon with fluorines are now accurately predicted, but an adjustment needs to be made for fluoroethylene and fluoroacetylene species where there are fluorine atoms on an adjacent carbon. The interaction values F//F, 2F//F, and 2F//2F for alkenes and F///F for alkynes are calculated from differences between the defined fluorinated hydrocarbon group values and the established thermodynamic properties of the parent compounds. $H_f°_{298}$ and C_p's for the F//F interaction are estimated by:

$$(CHFCHF) = (CD/F/H) \times 2 + (F//F) \qquad \text{---------- (12)}$$

$S°_{298}$ for the F//F interaction is calculated by:

$$(CHFCHF) = (CD/F/H2) \times 2 - R \times \ln(\sigma) + (F//F) \qquad \text{---------- (13)}$$

where $R = 1.987$ cal K^{-1} mol^{-1} and $\sigma = 2$ for CHFCHF

Other interaction values are estimated in the same manner. 2F//2F and F///F are unique groups; but the interactions are of value for evaluation of trends.

8.2.4 Gauche Interaction Estimation

The values of gauche interaction are calculated for eight fluoropropanes 1-fluoropropane, 1,1- and 1,2-difluoropropane, 1,1,1- and 1,1,2-trifluoropropane, 1,1,1,2- and 1,1,2,2-tetrafluoropropane, and 1,1,1,2,2-pentafluoropropane. Values are on a per F-CH3 gauche interaction for the varied molecular cases and the average F-CH3 gauche interaction value is derived. The calculation method of gauche interaction for 1-fluoropropane is explained below.

The group additivity method is applied for fluoropropanes using previously estimated fluorinated carbon groups and evaluated F-F interactions, where there is no F-F

interaction for 1-fluoropropane. The group additivity determined thermodynamic properties are subtracted from the thermodynamic properties ($\Delta H_f^{\circ}{}_{298}$, $S^{\circ}{}_{298}$, and $C_p(T)$'s, $300 \leq T/K \leq 1500$) of 1-fluoropropane. Then the respective differences are divided by the number of gauche interactions (1 for 1-fluoropropane). The counting of F-CH3 gauche interaction is different from traditional hydrocarbon gauche interaction. The rotational barrier calculations for fluoropropanes indicate that the F-CH3 gauche conformation has lower energy than anti-gauche conformation[27]. Therefore the gauche number has to be counted as the maximum possible for fluorinated carbons. Gauche interactions have a stabilizing or energy lowering effect in enthalpies of formation.

8.3 Results and Discussion

8.3.1 Thermodynamic Properties: Estimation of 2-fluoro,2-methylpropane Geometries and Frequencies

Table 8.1 lists the HF/6-31G* determined frequencies of 2-fluoropropane and 2-fluoro, 2-methylpropane. Asterisks indicate torsional frequencies where contributions are excluded from $S^{\circ}{}_{298}$ and $C_p(T)$ calculations. Figure 8.1 and 8.2 illustrate MP2(full)/6-31G* determined geometries of 2-fluoropropane and 2-fluoro,2-methylpropane.

Enthalpies of Formation ($\Delta H_f^{\circ}{}_{298}$)

G2MP2 determined total energies and the $\Delta H_f^{\circ}{}_{298}$ from literature are tabulated in Table 8.2 and 8.3 respectively. $\Delta H_f^{\circ}{}_{298}$ for 1-fluoropropane and 2-fluoropropane are calculated to evaluate the systematic error in estimation of enthalpies of formation for

2-methyl,2-fluoropropane. $\Delta H_f^{\circ}{}_{298,rxn}$ for reaction (2) is calculated using G2MP2

determined total energies as:

$CH_3CH_2CH_3 + CFH_2CH_3 - (CH_3CHFCH_3 + CH_3CH_3) = 5.07$ kcal/mol.

$\Delta H_f^{\circ}{}_{298}$ of 2-fluoropropane is calculated using the known $\Delta H_f^{\circ}{}_{298}$ for ethane, propane,

and fluoroethane, with the calculated $\Delta H_f^{\circ}{}_{298,rxn}$. This calculation yields -72.55 kcal/mol

as shown in Table 8.7, which also shows literature values[20,22]. Our result underestimate

$\Delta H_f^{\circ}{}_{298}$ by 2.40 to 3.55 kcal/mol compared with the literature values. $\Delta H_f^{\circ}{}_{298}$ of 2-

fluoro,2-methylpropane is calculated in the same manner and listed in Table 8.7.

The isodesmic reaction to calculate $\Delta H_f^{\circ}{}_{298}$ for 1-fluoropropane conserves both

bonds and groups in reaction (1). Comparison of the calculation results using this

isodesmic reaction between the two literature sources shows differences of +0.37 and -

0.26 kcal/mol relative to Frenkel et al.'s and Stull et al.'s data respectively[20,22].

The groups used in reaction (1) are three C/C/H3's, one C/C/F/H2, and C/C2/H2. These

group types are conserved for both the left and right sides of the reaction. Reaction (2)

for 2-fluoropropane conserves only bond types and the calculation results underestimate

$\Delta H_f^{\circ}{}_{298}$ for this compound by -2.40 and -3.55 kcal/mol in comparison with Frenkel et

al.'s and Stull et al.'s data respectively[20,22]. Groups used in left side of reaction (2) are

four C/C/H3's and one C/C2/F/H, and those used in right side are three C/C/H3's, one

C/C/F/H2, and one C/C2/H2. The unbalanced groups are one C/C/H3 and one C/C2/F/H

for left side, and one C/C/F/H2 and one C/C2/H2 for right side of equation. This loss of

group conservation may cause a systematical error in the calculation of $\Delta H_f^{\circ}{}_{298}$ of 2-

fluoropropane. The correction values are chosen to account for this underestimation in

estimation on $\Delta H_f^{\circ}{}_{298}$ of 2-methyl,2-fluoropropane.

Table 8.1 Vibrational Frequencies[a] (ν cm^{-1})

Species	CH$_3$CFHCH$_3$	(CH$_3$)$_3$CF
ν1	233*	212*
ν2	276*	273*
ν3	375	273*
ν4	438	357
ν5	512	358
ν6	886	431
ν7	1015	492
ν8	1027	492
ν9	1059	801
ν10	1256	1006
ν11	1279	1006
ν12	1312	1016
ν13	1516	1053
ν14	1523	1147
ν15	1572	1147
ν16	1575	1370
ν17	1626	1402
ν18	1631	1402
ν19	1635	1563
ν20	1655	1563
ν21	3210	1582
ν22	3215	1616
ν23	3241	1630
ν24	3275	1630
ν25	3285	1642
ν26	3286	1642
ν27	3292	1665
ν28		3211
ν29		3211
ν30		3221
ν31		3278
ν32		3278
ν33		3282
ν34		3289
ν35		3289
ν36		3290

[a] Non-scaled. Frequencies are calculated at the HF/6-31G* level of theory.
* Torsional Frequencies. These frequencies are not included in the calculation of entropies S°$_{298}$'s and heat capacities C$_p$(T)'s. Instead, an exact contribution from hindered rotations about the C-C is included. See text.

Bond	Length (Å)
C1-C2	1.511
C2-C3	1.511
C1-H	1.092
	1.093
	1.093
C2-F	1.408
C2-H	1.096
C3-H	1.092
	1.093
	1.093

Bond	Angle (degree)
$\angle C_1C_2C_3$	113.9
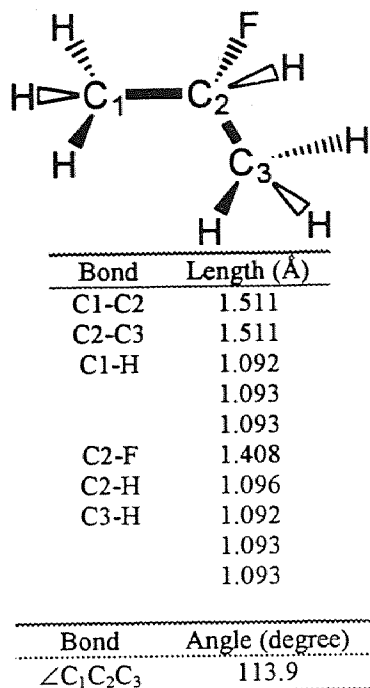
Figure 8.1 MP2(full)/6-31G(d) Determined Geometry of 2-Fluoropropane

Bond	Length (Å)
C1-C2	1.516
C1-C3	1.516
C1-C4	1.516
C2-H	1.093
C3-H	1.093
C4-H	1.093
C1-F	1.418

Bond	Angle (degree)
$\angle C_xC_1C_y$	112.4
$\angle C_xC_1F$	106.4
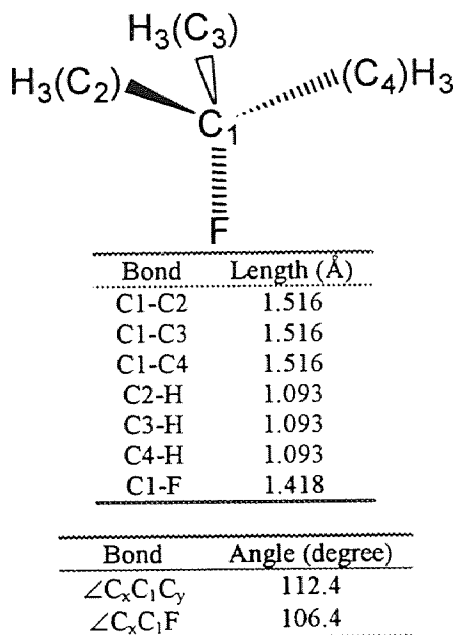
Figure 8.2 MP2(full)/6-31G(d) Determined Geometry of 2-Methyl,2-fluoropropane

Table 8.2 G2MP2 Total Energy Calculation Result

Species	Total Energy[a]
CH_3CH_3	-79.624450
CFH_2CH_3	-178.775281
CF_2HCH_3	-277.942239
CF_3CH_3	-377.116202
CH_2FCH_2F	-277.921576
CHF_2CH_2F	-377.084329
CHF_2CHF_2	-476.244755
CF_3CH_2F	-476.254995
CF_3CHF_2	-575.412385
$CH_3CH_2CH_3$	-118.847504
$CH_2FCH_2CH_3$	-217.998301
CH_3CFHCH_3	-218.006412
$(CH_3)_3CH$	-158.074011
$(CH_3)_3CF$	-257.238481

[a] ZPVE's and thermal corrections to 298 K are included.

Table 8.3 Literature Values for Known $\Delta H_f^{\circ}{}_{298}$ for Use in Isodesmic Reactions

Compounds	$H_f^{\circ}{}_{298}$ (kcal/mol)
CH_3CH_3	-20.24[a]
CFH_2CH_3	-62.90[b]
CF_2HCH_3	-119.70[b]
CF_3CH_3	-178.20[b]
$CH_3CH_2CH_3$	-24.82[a]
$CH_2FCH_2CH_3$	-67.20[a]
	-67.83[c]
CH_3CFHCH_3	-69.00[a]
	-70.15[c]
$(CH_3)_3CH$	-32.27[c]

[a] reference 20. [b] reference 1.
[c] reference 22

The calculation result for $\Delta H_f^{\circ}{}_{298}$ of 2-methyl,2-fluoropropane is -81.09 kcal/mol.

The unbalanced groups for reaction (3) are one C/C3/F and one C/C2/H2 for left side,

and one C/C3/H and one C/C2/F/H for right side of reaction. Reaction (2) and (3) have

one fluorine, and ethane is used for estimation of 2-fluoropropane as reference

compound, and propane is used for 2-methyl,2-fluoropropane as reference compounds

correcting for the underestimation observed in 2-fluoropropane, 3.0 kcal/mol (average

difference from two literature values). $\Delta H_f^{\circ}{}_{298}$ of 2-methyl,2-fluoropropane is estimated

as –78.1 kcal/mol.

Rotational Barriers

Figure 8.3 and 8.4 shows the rotational barriers for 2-fluoropropane and 2-fluoro,2-

methylpropane respectively. The barriers for internal rotations are calculated as the

difference between the total energy of each conformation and that of the global

equilibrium plus the scaled ZPVE difference (see Table 8.4). The curves are fit by a

truncated Fourier series (4). Table 8.6 lists the coefficients of the respective Fourier

series.

Table 8.4 Barriers for Internal Rotors and ZPVE

Compounds & Rotor[a]	MP2/6-31G*	ZPVE (No scale)	Total Energy[b]	Rotational Barrier Height (kcal/mol)
CH3-CFHCH3 S	-217.6827061	0.102981	-217.5912274	0.000
CH3-CFHCH3 E	-217.6767316	0.1026772	-217.5850511	3.876
CH3-C(CH3)2F S	-256.856998	0.132414	-256.739196	0.000
CH3-C(CH3)2F E	-256.8508856	0.13215	-256.7328889	3.958

[a] S at the end of species stands for "staggered", E stands for "eclipsed".
[b] Total Energies are calculated as the difference in MP2/6-31G* determined total energies plus scaled ZPVE. The corresponding torsional frequency is excluded.
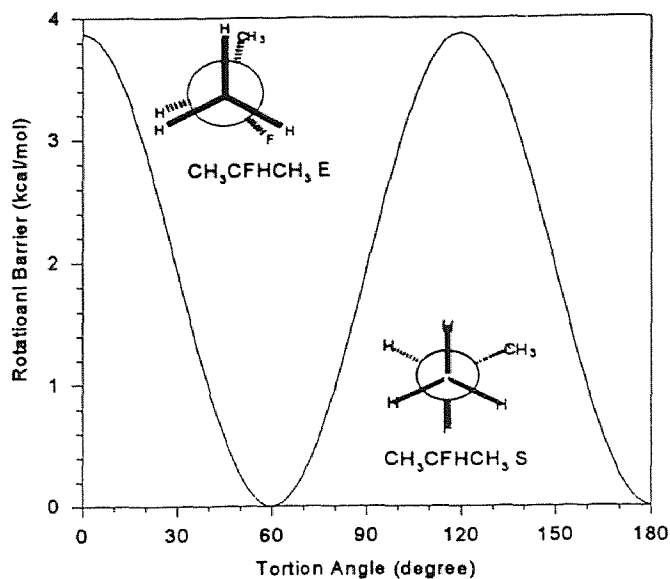
Figure 8.3 Potential Barriers for Internal Rotations about C-C Bonds of CH_3-$CFHCH_3$
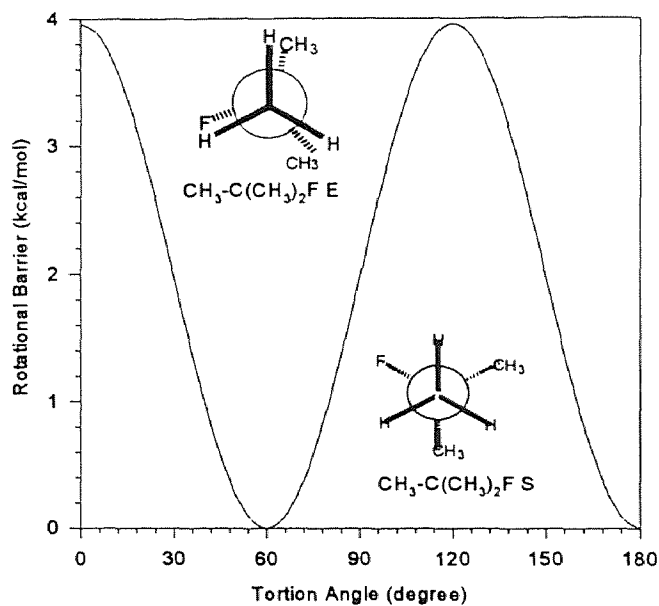
Figure 8.4 Potential Barriers for Internal Rotations about C-C Bonds of CH_3-$C(CH_3)_2F$

Table 8.5 Rotational Constants[a]

Species	I_a	I_b	I_c
CFH$_2$CH$_2$CH$_3$	14.64	5.171	4.349
CH$_3$CFHCH$_3$	8.898	8.106	4.841
(CH$_3$)$_3$CF	4.776	4.775	4.528

[a] Unit in GHz

Table 8.6 Coefficients of Truncated Fourier Series Representation Expansions for Internal Rotation Potentials[a]

Rotors	a_0	a_1	a_2	a_3
CH$_3$-CFHCH$_3$	1.938	0	0	1.938
CH$_3$-C(CH$_3$)$_2$F	1.979	0	0	1.979

Values of rotational barriers computed at the MP2(full)/6-31G(d,p) level of theory are used to calculate the coefficients. Equation (4) in text. See text. [a] Unit in kcal/mol

Standard Entropy ($S°_{298}$) and Heat Capacities ($C_p(T)$'s, $300 \leq T/K \leq 1500$):

$S°_{298}$ and $C_p(T)$'s are listed in Table 8.7. The literature values for 2-fluoropropane are in agreement with our calculation[20,22]. Our estimations of $S°_{298}$ and $C_p(T)$'s for 2-fluoropropane are around 0.2 and 0.5 cal/mol-K higher than Frenkel et al.'s and Stull et al.'s data respectively. Our estimation of $S°_{298}$ for 2,2-difluoropropane is in good agreement with Frenkel et al.'s data[22]. Our estimation of heat capacities ($C_p(T)$'s $300 \leq$ T/K $\leq$ 600) for 2-methyl,2-fluoropropane are 0.3 to 0.6 cal/mol-K above the value of Frenkel et al.'s data[22].

Table 8.7 Ideal Gas Phase Thermodynamic Properties Obtained by G2MP2 Calculation[a]

Species and Symmetry #		$H_f°_{298}$[b]	$S°_{298}$[c]	C_{p300}[c]	C_{p400}	C_{p500}	C_{p600}	C_{p800}	C_{p1000}	C_{p1500}
CH_3CFHCH_3	TVR[d]		62.16[e]	16.09	20.91	25.47	29.47	35.89	40.65	47.92
(9)	Internal Rotor 1,2[f]		4.06	2.06	2.20	2.19	2.10	1.86	1.65	1.35
	Values are for each rotor									
	Total	-72.55	70.28	20.20	25.31	29.85	33.67	39.60	43.95	50.61
	Frenkel et. al.[g]	-70.15	70.03	20.00	25.19	29.71	33.51	39.39	43.81	***
	Stull et. al.[h]	-69.00	69.82	19.68	24.72	29.27	33.14	39.14	43.55	***
$(CH_3)_3CF$	TVR		62.26[e]	20.43	26.27	32.50	37.65	45.79	51.84	61.10
(81)	Internal Rotor 1,2,3[i]		4.05	2.05	2.20	2.20	2.11	1.88	1.67	1.36
	Values are for each rotor									
	Total	-78.1	74.41	26.57	32.87	39.10	43.99	51.42	56.85	65.18
	Frenkel et. al.	***	74.50	26.24	32.83	38.85	43.37	***	***	***

[a] Thermodynamic properties are referred to a standard state of an ideal gas of pure enantiometer at 1 atm. Torsional frequencies are excluded in the calculations of entropies and heat capacities. Instead, an exact contribution from hindered rotations about the C-C is included. See text. [b] Units in kcal/mol. [c] Units in cal/mol-K. [d] Sum of contributions from translations, vibrations, and external rotations.
[e] Symmetry number is taken into account (-R x ln (number of symmetry)). [f] Contribution from internal rotation about two CH_3-$CFHCH_3$ symmetrical bonds. [g] reference [22]. [h] reference [20]. [i] Contribution from internal rotation about three CH_3-$C(CH_3)2F$ symmetrical bonds. *** indicates no available data.

8.3.2 ab initio Calculations for $\Delta H_f°_{298}$ Estimation of Five Fluorinated Ethanes

The G2MP2 composite calculation method and isodesmic reactions, (5) - (9), are used to estimate enthalpies of formations for 1,2-difluoroethane, 1,1,2-trifluoroethane, 1,1,2,2-tetrafluoroethane, 1,1,1,2-tetrafluoroethane, and pentafluoroethane. The F-F interaction terms are estimated using those $\Delta H_f°_{298}$ and group values C/C/H2/F, C/C/H/F2, and C/C/F3, which were estimated in chapter 6. Results of the interaction terms are tabulated in Table 8.9. Interaction values are slightly increased (less than 1 kcal/mol) except F-F interaction, which is 3.9 kcal/mol higher in this study compared with our previous data[26].

Chen et. al calculated $\Delta H_f°_{298}$ for 1,1,2-trifluoroethane and 1,1,2,2-tetrafluoroethane using MP4/6-311G**//6-31G* calculation method and same isodesmic reactions as

ours[3]. Our G2MP2 calculation results show good agreement with their data. $\Delta H_f°_{298}$ for

1,1,1,2-tetrafluoroethane and 1,1,1,2,2-pentafluoroethane are close to Chen 's

recommended value[1]. Zachariah et al. also reported $\Delta H_f°_{298}$ for about 100 closed and

open shelled fluorocarbon species using BACMP4 method. Most of their values on

compounds in this study are about 4 kcal/mol lower than our estimation.

Table 8.8 Summary of Ideal Gas Phase Thermodynamic Properties

Species and Symmetry #	$H_f°_{298}$	$S°_{298}$	C_{p300}	C_{p400}	C_{p500}	C_{p600}	C_{p800}	C_{p1000}	C_{p1500}	Source
CFHCH₂ (2)[a]	-33.20	62.71	12.10	14.81	17.14	19.05	21.94	24.04	27.27	b
CF₂CH₂ (4)	-80.50	63.41	14.18	17.16	19.49	21.32	23.95	25.75	28.37	b
	-76.84	63.38	14.18	17.16	19.51	21.32	23.95	25.74	***	c
CFHCFH (2)	-77.01	64.23	14.00	16.80	19.14	21.00	23.71	25.56	28.25	b
CF₂CFH (2)	-117.30	69.95	16.60	19.39	21.59	23.29	25.68	27.22	29.30	b
	-118.50	69.94	16.60	19.39	21.59	23.30	25.69	27.23	***	c
CF₂CF₂ (4)	-157.40	71.68	19.29	21.97	23.99	25.53	27.61	28.86	30.35	d
	-157.41	71.73	19.29	21.96	23.99	25.53	27.61	28.86	30.35	b
	-157.40	71.69	19.29	21.97	23.99	25.53	27.61	28.86	***	c
CFCH (1)	30.00	55.41	12.54	13.91	14.85	15.57	16.66	17.49	18.85	d
CFCF (2)	5.00	58.31	13.54	15.12	16.24	17.11	18.31	19.05	19.96	d
CH₃CFHCH₃ (9)	-70.15	70.03	20.00	25.19	29.71	33.51	39.39	43.81	***	b
	-69.00	69.82	19.68	24.72	29.27	33.14	39.14	43.55	***	c
	-72.55	70.28	20.19	25.31	29.85	33.67	39.60	43.86	50.61	e
CH₃CF2CH₃ (18)	-124.88	72.38	22.87	28.22	32.52	36.34	41.76	45.64	***	b
	***	72.46	22.87	28.21	32.71	36.37	41.87	45.80	51.70	e
(CH₃)₃CF (81)	-78.1	74.41	26.57	32.87	39.10	43.99	51.42	56.85	65.18	e
	***	74.50	26.24	32.83	38.85	43.37	***	***	***	b

[a] Number in parenthesis show symmetry number. [b] reference [22].
[c] reference [20]. [d] reference [28]. [e] this study. *** indicates no available data.

8.3.3 Estimation of Group and F –F Interaction Values

The thermodynamic properties ($\Delta H_f°_{298}$, $S°_{298}$, and C_p(T)'s (300 ≤ T/K ≤ 1500)) which

are used to calculate group values and interaction terms are listed in Table 8.8. All data

except thermodynamic properties for 2-methyl,2-fluoropropane are adopted from Frenkel et al.[22].

Thermodynamic properties of fluorinated hydrocarbon groups and their interaction terms are listed in Table 8.12. The group values C/C/H3 and C/C2/H2 are taken from existing literature value[7]. Thermodynamic properties of fluorinated hydrocarbon groups and interaction terms determined in the previous study[26] are also listed in Table 8.11 for comparison.

The group values for $\Delta H_f°_{298}$ for C/C2/F/H, C/C2/F2, and C/C3/F are determined as -50.2, -104.9, and -48.0 kcal/mol respectively. The $S°_{298}$ values are 13.6, 17.3, and −8.09 cal/mol-K respectively.

The improved interaction terms for $\Delta H_f°_{298}$ of fluoroalkanes evaluated in this study are: 3.1, 5.7, 7.8,9.8, and 13.8 kcal/mol for F/F, 2F/F, 3F/F, and 3F/2F respectively. Interaction terms for fluoroalkenes increase strongly with increased fluorine substitution,;1.9, 8.9, and 16.1 kcal/mol for F//F, 2F//F, and 2F//2F respectively.

The interaction terms for $\Delta H_f°_{298}$ of F-F decrease with strength of C-C bond: 3.1, 1.9, and -0.5 kcal /mol for alkane, alkene, and alkyne respectively. Increased distance between F's on adjacent carbons is probably the contributing factor.

There are large corrections for $S°_{298}$'s, of fluoroalkene and alkyne groups, while corrections of less than 1.0 cal/mol-K apply to alkane groups (Table 8.11). For example, $S°_{298}$ interaction terms for F/F, 2F/F, and 2F/2F are 0.92, 0.38, and 0.85 cal/mol-K respectively, while those for F//F, 2F//F, and 2F//2F are −7.34, -3.70, and -2.62 cal/mol-K respectively. Only small corrections are necessary for heat capacities $C_p(T)$'s of fluoroalkenes and alkynes.

Table 8.9 Evaluated Enthalpies of Formations ($\Delta H_f^\circ{}_{298}$) for Fluorinated Ethanes and Fluorine – Fluorine Interactions[a]

Compounds and Interactions	This Study	Number used in Previous Study[b]	BAC-MP4[c]	Other Sources
CH_2FCH_2F	-102.7	-106.6	-106.6	-103.7[c]
CHF_2CH_2F	-156.9	-157.8	-160.5	-156.8[d]
CHF_2CHF_2	-209.6	-210 .1	-211.1	-209.1[d]
CF_3CH_2F	-213.3	-214.1	-218.3	-214.1[e]
CF_3CHF_2	-264.1	-264.0	-268.7	-264.0[e]

Compounds and Interactions	This Study	Number used in Previous Study[b]
F/F[f]	3.1	-0.8
2F/F	5.7	4.8
2F/2F	9.8	9.3
3F/F	7.8	7.0
3F/2F	13.8	13.9

[a] Unit in kcal/mol. [b] reference [26]. [c] reference [2]. [d] reference [3]. [e] reference [1]. [f] "*f*" indicates interaction for alkane.

8.3.4 Estimation of F-CH3 Gauche Interaction

The previous study reported that the F-CH3 gauche staggered conformation was more stable than anti staggered conformation in fluoropropanes[27]. There are five F-CH3 gauche interaction systems to calculate thermodynamic properties resulting from F-CH3 gauche interactions. The composite table in Table set 8.10 shows the process to estimate the thermodynamic properties of the F-CH3 gauche interaction.

The first table set is the *ab initio* determined thermodynamic properties which were reported in the previous study[27].

The second table set is the Group Additivity (G.A.) determined thermodynamic properties using fluorinated carbon groups determined in the chapter 6 including F-F interactions terms which are estimated in this chapter without F-CH3 gauche interaction.

Table 8.10 F - CH3 Gauche Interaction Estimation Table

ab-initio Determined Thermodynamic Properties for Fluoropropanes

Species	$H_f^{\circ}{}_{298}{}^a$	$S^{\circ}{}_{298}{}^b$	$C_{p300}{}^b$	C_{p400}	C_{p500}	C_{p600}	C_{p800}	C_{p1000}	C_{p1500}
$CH_2FCH_2CH_3$	-67.5	73.39	19.70	24.74	29.35	33.27	39.38	43.82	50.57
$CHF_2CH_2CH_3$	-123.7	77.51	21.64	26.89	31.51	35.35	41.18	45.33	51.47
$CF_3CH_2CH_3$	-183.1	78.79	24.32	29.77	34.32	37.99	43.41	47.15	52.55
$CH_2FCHFCH_3$	-110.0	77.74	22.21	27.26	31.79	35.56	41.33	45.46	51.61
CHF_2CHFCH_3	-164.9	80.35	24.50	29.93	34.63	38.46	44.02	47.76	52.95
$CHF_2CF_2CH_3$	-214.7	82.72	27.92	33.84	38.46	41.97	46.82	49.94	54.14
CF_3CHFCH_3	-221.6	82.63	26.72	32.31	36.88	40.47	45.56	48.92	53.53
$CF_3CF_2CH_3$	-271.1	86.06	29.57	35.26	39.75	43.17	47.82	50.94	54.56

G. A. Determined (w/o Gauche Interaction) Thermodynamic Properties for Fluoropropanes

Species	$H_f^{\circ}{}_{298}{}^a$	$S^{\circ}{}_{298}{}^b$	$C_{p300}{}^b$	C_{p400}	C_{p500}	C_{p600}	C_{p800}	C_{p1000}	C_{p1500}
$CH_2FCH_2CH_3$	-67.8	73.73	19.73	24.64	29.17	33.04	39.13	43.61	50.36
$CHF_2CH_2CH_3$	-124.6	77.84	21.87	27.02	31.57	35.36	41.13	45.26	51.36
$CF_3CH_2CH_3$	-183.1	80.18	24.44	29.84	34.36	38.00	43.36	47.09	52.46
$CH_2FCHFCH_3$	-109.9	78.81	21.64	26.95	31.52	35.32	41.07	45.30	51.62
CHF_2CHFCH_3	-164.1	82.38	24.29	29.83	34.40	38.09	43.44	47.22	52.71
$CHF_2CF_2CH_3$	-214.8	85.27	28.47	33.82	37.81	41.25	45.87	49.03	53.76
CF_3CHFCH_3	-220.5	85.19	26.42	32.20	36.78	40.37	45.38	48.81	53.65
$CF_3CF_2CH_3$	-269.3	88.79	29.51	35.28	39.53	43.07	47.60	50.51	54.67

Difference (*ab initio* - G.A.) and Number of F-CH₃ Gauche Interaction

Species	# of Gauche Ineraction	$H_f^{\circ}{}_{298}{}^a$	$S^{\circ}{}_{298}{}^b$	$C_{p300}{}^b$	C_{p400}	C_{p500}	C_{p600}	C_{p800}	C_{p1000}	C_{p1500}
$CH_2FCH_2CH_3$	1	0.4	-0.34	-0.03	0.10	0.18	0.23	0.25	0.21	0.21
$CHF_2CH_2CH_3$	2	1.0	-0.33	-0.23	-0.13	-0.06	-0.01	0.05	0.07	0.11
$CF_3CH_2CH_3$	2	0.0	-1.39	-0.12	-0.07	-0.04	-0.01	0.05	0.06	0.09
$CH_2FCHFCH_3$	1	0.0	-1.07	0.57	0.31	0.27	0.24	0.26	0.16	-0.01
CHF_2CHFCH_3	2	-0.7	-2.03	0.21	0.10	0.23	0.37	0.58	0.54	0.24
$CHF_2CF_2CH_3$	2	0.0	-2.55	-0.55	0.02	0.65	0.72	0.95	0.91	0.38
CF_3CHFCH_3	2	-1.0	-2.56	0.30	0.11	0.10	0.10	0.18	0.11	-0.12
$CF_3CF_2CH_3$	2	-1.9	-2.73	0.06	-0.02	0.22	0.10	0.22	0.43	-0.11
Standard Deviation		0.6	1.63	0.26	0.11	0.22	0.22	0.32	0.31	0.16

Estimated Thermodynamic Properties of F-CH₃ Gauche Interaction

Gauche Group	$H_f^{\circ}{}_{298}{}^a$	$S^{\circ}{}_{298}{}^b$	$C_{p300}{}^b$	C_{p400}	C_{p500}	C_{p600}	C_{p800}	C_{p1000}	C_{p1500}
$F - CH_3$	-0.1	-0.90	0.05	0.05	0.13	0.14	0.19	0.18	0.06

[a] unit in kcal/mol. [b] unit in cal/mol-K

The third table is the difference between first and second table and number of maximum F-CH3 gauche interaction.

The last table is the estimated thermodynamic properties of F-CH3 gauche interaction. The difference of thermodynamic properties are divided by the number of F-CH3 gauche interactions for each of the eight species and the average is taken.

G.A. method without gauche interaction underestimates $\Delta H_f°_{298}$ by 1 kcal/mol for 1,1-difluoropropane and overestimates by 1.0, and 1.9 kcal/mol for 1,1,1,2-tetrafluoropropane and 1,1,1,2,2-pentafluoropropane. G. A. method without gauche interaction overestimate $S°_{298}$ for all fluorinated propanes and difference increases with number of fluorine which is 0.34 to 2.73 cal/mol-K. G.A. method for the estimation of heat capacities ($C_p(T)$'s $300 \le T/K \le 1000$) are quite close to *ab initio* determined thermodynamic properties. The thermodynamic properties of F-CH3 gauche interaction are then calculated as explained above and shown in the lowest section of Table 8.10.

Table 8.11 shows F-CH3 gauche interaction included G. A. determined thermodynamic properties and the difference from *ab initio* calculations. The gauche correction term for $\Delta H_f°_{298}$, which is -0.1 kcal/mol, does not improve accuracy significantly. An increase of standard deviation from *ab initio* calculation results by factor of 0.1 indicates the use of no correction would be better. The correction for $S°_{298}$, which is -0.9 cal/mol-K, improves the accuracy for the standard deviation, which decreases from 1.63 to 0.66 cal/mol-K. The G. A. determined $S°_{298}$ for 1,1-difluoropropane is underestimated by 1.47cal/mol-K and the G. A. determined $S°_{298}$ for 1,1,1,2,2-pentafluoropropane is overestimated by 0.93 cal/mol-K. Other differences are

Table 8.11 F - CH3 Gauche Interaction value Included G. A. Determined Thermodynamic Properties for Fluoropropanes and Difference from *ab-initio* Determined Thermodynamic Properties

G.A. Determined (include F-CH3 Gauche)Thermodynamic Properties

Species	$H_f^{\circ}{}_{298}$ [a]	$S^{\circ}{}_{298}$ [b]	C_{p300} [b]	C_{p400}	C_{p500}	C_{p600}	C_{p800}	C_{p1000}	C_{p1500}
CH₂FCH₂CH₃	-67.9	72.83	19.78	24.69	29.30	33.18	39.32	43.79	50.42
CHF₂CH₂CH₃	-124.9	76.04	21.96	27.12	31.82	35.64	41.51	45.62	51.48
CF₃CH₂CH₃	-183.4	78.38	24.53	29.94	34.61	38.28	43.74	47.45	52.58
CH₂FCHFCH₃	-110.1	77.91	21.69	27.00	31.64	35.46	41.26	45.48	51.68
CHF₂CHFCH₃	-164.4	80.58	24.39	29.93	34.65	38.37	43.82	47.58	52.83
CHF₂CF₂CH₃	-215.0	83.47	28.56	33.92	38.06	41.53	46.25	49.39	53.88
CF₃CHFCH₃	-220.8	83.39	26.52	32.30	37.03	40.65	45.76	49.17	53.77
CF₃CF₂CH₃	-269.5	86.99	29.60	35.38	39.78	43.35	47.98	50.87	54.79

Differences (*ab initio* - G. A.)

Species	$H_f^{\circ}{}_{298}$ [a]	$S^{\circ}{}_{298}$ [b]	C_{p300} [b]	C_{p400}	C_{p500}	C_{p600}	C_{p800}	C_{p1000}	C_{p1500}
CH₂FCH₂CH₃	0.5	0.56	-0.08	0.05	0.05	0.09	0.06	0.03	0.15
CHF₂CH₂CH₃	1.2	1.47	-0.32	-0.23	-0.31	-0.29	-0.33	-0.29	-0.01
CF₃CH₂CH₃	0.3	0.41	-0.21	-0.17	-0.29	-0.29	-0.33	-0.30	-0.03
CH₂FCHFCH₃	0.1	-0.17	0.52	0.26	0.15	0.10	0.07	-0.02	-0.07
CHF₂CHFCH₃	-0.5	-0.23	0.11	0.00	-0.02	0.09	0.20	0.18	0.12
CHF₂CF₂CH₃	0.3	-0.75	-0.64	-0.08	0.40	0.44	0.57	0.55	0.26
CF₃CHFCH₃	-0.8	-0.76	0.20	0.01	-0.15	-0.18	-0.20	-0.25	-0.24
CF₃CF₂CH₃	-1.6	-0.93	-0.03	-0.12	-0.03	-0.18	-0.16	0.07	-0.23
Standard Deviation	0.7	0.66	0.26	0.12	0.18	0.21	0.24	0.21	0.14

[a] unit in kcal/mol. [b] unit in cal/mol-K

small, less than 0.76 cal/mol-K. The correction factor for heat capacities ($C_p(T)$'s $300 \leq T/K \leq 1500$) shows small improvement. Since original difference between modified G. A. and *ab initio* is very small, the improvement is not significant. The bottom of Table 8.12 shows final values of F-CH3 gauche interactions. No correction is chosen for enthalpy of formation. The result is an average deviation of ±1.3 kcal/mol in estimation of $\Delta H_f^{\circ}{}_{298}$.

Table 8.12 Summery of Groups and Interactions

Groups	$H_f°_{298}$[a]	$S°_{298}$[b]	C_{p300}[b]	Cp_{400}	Cp_{500}	Cp_{600}	Cp_{800}	Cp_{1000}	Cp_{1500}
C/C/H3[c]	-10.0	30.41	6.19	7.84	9.4	10.79	13.02	14.77	17.58
C/C/F/H2[d]	-52.9	35.00	8.04	9.85	11.52	12.9	15.04	16.5	18.58
C/C/F2/H[d]	-109.7	39.11	10.18	12.23	13.92	15.22	17.04	18.15	19.58
C/C/F3[d]	-168.2	42.55	12.75	15.05	16.71	17.86	19.27	19.98	20.68
C/C2/F/H	-50.2	13.58	7.62	9.51	10.91	11.93	13.35	14.27	15.52
C/C2/F2	-104.9	17.30	10.49	12.54	13.72	14.76	15.72	16.10	16.26
C/C3/F	-48.1	-8.09	8.00	9..35	10.90	11.62	12.36	12.54	12.44
CD/H2	6.3	27.61	5.10	6.36	7.51	8.50	10.07	11.27	13.19
CD/F/H	-39.5	36.48	7.0	8.5	9.6	10.5	11.9	12.8	14.1
CD/F2	-86.8	38.55	9.1	10.8	12.0	12.8	13.9	14.5	15.2
CT/H	27.3	24.70	5.28	5.99	6.49	6.87	7.47	7.96	8.85
CT/F	2.8	32.08	7.26	7.92	8.36	8.70	9.19	9.53	10.00

Interaction	$H_f°_{298}$[b]	$S°_{298}$[c]	Cp_{300}[c]	Cp_{400}	Cp_{500}	Cp_{600}	Cp_{800}	Cp_{1000}	Cp_{1500}
F/F	3.1	0.92	-0.21	-0.25	-0.31	-0.3	-0.34	-0.24	0.01
F/2F	5.7	0.38	0.3	0.25	0.17	0.15	0.03	0.03	0.1
F/3F	7.8	0.85	-0.14	-0.2	-0.24	-0.21	-0.26	-0.21	-0.06
2F/2F	9.8	-0.45	1.61	1.21	0.77	0.48	0.09	0.01	0.06
2F/3F	13.8	0.73	0.08	-0.15	-0.3	-0.34	-0.41	-0.34	-0.13
3F/3F[d]	15.5	0.54	0.24	-0.09	-0.28	-0.34	-0.39	-0.31	-0.13
F//F[e]	1.91	-7.34	-0.01	-0.10	-0.12	-0.09	-0.03	0.03	0.10
2F//F	8.91	-3.70	0.51	0.15	-0.02	-0.07	-0.07	-0.03	0.05
2F//2F	16.1	-2.62	1.12	0.37	0.02	-0.11	-0.15	-0.10	0.00
F///F[f]	-0.5	-5.17	-0.97	-0.72	-0.48	-0.29	-0.08	-0.02	-0.03

Gauche	$H_f°_{298}$[b]	$S°_{298}$[c]	Cp_{300}[c]	Cp_{400}	Cp_{500}	Cp_{600}	Cp_{800}	Cp_{1000}	Cp_{1500}
F - CH3	0.0	-0.90	0.05	0.05	0.13	0.14	0.19	0.18	0.06

[a] Units in kcal/mol. [b] Units in cal/mol-K. [c] reference 7. [d] reference 26.
[e] // indicates correction for alkene group. [f] /// indicates correction for alkyne group.

8.4 Summary

Thermodynamic properties ($\Delta H_f^\circ{}_{298}$, $S^\circ{}_{298}$, and $C_p(T)$'s ($300 \leq T/K \leq 1500$)) for fluorinated carbon groups, C/C2/F/H, C/C2/F2, CD/F/H, CD/F2, and CT/F are estimated using the existing literature data and existing group value of C/C/H3. Those for C/C3/F are estimated from thermodynamic properties of 2-methyl,2-fluoropropane, which is calculated with G2MP2 method, and existing group value of C/C/H3. Interaction values F//F, 2F//F, and 2F//2F for fluorinated alkenes and F///F for fluorinated alkynes are also calculated. $\Delta H_f^\circ{}_{298}$ of 2-methyl,2-fluoropropane, 1-fluoropropane, and 2-fluoropropane are calculated using G2MP2 results and isodesmic reactions. $\Delta H_f^\circ{}_{298}$ of 1-fluoropropane, and 2-fluoropropane are compared with experimental data and systematic error is evaluated. It is concluded that the error would be 3.0 kcal/mol for $\Delta H_f^\circ{}_{298}$ of 2-methyl,2-fluoropropane with G2MP2 calculation and isodesmic reaction, which is calculated as 81.09 kcal/mol. The $\Delta H_f^\circ{}_{298}$ for 2-methyl,2-fluoropropane is estimated as -78.1 kcal/mol. Calculated $S^\circ{}_{298}$ and $C_p(T)$'s of 2-methyl,2-fluoropropane are expected to be reasonable. Group values and interaction terms for of fluorinated carbons are presented.

REFERENCES

(1)   Chen, S. S.; Rodgers, A. S.; Wilhoit, R. C.; Zwolinski, B. J. *J. Phys. Chem. Ref. Data* **1975**, *4*, 441 .

(2)   Zachariah, M. R.; Westmoreland, P. R.; Burgess, D. R.; Tsang, W.; Mellius, C. F. *J. Phys. Chem.* **1996**, *100*, 8737 .

(3)   Chen, Y.; Paddison, S. J.; Tschuikow-Roux, E. *J. Phys. Chem.* **1994**, *98*, 1100 .

(4)   Berry, R. J. *J. Phys. Chem.* **1997**, *100*, 7405.

(5)   Marshall, P.; M., S. *J. Phys. Chem.* **1997**, *101*, 2906.

(6)   Benson, S. W. *Thermochemical Kinetics*; A Wiley-Interscience Publication: New York, NY, 1976.

(7)   Cohen, N. *J. Phys. Chem. Ref. Data* **1996**, *25*, 1411.

(8)   Burgess, D. R. F.; Zachariah, M. R.; Tsang, W.; R., W. P. "Thermochemical and Chemical Kinetic Data for Fluorinated Hydrocarbons," NIST, 1995.

(9)   Lacher, J. R.; Skinner, H. A. *J. Chem. Soc. (A)* **1968**, 1034 .

(10)   Frisch, M. J.; Trucks, G. W.; Schlegel, H. B.; Gill, P. M. W.; Johnson, B. G.; Robb, M. A.; Cheeseman, J. R.; Keith, T.; Petersson, G. A.; Montgomery, J. A.; Raghavachari, K.; Al-Laham, M. A.; Zakrzewski, V. G.; Ortiz, J. V.; Foresman, J. B.; Cioslowski, J.; Stefanov, B. B.; Nanayakkara, A.; Challacombe, M.; Peng, C. Y.; Ayala, P. Y.; Chen, W.; Wong, M. W.; Andres, J. L.; Replogle, E. S.; Gomperts, R.; Martin, R. L.; Fox, D. J.; Binkley, J. S.; Defrees, D. J.; Baker, J.; Stewart, J. P.; Head-Gordon, M.; Gonzalez, C.; Pople, J. A. Gaussian 94; Gaussian, Inc.: Pittsburgh, PA, 1995.

(11)   Hehre, W. J.; Radom, L.; Schleyer, P. R.; Pople, J. A. *Ab-Initio Molecular Orbital Theory*; John Wiley &Sons, Inc: New York, NY, 1986.

(12)   McQuarrie, D. A. *Statistical Mechanics*; Harper & Row: New York, 1976.

(13)   Villamanan, R. M.; Chen, W. D.; Wlodarczak, G.; Demaison, J. *J. Mol. Spectrosc.* **1995**, *171*, 223.

(14)   Danti, A.; Wood, J. L. *J. Chem. Phys.* **1959**, *30*, 582.

(15)   Eltayeb, S.; Guirgis, G. A.; Fanning, A. R.; R., D. J. *J. Raman Spectrosc.* **1996**, *27*, 111.

(16)   Gallaher, K. L.; Yokozaki, A.; Bauer, S. H. *J. Phys. Chem* **1974**, *78*, 2389.

(17)   Parra, R. D.; Zeng, X. C. *J. Phys. Chem.* **1998**, *102*, 654.

(18)   Papasavva, S.; Illinger, K. H.; Kenny, J. E. *J. Phys. Chem.* **1996**, *100*, 10100 .

(19)   Durig, R. J.; Liu, J.; Little, T. S.; Kalasinsky, V. F. *J. Phys. Chem.* **1992**, *96*, 8224.

(20)   Stull, D. R.; Westrum, E. F.; Sinke, G. C. *The Chemical Thermodynamics of Organic Compounds*; Robert E. Krieger Publishing Company: Malabar, FL, 1987.

(21)   Pitzer, K. S. *J. Chem. Phys* **1946**, *14*, 239.

(22)   Frenkel, M.; Kabo, G. J.; Marsh, K. N.; Roganov, G. N.; Wilhoit, R. C. *Thermodynamics of Organic Compounds in the Gas State*; Texas A&M University System: , 1994; Vol. 2.

(23)   Curtiss, L. A.; Raghavachari, K.; Trucks, G. W.; Pople, J. A. *J. Chem Phys.* **1991**, *94*, 7221.

(24)   Lay, T. H.; Krasnoperov, L. N.; Venanzi, C. A.; Bozzelli, J. W. *J. Phys. Chem.* **1996**, *100*, 8240.

(25)   Krasnoperov, L. N.; Lay, T. H.; Shokhirev, N. V. *Thermodynamic Properties of Hindered Rotor by Diagonalization of Hamiltonian Matrix* .

(26)   Yamada, T.; Lay, T. H.; Bozzelli, J. W. *J. Phys.Chem* **1998**, *102*, 7286.

(27)   Yamada, T.; Bozzelli, J. W. *J. Phys. Chem* **1998**, in progress.

(28)   Stull, D. R. P., H, *JANAF Thermochemical Tables, 2nd ed.; NSRDS-NBS37 Second Edition*; U.S. Govermental Printing Office: Washington D. C., 1971.